CHALLENGES AND RECENT ADVANCE IN GEOTECHNICS FOR FOUNDATION ENGINEERING

30 May 2014

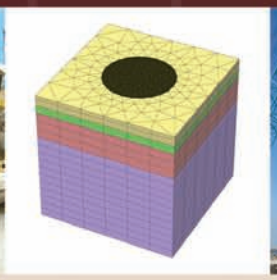

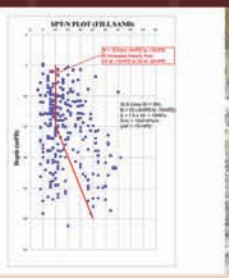

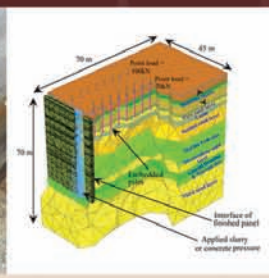

HK工E THE HONG KONG INSTITUTION OF ENGINEERS 香港工程師學會

GEOTECHNICAL DIVISION 岩土分部

HKGES 香港岩土工程學會

Since 2003





With the Compliments

of

New Concepts Foundation Ltd.

Rm 1812, 18/F, Nan Fung Commercial Centre, 19 Lam Lok Street, Kowloon Bay, Kowloon.
Tel: (852) 2750 7008 Fax: (852) 2363 2162 E-mail Address: ncfl@netvigator.com

ISO 9001:2008
Certificate No. 131030-HK

ISO 14001:2004
Certificate No. 131031-HK

ISO 50001:2011
Certificate No. EnMS-HK-10003

OHSAS 18001:2007
Certificate No. OH-HK-10071




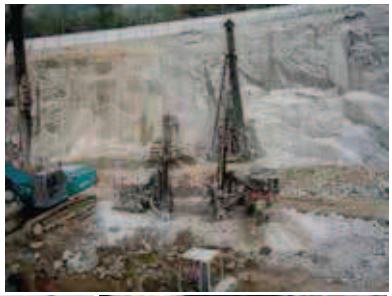








With The Compliments
to
The Hong Kong Institution of Engineers
Geotechnical Division 34th Annual Seminar




Our Business includes:

- Design and Construction of Land Pile Works
- Construction of Landslip Preventive and Mitigation Works to Slopes and Retaining Walls
- All Sorts of Civil Engineering Works




中國地質工程集團公司
CHINA GEO-ENGINEERING CORPORATION

香港灣仔港灣道 30 號新鴻基中心 24 樓 2421-25 室
Rm. 2421-25, 24/F., Sun Hung Kai Centre, 30 Harbour Road, Wanchai, Hong Kong
Tel: (852) 2511 9001 Fax: (852) 2580 0697

Meeting complex challenges

Wherever difficult ground conditions, sensitive environments or ambitious structures present geotechnical challenges, Arup provides robust and advanced solutions to reshape our cities.


1

Images

1. Non-dredged Cellular Seawall to create 150-hectare Artificial Island, Hong Kong Boundary Crossing Facilities
2. Driven Steel Tubular Piles for Residential Development at TCTL 36, Area 55A, Tung Chung
3. Mechanical Excavation of Large Span 4-lane Carriageway Tunnel underneath Scenic Hill, Hong Kong Link Road
4. Fabrication of 31m Internal Diameter Circular Steel Cells, Hong Kong Boundary Crossing Facilities


2

3

4

泰錦建築工程有限公司
Tai Kam Construction Engineering Company Limited

Slope Stabilization & Site Formation

Specialist Contractor

Director : K S LAU
BSc(Hon) Msc DIC LLB(Hon)
MHKIE FHKIHT RPE(Civil) RSO RSA ASA

Address : Room 1114, 11/Floor, Wealth Commercial Centre,
42 - 56 Kwong Wa Street, Mong Kok, Kowloon, HK.

Tel.: 2473 4428 Fax : 2473 4418

e-mail : taikamsafety@hotmail.com

陳運圖工程顧問有限公司
W T Chan & Associates Limited

Website : http//www.wtchan.com.hk

W T Chan & Associates Limited is a professional consulting engineering firm specializes in Civil, Structural and Geotechnical Engineering.

We are specialize in following areas,

- Structural Design
- Site Formation Design
- Excavation and Lateral Support
- Ground Investigation and Ground Treatment
- Foundation Design – Piling and Footing
- Slope remedial Works Design
- Settlement Analysis
- Drainage Design and Seepage Analysis
- Project Management
- Boulders Survey
- Natural Terrain Studies

C M WONG & ASSOCIATES LTD
Consulting Engineers

黃志明
建築工程師
有限公司

C M Wong & Associates Ltd is a multi-disciplinary firm of consulting engineers providing services for all stages of the development process including feasibility studies, design, contract administration, and construction phase services for building and civil engineering projects.

The reputation of the firm is based on the ability of the practice to produce **Innovative, economical and elegant** engineering solutions for a wide range of project.







11/F, Universal Trade Centre, 3-5A Arbuthnot Road, Hong Kong
Web Site: www.cmwal.com ◆ Email: cmwal@cmwal.com
Tel: (852) 2522 1068 ◆ Fax: (852) 25263111

Mott MacDonald's foundation and geotechnical engineers have extensive skills that have supported the delivery of innovative foundation solutions for projects in the building, transportation, infrastructure, maritime and utilities sectors. Our experience covers the design and supervision of both shallow and deep foundations on land and at sea.

With geotechnical skills expanding well beyond foundations, Mott MacDonald has worked on many ground and underground projects, providing services including:

- Geotechnical investigation and appraisal
- Site formation
- Natural terrain hazard assessment
- Deep excavation
- Geo-environmental study
- Slope engineering and maintenance
- Tunnelling
- Reclamation
- 3D ground modelling

HKUST - New Academic Building

HZMB - Hong Kong Link Road

Mott MacDonald

Foundation design

North Lantau Hospital

Cai Mep Maritime Terminal

For general enquiries:

Mott MacDonald
T +852 2828 5757
E marketing.hk@mottmac.com.hk
W www.mottmac.com/hong-kong

Mott MacDonald

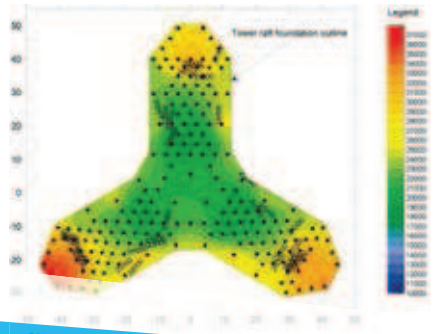

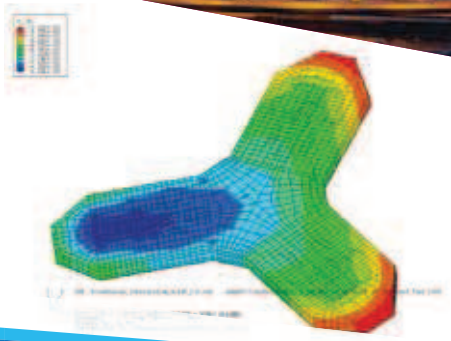

The Next Evolution
in Design and Engineering Consultancy

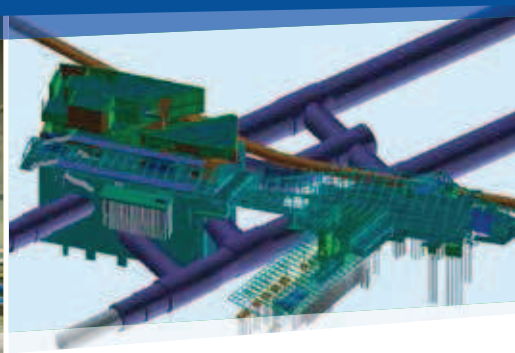

Hyder Consulting Limited

47/F Hopewell Centre, 183 Queen's Road East, Wan Chai, Hong Kong

Tel: (852) 2911 2233 Fax: (852) 2805 5028

E-mail: hyder.hk@hyderconsulting.com

www.hyderconsulting.com

Hyder

AQUATERRA CONSULTANTS LIMITED
SHAPING THE WORLD BY DESIGN


Slope Protection


Channels & Ditches

CONCRETE CANVAS™

Concrete Impregnated Fabric...

CONCRETE CANVAS: CC5, CC8 & CC13

Available 5 mm, 8mm or 13 mm thick
Small or large rolls for:

SLOPE PROTECTION & DITCH LINING

TEMPORARY & PERMANENT WORKS

For more information contact us at:
INFO@AQUATERRA.COM.HK
WWW.CONCRETECANVAS.CO.UK
Call TEL: +852 2808 1829 or +852 9222 8826


Hong Kong Trial – Ditch Lining
XRL – C810A


CC Batched Rolls


CC Bulk Rolls

WHAT IS CONCRETE CANVAS? A versatile cement-fabric used for protection or repair. Rapidly installed using unskilled labour.

WHY USE CONCRETE CANVAS? – 24 hour hardening, rapid repairs to drainage channel / surface protection in inclement weather.

CONCRETE CANVAS USES?


Rock Slope Protection


Soil Bund Protection

10 day properties of Concrete Canvas:

- Compressive strength = 40kPa
- Young's Modulus = 1,500 MPa
- Bending stress & E_b = 3.4 MPa & 180 MPa
- Abrasion Resistance = 0.1g.cm^2
- MOHS hardness test = 4 to 5
- CBR puncture resistance = 2.69 kN
- Material Density = 2 .00 Mg/m^3
- Fire proof / erosion proof / UV proof


Fast slope protection

- Weatherproofing slope surfaces
- Gabion reinforcing covering
- Track surface or floor matting
- Pipe protection / cable coverings


Lay in Wet Weather

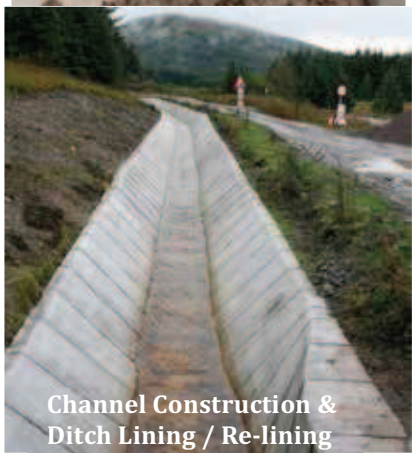
Channel Construction & Ditch Lining / Re-lining

With Compliments from

Golder Associates (HK) Limited

20/F, Henan Building, 90 Jaffe Road, Wanchai, HK
Tel: +852 2591 1774 Fax: +852 2591 1730
Email: info@golder.com.hk

Following the merger with Geotechnical Consulting Group (Asia) Ltd (GCG Asia) in 2012, Golder Associates Hong Kong Ltd (GAHK) has expanded the geotechnical and engineering services previously provided by GCG (Asia). Golder Associates (GA) employs more than 8,000 professional staff worldwide who practise in the fields of geotechnical and environmental engineering. A core discipline of GA relates to the geotechnical design and construction of deep excavations, foundations, ground treatment, instrumentation and monitoring, reclamation, rock/geological engineering, site formation works and soft/hard ground tunnelling.

Although the majority of the works carried out by GAHK serves the Hong Kong construction industry, by working with other GA offices GAHK is well placed to work on projects throughout Southeast Asia. GA has offices in China, Singapore, Jakarta and Manila. GAHK is currently working on projects as far afield as Australasia and the Middle East. GAHK offers civil/geotechnical consultancy services in the fields of specialist advice/design on major infrastructure projects, technical innovation, high level numerical analysis, expert advice, independent review and representation.

JACOBS®

Jacobs is one of the world's largest and most diverse providers of professional technical services. With 2013 revenues of over $12 billion, we offer full-spectrum support to industrial, commercial, and government clients across multiple markets. **Jacobs'** services include scientific and specialty consulting as well as all aspects of engineering and construction, and operations and maintenance.

As a broad-based technical professional consulting firm, we offer a complete range of services to help our clients maintain a competitive edge in their respective markets. From feasibility studies and planning to operations and maintenance (O&M), we customize our services to meet our clients' business and project goals.

BEYOND ZERO®
A Culture of Caring

www. jacobs.com

Proceedings of the 34th Annual Seminar
Geotechnical Division, The Hong Kong Institution of Engineers

Challenges and Recent Advance in Geotechnics for Foundation Engineering

30 May 2014
Hong Kong

Jointly organized by:
Geotechnical Division, The Hong Kong Institution of Engineers
Hong Kong Geotechnical Society

Captions of Figures on the Front Cover

Top: Foundation Design for a Residential Development in Adverse Ground Condition at Designated Area of Northshore Lantau (By courtesy of Ove Arup & Partners Hong Kong Ltd)

Bottom From Left to Right:

1) Feasibility of Bored Pile Foundation Modification in Hong Kong (By courtesy of AECOM Asia Co Ltd)
2) Design and Analysis of a Piled-Raft Foundation in Doha (By courtesy of Hyder Consulting Ltd)
3) A Case Study of Marine Structures Foundation Design (By courtesy of AECOM Asia Co Ltd)
4) Geotechnical Design at Tseung Kwan O Reclamation Development (By courtesy of AECOM Asia Co Ltd)
5) Foundation Design for a Residential Development in Adverse Ground Condition at Designated Area of Northshore Lantau (By courtesy of Ove Arup & Partners Hong Kong Ltd)
6) Pile Settlement Induced by Diaphragm Wall Installation (By courtesy of Golder Associates (HK) Ltd)

Soft copy of the proceedings can be downloaded from the HKIE Geotechnical Division's website http://hkieged.org/geodiv/annualseminar.aspx

ORGANISING COMMITTEE

Chairman
Ir Chris Lee

Members
Ir Sammy Cheung
Ir David Lai
Ir K C Lam
Ir Dr S W Lee
Dr Ryan Yan
Ir Patrick Yong
Ir Irene Yu
Ir Ringo Yu
Dr Y H Wang

Technical Sub-committee
Ir David Lai
Ir Kenneth Lai
Ir Chris Lee
Ir Darkie Lee
Dr Andy Leung
Ir Angus Sum
Ir Dr H W Sun
Ir Patrick Yong
Ir Irene Yu
Dr Y H Wang

Published by:
Geotechnical Division
The Hong Kong Institution of Engineers
9/F., Island Beverley, 1 Great George Street, Causeway Bay, Hong Kong
Tel: 2895 4446 Fax: 2577 7791

Printed in Hong Kong

FOREWORD

This volume of proceedings contains papers of the 34th Annual Seminar organised by the Geotechnical Division of The Hong Kong Institution of Engineers. Over the years, the Geotechnical Division has organised seminars annually on a variety of geotechnical subjects. These annual seminars served to provide a platform for geotechnical practitioners and researchers to consolidate their engineering experience and expertise in various topics of geotechnical engineering.

This year, the Geotechnical Division has chosen the title "Challenges and Recent Advance in Geotechnics for Foundation Engineering" to be the theme of this 34th Annual Seminar. Demands for tall buildings driven by economic and population growth have posed great challenge to the geotechnical profession, in particular where the ground conditions are difficult and with complex geology. In response to the challenges, geotechnics for foundation engineering have made much advancement with respect to ground investigation, design methodology, construction techniques and risk management. The papers included in this volume of proceedings present a lot of valuable geotechnical engineering experience and insight gained in the advancement in these areas. They also give foresight to areas of foundation solutions requiring research and development for cost reduction as well as further improvement in safety and environmental performances.

This set of proceedings differs from its predecessors in one respect. There is a report on the HKIE Geotechnical Paper Award. The report describes the selection mechanism and the reasons for selecting the two papers for the award. It is worth reading.

On behalf of the Geotechnical Division, I would like to thank the Hong Kong Geotechnical Society for jointly organising this seminar. In particular, I am grateful to our Guest-of Honour - Ir Wai Chi-sing JP**,** Permanent Secretary for Development (Works) of the Government of the Hong Kong Special Administrative Region; the Invited Speakers - Ir Prof CM Wong and Ir Prof Charles Ng; the speakers and the authors of the papers for their contributions to this seminar. Lastly, I must thank the Organising Committee, under the leadership of Ir Chris Lee, for their hard work in making this seminar possible.

Ir Terence Chan
Chairman, Geotechnical Division
Hong Kong Institution of Engineers (2013/2014 Session)
May 2014

The HKIE Geotechnical Paper Award

I have been asked by the Assessment Board to introduce the Award to readers of this set of seminar proceedings. I shall be brief.

Professor Wilson Tang of HKUST served on the HKIE Geotechnical Division Committee between 1998 and 2001. He proposed to set up an award for high quality papers. The Best Geotechnical Paper Award scheme was introduced to recognize outstanding geotechnical research or project work. It ran for five years but interest in the local geotechnical profession gradually waned to the extent that it was suspended in 2006.

Professor Tang passed away in 2012. In the memorial service that March, Professor Tang's aspiration for an award was mentioned and inspired the Geotechnical Division Committee to look into the feasibility of revitalizing the initiative. The result is the HKIE Geotechnical Paper Award, of which the present exercise is the first one. We plan to hold award exercises every two years, for papers published in Hong Kong or authored by geotechnical engineers based in Hong Kong but published elsewhere in the five years before the exercise.

To ensure high quality assessment of the papers, an Assessment Board Panel has been formed with eminent members of the geotechnical profession. There are at present sixteen on the Panel. An Assessment Board is formed for each Award exercise, to be chaired by the Chairman of the Geotechnical Division Committee (GDC) of that year, and with the Deputy Chairman of GDC and five others from the Panel as members. For the present exercise, it comprises Ir Terence Chan, Ir Rupert Leung, Ir Y C Chan, Ir Y C Koo, Ir Dr C K Lau, Ir Victor Li and Ir Professor George Tham.

The first exercise received warm support from authors local and overseas. A total of 36 entries were received. To facilitate frank and critical views from members, and to help assure those who entered papers that their entries will be handled with discretion and upmost fairness, a strict code of confidentiality was exercised. Members received information on a need-to-know basis. They passed views to a designated member of the Board who then redirected it upon removal of any identity tags. The final decision on winners was by rounds of secret ballot with the summary of views in hand. The Board has found this arrangement to be fair and fruitful, such that the Board as a whole could develop in-depth appreciation of the relative strength and specialties of the contending papers, with time to ponder and dig up supporting information, and with room for contention without tension.

The Board noted that the contending papers fall into two broad groups: those reporting research efforts that led to changes in practice, and those aiming at sharing experience. The former differs from the latter in the need to put in sufficient details for readers to replicate the study if they so desire. For the papers in hand, the Board felt it difficult to compare fairly across the groups. It has therefore selected one from each for the Award.

Hence, for experience-sharing type papers

Tattersall, J.W., Tam, J.K.W., Garshol, K.F. & Lau, K.C.K. (2012). Engineering geological approach for assessment of quantities and programme for deep tunnels in Hong Kong. Proceedings of the HKIE Geotechnical Division 32nd Annual Seminar "Geotechnical Aspects of Tunnelling for Infrastructure", pp 81-87

and, for research type papers

Cheung, R.W.M. & Lo, D.O.K. (2011). Use of time domain reflectometry for quality control of soil nailing works. Journal of Geotechnical and Geoenvironmental Engineering, ASCE, Vol. 137, No. 12, pp 1222-1235

The Board selected them for their potential to advance local geotechnical practice and their quality of writing for the readership of practicing geotechnical engineers, which are summarized as follows.

The paper Tattersall et al (2012) provides a succinct and focussed account of a novel and substantial attempt to correlate ground conditions and water inflow, through analysing a large volume of ground information in the public domain and measurements taken in the first stage of a project, for better certainty of cost and programme estimates for the second stage of the project. The effort underscores the commitment of the local geotechnical profession to improve project management in the face of geological uncertainties. The paper offers the possibility of initiating a good practice among the local profession and inspiring other uses of big datasets in the service of the construction industry. It is well illustrated with clear figures and tables and is readable even to engineers not attuned to engineering geology or familiar with tunnelling.

The paper Cheung & Lo (2011) gives a brief overview, illustrated with cases, of the technique of Time Domain Reflectometry for quality control on soil nails, and a more detailed account of the attention to its reliability for practical use. It provides leads to relevant publications and background information for users of the technique. When viewed with these publications, the paper demonstrates the commitment and mental flexibility of the geotechnical profession in the process of enhancing quality control of the most commonly used technique in improving slope safety. By itself, the paper offers an example of the detailed considerations and care required to turn a concept into a practical tool for industry-wide application. The field measurement trials, in particular, highlight the importance of physical data and statistical concepts in handling human and material uncertainties. The paper is simple in structure, clearly illustrated with figures and tables, and supported by demonstrative cases to capture the attention of a wide range of practicing geotechnical engineers. Work reported by a paper may be less than perfect. An example in this paper is the low number of operators in the multi-operator trial. The authors appear to be aware of the shortcoming as the number was significantly increased in a later trial reported in one of the references cited. It is good that the paper includes this part for completeness.

The launching of the HKIE Geotechnical Paper Award scheme and the successful completion of the current exercise is the result of joint effort. Peers involved in the predecessor scheme of the early 2000's shared generously their experience and insights, from which the present scheme developed. Eminent members of the profession kindly committed themselves to membership of the Assessment Board Panel and contributed their time and wisdom on details of the scheme. Authors of papers and members of the HKIE Geotechnical Discipline supported by entering their papers warmly. Members of GDC and senior members of key geotechnical entities in Hong Kong mobilised geotechnical engineers to take part in a reading exercise to look for hints on readability of papers to practising geotechnical engineers. Finally, members of the Panel made available their time amply amidst their heavy work schedule, for fair and insightful assessment of the contending papers.

Each winner will be presented a trophy, the working design of which is shown below, to be kept until the time of the next award exercise. Each author of a winning paper will receive for their personal retention a plaque based on the trophy and also a certificate. The title of the winning paper and the name of its authors will be inscribed at the back of the trophy. When the space is full a decade or so later, the trophy will be passed to the organization that has originated the most number of winners inscribed there, for permanent retention. This is a tentative thought the details of which will have to be worked out in due course.

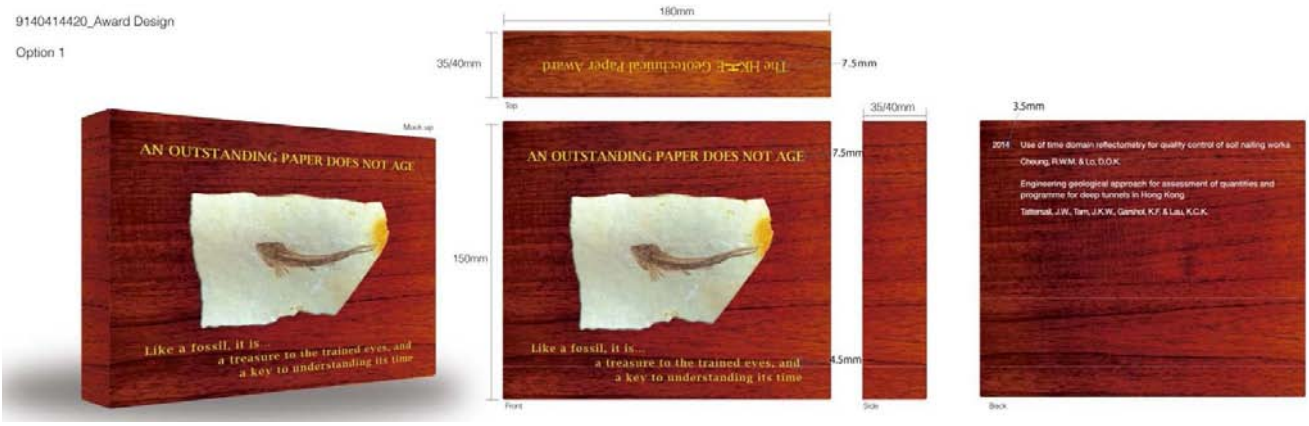

Meanwhile, readers interested in knowing more about the scheme and tracking its development may refer to the HKIE Geotechnical Paper Award webpage http://hkieged.org/geodiv/geopaperaward.aspx.

Ir Y C Chan
Secretary, Assessment Board
The 2014 HKIE Geotechnical Paper Award
May 2014

ACKNOWLEDGEMENTS

The Organising Committee would like to express sincere thanks to the following sponsors for their generous support of the Seminar:-

AECOM Asia Co Ltd.
New Concepts Foundation Limited
Arup
China Geo-Engineering Corporation
Fugro Geotechnical Services Ltd.
Earth Products China Ltd.
Aquaterra Consultants Ltd.
C M Wong & Associates Ltd.
Hyder Consulting Ltd
Mott MacDonald Hong Kong Ltd.
Tai Kam Construction Engineering Co Ltd.
W T Chan & Associates Ltd.
Golder Associates (HK) Ltd.
Jacobs China Limited
Konwall Construction & Engineering Co., Ltd.
Lambeth Associates Limited

TABLE OF CONTENTS

	Keynote Lectures	Page No.
1	Effects of Stress Relief due to Deep Excavation and Tunnelling on the Capacity and Deformation of Piles *Charles W W Ng, Hu Lu & Kelvin S Y Peng*	1 - 25
2	Overview of Development and Challenges in Foundation Design and Construction in Hong Kong *C M Wong*	27 - 52
	Papers	
3	Modelling of Combined Piled-Raft Foundations using 3-D FEM *William W L Cheang, Noppadol Pien-wej, Harry S A Tan & Kamol Almornfa*	53 - 63
4	The Capacity of Driven Steel H-Piles *Leonard John Endicott, Xu Zhang & Limin Zhang*	65 - 70
5	Feasibility of Bored Pile Foundation Modification in Hong Kong *Edmond K L Fung*	71 - 76
6	Recent Development of Shaft-grouted Piles in Hong Kong *A K M Lam, G K F Yam & A Y T Liu*	77 - 83
7	Pile Settlement Induced by Diaphragm Wall Installation *I S Haryono & M Korff*	85 - 93
8	Some Suggestions for Updating the Foundation Code *Victor Li*	95 - 107
9	Installation of Prestressed Spun High Strength Concrete Piles by Hydraulic Jacking *Albert T Yeung*	109 - 115
10	Is my Geotechnical Modelling Conservative or Aggressive? – A Challenge in the Design of a Deep Foundation Excavation *Gavin S H Toh*	117 - 125

11	The Adoption of Rock-head Level for Foundation Design and Construction in Hong Kong *N R Wightman & A D Mackay*	127 - 134
12	Impact of Changing Geological Conditions for Foundation Design and Construction in Tung Chung New Town Area *N R Wightman & J F Benson*	135 - 141
13	Foundation Design for a Residential Development in Adverse Ground Condition at Designated Area of Northshore Lantau *J W C Sze, J C Y Li & C K Lau*	143 - 149
14	Design Principles for Soil Friction Pile Derived from Fundamental Theories & Field Data *H Y Wong, C Y Kan, C T Wong & M K Leung*	151 - 159
15	Geotechnical Design at Tseung Kwan O Reclamation Development *S L Chiu, Vic Pun & P H Lam*	161 - 169
16	Foundation Design for the District Cooling System Building at Kai Tak *Leslie H Swann & Irene Chung*	171 - 177
17	Design and Analysis of a Piled-raft Foundation in Doha *L Tony Chen*	179 - 185
18	Padma Bridge, Bangladesh – Seismic Design Approach of the Pile Foundations *Suraj De Silva, Chao Li, Eric Yung & Guoxiong Yu*	187 - 196
19	Tianjin 117 Mega Tower Deep Foundation *G X W Ge, F H Y Chu, W W B Wei & S Y Gao*	197 - 204
20	3D Finite Element Analysis for Deep Foundation Case Histories *F Tschuchnigg & H F Schweiger*	205 - 211
21	A Case Study of Marine Structures Foundation Design *Henry Wang, Herman Wong & Eddie Wong*	213 - 222
22	Seismic Geotechnical Design of T-Shape Barrette Piles *Herman Wong, Henry Wang & Eddie Wong*	223 - 229

Effects of Stress Relief due to Deep Excavation and Tunnelling on the Capacity and Deformation of Piles

Charles W.W. Ng, Hu Lu & Kelvin S.Y. Peng
Department of Civil and Environmental Engineering,
Hong Kong University of Science and Technology

ABSTRACT

To increase the use of underground space for infrastructural needs while minimizing environmental impacts, an increasing number of tunnels and ever deeper basements are being constructed in densely populated cities like Hong Kong. Engineers and designers are also facing tougher and tougher geotechnical challenges. In this keynote lecture, the effects of stress relief due to deep excavation and twin tunnelling on the capacity and deformation of piles are discussed. In the first part of the lecture, centrifuge model tests carried out to investigate the capacity and deformation of a single floating pile with and without considering vertical stress relief due to a 20 m deep basement excavation are reported. For comparison purposes, in-flight pile load tests were conducted both at the ground surface and at the formation level after an in-flight simulation of the excavation. A non-dilatant pile-soil interface was adopted for simulating piles installed in normally consolidated clays and loose sands, whereas a dilatant pile-soil interface was used for modelling piles constructed in overconsolidated clays and dense sands. In addition, discrete element modelling (DEM) of these two pile-soil interfaces was carried out to reveal the governing mechanisms and the changes in pile shaft resistance. A simple calculation method allowing for the effects of vertical stress relief on pile capacity is then proposed. In the second part of the lecture, a series of three-dimensional centrifuge model tests and numerical back-analyses conducted to study the influence of twin tunnelling on an adjacent pile and a piled raft are described. Moreover, the effects of the construction sequence of twin tunnelling on an existing pile are explained. Design implications of these two types of stress relief (i.e., vertical and horizontal) on piled foundations are highlighted.

1 INTRODUCTION

To meet the increasing demands for underground space for infrastructural needs while minimizing environmental impacts, a growing number of tunnels and ever deeper basements are being constructed in densely populated cities like Hong Kong, Shanghai and London. When the top-down construction method is used, piles are subjected to increasing vertical stress relief from the excavation of basements above. These piles are generally designed according to pile load tests carried out at the ground surface ignoring any vertical stress relief, and so their capacity when subjected to vertical stress relief is questionable. It has been reported that concrete piles were damaged severely by excessive tensile force induced by soil heave after deep excavation (Zhu and Sun, 2005). Even though a sleeve may be used in a conventional load test to eliminate the shaft resistance along the entire depth of a planned excavation, the effects of vertical stress relief due to basement excavation on pile performance have not been considered explicitly. It is not common to carry out a load test at the bottom of a deep excavation, although some design codes (e.g., Eurocode7, 1997) recommend conducting a pile load test where the ground conditions are the most adverse. The influence of vertical stress relief on the capacity and stiffness of piles underneath a basement is not fully understood, particularly with different pile-soil interfaces.

Similar to piles subjected to stress relief due to excavations, the capacity of existing piled foundations can also be adversely affected by stress relief due to tunnel construction in congested cities. Loganathan *et al*. (2000) carried out centrifuge model tests to investigate the effects of stress relief due to tunnelling on ground deformations and their adverse effects on pile foundations in clay. They investigated the tunnelling-induced bending moment and axial force in the piles of a pile group by modelling the volume loss of a tunnel in a

single stage. They concluded that the tunnelling-induced bending moment may be critical when the centreline of the tunnel is located near the pile toe. Jacobsz*et al*. (2004) investigated the adverse effects of tunnelling beneath a pile in dry sand. An influence zone was identified above and around the tunnel in which the pile could undergo significant settlement. Marshall and Mair (2011) carried out centrifuge model tests to investigate the effects of tunnelling beneath driven or jacked end bearing piles in sand. They found that the volume–loss-induced pile failure, as reflected in a significant increase in the rate of pile settlement, is closely related to the distance between the tunnel and the pile toe. Very few researchers, however, have reported the effects of twin tunnelling on piles. Pang (2007) reported field monitoring results and a numerical study of the effects of twin tunnelling on an adjacent pile foundation in Singapore, where a northbound tunnel and a southbound tunnel were constructed near piles one after the other. The smallest clear distance between the tunnels and piles was just 1.6 m. Results of the field study showed that the piles were subjected to a large dragload due to the settlement induced in the residual soil. Ng *et al*. (2014) investigated the response of a 2x2 pile group under a working load subjected to the advancement of twin tunnels in dry sand. Side-by-side twin tunnels (excavated one after the other on either side of the pile group) were simulated in-flight in centrifuge. Among the three tunnelling tests conducted, twin tunnelling below the pile toe caused the largest settlement of the pile group (2.4% of pile diameter), resulting in an apparent loss of capacity of 40%. Meanwhile, the largest induced transverse tilting of the pile cap reached the limit of 0.2% suggested by Eurocode 7. Despite all these studies, the effects of twin tunnelling on pile capacity and deformation remain ill understood in different ground conditions. Moreover, the influence of the sequence of twin tunnel construction on the response of piles and piled rafts has not been thoroughly investigated.

This keynote lecture consists of two major parts. In the first part of the lecture, centrifuge model tests carried out to investigate the capacity and deformation of a single floating pile with and without considering vertical stress relief due to a 20 m deep basement excavation are reported. For comparison purposes, in-flight pile load tests were conducted both at the ground surface and at the formation level after an in-flight simulation of the excavation. Two different pile-soil interfaces were considered in the tests. A non-dilatant pile-soil interface (i.e., low friction) was adopted for simulating piles installed in normally consolidated clays and loose sands, whereas a dilatant pile-soil interface (i.e., high friction) was used for modelling piles constructed in overconsolidated clays and dense sands. In addition, discrete element modelling (DEM) of these two types of pile-soil interfaces was carried out to reveal the governing mechanisms and changes in pile shaft resistance. A simple calculation method allowing for the effects of vertical stress relief on pile capacity is then proposed. In the second part of the lecture, a series of three-dimensional centrifuge model tests and numerical back-analyses conducted to study the influence of twin tunnelling on an adjacent pile and a piled raft are described. Moreover, the effects of the construction sequence of twin tunnelling on an existing pile are explained. Design implications of these two types of stress relief (i.e., vertical and horizontal) on piled foundations are highlighted. Essentially, this keynote paper provides a summary of two PhD theses (i.e., Lu, 2013 and Peng, 2012) and highlights key findings from four published studies (i.e., Zheng *et al*., 2012, Peng *et al*., 2012; Ng *et al*., 2013 and Ng & Lu, 2014).

2 CENTRIFUGE MODELLING

The centrifuge model tests reported in this keynote were carried out at the Geotechnical Centrifuge Facility (GCF) of the Hong Kong University of Science and Technology (HKUST) (Ng *et al*., 2001b; Ng *et al*., 2002; Ng, 2014). For simplicity, dry Toyoura sand was used in all the tests reported. Toyoura sand is a uniformly fine sand consisting of sub-rounded and sub-angular particles having a mean grain size (D_{50}) of 0.17 mm, a maximum void ratio of 0.977, a minimum void ratio of 0.597, a specific gravity of 2.65 and an angle of friction at critical state ϕ'_{cv} of 31^o (Ishihara 1993). The pluvial deposition method was used to prepare all the centrifuge models. To obtain a relatively uniform soil bed, a hopper deposited sand onto the surface from a distance of 500 mm above. Scaling factors relevant to this study are summarised in Table 1.

In this keynote, model preparation and test procedures for studying the effects of vertical stress relief due to excavation on piles are described first and then the investigations of the effects of stress relief due to twin tunnelling on piles and piled rafts are reported.

2.1 Experimental program and setup for simulating piles subjected to vertical stress relief due to basement excavation

Figure 1(a) shows a schematic diagram of model container LN, where L indicates "low friction interface" piles and N denotes "no excavation effects simulated". Load tests on three low friction piles were carried out at the ground surface, as in conventional load tests. More details of modelling the pile-soil interface will be given later. During centrifuge tests, model piles were arranged at different distances from a circular diaphragm wall that is 320 mm in diameter (or 32 m in prototype when tested at 100g). The pile located in the middle of the excavation area is referred to as pile LNM, where M denotes middle. Pile LNW (low friction interface; no excavation effects simulated; close to the diaphragm wall) was located closer to the diaphragm wall, at a distance of 30 mm, which was about 1.8 times the pile diameter (dp), where dp is 16mm (or 1.6m in prototype). To minimise interaction between piles, the distance between piles LNM and LNW was more than 8dp. The third pile, LNF, was located outside the circular excavation to serve as a reference. The three model piles were 500 mm long. A 200 mm long sleeve was used to eliminate shaft resistance along the upper portion of each pile. Thus, the effective pile length was 300 mm (or 30m in prototype). More details of the tests are available from Peng (2012) and Zheng *et al*. (2012).

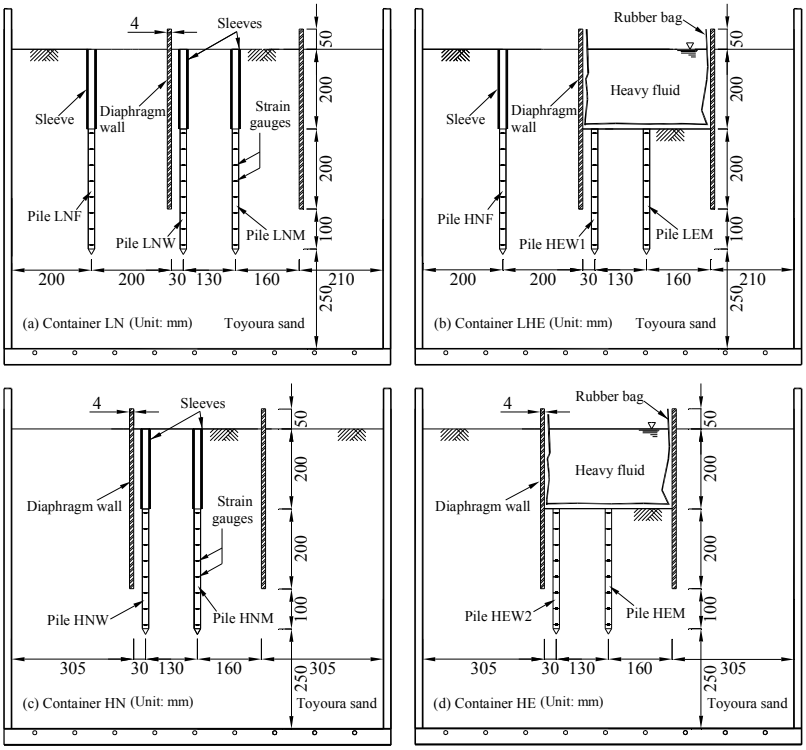

Figure 1: Schematic diagrams of centrifuge models for single pile tests with and without simulating vertical stress relief: (a) container LN; (b) container LHE; (c) container HN and (d) container HE. Dimensions in model scale.

Figure 1(b) shows model container LHE, in which both low and high friction interface piles and excavation effects were simulated. A basement excavation was simulated in-flight at 100g by draining away the heavy fluid (zinc chloride solution). The density of the heavy fluid was 1.53 kg/m3, which was the same as the target density of Toyoura sand. The excavation depth was 200 mm (20 m in prototype). Two piles, LEM and HEW1, were located underneath the excavation and at different distances from the diaphragm wall. In-flight load tests on these two piles were carried out after the excavation. A third pile, HNF, was located outside the excavation to serve as a reference. Piles HEW1 and HNF had high friction (dilative) interface sand were used to study the influence of dilative interface on pile behaviour. The locations of the three piles were the same as those in container LN. Figure 1(c) shows container HN in which high friction piles were simulated but not excavation effects, whereas Figure 1(d) shows container HE in which both high friction piles and excavation effects were

simulated. Two high friction piles, HEM and HEW2, were located below the excavation formation level. In-flight load tests on these two piles were carried out after the excavation.

The circular model diaphragm wall was made from mild steel. It had an internal diameter of 320 mm and a thickness of 4 mm. A load test was carried out on each pile using a hydraulic jack with a load cell installed in the piston. Pile settlement was measured with a linear variable differential transformer (LVDT). More details of this series of centrifuge tests are summarised in Table 2 (Peng, 2012; Zheng *et al*., 2012).

Table 1: Relevant scaling factors in centrifuge modelling

Quantity	Scale factor (model/prototype)
Acceleration	N
Length	$1/N$
Displacement	$1/N$
Stress	1
Strain	1
Density	1
Area	$1/N^2$
Force	$1/N^2$
Axial rigidity (EA)	$1/N^2$
Bending moment	$1/N^3$
Flexural stiffness(EI)	$1/N^4$

Table 2: Centrifuge test program for simulating piles subjected to vertical stress relief due to basement excavation

Container ID.*	Density (kg/m^3)	Relative density	Instrumented pile ID.*	Pile interface	Excavation effects
(1) LN	1527	66%	LNM	Low	No
			LNW	Low	No
			LNF	Low	No
(2) LHE	1510	62%	LEM	Low	Yes
			HEW1	High	Yes
			HNF	High	No
(3) HN	1529	67%	HNM	High	No
			HNW	High	No
(4) HE	1529	64%	HEM	High	Yes
			HEW2	High	Yes

*Note: L – **l**ow friction interface; H – **h**igh friction interface; N – **n**o excavation effects; E – subjected to **e**xcavation; M – in the **m**iddle of the excavation; W – close to diaphragm **w**all; F – at **f**ar field

2.1.1 Modelling of different pile-soil interfaces

Various researchers have shown that the characteristic of the pile-soil interface has profound effects on the capacity of a pile (e.g., Paikowsky *et al*., 1995; Garnier and Konig, 1998). In this study, the governing mechanisms of piles in non-dilatant and dilatant soils were modelled for two distinct pile-soil interfaces (see Figure 2).The first type of interface was made of aluminium. Piles with this type of interface are referred to as low friction piles, as they are intended to simulate piles in non-dilatant soils, such as normally consolidated clays. The measured normalised roughness (R_n, Kishida and Uesugi (1987)) of the interface was 0.013, which was lower than the threshold for a substantially smooth interface of $R_n < 0.020$ (Fioravante, 2002). Shearing failure was expected to occur along the pile-soil interface. The limit shaft resistance (τ_p) of piles with this type of interface is given by

$$\tau_p = \sigma'_n \tan \delta \quad (1)$$

where σ'_n is the initial normal effective stress on the pile shaft and δ is the friction angle of the pile-sand interface.

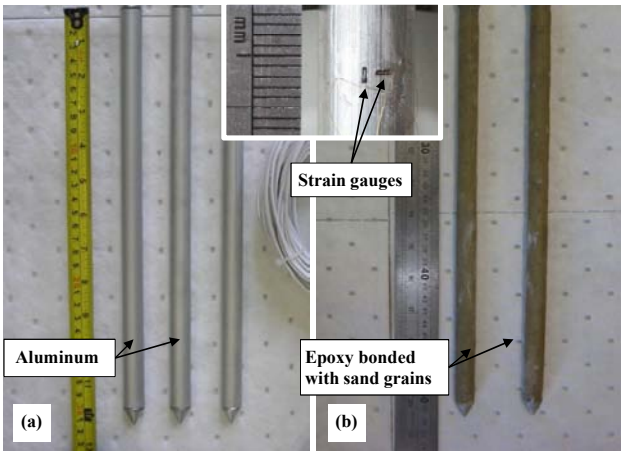

Figure 2: Model piles with (a) non-dilative and (b) dilative interfaces and instrumentation

The other type of interface was made completely rough by bonding sand grains to the piles. These piles are referred to as high friction piles and are used to simulate piles in dilatant soils, such as heavily overconsolidated clays and dense sands. The normalised roughness R_n of the interface was 0.21, which satisfied the criterion of $R_n > 0.10$ for a substantially rough interface (Fioravante, 2002). When a pile with this type of interface is sheared, the sand in the shear band dilates resulting in changes in normal stress, which in turn affect the mobilised shear stress at the interface. The limit shaft resistance (τ_p) of a pile with this type of interface is given by the following equation:

$$\tau_p = (\sigma'_{n0} + \Delta\sigma'_n) \tan \delta \quad (2)$$

where $\Delta\sigma'_n$ is the change in normal stress due to dilation of soil at the interface.

This is the fundamental governing equation for the shaft resistance of a pile with a dilatant interface. Governing mechanisms for the two distinct interfaces are briefly discussed later in this paper. More details are provided by Peng (2012) and Peng *et al.* (2012).

As shown in Figure 2, aluminium tubes with Young's modulus of 70 GPa were used as model piles. The tubes had an internal diameter of 4 mm and an external diameter of 10 mm. Eight levels of semiconductor strain gauges (SGs) were installed at a spacing of 40 mm between two consecutive levels to measure the axial load transfer along the pile shaft. A full Wheatstone bridge circuit was arranged for each level to minimise temperature effects. SGs were coated with a layer of epoxy resin for protection. Figure 2(a) shows the model piles with a low friction interface. The thickness of the epoxy resin layer was 2.5 mm. To minimise interface friction, another smooth aluminium tube that was 15.5 mm in internal diameter and 0.5 mm thick was prepared to enclose the epoxy resin layer. For modelling the dilative interface, on the other hand, Toyoura sand grains were bonded to the surface of the model pile (see Fig. 2(b)). The final external diameter of each pile was 16 mm. The techniques of modelling both low and high friction interfaces were verified in shearbox tests. Details of the tests are reported by Peng (2012) and Zheng *et al.* (2012).

2.1.2 Simulation procedures for modelling piles subjected to vertical stress relief due to basement excavation

Figure 3 shows a photograph of a typical model setup (container HE). A rubber bag containing heavy fluid was made from a sheet of latex membrane to simulate the soil mass retained by the model diaphragm wall.

The measured soil densities in all models ranged from 1.51 to 1.53 kg/m^3, with a difference within ±1.0%. The average relative density of sand in each container was calculated to be about 65%.

The model tests to study excavation effects on piles were carried out at 100g. For tests in which excavation effects were not simulated (i.e. those involving containers LN and HN), an in-flight load test was first carried out on the centre pile. An incremental load testing procedure was applied to the pile at 100g using a hydraulic jack, which was equipped with an in-flight load-control system. A load increment was maintained until no further pile settlement could be recorded. Once a pile settlement larger than 10% d_p was obtained, the pile was unloaded in steps until the load was reduced to zero. For tests in which excavation effects were simulated (i.e. those involving containers LHE and HE), the only difference in the testing procedure was that in-flight excavation was simulated first by draining away the heavy fluid at 100g, before a pile load test was carried out at the bottom of the excavation. More details of centrifuge modelling are available from Zheng *et al.* (2012).

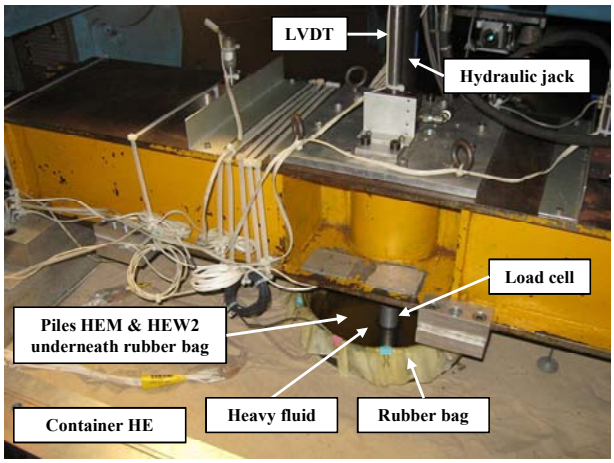

Figure 3: Model setup and instrumentation at and above the ground surface

2.2 Centrifuge test program for simulating piles and a piled raft subjected to stress relief due to twin tunnelling

For investigating the effects of stress relief due to twin tunnelling on piles, nine centrifuge model tests were carried out at an acceleration of 40g at GCF of HKUST. The effects of twin tunnelling with different construction sequences on existing single piles and a piled raft were also studied. A summary of the test program is given in Table 3.

Figure 4(a) shows a schematic elevation view of three separate tests (i.e., Tests SS, TT and BB). A single pile was located at the centre of each model container. The model pile had a diameter of 20 mm (0.8 m in prototype) and was 600 mm long (24.0 m in prototype). The pile cap was elevated by 110 mm and so the embedded depth of each pile was 490 mm (19.6 m in prototype). The tunnel diameter (D) was 152 mm (6.08 m in prototype).The horizontal distance from the centreline of the tunnel to the pile was 0.75D. To determine the load settlement curve of the type of single pile without the presence of any tunnel, a separate test (Test PL) was carried out (refer to Table 3). This test had the same configuration as other tests except no model tunnel was present.

Table 3: Test program of centrifuge tests for simulating piles and a piled raft subjected to stress relief due to twin tunnelling

Test ID	*C/D*	Relative density of sand	Void ratio of sand	Surface settlement due to rising g-level (mm)	Remark
PL	N/A	60%	0.75	2.3	Pile load test
T	2.7	60%	0.75	2.4	Effects of C/D ratios of twin tunnelling on a single pile
TT	1.5	65%	0.73	2.1	

SS	2.7	62%	0.74	2.2	
BB	3.7	65%	0.73	2.2	
ST	1.5, 2.7	65%	0.73	2.1	Effects of the construction sequence of twin tunnelling on a single pile
TS	2.7, 1.5	65%	0.73	2.1	
GR-SS	1.5	66%	0.73	2.1	Effects of twin tunnelling on a piled raft
GR-TT	2.7	65%	0.73	2.1	

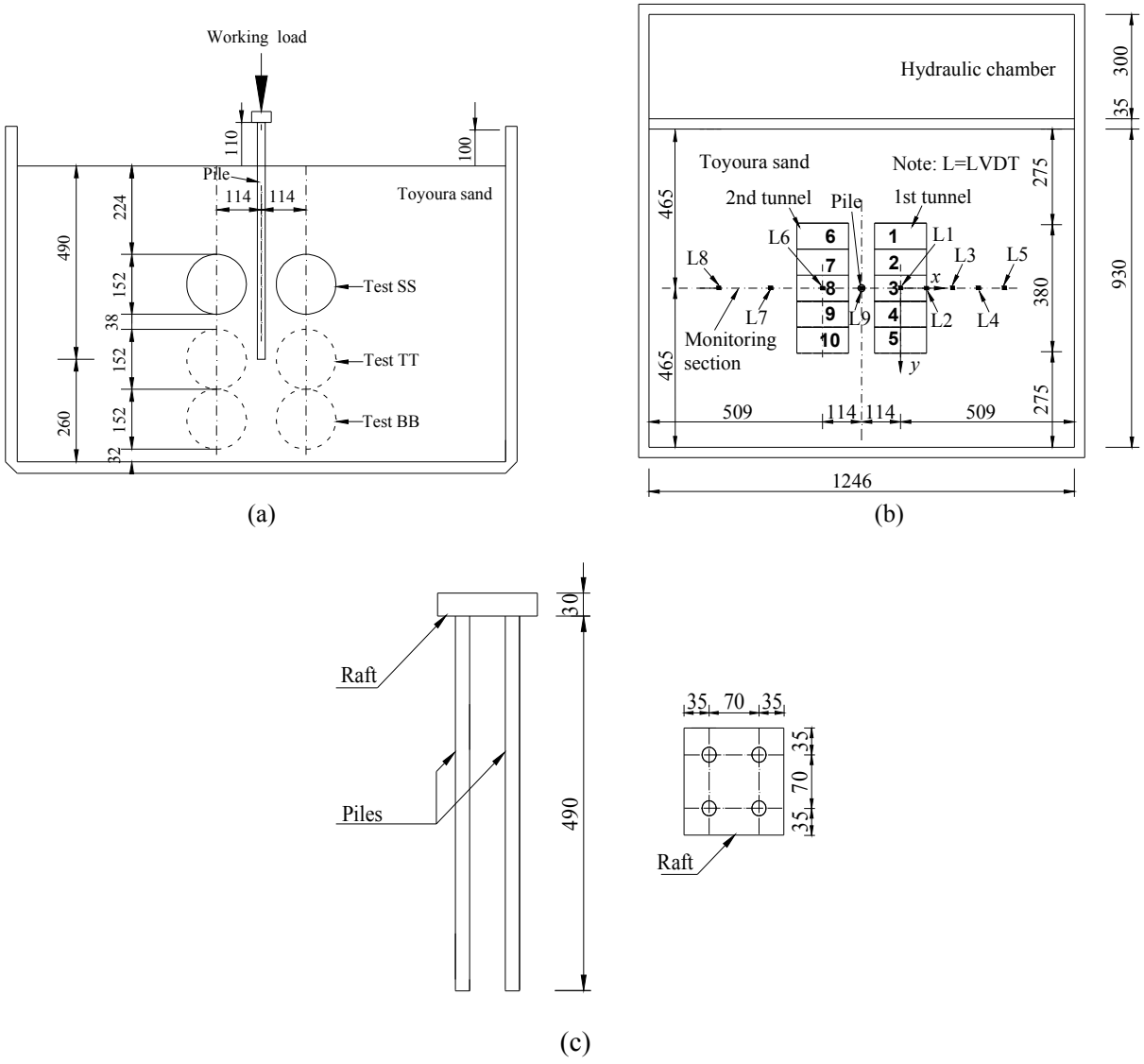

Figure 4: Configurations of the model piled foundation and twin tunnels: (a) Elevation view of a single pile and tunnels; (b) Plan view of a single pile and tunnels; (c) Dimensions of a 2x2 model piled raft. All dimensions are in mm in model scale.

As shown in Figure 4(a), the twin tunnels were located at different *C*/*D* ratios in the three tests (i.e., Tests SS, TT and BB). Test SS was designed to investigate pile responses induced by the construction of twin tunnels, one after the other, near the mid-depth of pile shaft. In Test TT, the effects of twin tunnelling near the pile toe on the pile were investigated. Test BB was designed to study the effects of twin tunnelling below the pile toe on the pile.

To investigate the effects of tunnelling sequence, two separate tests were carried out (i.e., Tests TS and ST in Table 3). In Test TS, a tunnel was first constructed near the pile toe before a second tunnel was excavated near the mid-depth of the pile shaft. In Test ST, a tunnel was excavated near the mid-depth of the pile shaft before a second tunnel was constructed near the pile toe. Figure 4(b) shows a plan view of a typical model. The longitudinal length of each tunnel was 380 mm, which was equivalent to 2.5*D*.The three-dimensional tunnel construction was simulated in five stages, with the tunnel face advancing by a distance of 0.5*D* in each stage.

To study the effects of twin tunnelling at different depths on a piled raft, two model tests were carried out. Figure 4(c) shows the dimensions of the model piled raft. Each pile had an embedded depth of 490 mm, corresponding to 19.6m in prototype. The twin tunnels were built near the pile toe in Test GR-TT and near the mid-depth of the pile shaft in Test GR-SS.

2.2.1 Model piles and a piled raft subjected to stress relief due to twin tunnelling

Aluminium alloy tubes were used as instrumental model piles based on relevant scaling laws shown in Table 1. Nine levels of full Wheatstone bridge of strain gauges were installed to record the bending moment and axial force along the entire pile length. The strain gauges were protected by a thin layer of epoxy. For structural elements, the bending stiffness (EI) of a pile was scaled. The scaling requirement for a model pile $(EI)_m$ is equal to $N^4(EI)_p$ (refer to Table 1), where N is the number of times gravity is enhanced in a centrifuge test, E is Young's modulus, I is the second moment of area for a cross-section, and subscripts m and p refer to the model and prototype scale, respectively. Each model pile had an axial rigidity (E_mA_m) of 7,473 kN and a bending rigidity (E_mI_m) of 273 Nm^2, corresponding to prototype E_pA_p of 11,957 MN and E_pI_p of 701 MNm^2 of a real concrete pile, respectively.

To support the raft, a two by two pile group was constructed. The raft was made from aluminum alloy with Young's modulus (E_r) of 70 GPa and had a thickness (t_r) of 30 mm. To support the raft effectively, the pile spacing was 70 mm (= 3.5*D*) and the width (B) of the square cap was 140 mm (= 7*D*). To quantify the relative rigidity of the cap, a cap-soil stiffness ratio defined by Horikoshi and Randolph (1997) was adopted and calculated to be about 34, which was greater than 1.5 for a rigid cap (Randolph, 2003). See Lu (2013) for more details of the calculations.

2.2.2 Procedures for simulating twin tunnelling in centrifuge

In engineering design, the amount of volume loss resulting from various tunnelling activities is often used to assess ground settlements and induced deformations of adjacent buildings (Mair, 2008). Obviously, this means that the effects due to construction activities such as erection and deformation of tunnel liners, stiffness of liners and workmanship are not considered separately. Similarly, tunnel advancement is simulated by controlling volume loss (Taylor, 1995), as opposed to simulating a series of construction steps in centrifuge. Although this type of modelling is not ideal, it does capture the essential effects (i.e., volume loss) of tunnelling and at the same time meets the objective of comparing different simulated cases in this paper.

As shown in Figure 4(b), each model tunnel consisted of five cylindrical rubber bags. Each rubber bag was filled with de-aired water. Between two rubber bags was a rigid aluminium divider to control and separate the volume of water inside. Volume change in each rubber bag (i.e., the tunnel volume loss) can then be controlled independently. Three-dimensional tunnel construction was simulated in-flight by draining away the water in the rubber bags one at a time. The amount of water drained from a bag was controlled to simulate an equivalent volume loss of 1.0% of the excavated cross-sectional area of the tunnel face during each stage of tunnel construction. Since the effects of tunnel excavation were modelled by inducing a volume loss equivalent to that from various construction activities and tunnel conditions, a tunnel liner was not separately simulated in the centrifuge tests (Lu, 2013).

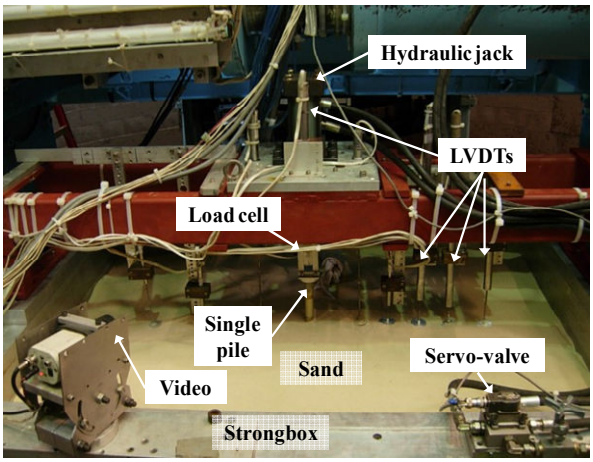

Figure 5: Model setup

2.2.3 Procedures of centrifuge tests investigating twin tunnelling effects on existing piles and a piled raft in-flight

Prior to each centrifuge test, the model pile was "wished-in-place" in the sand bed. Effectively, this simulated an equivalent bored pile in the field. Figure 5 shows a typical centrifuge model setup. To determine the capacity of the model pile, a separate centrifuge test was carried out at 40g (i.e., Test PL in Table 3). The pile was loaded in-flight (i.e., while the centrifuge was spinning) using a hydraulic jack in a number of steps to determine the pile load-settlement characteristic (Lu, 2013). A load cell was installed at the piston of the jack to control the applied load. Settlement of the pile was measured with a linear variable differential transformer (LVDT) located at the pile head.

To simulate tunnelling effects on the piled foundation (see model tests summarised in Table 3), each model pile was loaded in-flight at 40g in a number of steps until the working load—determined from Test PL—was reached. In each step, an incremental vertical load of 100 N (160 kN in prototype) was applied. Each load increment was maintained for three minutes. Once the load had reached the working load (1,200 N), tunnel construction with the designed volume loss of 1.0% commenced. As shown in Figure 4(b), various construction stages were simulated in-flight by draining away the water in the rubber bags one at a time, until all ten tunnel construction stages were completed. Throughout each test, ground surface settlement, settlement of the pile, induced bending moment and axial force along the pile were recorded.

3 NUMERICAL MODELLING

3.1 Discrete element modelling (DEM) of soil-pile interface behaviour due to stress relief

Depending on the stress state, soil at the pile-soil interface may dilate or contract when subjected to shearing. It is thus difficult to predict $\Delta\sigma'_n$ in Equation (2) accurately during shearing after stress relief due to excavation. DEM was therefore carried out to study the pile-soil interaction after stress relief. The fundamental mechanism of the pile-soil interaction at the interface is the key to quantifying the shaft resistance of a pile. This is because dilation at the interface soil (if any) results in a change in normal stress, which in turn influences the mobilised shear stress at the interface, as Equation (2) shows. The interaction between pile and soil may be simulated in a shear box under constant normal stiffness (CNS) conditions (Boulon and Foray, 1986).

Fig. 6 shows a typical DEM of a direct shear box. The objectives of this DEM were to investigate the shearing mechanisms at the pile-soil interface and to quantify any increase in normal stress, i.e., $\Delta\sigma'_n$ in Equation (2), which contributes to pile shaft resistance when a pile is subjected to stress relief due to deep excavation. All numerical simulations of direct shear box tests were performed using Particle Flow Code (PFC) in Two Dimensions (PFC^{2D}) (Itasca, 2002). Shear box tests under CNS conditions were simulated to study responses at the interface with and without considering stress relief due to excavation. For comparison

purpose, the extreme boundary conditions of a constant normal load (CNL) and a constant volume (CV) were also modelled. More details of the numerical setup, input parameters, boundary conditions and modelling procedures are described by Peng (2012) and Peng *et al.*, (2013).

In order to make use of computed results from two-dimensional shear box simulations to estimate the shaft friction of a pile (an axisymmetric problem), cylindrical cavity expansion theory was adopted (Houlsby, 1991). The cavity stiffness k_n constraining a pile-soil interface is given by the following equation:

$$k_n = 4G/d_p \tag{3}$$

where G is the average shear modulus of soil near the interface and d_p is the pile diameter. For a given pile, k_n may be estimated and considered as an equivalent normal stiffness applied to a two-dimensional DEM shear box.

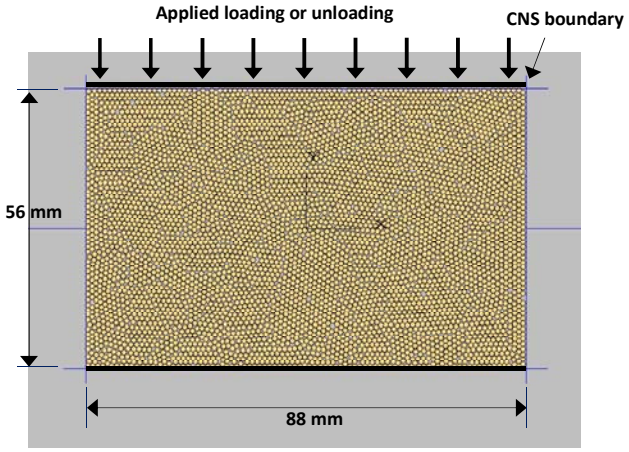

Figure 6: A typical DEM shear box model

3.2 Three-dimensional finite element (FE) mesh and procedures for simulating tunnelling effects on piles

In order to provide more insight into the load transfer mechanism of the twin tunnel-pile interaction, three-dimensional numerical back-analyses of centrifuge tests were carried out. The FE software PLAXIS-3D (Brinkgreve, *et al*. 2012). Figure 7 shows a typical three-dimensional FE mesh for the numerical analyses. The mesh had the same geometry as that used in the centrifuge tests. Roller supports were assigned on all vertical sides of the mesh and pinned supports were specified at the base of the mesh. In this study, a hardening soil model with small-strain stiffness was adopted to capture key behaviour of Toyoura sand. The relative density of the sand was taken to be 65%, corresponding to a unit weight of 15.3 kN/m^3. According to Ishihara (1993), the friction angle (ϕ') at critical state for Toyoura sand is 31^o. The empirical equation proposed by Bolton (1986) was used to approximate the angle of dilation (ψ), which was found to be 5^o. The model pile was modelled as a linear elastic material with Young's modulus of 70 GPa. Its density and Poisson's ratio were assumed to be 2700 kg/m^3 and 0.2, respectively.

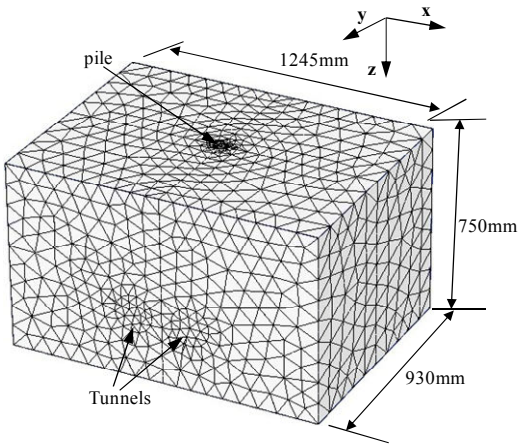

Figure 7: A typical three-dimensional finite element mesh

The numerical analysis followed the same procedures as those adopted in the centrifuge tests. The steps were:

1. Set up the initial boundary conditions and the initial stress conditions (i.e., static stress condition with K_0=0.5) at 1 g.
2. Increase the centripetal acceleration of the numerical model incrementally from 1g to 40g.
3. Apply the working load (1200 N) to the pile.
4. Excavate the first tunnel section by section three-dimensionally using the surface contraction method to simulate the effects of volume loss.
5. Excavate the second tunnel in the same manner.

4 INTERPRETATION OF EXPERIMENTAL AND NUMERICAL RESULTS FORPILES SUBJECTED TO VERTICAL STRESS RELIEF

In this paper, all interpreted results are expressed in prototype scale unless stated otherwise.

4.1 Capacity and stiffness of piles subjected to stress relief in non-dilatant soils

To investigate the effects of stress relief due to excavation on pile performance, the measured results of two low friction piles LNM and LEM are directly compared in Figure 8. For simplicity, the measured load-settlement relationships of the other two low friction piles tested (i.e., piles LNW and LNF) are not reported in this paper but are available from Peng (2012). Only the measured settlement due to the load applied at each pile head is shown in the figure (i.e., induced settlements and axial loads due to negative skin friction and body weight of each pile during the rise of g-level are excluded). The measured settlement of each pile was normalised by the pile diameter d_p. When the settlement was smaller than 1.5%d_p, the observed load-settlement relationship for each pile may be considered as linear. There was no noticeable difference between the two piles. When settlement was larger than 1.5%d_p, however, the piles exhibited different stiffness responses. Pile LNM, which was loaded at the ground surface and was not subjected to stress relief, showed a stiffer response than pile LEM tested at the bottom of the excavation zone after unloading.

To compare the capacities of the two piles, the failure criterion proposed by Ng *et al.* (2001a) was used. This semi-empirical method was derived from 38 full-scale pile load tests conducted in Hong Kong and may be used to determine a moderately conservative failure load. For piles constructed in soils, the criterion is given by:

$$\Delta_M = 0.045d_p + 0.5PL/AE \quad (4)$$

where Δ_M is the maximum pile head movement (in mm) which defines the ultimate load; P is the applied test load; L is the pile length; A is the pile shaft cross-sectional area; and E is the pile shaft modulus of elasticity.

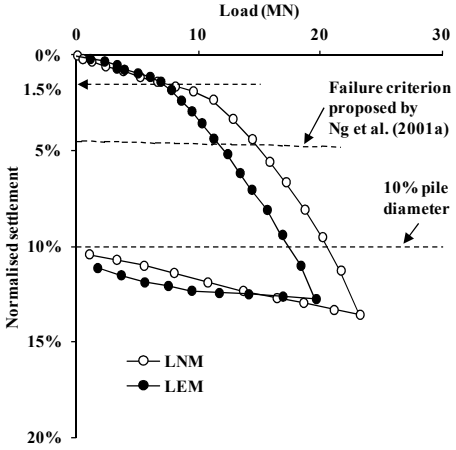

Figure 8: Measured load-settlement relationships of piles with a non-dilatant interface (i.e., low friction)

From Equation (4), it can be readily deduced that the capacity of pile LEM was only 80% of that of pile LNM. For comparison purpose, the failure criterion based on a settlement of 10% of d_p is also illustrated in the figure. The capacity of pile LEM was about 84% of that of pile LNM. It is clear from these results that the capacity of a low friction pile is reduced when subjected to stress relief. This implies that any design based on a pile load test at the ground surface without considering stress relief due to excavation would not be on the conservative side. On the other hand, the piles exhibited similar rebound stiffness with and without considering the effects of stress relief.

Figure 9 compares measured axial load distributions along piles LNM and LEM at various loading stages. The induced compressive axial loads (if any) resulting from negative skin friction and body weight due to the rise of g-level in the centrifuge are not shown in the figure. As expected, the shaft resistance of pile LNM was gradually mobilised along the entire length of the pile when the applied load at the pile head was increased. The toe resistance, however, was not mobilised until the applied load reached 11.1 MN. The slope of the measured axial load distribution along the entire shaft was almost constant as the applied load further increased from 11.1 to 14.3 MN, suggesting that shaft resistance was fully mobilised and the pile toe resisted the addition applied loads. In contrast, the measured axial load distribution along pile LEM behaved differently. At the end of excavation, tensile force was induced by vertical stress relief due to excavation and the maximum tensile force induced was about 4 MN at a depth of 45 m. This suggests that a sufficient amount of steel reinforcements must be installed to give the pile tensile resistance. As the applied load increased, both the shaft and toe resistances were mobilised gradually. The shaft resistance was fully mobilised under a load of 5.0 MN, which was much smaller than the 11.1 MN induced in pile LNM. This can be attributed to the reduction in vertical stress and hence confining stress surrounding pile LEM after excavation.

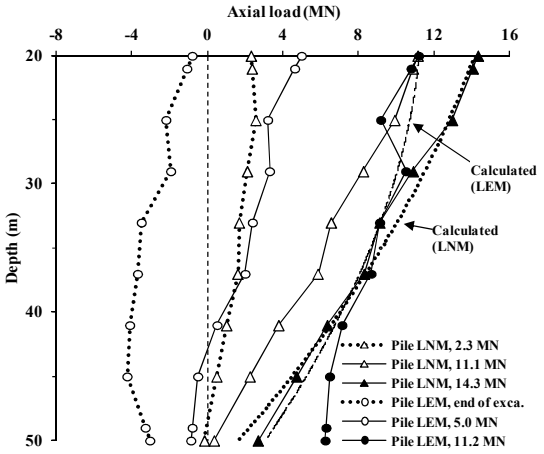

Figure 9: Measured axial load distributions in piles with a non-dilative interface at various loading stages

To investigate the load distributions relative to the shaft and the toe in each pile, a comparison can be made between pile LNM under 11.1 MN and pile LEM under 11.2 MN (i.e. when the two piles were subjected to similar applied loads). At these applied loads, the shaft resistances were fully mobilised in both piles. But pile LNM ultimately had a much higher shaft resistance than pile LEM, as revealed by the slopes of the two corresponding curves. Correspondingly, the toe resistance of LNM was only 0.3 MN, which was 3% of the total load applied at the pile head. In contrast, the toe resistance of LEM was 6.1 MN, which was 55% of the total load. For a given total load, the two piles contributed to different proportions of shaft and toe resistances.

To understand the reduction in capacity of pile LEM, some simple theoretical calculations for the low friction piles can be made. By assuming that $K_o = (1 - \sin \phi')$ and using the angle of friction at the pile-soil interface of $\delta = 18^o$ measured from shear box tests (Peng, 2012), the unit shaft resistance can be estimated from Equation (1). The axial load distribution along each pile can then be calculated by integrating the unit shaft resistance along depth, applying the same load at the pile head as that measured in centrifuge tests. Figure 9 compares the calculated and measured axial load distributions for LNM and LEM at their respective maximum applied loads. The measured and calculated results for pile LNM tested at the ground surface without stress relief are consistent. On the contrary, although the calculated shaft resistance along the upper portion (about 15m) of pile LEM agreed with the measured axial loads in general, that along the lower portion of the pile did not. A large toe resistance was mobilised in pile LEM to compensate for the reduction in shaft resistance due to stress relief resulting from the excavation. The pile settlement required to mobilise toe resistance is usually larger than that required to mobilise shaft resistance. This larger pile settlement may counteract pile heave induced by excavation.

4.2 Capacity and stiffness of piles subjected to stress relief in dilatant soils

Figure 10 shows the measured load-settlement relationships for two high friction piles (i.e., HNM and HEM). As the applied load was increased, the stiffness of each pile reduced gradually. In contrast to the result for the low friction pile LEM shown in Figure 8, pile HEM subjected to stress relief resulting from the excavation had a stiffer response than pile HNM tested at the ground surface. These observations are in contrast to the measured results for the low friction piles (refer to Figure 8). If the failure criterion defined by Equation (4) is adopted, the capacity of pile HEM would be 27 MN, which is 57% higher than that of Pile HNM (17 MN). Similar results can be obtained if ISSMGE's criterion of 10% of pile diameter is adopted. The higher pile capacity after excavation was the result of strong dilation taking place at the pile-soil interface during shearing. The fundamental shearing mechanism of a pile with a dilatant interface, when it is subjected to stress relief, is distinct from that of a low friction pile. This issue is further discussed later.

Comparing the two piles tested at the ground surface (i.e., LNM and HNM in Figures 8 and 10, respectively), the capacity of the low friction pile LNM is about 85% of that of the high friction pile HNM when the failure criterion defined by Equation (4) is used. Due to the increase in lateral stress, i.e., $\Delta\sigma'_n$ in Equation (2), resulting from dilation at the pile-soil interface after excavation, the high friction pile HEM is

about 2.3 times higher in capacity than the low friction pile LEM. More detailed explanations are given in sections 4.3 and 4.4.

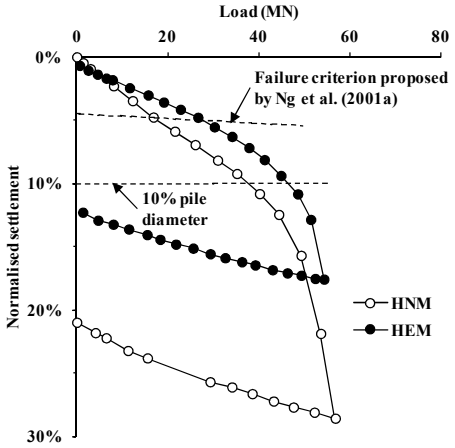

Figure 10: Measured load-settlement relationships of piles with a dilatant interface

Figure 11 compares axial load distributions along piles HNM and HEM at various loading stages at 100g. An applied load between0 and 3.0 MN was almost entirely carried by the shaft resistance of pile HNM. A load between 3.0 and 51.7 MN was supported partly by shaft resistance and partly by toe resistance. As expected, the pile experienced compression throughout the loading stages. On the contrary, a tensile force up to about 5 MN was induced along pile HEM by the upward movement of the soil due to stress relief after excavation (Peng, 2012). This implies that a sufficient amount of steel reinforcements should be deployed in the pile underneath the excavation. As the load was applied at the pile head gradually, a positive shaft resistance—as well as toe resistance—was mobilised along the entire pile length. At similar final applied loads on piles HNM and HEM (51.7 MN and 51.6 MN, respectively), the former pile tested at the ground surface mobilised a larger toe resistance, whereas the latter—having been subjected to vertical stress relief—developed a higher shaft resistance, to support their respective applied loads. Similar behaviour can be observed for the two piles (i.e., LNM and LEM) with a non-dilative interface as shown in Figure 9.

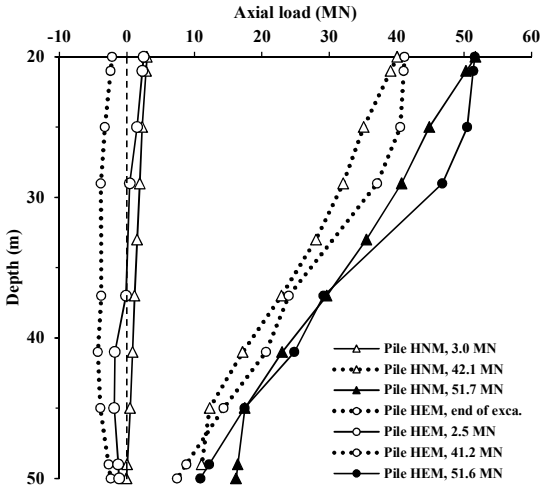

Figure 11: Measured axial load distributions in piles with a dilatant interface at various loading stages

4.3 Pile-soil interface behaviour revealed by DEM

To quantify and explain the increase in capacity of a pile tested at the bottom of an excavation after stress relief given a dilatant interface (i.e., for piles constructed in medium-to-dense sands and stiff clays), Peng *et al.* (2013) carried out a systematic numerical parametric simulation of direct shear box tests using DEM (refer to section 3.1 for more details). They demonstrated that the magnitude of $\Delta\sigma'_n$ (incremental normal effective stress) at the pile-soil interface depended on the state of the interface soil (e_0 and σ'_{n0}) and the cavity stiffness constraining the interface (i.e., Equations (2) and (3)). Figure 12(a) shows computed relationships between mobilised stress ratios (τ / σ'_n) and increasing shear strain from two dense specimens with different stress histories(i.e., with and without a history of stress unloading) prior to shearing in a "shear box".Shear strain is calculated as the applied shear displacement normalised by the height (H) of the shearbox. Both specimens were given the same initial density (refer to Peng, 2012 for details). For the specimen subjected to stress relief, an initial normal stress σ'_{n0} of400 kPa was applied which was later reduced to 100 kPa before shearing under a constant normal stiffness (k_n) of 2,000 kPa/mm. As shown in the figure, a strain-softening response can be observed. The peak stress ratio was about 1.0, which was mobilised at a shear strain of about 1.0%. For the specimen placed under a constant applied initial stress of 400 kPa, the peak stress ratio was about 0.70 and was mobilised at a shear strain of about 3.0%. This specimen showed a strain-hardening response. It is clear that the first specimenshowed a higher peak stress ratio at a lower shear strain. At the final stage, when the applied shear strain neared 10%, the stress ratios for both specimens approached 0.7.

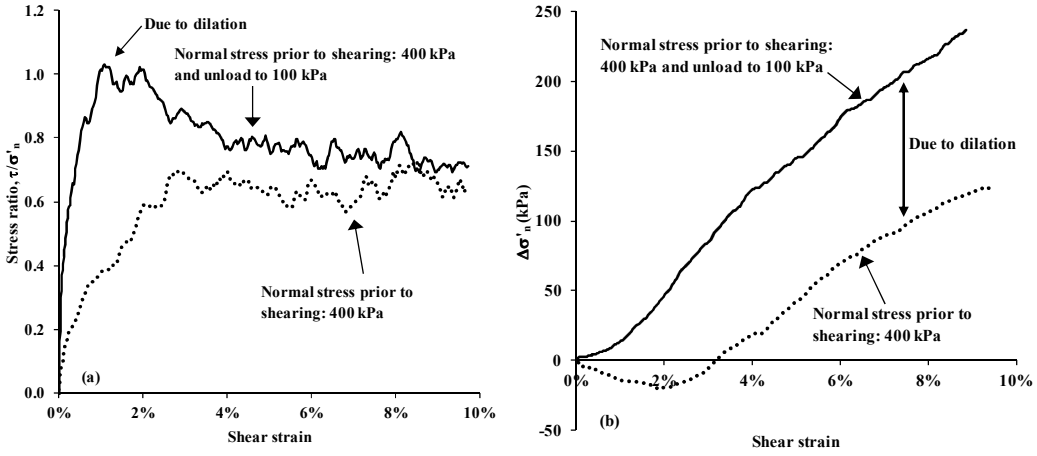

Figure 12: Computed results for two dense specimens under k_n of 2,000 kPa/mm: (a) mobilised stress ratio and (b) normal stress increment ($\Delta\sigma'_n$) with increasing shear strain

To illustrate the influence of stress relief on induced normal stress ($\Delta\sigma'_n$) during shearing under a normal stiffness of 2,000 kPa/mm, Figure 12(b) shows computed $\Delta\sigma'_n$for the two specimens. The magnitude of $\Delta\sigma'_n$ was affected by the stress leveland the unloading history prior to shearing. The specimen subjected to a constant stress σ'_{n0} of 400 kPa showed a slight reduction in normal stress when shear strain was below 1.0%. As the applied shear strain increased, the normal stress rose above 100 kPa due to the dilative response of the sample. The magnitude of $\Delta\sigma'_n$ reached about 125kPa at a strain level close to 10%. On the other hand, the specimen subjected to an initial stress σ'_{n0} of 400 kPa which was later reduced to 100 kPa showed an increase in normal stress from the very beginning of shearing. At any given strain, the induced magnitude of $\Delta\sigma'_n$ was always higher than that for the specimen subjected to a constant stress of 400 kPa. The final $\Delta\sigma'_n$ reached about 230 kPa, which was 84% higher than that for the specimen subjected to a constant stress. Clearly a much higher normal stress was induced for the specimen subjected to an initial normal stress unloading of 300 kPa prior to shearing. This higher induced normal stress explains the measured centrifuge test results reported in Figures 10 and 11 in which the pile tested at the bottom of the excavation area after stress relief exhibiteda stiffer response and a higher average mobilised shear resistance than the pile tested at the ground surface. More detailed comparisons are discussed and explained later.

To quantify the magnitude of $\Delta\sigma'_n$ at various soil states (i.e., initial void ratio and stress level), systematic DEM simulations of shear box tests under CV and CNS conditions were carried out (Peng, 2012; Peng *et al.*, 2013). Figure 13(a) shows computed results for specimens with different initial densities under various normal stresses. A fairly consistent relationship between normalised $\Delta\sigma'_{n,max}$ and k_n was obtained. The magnitude of $\Delta\sigma'_{n,max}$ increased by about 100% as k_n increased from 1,000 to 10,000 kPa/mm, at which dilation at the interface suffered more constrained. The maximum $\Delta\sigma'_n$ was obtained when k_n was about 10,000 kPa/mm.

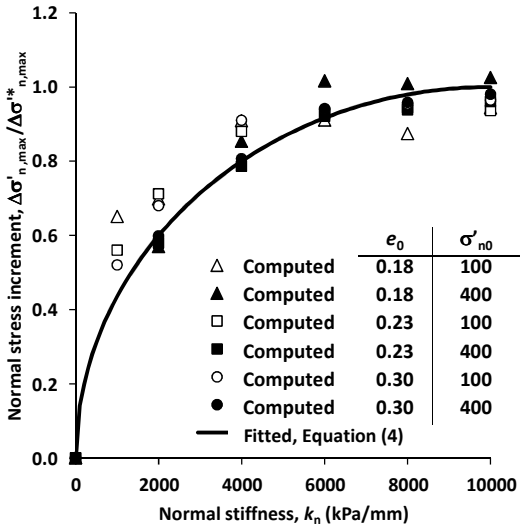

Figure 13: Relationship between $\Delta\sigma'_{n,max}$ and normal stiffness (k_n) for soil specimens with different densities and under various normal stresses

Based on the computed results, the normalised relationship between $\Delta\sigma'_{n,max}$ and k_n relationship is fitted using the following equation:

$$\left(\frac{\Delta\sigma'_n}{\Delta\sigma'^*_n}\right)+\left(1-\frac{k_n}{k^*_n}\right)=1 \tag{5}$$

where k_n^* of 10,000 kPa/mm is a reference normal stiffness to represent CV simulation conditions.

The upper limit ($\Delta\sigma'^*_n$) was obtained from a CV simulation test. Equation (5) reasonably describes the computed relationship between $\Delta\sigma'_{n,max}$ and k_n for various soil states in a unified way. The equation considers the state of the interface soil (e_0 and σ'_{n0}) and the stiffness constraining a given pile-soil interface. Note, however, that other factors such as the shape and size of soil particles which may also affect the changes in normal stress for a given interface were not investigated in this study.

4.4 Back-analysis of measured axial load distributions using DEM results

Computed results (i.e., Equation (5)) from the DEM simulations were applied to estimate the unit shaft resistances of piles tested in centrifuge. The calculated shaft resistances can be integrated along the pile shaft to obtain the axial load distributions of the piles. The calculated results are compared with measured values in Figure 14 for piles tested at the bottom of the excavation zone. For back-analysis, axial loads were calculated with and without considering the contribution from $\Delta\sigma'_n$. For the calculation ignoring $\Delta\sigma'_n$, normal stress was estimated as $K_0\sigma'_v$, where K_0 is the coefficient of lateral earth pressure and σ'_v is the vertical effective stress. The friction angle of the interface was assumed to be the same as that at the critical state ($\varphi'_{cv} = 31^o$)

of Toyoura sand (Ishihara, 1993). When $\Delta\sigma'_n$ was ignored, the calculated shaft resistance was in general considerably lower than the measured results. For the three high friction piles (HEM, HEW1 and HEW2) tested at the formation level at a depth of 200 mm (or 20 m in prototype) after excavation, the calculated unit shaft resistances were generally much lower than the measured ones. To consider the effects of $\Delta\sigma'_n$, the proposed relationship between $\Delta\sigma'_{n,max}$ and k_n (i.e., Equation (5)) was used with $\Delta\sigma'_{n,max}$ of 252 kPa obtained from the CV simulation test on a specimen with e_0 of 0.23 and σ'_{n0} of 100 kPa. It can be seen in Figure 14 that although the calculated and measured values do not match perfectly, the contribution of $\Delta\sigma'_n$ towards axial load distributions must be taken into account if the pile shaft resistance in dilative soils is to be correctly determined.

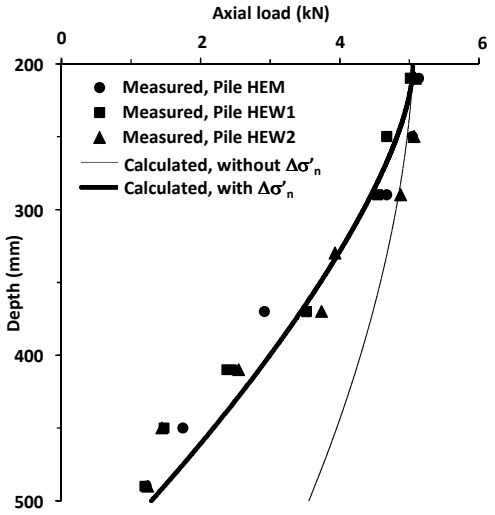

Figure 14: Comparison of measured and calculated axial loads along the pile shaft for piles tested at the bottom of the excavation zone after stress relief

It should be pointed out that the contribution of $\Delta\sigma'_n$ towards the pile shaft resistance and capacity is usually overestimated in small-scale centrifuge model tests, due to the reduced size of the model pile used. For a full-scale pile with a large diameter used in the field, the contribution of $\Delta\sigma'_n$ is in fact limited as revealed by the inverse relationship between k_n and the pile diameter (Houlsby, 1991) (i.e., Equation (3)). Therefore, $\Delta\sigma'_n$ for a full-scale pile is much lower than that for a model pile in centrifuge. Such scale effects on the pile shaft resistance have previously been reported by several researchers (e.g., Garnier and Konig, 1998).For a conservative design of piles in the field, the contributions of $\Delta\sigma'_n$ in dilative soils should therefore be ignored. The reduction in overburden pressure due to excavation (but excluding dilation contributions if any), however, should be considered in the design of piles for use in both non-dilative (e.g., soft clay) and dilative (e.g., stiff clay) soils.

5 INTERPRETATION OF TEST AND COMPUTED RESULTS FOR PILES AND A PILED RAFT SUBJECTED TO STRESS RELIEF DUE TO TWIN TUNNELLING

All interpreted results are expressed in prototype scale unless stated otherwise. Due to page constraints, measured and computed axial load distributions in pile with depth due to stress relief resulting from tunnelling are not provided in this paper. Detailed results and discussions are given by Lu (2013), Ng *et al.*, (2013) and Ng & Lu (2014).

5.1 Apparent loss of pile capacity (ALPC) due to twin tunnelling

To determine the working load of the single model pile for the tests summarised in Table 3, it is necessary to obtain the pile's load-settlement characteristic. An in-flight pile load test (i.e., Test PL) was carried out in a

separate centrifuge model in the absence of model tunnels. Figure 15a shows the measured load settlement relationship. The load applied to the pile cap was gradually increased to 4 MN at increments of 100kN. The ultimate axial load capacity was determined using Equation (4). As shown in the figure, the ultimate load capacity of the pile was 2,880kN. By using a factor of safety (FOS) of 1.5, a working load of 1,920kN was determined and adopted in all other tests summarised in Table 3. At this working load, a pile settlement of 1.6% of d_p was observed.

Since pile capacity is often interpreted using a settlement criterion, any additional pile settlement induced by tunnelling can be considered and converted as an apparent loss of pile capacity (ALPC) using the measured load settlement relationship from Test PL. To illustrate the conversion, measured results of additional pile settlement due to stress relief from the excavation of a single tunnel (i.e., Test T) are shown in the figure. Before the tunnel excavation, the pile settled 12 mm due to the initial applied working load (1,920 kN). An additional pile head settlement of 15 mm (0.24%d_p) was induced due to tunnelling. Based on the load-settlement relationship obtained from Test PL, a total pile settlement of 27 mm may be regarded as applying an equivalent load of 2,490 kN to the pile as illustrated in the figure. Thus, the increase in equivalent pile load can be calculated to be 570kN (i.e., 2,490 – 1,920kN) due to stress relief from the tunnel excavation. Since the ultimate load capacity of the pile was 2,880kN, the current FOS may be considered to be 1.16 (i.e., 2880/2490).That equates to an ALPC of about 23% from the initial FOS of 1.5 due to the tunnel excavation.

Figure 15b illustrates the reductions in FOS due to twin tunnelling in Tests TT and BB. The equivalent pile load was 2,520 kN after the first tunnelling in Test TT, corresponding to an FOS of 1.14 (i.e., 2880/2520), which is consistent with the FOS of 1.16 obtained in Test T. After the second tunnelling, the pile settled even more due to further stress relief. The equivalent pile load further increased to 2,960 kN, which is larger than the determined pile capacity of 2,880 kN, suggesting that the pile failed if Equation 4 had been adopted. In other words, the ALPC was about 21% after excavating the first tunnel and it further increased to about 36% after the second tunnel was constructed in Test TT. Similarly, measured pile settlements due to twin tunnelling in Test BB are illustrated in the figure. The ALPCs or the resultant FOSs due to tunnelling are summarised in Table 4 for all the tests. It is clear that the serviceability limit state of a pile after tunnelling should be considered carefully. The case of constructing twin tunnels at the mid-depth of the pile (i.e., Test SS) had the least impact on the existing pile among the three cases considered. However, the construction of shallow tunnels (i.e., C/D=1.5 in Test SS) could induce large ground surface settlement. As reported by Ng *et al.* (2013), maximum ground surface settlement measured in Test SS was almost twice that measured in Test TT (C/D=2.7). Engineers should assess both the induced pile settlement and the ground surface settlement critically to see which one governs their designs.

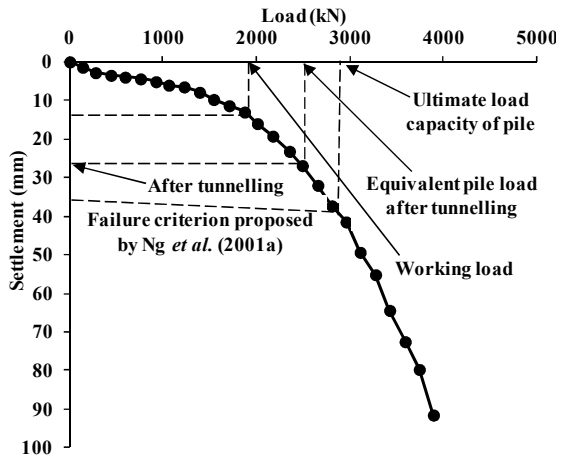

Figure 15a: Load–settlement relationship obtained from load test with and without tunnelling (Test PL and Test T)

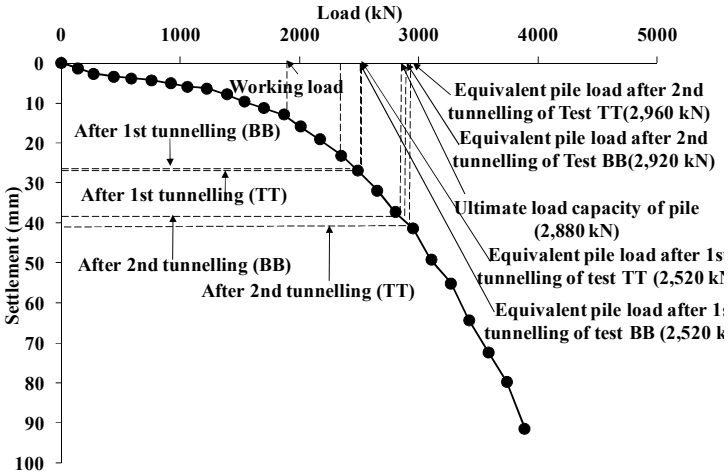

Figure 15b: Comparison of the apparent loss of pile capacity (ALPC) in Tests TT and BB

Table 4: A summary of equivalent FOS or ALPCs from an initial value of 1.5 for Tests TT, SS, BB, TS and ST

Test ID	After first tunnelling	After second tunnelling
T	1.16	not applicable
TT	1.14	0.97
SS	1.24	1.15
BB	1.14	0.99
TS	1.13	1.05
ST	1.24	0.94

5.2 Relationships between induced pile settlement and tunnel depth

Figure 16 shows the normalised settlement of the pile (where S_p and D are pile settlement and tunnel diameter, respectively) induced by twin tunnelling at different depth ratios (Z/L). Due to the excavation of the first tunnel, the induced pile settlement increased as Z/L increased from 0.6 to 1.0. This is because a larger stress relief was experienced by the pile when the first tunnel was excavated at a greater depth. This means that a larger pile settlement was required to mobilise sufficient resistance to support the pile under the working load. As Z/L further increased to 1.3, there was no obvious increase in pile settlement (in Test BB). Similarly, the computed pile settlement also increased with Z/L for $Z/L \leqslant 1.0$. When Z/L reached 1.3, however, a slight reduction in S_p/D was predicted, suggesting there was vertical stress transfer from a deeper soil stratum to support the pile under the working load.

After the second tunnelling, pile settlement continued to increase as a result of further stress relief in each test. The pile settlements in the three tests exhibited a similar trend to those induced by the first tunnelling in each case. The maximum pile settlement was induced by the second tunnelling at the pile toe (i.e., Test TT). This is because the soil was highly stressed near the toe before the second tunnelling. For a 1% volume loss resulting in a relatively large stress relief, a relatively large pile settlement was required to mobilise sufficient resistance to support the pile. The stress relief from the excavation of a tunnel at a shallower depth (i.e., in Test SS) was smaller for a given volume loss.

On the other hand, as the second tunnel was constructed at a greater depth than the pile toe (i.e., Test BB), the influence of stress relief on the pile was less significant and hence the magnitude of pile settlement required to mobilise enough resistance to support the pile was reduced (i.e. smaller than that in Test TT). Although there was a consistent trend between the measured and computed results after the second tunnelling, the computed pile settlements were generally smaller than the corresponding measured ones in Tests TT and BB (or when $Z/L \geqslant 1.0$). This discrepancy may be caused by an overestimation of the shear strength and/or stiffness of soils.

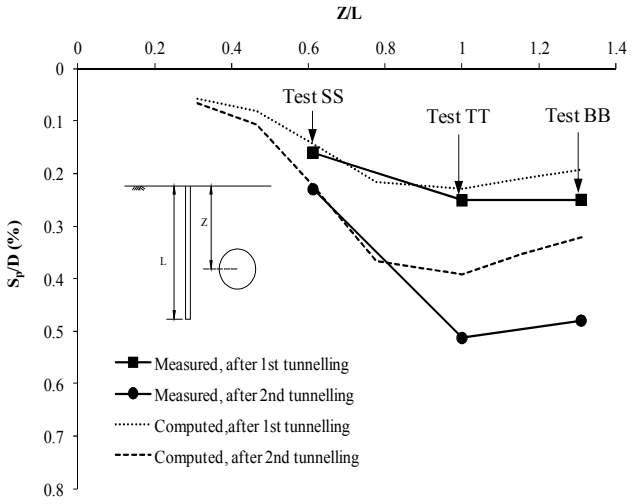

Figure 16**:** Comparison of measured and computed settlement of a single pile with different Z/L ratios

5.3 Influence of different configurations of twin tunnels on induced bending moments (BMs)

Figure 17(a) shows the measured tunnelling-induced bending moments along the piles in Test SS and Test TT. Bending moments are taken to be positive if tensile stress is induced at the side facing the first tunnel. For comparisons, centrifuge test results reported by Loganathan *et al.* (2000) are also shown in the figure. In Test SS, after the first tunnel was excavated, the maximum positive BM was recorded above the tunnel crown (i.e., z/D = 0.8). The magnitude of BM was 113kNm, which was only about 14% of the BM capacity of the pile (M_{yield} = 800 kNm). Unexpectedly, a large negative BM of -125 kNm was recorded near the ground surface. This was caused by the moment constraint of the hydraulic jack. After the second tunnelling, the maximum BM was measured to be 136 kNm (17.0% of M_{yield}). Due to the unexpected constraints imposed by the hydraulic jack, the maximum positive BM is likely to be underestimated. Nevertheless, the maximum BM induced by the twin tunnels in Test TT cannot possibly exceed 50% of M_{yield} of the pile.

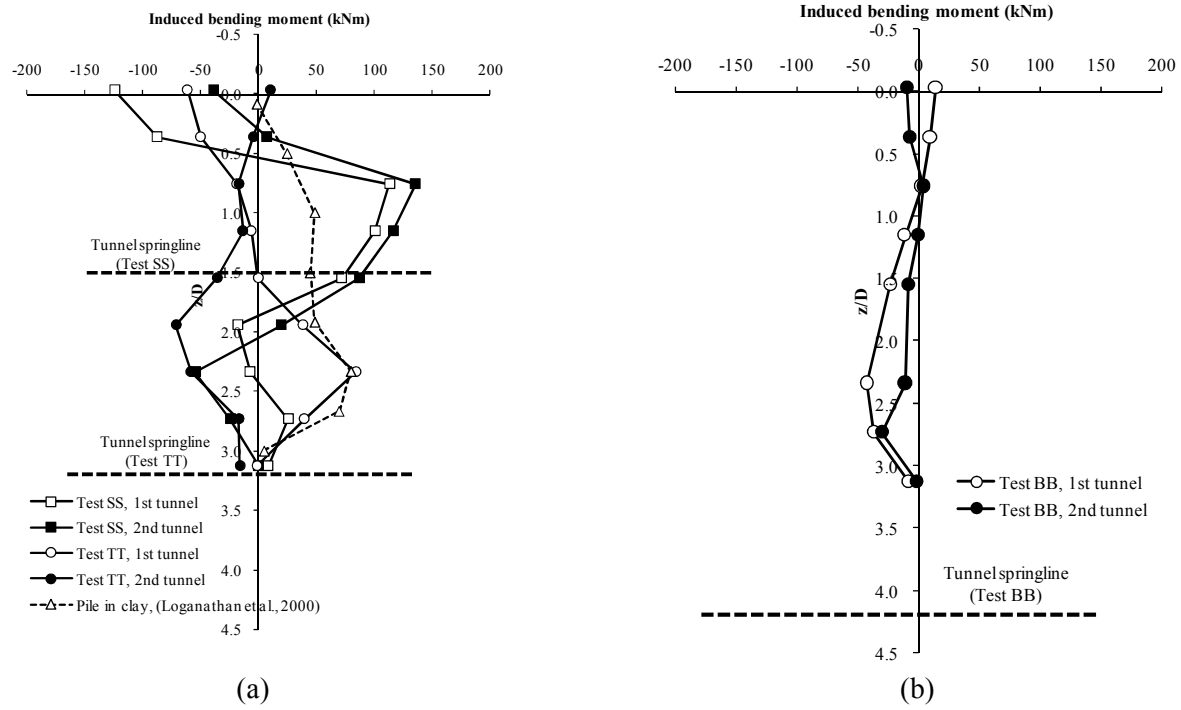

Figure 17: Tunnelling-induced bending moment along the piles in (a) Tests SS and TT; and (b) Test BB

In Test TT, the maximum BM was measured above the crown of the first tunnel (i.e., z/D = 2.7) after excavation. The maximum positive bending moment was only 84kNm (10.5% of M_{yield}). After the excavation of the second tunnel, the maximum negative BM was 71kNm (8.9% of M_{yield}). Loganathan *et al.*, (2000) also observed a small maximum bending moment along a pile constructed in clay above the tunnel crown.

Figure 17(b) shows measured tunnelling-induced BM along the pile in Test BB. After the first tunnel was excavated, the maximum BM was observed at z/D = 2.3 and its magnitude was only 47 kNm (5.8% of M_{yield}).Due to the constraints of the hydraulic jack, as mall bending moment of 14.4kNm was recorded near the ground surface. After the second tunnelling, the bending moments induced along the pile were generally smaller than 5% of M_{yield}. Owing to the larger C/D of twin tunnels and larger distance from the pile in Test BB, the maximum induced BM was substantially smaller than those measured in Tests SS and TT.

5.4 Influence of tunnelling sequence (Test TS versus Test ST) on induced pile settlements

It is well understood that soils are stress- and path-dependent materials. The sequence of tunnelling in soil is expected to have significant impacts on existing piles. Figure 18(a) compares the development of measured S_p normalised by tunnel diameter (D) for each individual tunnel in twin tunnelling employing two different

sequences (i.e., sequence TS versus ST as summarised in Table 3). In the figure, the location of the tunnel face at any stage is denoted by the normalised distance between the tunnel face and the centreline of the pile (*y/D*). In Test TS, as the face of the first tunnel advanced at the same depth as the pile toe (i.e., at *C/D* = 2.7) from *y/D* = -1.25 to -0.25, a pile settlement of 0.06%*D* was measured. The measured pile settlement increased significantly to 0.19%*D* as the tunnel face advanced from *y/D* = -0.25 to 0.25. As the tunnel face continued to advance from *y/D* = 0.25 to 1.25, the pile settlement increased by a further 0.08%*D*. A total pile settlement of 0.28%*D* (2.1%d_p) was recorded at the completion of the first tunnel simulation.

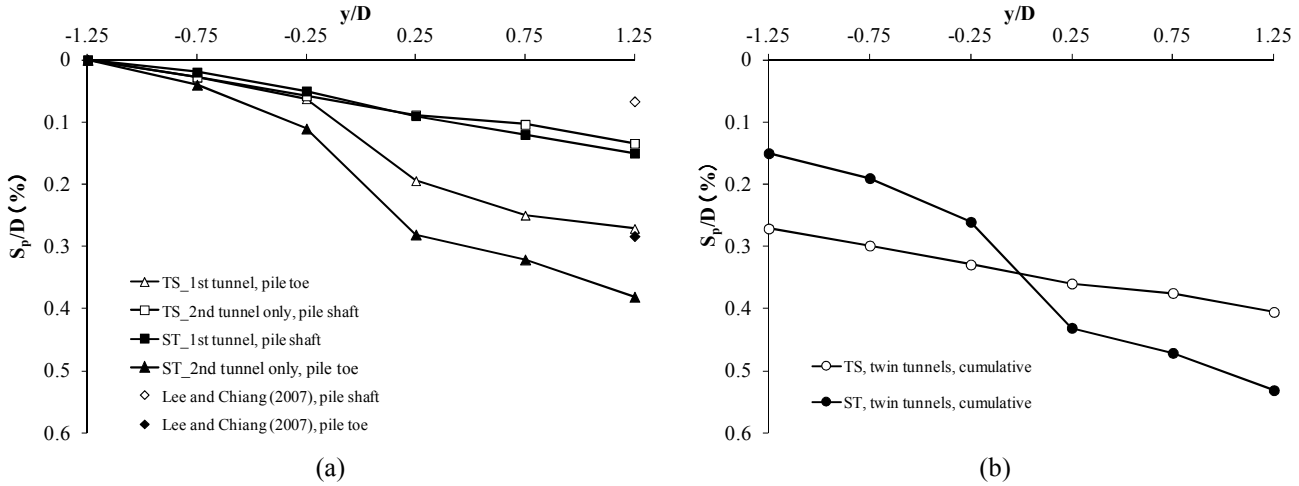

Figure 18: Pile settlement induced by excavations of twin tunnels in Test TS and ST: (a) individual tunnel; (b) after second tunnel (cumulative)

When the second tunnel was excavated near the mid-depth of the pile shaft (i.e., at *C/D* = 1.5) in Test TS, the pile settlement increased almost linearly with the advancement of the tunnel face. This is significantly different from the step jump in pile settlement observed when the first tunnel advanced from *y*/D=-0.25 to *y*/D=0.25. The pile settlement induced by the construction of the second tunnel only was 0.13%*D* (0.99%d_p), which was only 48% of that induced by the construction of the first tunnel only. This is mainly because the stress relief from the excavation of the second tunnel located at a shallower depth was smaller than that induced by the first tunnel constructed at a greater depth for a given volume loss. Hence, a smaller pile settlement was required to mobilise resistance to compensate for the loss of capacity of the pile. Lee and Chiang (2007) also measured pile settlement in centrifuge tests. Their results are shown in the figure for comparisons. They also reported that pile settlement induced by tunnelling near the mid-depth of the pile shaft was smaller than that induced by tunnelling near the pile toe. As expected, the pile settlement induced by tunnelling is closely related to the depth of a tunnel relative to the pile length.

In Test ST, the induced pile settlement increased almost linearly as the excavation of the first tunnel progressed at *C/D* = 1.5 (i.e., near the mid-depth of the pile). This was almost identical to the pile settlement induced by the construction of the second tunnel located at the same *C*/*D* ratio in Test TS. After the excavation of the first tunnel, a pile settlement of 0.15%*D* (1.1%d_p) was measured. When the second tunnel located near the pile toe (i.e., at *C/D* = 2.7) advanced from *y*/D=-0.25 to *y*/D=0.25, a step jump in pile settlement was also observed in Test ST. At the end of the second tunnel construction, the pile settlement induced only by this second tunnel was 0.38%*D* (2.9%d_p), which was about 2.6 times that induced by the first tunnel. By comparing the effects of different tunnelling sequences on pile settlement, it can be seen that the pile settlement induced only by the second tunnel near the pile toe in Test ST was 40% larger than that induced only by the first tunnel (also located near the pile toe) in Test TS. This is because a significant amount of the vertical load applied to the pile head had been transferred downwards to the pile toe after the excavation of the first tunnel in Test ST. For a given volume loss simulated, a larger pile settlement due to the subsequent excavation of the second tunnel near the highly stressed soil around the pile toe was required to mobilise resistance to compensate for the larger loss of pile capacity under the applied working load. In other words, it is not advisable to construct a tunnel near the mid-depth of the pile first and then excavate another one near

the pile toe (i.e., Test ST). Furthermore, the ultimate limit state and the serviceability limit state of piles should both be considered carefully before tunnelling.

Figure 18(b) compares measured cumulative normalised pile settlements after twin tunnel construction in both tests. After the excavation of twin tunnels in Test ST, the measured cumulative settlement was 0.53%D (4.0%d_p), which was 33% larger than that in Test TS. As previously shown in Figure 18(a), a step jump in pile settlement was observed during the advancement of the second tunnel near the pile toe (i.e., from y/D = -0.25 to 0.25) in Test ST. This is due to significantly increased yielding of the soil beneath the pile toe when the second tunnel passed by, as revealed in numerical back-analyses (Lu, 2013). On the other hand, the measured pile settlement increased almost linearly as the second tunnel advanced near the mid-depth of the pile shaft in Test TS. The measured results clearly demonstrate that the tunnelling sequence has a significant effect on the pile settlement induced by twin tunnelling at different depths.

5.5 Influence of twin tunnelling on titling of a piled raft

Due to page constraints, only transverse tilting of the piled raft measured in Tests GR-SS and GR-TT are reported and discussed in this paper. Other results of the two tests are described by Lu (2013).

Figure 19(a) compares the transverse tilting of the piled raft measured in Test GR-SS and Test GR-TT due to the construction of the first tunnel. In Test GR-SS, the raft tilted towards the first tunnel as the latter was being excavated. The magnitude of maximum induced tilting was 0.04% at the end of the first tunnel simulation. Interestingly, the magnitude of tilting decreased as the second tunnel was being excavated (see Figure 19(b)). When the excavation of the twin tunnels was completed, the final tilting of piled raft was almost zero. Similar observations were made in Test GR-TT. The raft tilted towards the first tunnel as the latter was being excavated. The magnitude of tilting increased as the tunnel face advanced from y/D = -0.25 to 1.25 but at a reduced rate. When the simulation of the first tunnel was completed, the tilting reached 0.18%, which was close to the tilting limit of 0.20% for tall buildings proposed by Eurocode 7 (2001). During the excavation of the second tunnel, a significant reduction in tilting occurred as the tunnel face moved from -1.25 to 0.25. When the excavation of the twin tunnels was completed, the final tilting of the piled raft was very small. So the maximum tilting of the piled raft in fact occurred at the end of first tunnelling, and not at the end of the second tunnelling as one might have thought.

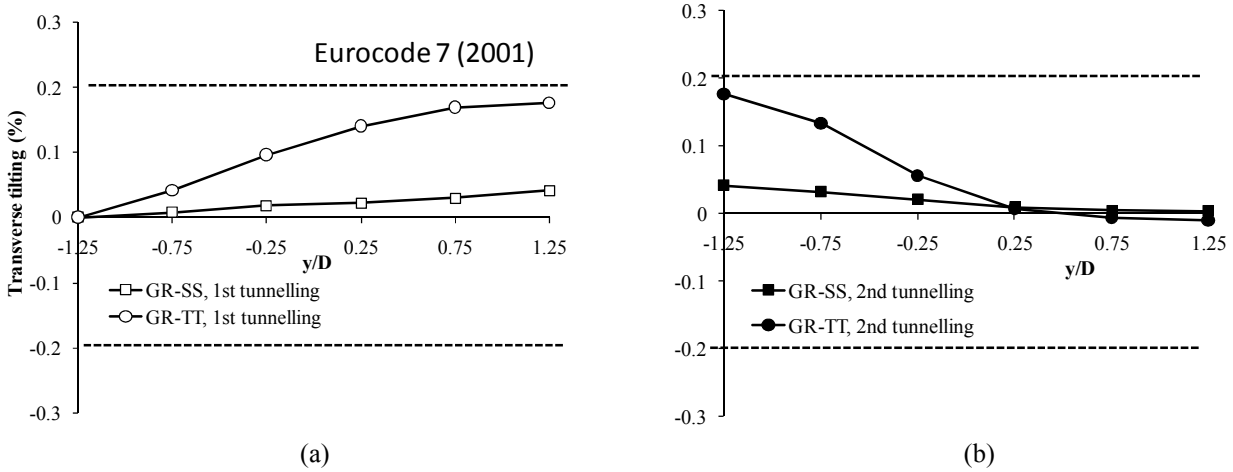

Figure 19: Measured transverse tilting of the piled raft during excavation of: (a) the first tunnel; (b) the second tunnel

6 CONCLUSIONS

Based on the first series of centrifuge model tests on piles with and without subjecting them to stress relief due to an excavation and the detailed analysis of soil-pile interface behaviour using DEM, the following conclusions may be drawn:

(a) For a single pile with a non-dilatant pile-soil interface (e.g., piles constructed in soft clay), the capacity was reduced by about 20% due to stress relief resulting from a 20 m deep excavation. The reduction in shaft resistance was found to be proportional to the normal stress acting on the pile shaft and hence the depth of excavation. For the design of piles underneath of a basement using the top-down construction method, the most adverse location to carry out a pile load test should be at the formation level after the excavation. When such a pile load test is not practically viable, the shaft resistance should be reduced in proportion to stress relief when deducing the pile capacity from a conventional load test at the ground surface.

(b) For a pile installed in stiff clay and dense sand (with a dilatant pile-soil interface), the observed capacity of a 30 m long pile subjected to the 20 m deep excavation was even higher than that of a sleeved pile tested at the ground surface. The increase in pile capacity was attributed to soil dilation at the pile-soil interface, resulting in an increase in normal stress ($\Delta\sigma'n$) acting on the pile shaft and hence the pile capacity. The DEM of direct shear box tests revealed that an unloading of normal stress from 400 to 100 kPa can lead to a 30% increase in $\Delta\sigma'n$. By considering the increase in $\Delta\sigma'n$, centrifuge model test results were reasonably predicted by DEM.

(c) The capacity of a pile, installed in a dilatant soil and subjected to stress relief due to excavation, is governed by two counteracting terms in Equation (2), i.e., a reduction in $\sigma'n0$ proportional to the magnitude of stress relief and an increase in normal stress ($\Delta\sigma'n$) due to dilation at the soil-pile interface. However, it should be noted that the magnitude of soil dilation (i.e., an increase in normal stress ($\Delta\sigma'n$)) is often overestimated in centrifuge model tests since a much smaller pile diameter is adopted in model tests than that in the field. Therefore, the effects of stress relief should not be overlooked in pile design, not only in non-dilative soils such as loose sand and soft clay but also in dilative soils such as dense sand and stiff clay.

Based on the second series of three-dimensional centrifuge model tests and finite element numerical back-analyses conducted to study the influence of twin tunnelling on an adjacent pile and a piled raft, the following conclusions may be drawn:

(d) The settlement of a pile induced by twin tunnelling is closely related to the depth of each tunnel relative to the pile. The maximum cumulative pile settlement occurred when twin tunnels were constructed at the pile toe. Near the pile toe (i.e., Test TT), the cumulative pile settlement induced by twin tunnelling was 3.7% of the pile diameter. On the other hand, the induced cumulative pile settlements in Test SS and BB were 1.6% and 3.6% of the pile diameter, respectively. Based on the displacement-failure load criterion proposed by Ng et al. (2001a), the apparent loss of pile capacity (ALPC) was about 21% after the construction of the first tunnel, and increased to about 36% (cumulative) after the construction of the second tunnel in Test TT. The ALPCs due to twin tunnelling in Tests SS and BB were 20% and 35% of the pile diameter, respectively. In other words, twin tunnelling near and below the pile toe would be more critical for the ultimate and serviceability limit states of existing piles. However, twin tunnelling at a shallow depth (i.e., at small C/D ratio) could result in large ground surface settlements.

(e) The induced bending moment due to twin tunnelling may not be significant. It was typically less than 20% of the ultimate bending moment capacity of the pile for the cases considered in this paper.

(f) The construction sequence of twin tunnels at different depths has a significant effect on the cumulative induced pile settlement and hence the ultimate and serviceability limit states of existing piles. The measured pile settlement induced by first tunnelling near the mid-depth of the pile shaft followed by tunnelling near the pile toe (i.e., Test ST) was 33% larger than that induced by first tunnelling near the pile toe followed by tunnelling near the mid-depth of the pile shaft (i.e., Test TS). The deduced ALPCs were 40% and 29% for tunnelling sequences ST and TS, respectively.

(g) For the two by two piled rafts simulated, the maximum measured transverse tilting was 0.18%, which was very close to the limit of 0.20% for tall buildings proposed by Eurocode 7 (2001). The most critical transverse tilting occurred after the construction of the first tunnel near the pile toe, rather than after the completion of twin tunnels near the pile toe. On the contrary, an insignificant amount of tilting was observed when tunnelling near the mid-depth of the pile shaft.

ACKNOWLEDGEMENTS

The authors would like to acknowledge the financial support provided by the Research Grants Council of the HKSAR under grant numbers GRF617608 and 617511.

REFERENCES

Boulon, M. and Foray, P. (1986). Physical and numerical simulation of lateral shaft friction along offshore piles in sand. *3rd International Conference on Numerical Methods in Offshore Piling*, 127-147.

Bolton, M.D. (1986). The strength and dilatancy of sands. *Géotechnique*, 36(1), 65-78.

Brinkgreve, R. B.J., Engin,E. and Swolfs,W. M. (2012). *Plaxis 3D – 2012* User *manual*. Plaxis bv Delft.

CEN (2001). *Eurocode 7 part 1*: *Geotechnical design: General rules*, *Final Draft prEN 1997–1*. Brussels: European Committeefor Standardization (CEN).

Eurocode7. (1997). *Eurocode 7: geotechnical design*. Part 1: general rules. British Standards Institution DD ENV 1997-1.

Evgin, E. and Fakharian, K. (1996). Effect of stress paths on the behaviour of sand-steel interfaces. *Canadian Geotechnical Journal*, 33(6), 853-865.

Fioravante, V. (2002). On the shaft friction modelling of non-displacement piles in sand. *Soils and Foundations,* 42(2), 23-33.

Garnier, J. and Konig, D. (1998). Scale effects in piles and nails loading tests in sand. *Proceedings of Centrifuge 98*, 205-210.

Horikoshi, K. and Randolph, M. F. (1996). Centrifuge modelling of piled raft foundations on clay. *Geotechnique,* 46(4), 741-752.

Horikoshi, K. and Randolph, M. F. (1997). On the definition of raft-soil stiffness ratio for rectangular rafts. *Geotechnique,* 47(5), 1055-1061.

Houlsby, G. T. (1991). How the dilatancy of soils affects their behaviour. *10th European Conference on Soil Mechanics and Foundation Engineering, Florence, Italy*, 1189-1202.

Ishihara, K. (1993). Liquefaction and flow failure during earthquakes. *Geotechnique*, 43(3), 351-415.

ISSMFE. (1985). Axial pile loading test -- part 1: static loading. *Geotechnical Testing Journal*, 8(2), 79-90.

Itasca. (2002). *PFC2D - Particle flow code in two dimensions.* Itasca Consulting Group, Inc., Minneapolis, MN, USA.

Jacobsz, S.W., Standing, J.R., Mair, R.J., Hahiwara, T. and Suiyama, T. (2004). Centrifuge modeling of tunnelling near driven piles. *Soil and Foundations*, 44(1), 49-56.

Kishida, H. and Uesugi, M. (1987). Tests of the interface between sand and steel in the simple shear apparatus. *Geotechnique*, 37(1), 45-52.

Lee, C. J., Al-Tabbaa, A. and Bolton, M. D. (2001). Development of tensile force in piles in swelling ground. *Proc. 3rd Int. Conf. Soft Soil Engineering,* 345-350. Swets & Zeitlinger. (eds. C. F. Lee, C. K. Lau, C. W. W. Ng, A. K. L. Kwong, P. L. R. Pang, J. H. Yin, Z. Q. Yue).

Lee, C.J. and Chiang K.H. (2007). Responses of single piles to tunnelling-induced soil movements in sandy ground. *Canadian Geotechnical Journal*, 44(10), 1224-1241.

Lee, T.K. and Ng, C.W.W. (2005). Effects of advancing open face tunnelling on an existing loaded pile. *Journal of Geotechnical and Geoenvironmental Engineering*, *ASCE*, 131(2), 193-201.

Lehane, B. M., Gaudin, C. and Schneider, J. A. (2005). Scale effects on tension capacity for rough piles buried in dense sand. *Geotechnique*, 55(10), 709-719.

Loganathan, N., Poulos, H.G., and Stewart, D.P. (2000). Centrifuge model testing of tunnelling-induced ground and pile deformations. *Géotechnique*, 50(3), 283-294.

Lu, H. (2013). Three-dimensional centrifuge and numerical modelling of twin tunnelling effects on piles. *PhD thesis, Hong Kong University of Science and Technology*.

Mair, R. J. (2008). Tunnelling and geotechnics: new horizons. *Geotechnique* 58, No. 9, 695–736.

Marshall, A.M. and Mair, R.J., (2011). Tunneling beneath driven or jacked end bearing piles in sand. *Canadian Geotechnical Journal*. 48(12), 1757-1771.

Ng, C. W. W., Yau, T. L. Y., Li, J. H. M. and Tang, W. H. (2001a). New failure load criterion for large diameter bored piles in weathered geomaterials. *Journal of Geotechnical and Geoenvironmental Engineering*, 127(6), 488-498.

Ng, C. W. W., Van Laak, P. A., Tang, W. H., Li, X. S. and Zhang, L. M. (2001b). The Hong Kong geotechnical centrifuge. *Proc. 3rd Int. Conf. Soft Soil Engineering, Hong Kong.* 225-230. Swets & Zeitlinger. (eds. C. F. Lee, C. K. Lau, C. W. W. Ng, A. K. L. Kwong, P. L. R. Pang, J. H. Yin, Z. Q. Yue).

Ng, C. W. W., Van Laak, P. A., Zhang, L. M., Tang, W. H., Zong, G. H., Wang, Z. L., Xu, G. M. and Liu, S. H. (2002). Development of a four-axis robotic manipulator for centrifuge modeling at HKUST. *Proc. Int. Conf. Physical Modelling in Geotechnics, St. John's Newfoundland, Canada,* 71-76.

Ng, C.W.W, Zhang, L.M. and Wang, Y.H. (2006). Co-editors of the proceedings of 6th Int. Conf. on Physical Modelling in Geotechnics (TC2). Publisher: Taylor & Francis. Vols 1 and 2. ISBN: 978-0-415-41587-3 and 978-0-415-41588-0.

1608p.
Ng, C. W. W., Lu, H., and Peng, S. Y. (2013). Three-dimensional centrifuge modelling of the effects of twin tunnelling on an existing pile. *Tunnelling and underground space technology,* 35, 189-199.
Ng, C.W.W., and Lu, H. (2014). Effects of the construction sequence of twin tunnels at different depths on an existing pile. *Canadian Geotechnical Journal*, 51(2): 173-183.
Ng, C.W.W. (2014). The 6th ZENG Guo-xi Lecture: The State-of-the-Art centrifuge modelling of geotechnical problems at HKUST. *Journal of Zhejiang University-Science A (Applied Physics & Engineering)*. Vol. 15, No. 1, 1-21.
Ng, C. W.W. ,Soomro, M.A. &Hong, Y. (2014). Three-dimensional centrifuge modelling of pile group responses to side-by-side twin tunnelling. *Tunnelling and Underground Space Technology.* Under re-review.
O'Neill, M.W., and Reese, R.C. (1999). *Drilled shaft: construction procedures and design methods*, Federal Highway Administration, Washington, D.C.
Paikowsky, S. G., Player, C. M. and Connors, P. J. (1995). A dual interface apparatus for testing unrestricted friction of soil along solid surfaces. *Geotechnical Testing Journal*, 18(2), 168-193.
Pang, C.H. (2007). The effect of tunnel construction on nearby pile foundation. *Ph.D. thesis. National University of Singapore.*
Peng, S. Y. (2012). Influence of stress relief due to deep excavation on capacity of pile foundations. *PhD thesis, Hong Kong University of Science and Technology*.
Peng, S. Y., Ng, C. W. W. and Zheng, G. (2013). The dilatant behaviour of sand–pile interface subjected to loading and stress relief. *Acta Geotechnica*, Published online on 20 April.
Poulos, H. G. (2001). Piled raft foundations: Design and applications. *Geotechnique,* 51(2), 95-113.
Randolph, M. F. (2003). Science and empiricism in pile foundation design. *Geotechnique,* 53(10), 847-875.
Weltman, A. J. (1980). *"Pile load testing procedures."* DOE and CIRIA Piling Devel. Group Rep. PG7, Construction Industry Research and Information Association, London.
Taylor, R.N. (1995). *Geotechnical centrifuge technology*. Blackie Academic and Professional, London.
Zheng, G., Peng, S. Y., Ng, C. W. W. and Diao, Y. (2012). Excavation effects on pile behaviour and capacity. *Canadian Geotechnical Journal*, 49(12), 1347-1356.
Zhu, H. G. and Sun, J. P. (2005). The influence of basal heave on piles during deep excavation in Shanghai. *Geotechnical engineering world*, 8(3), 43-46.

Overview of Development and Challenges in Foundation Design and Construction in Hong Kong

C. M. Wong
C M Wong & Associates Limited

ABSTRACT

This paper presents an overview of the development and challenges in foundation design and construction in Hong Kong, as a result of heavier buildings, more restrictive site terrain, more difficult ground conditions and higher public demand for quieter construction. It starts with the challenges in post hand-dug caisson era, followed by the development of the frictional barrettes and bored piles, with friction values enhanced by applying pressure grouting at the soil/concrete interface. The advancement in designing and installing small sized piles, like minipiles, prebored H-piles and jacked piles, is also discussed.

1 INTRODUCTION

Hong Kong is hilly and land is scarce. Throughout the years, there is a clear trend that there are more site constraints on the development, especially those in the urban area, and that buildings are getting taller. Together with the rising concern on industrial safety, the lower tolerance to nuisance during construction, as well as the complex nature of the geology in Hong Kong, foundation design and construction has become increasingly challenging.

This paper will look at the development in different pile types and how to overcome the recent challenges arising from taller and heavier buildings, geological difficulties and social issues.

2 LARGE REPLACEMENT PILES

2.1 Hand-dug caissons

One of the most significant changes in statutory control on foundation works in the past 20 years is the banning of hand-dug caissons.

Hand-dug caissons were first introduced to Hong Kong in the 1960s (Choy & Wong 2007). They were widely used in Hong Kong as large replacement piles before the mid-nineties. Other than foundation works, hand-dug caissons were often used as earth retaining structures.

Despite all the advantages, the construction process caused safety hazards and long-term health problems to the workers such as pneumoconiosis. The bill of banning hand-dug caissons was passed in the Legislation Council in 1995, soon after the accident in the Smithfield Road flyover extension project, where two workers were killed by the collapsed reinforcement cage while fixing the reinforcement inside the caisson shaft (SCMP 1996).

Although hand-dug caissons have been banned, there are still exceptional circumstances that no foundation type other than hand-dug caisson is viable. Since the banning in 1995, hand-dug caissons have been successfully adopted in several projects. One of these is the fill slope stabilisation works at the peak (Wong et. al. 2011a).

The loose fill slope was located below the then Peak Café (now known as Peak Lookout), which is a Grade II Historic Building and constructed of brick walls and timber trusses. The site setting of the slope is shown in Figure 1. Site access and construction space was very limited. The geology of the slope consists of approximately 10m of loose fill overlying Completely Decomposed Tuff (CDT) and bedrock, with a relatively low groundwater table, as indicated in Figure 2.

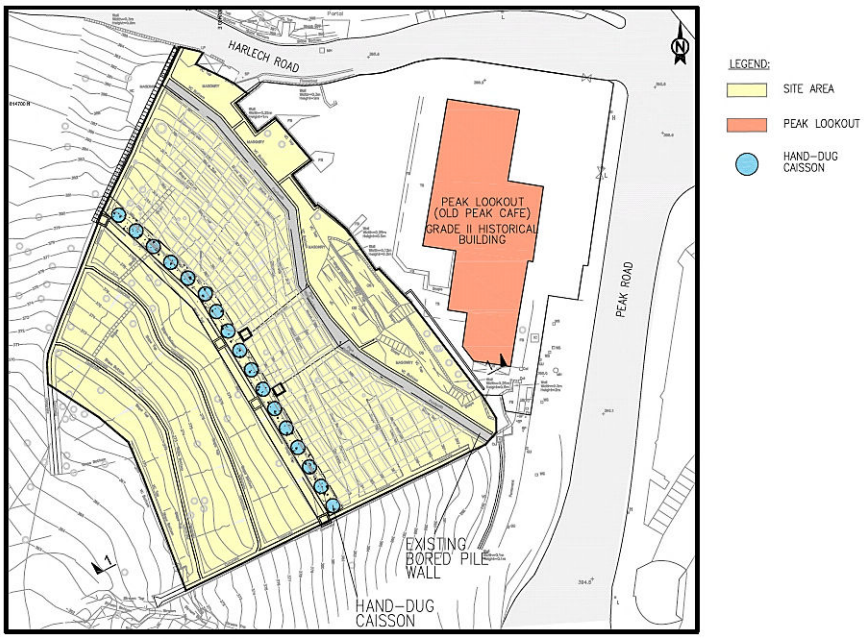

Figure 1: Site setting plan of slope upgrading works

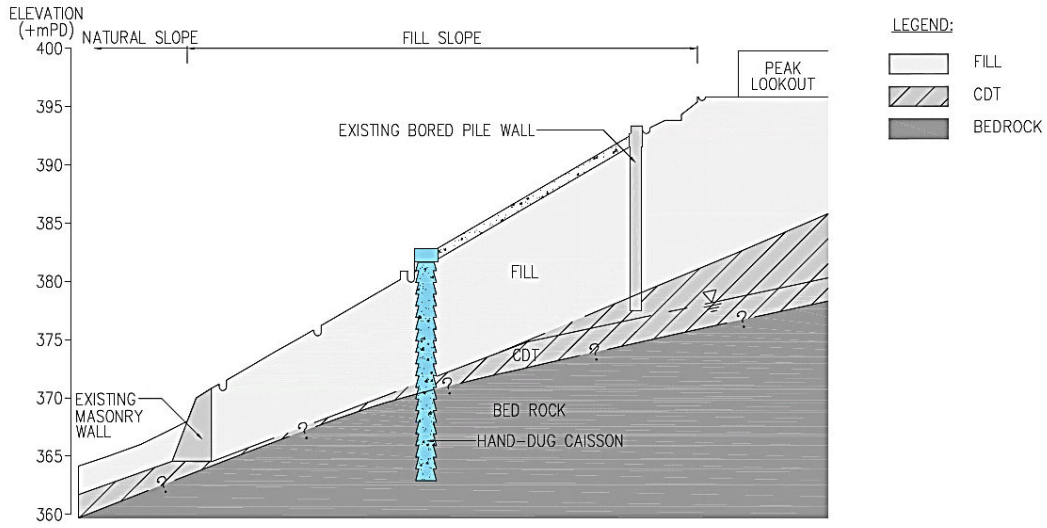

Figure 2: Geology of the slope

A bored pile (450mm diameter) wall with tie back by soil nails were proposed to stabilise the slope and the works were commenced in 1997. However, excessive ground settlement and cracks in the Peak Café were observed during the bored pile construction. The works were therefore suspended after the bored pile wall had been completed. Further improvement works were to be carried out later.

In order to minimise the potential impact to the Grade II Historic Building and to overcome the sensitive geology of the slope, hand-dug caisson was considered to be the only feasible solution to tackle the problem. A row of 17 hand-dug caissons of 1.8m diameter and 3m spacing, with total length ranging from 17m to 23m, was constructed to stabilise the 27m high slope.

Health and safety was the major concern during the construction of hand-dug caissons. Extra attention was given to the ventilation system and the personal protective measures for the caisson workers. As shown in Plate 1, proper ventilation system was implemented to provide adequate fresh air into the caisson shaft. In

addition, during reinforcement bar fixing, the worker stays inside a protective cage, known as climbing mast, as shown in Plate 2. The climbing mast protects the worker from any collapse of reinforcements and falling objects.

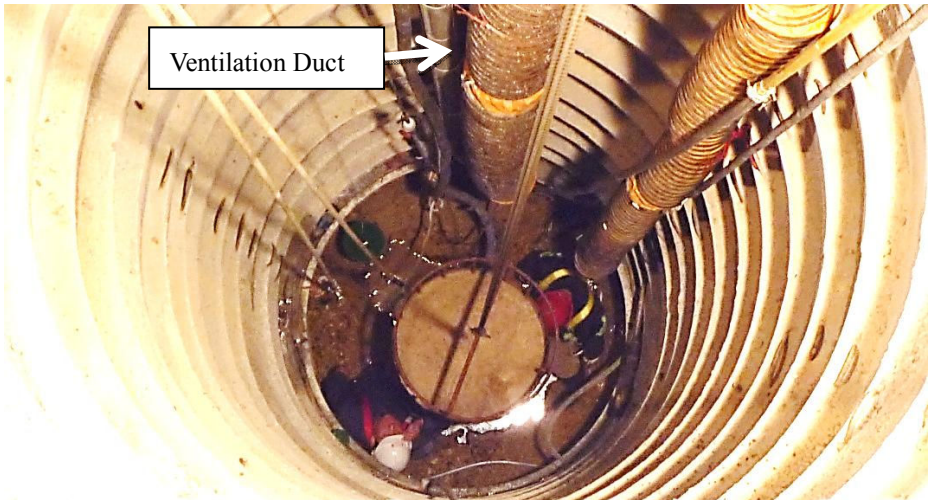

Plate 1: Provision of ventilation to the caisson shaft

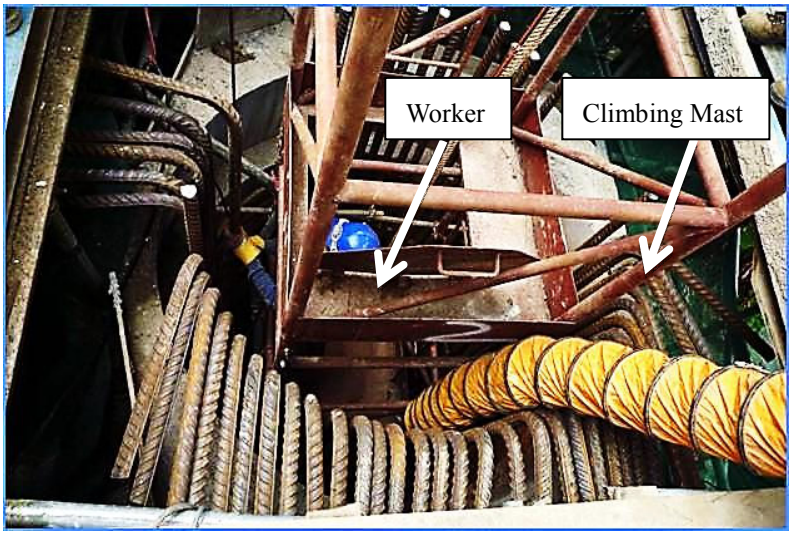

Plate 2: A worker inside the climbing mast during reinforcement bars fixing

The successful construction proves that, under special circumstances, hand dug caissons could still be a viable option with the implementation of proper health and safety measures. However, caisson works are no longer cost effective due to all these health and safety enforcements, as well as the lack of skilled labour supply.

2.2 Large Diameter Bored Piles

Bored piles were first introduced to Hong Kong in the 1970s. Typical size of these piles ranges from 1 m to 3 m in diameter. The maximum length of piles could be over 100 m. They are constructed by oscillating or rotating a steel casing into the ground and the materials inside the casing are removed by using large grabs

operated by cranes.

In 1976, the residential development at Kowloon Bay MTR station (Telford Garden) first adopted the Reversed Circulation Drilling (RCD) technique. RCD uses self-weight and rotary motion of the drill to crush hard materials. Crushed materials are then retrieved by circulation of fluids within the drillhole. This method effectively reduces the noise and vibration during the construction of rock sockets. Since then, RCD has become the common construction method for bored piles.

Since the banning of hand-dug caissons in 1995, large diameter bored piles have become one of the most common foundation types for high rise buildings. Large diameter bored pile walls have also been adopted to replace caisson walls as earth retaining structures.

In terms of safety, bored piles possess fewer hazards to the workers comparing with caissons, as all operations are carried out by mechanical plants. However, for sloping or terraced sites, temporary steel platforms would be required to support these heavy machineries. Such temporary steel platforms could be very costly and take long lead time to construct and dismantle.

One of the recent examples is the construction of bored piles for the redevelopment of previous government quarters at Mount Nicholson. To suit the new building layout, a row of bored pile wall was proposed along the lot boundary at the crest of a 20m high slope. The temporary steel platform, as shown in Plate 3 and Figure 3, contributed to about half of the bored pile construction cost.

Plate 3: The temporary steel platform for bored pile construction on slope

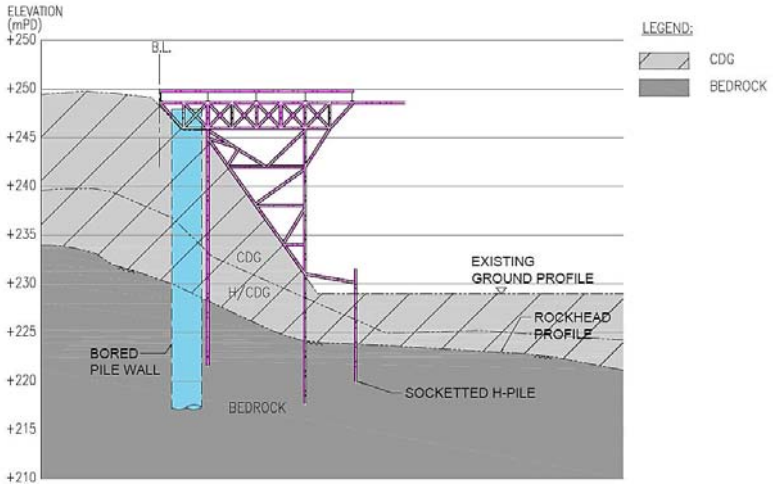

Figure 3: Section of the temporary steel platform

2.2.1 The development of presumed bearing pressure of granitic & volcanic rock

Bored Piles are conventionally designed as end-bearing piles and founded on bedrock. The use of presumed bearing pressure was first stipulated in the Building (Construction) Regulations (B(C)R) (HKG 1975) and amended in Practice Notes for Authorised Persons (PNAP) No.141 (BD 1990). It was latterly further revised in the Code of Practice for Foundation (CoP) (BD 2004). Table 1 illustrates the development of the presumed bearing pressure from B(C)R (1975) to CoP (2004).

Table 1: The development of the presumed bearing pressure

Category of Rock	General description of rock or soil*		Presumed bearing pressure (kPa)		
			B(C)R (1975)	PNAP14 1 (1990)	CoP (2004)
1 (a)	Fresh rock	TCR=100%	--	--	10,000
1 (b)	Fresh to Slightly decomposed	TCR>95%	--	7,500	7,500
1 (c)	Slightly to Moderately decomposed	TCR>85%	5,000	5,000	5,000
1 (d)	Moderately decomposed (better than Grade IV)	TCR>50%	3,000	3,000	3,000

*Note1: Description of rock or soil refers to Code of Practice for Foundation 2004
*Note2: B(C)R (1975) describes 1(c) as massive crystalline rock in hard sound and 1(d) as medium hard rock

2.2.2 Rock sockets

In the past, rock socket friction was not allowed to be considered in foundation design. Towards the late nineties, the Buildings Department started to allow the use of rock socket friction, subject to special approval.

The value of rock socket friction in minipiles and socketted steel H-piles was stipulated in PNAP66 (BD 2000) in 2000. However, other pile types such as large diameter bored piles were not included in that particular guideline. In 2004, the CoP was published (BD 2004) and allows the combination of rock socket friction (with length of up to 2 times the diameter of the pile) and presumed bearing pressure in bored piles. The allowable rock socket friction of CoP (BD 2004) is shown in Table 2.

Table 2: Presumed Allowable Bond or Friction Between Rock and Concrete for Piles

Category of Rock	Presumed allowable bond or friction between rock and concrete or grout for piles (kPa)	
	Under compression or transient tension	Under permanent tension
1 (c) or better	700	350
1 (d)	300	150

*Note: minipiles and socketted steel H-piles are limited to category 1 (c) or better only

2.3 Large Diameter Frictional Replacement Piles

2.3.1 Geology of Central - Sheung Wan Strip

The site specific ground investigation results of the projects at the locations shown in Figure 4 indicate that the bedrock is over 80m below ground level. Bored piles of over 80m in length are considered to be impractical in this congested urban area mainly due to the limitation of the concreting volume. As a result, this geology inhibits the use of end bearing piles founded on rock.

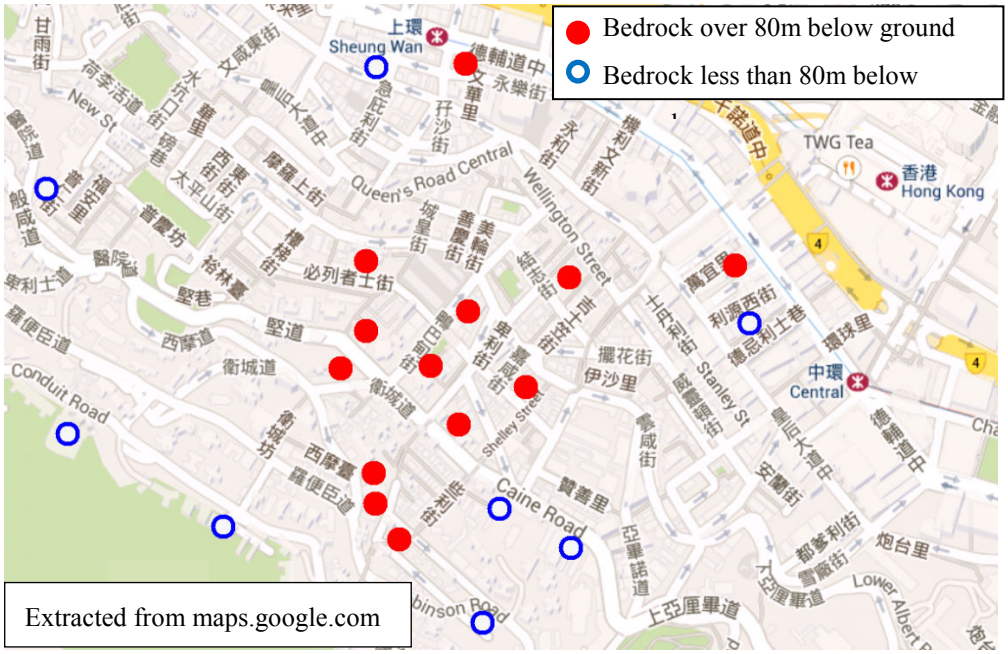

Figure 4: Site specific ground investigation results of the projects in the Central-Sheung Wan Strip

2.3.2 Frictional Bored Piles

In view of the deep rockhead in Central-Sheung Wan Strip, rock bearing piles become impractical and frictional bored piles were developed.

Frictional bored piles were first adopted in a residential development in Robinson Road in 1989. 50 bored piles, founded on CDG with SPT-N >240 (where N is the average SPT-N value), with 1m shaft diameter and approximately 70-80m long shaft, were constructed. The adopted friction coefficient of the piles was 1.4N (factor of safety = 2.0) and the loading capacity of each frictional bored pile was approximately 10,000kN.

2.3.3 Frictional Barrettes

Barrettes are simply rectangular variants of bored piles. The rectangular shafts are excavated by using grabs or milling machines. During excavation, the shaft is supported by bentonite slurry and because of their rectangular shape, barrettes can be oriented to provide optimum resistance to lateral loading.

Barrette foundations are commonly founded on saprolites and their loading capacities are mainly derived from skin friction. Frictional barrettes were first adopted in Hong Kong by the Kwun Tong Bypass project. The first building for which frictional barrettes were applied was the Heng Seng Bank Headquarters Project in 1987, with pile capacity of 20,000kN to 30,000kN.

Man Yee Building in Central, constructed in 1996, is the second private building project that adopted frictional barrette foundation. The site was located in close proximity to the MTR tunnel. It consists of fill materials underlain by alluvium, completely decomposed granite (CDG) and highly decomposed granite (HDG), while bedrock is around 90m below ground level. The geological profile of the site is shown in Figure 5.

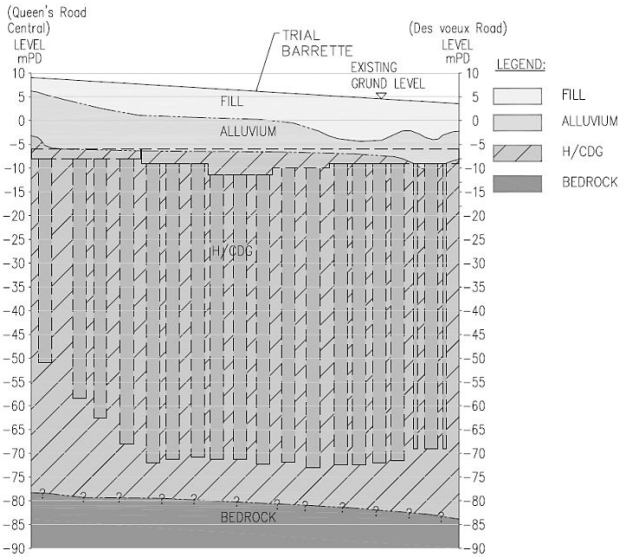

Figure 5: Geological profile of the Man Yee Building

As the rockhead level is about 90m below ground level, end bearing piles were impractical due to the constraint in concreting and frictional barrette was the most favourable option. The barrettes were designed to be founded on HDG with SPT-N value exceeding 240. The foundation design adopted a ultimate shaft resistance of 1.0N kPa (factor of safety 2.0), with a cap of 200kPa, and the working load capacity of the barrettes were around 18,000 kN.

For all barrettes, after completion of each barrette excavation, and immediately prior to placing the reinforcement cage, a special scrapping device will be used to scrape the sides of the trench, as shown in Plate 4. The scrapping process is aimed to remove the potential bentonite cake which could otherwise be formed at the soil/concrete interface. After scrapping, the bottom of the excavation will be cleaned by grab.

Plate 4: Trench surface scrapping device

A full scale instrumented trial barrette was constructed and load tested to twice the designed working load in order to verify the design assumption. The upper portion (35m) of the trial barrette was sleeved to reduce

the required test load to a practical value. The test focused on testing for the lower section of the pile and determining the friction coefficient of CDG.

The graphs of force against level and load against friction coefficient are shown in Figure 6 and Figure 7 respectively. The trend in Figure 7 hardly shows any sign of strain softening, which suggests that the shaft resistance of the barrette had not been fully mobilised at twice the working load. From the skin friction in CDG mobilised during the test at 200% working load, the correlation of shaft resistance (f_s) = 1.1N could be obtained. However, significant shaft resistance could be further mobilised if the applied load is further increased. This suggests the design assumption is conservative.

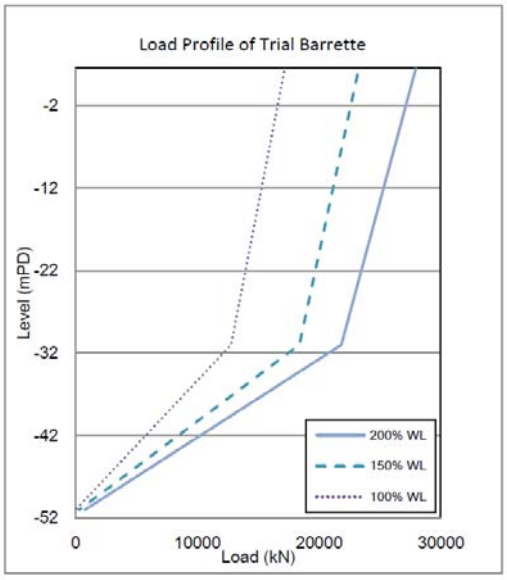

Figure 6: Graph showing the force against level

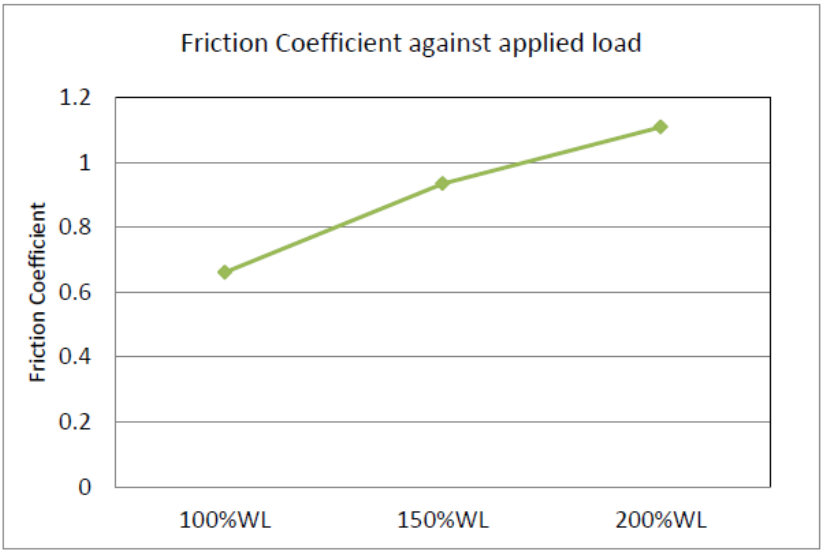

Figure 7: Graph showing load against friction coefficient

The designed friction coefficient and the mobilised friction coefficient are summarised in Table 3.

Table 3: Comparison of the designed and mobilised friction coefficient

	Designed friction coefficient	Mobilised friction coefficient
Under Working Load	0.5	0.65*
Under Ultimate Load	1.0	1.1*

*The shaft resistance of trial barrette was not fully mobilised

2.3.4 Post-shaft grouted bored piles & barrettes

New buildings are getting taller, which result in an increase of the loading acting on their foundations. Plain frictional piles have sometimes become inadequate to cater for the heavier loading. Shaft grouted piles are therefore becoming necessary in areas with deep rockhead level.

Shaft grouting can be applied to piles to enhance their frictional capacity. By injecting pressure grout along the pile shaft, the loose materials at the soil and pile interface are compacted and thus the frictional capacity of the pile is greatly increased.

Shaft-grouted bored piles and shaft grouted barrettes were first introduced to Hong Kong in the West Rail Project in the late 1990s (Plumbridge et al. 2000). Full-scale shaft-grouted piles and barrettes testing were carried out under the West Rail project. The results show a 2-3 times increase in shaft resistance, which agrees with test results from previous works in other countries. Since then, shaft-grouted barrettes were used on several projects in Hong Kong, including the MTRC Kowloon Station development and a residential development in Tung Chung (Sze et. al. 2007). Recently, shaft-grouted bored pile was also adopted in a development project at Caine Road, Mid-Levels.

The Caine Road project is a 50-storey residential development. It is in close proximity to Kam Tong Hall, which is graded as Monument and now converted to Dr. Sun Yat-Sen Museum. The site consists of fill materials underlain by colluvium, CDG and HDG, while bedrock is around 130m below ground level. The geological profile of the site is shown in Figure 8.

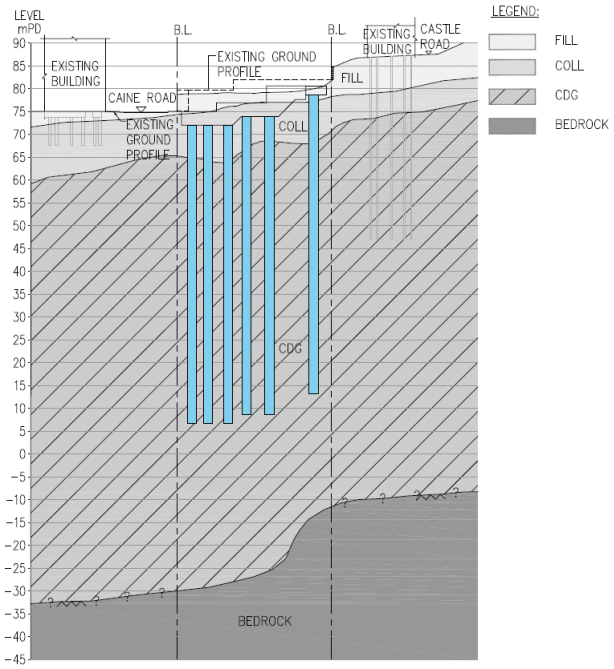

Figure 8: Geological profile of the site at Caine Road

Shaft grouted bored piles in this project was the first of its kind for which approval from the Buildings Department was sought. Approval for the use of such piles is subject to the results of the loading test on trial piles. Two instrumented trial piles of 1.2m diameter (T-P01 & T-P02) were constructed and load tested to 200% working load (which corresponds to 27,000kN and 31,000kN respectively) to determine the shaft resistance. The kentledge setup is shown in Plate 5.

Plate 5: Kentledge setup of T-P01

In order to determine the true friction value without the influence of end bearing condition, a soft base was set up at T-P01, as shown in Plate 6. The sand at the soft base was washed out after the pile was in place, as shown in Plate 7.

Plate 6: The soft base set up at T-P01

Plate 7: Sand being washed out

The construction of shaft-grouted piles involves various stages such as fixing of Tube-A-Manchette (TAM) pipes to the reinforcement bars, concreting of the pile, water cracking and pressure grout injection. These processes are shown in Plate 8, Plate 9 and Plate 10. The strain gauges, consisting of TAM pipes, are shown in Plate 11.

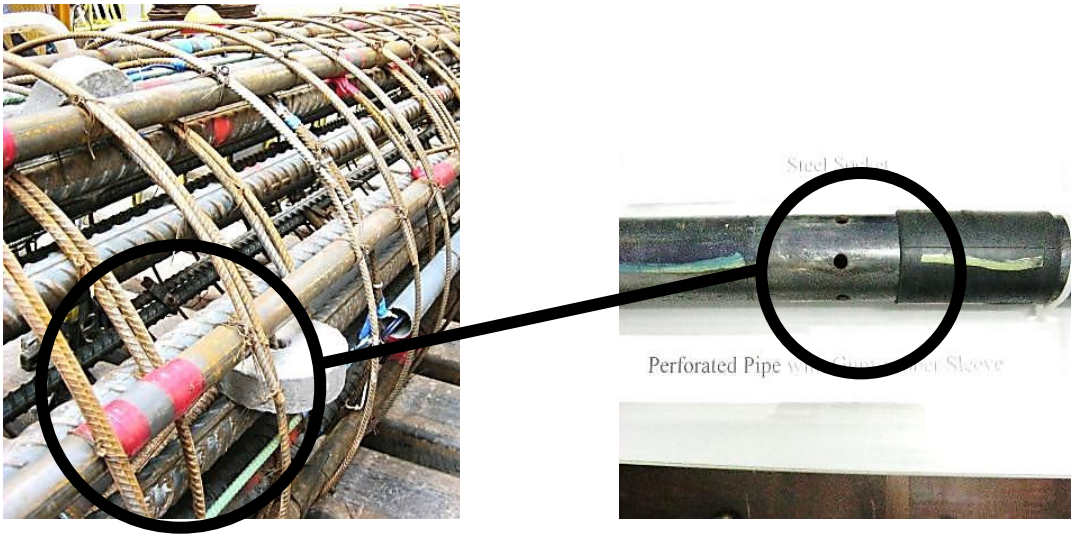

Plate 8: Tube-A-Manchette (TAM) pipe

Plate 9: The water cracking process

Plate 10: Pressure Grout Injection

Plate 11: Vibrating wire strain gauge attached to sister bar inside the trial pile

The pile head settlement during the load test is summarised in Table 4. Both the actual pile head settlement and residual settlement are less than a quarter of the allowable.

Table 4: The allowable and actual maximum settlement of T-P01 & T-P02

Pile No.	Test load	Allowable Maximum Settlement (mm)	Actual Maximum Settlement (mm)	Allowable Maximum Residual Settlement (mm)	Actual Maximum Residual Settlement (mm)
T-P01	27,000kN	76.1	21.2	N / A	4.2
T-P02	31,000kN	83.8	20.1	24.0	3.6

The results of the loadings along the pile shaft, estimated from strain gauge readings, are presented in Figure 9 and Figure 10.

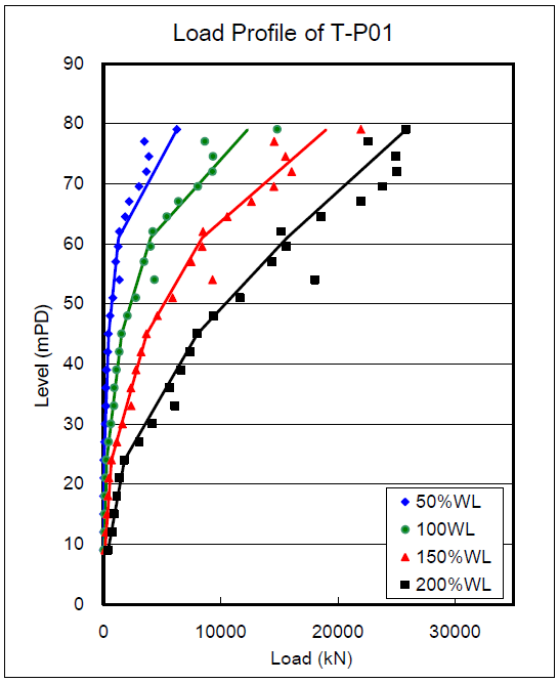

Figure 9: Load versus depth profile of T-P01

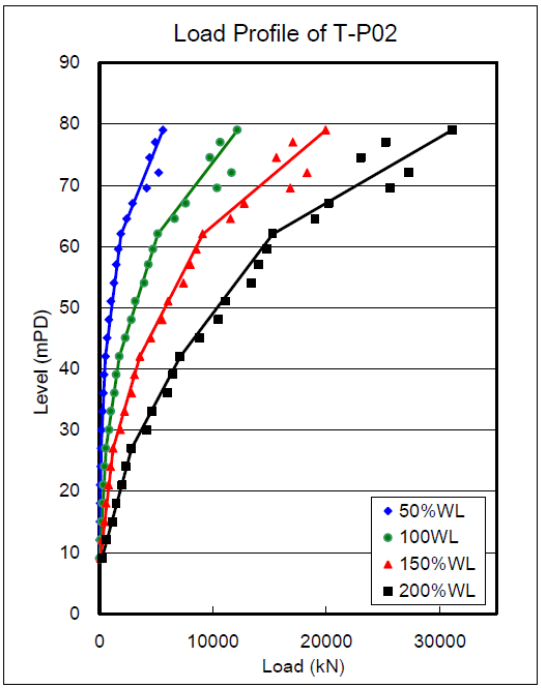

Figure 10 : Load versus depth profile of T-P02

As shown in the Figure 9 and Figure 10, there is no significant difference between the piles with and without soft toe. This shows that the end bearing capacity could hardly be mobilised even under the maximum test load.

The test results are divided into 6 groups (Zone A – Zone F) according to their depths and SPT-N values. The depth and the corresponding N value of each zone are shown in Table 5.

Table 5: The depth and the corresponding N values of different zones

	Level (mPD)		Material	Average SPT-N value	
	From	To		T-P01	T-P02
Zone A	75.5	60	Colluvium	33.4	23.9
Zone B	60	50	CDG	29.9	38.2
Zone C	50	40	CDG	53.4	73.4
Zone D	40	30	CDG	100.8	84.8
Zone E	30	20	CDG	129.9	167.4
Zone F	20	10	CDG/HDG	196.8	198

Based on the strain gauge readings, the mobilised shaft resistance along the pile segments can be estimated and the friction coefficients of the two trial piles are shown in Figure 11 and Figure 12. T-P01 and T-P02 have achieved shaft resistance of up to 4.6N kPa and 8.3N kPa in Zone A (Colluvium) under 200% working load; and 4.1N kPa and 3.4N kPa in Zone B (CDG), as shown in the corresponding figures.

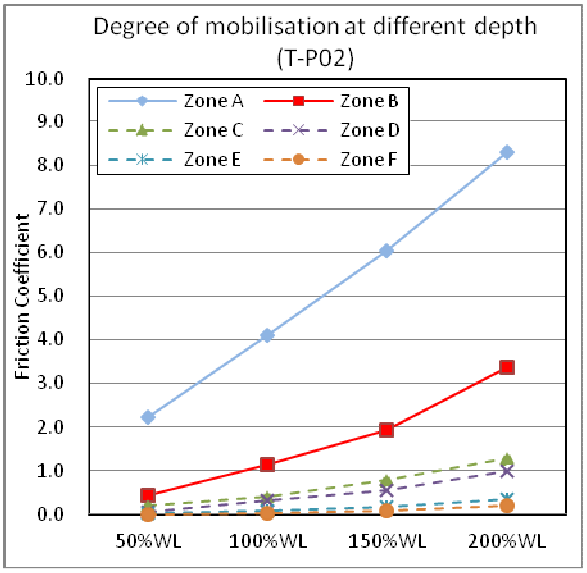

Figure 11: Friction coefficient of T-P01 under different test load

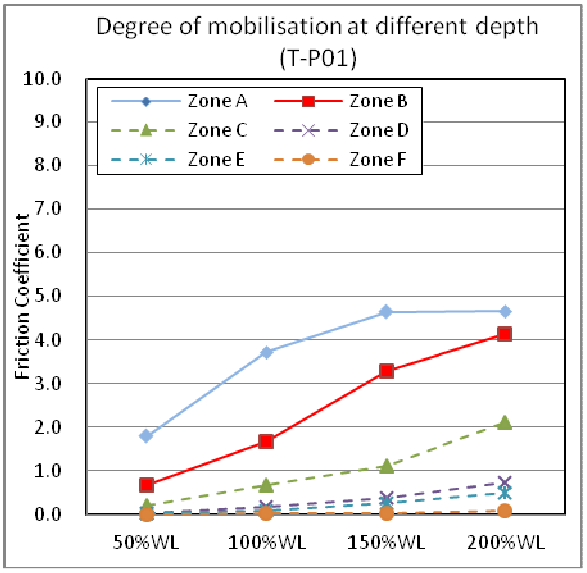

Figure 12 : Friction coefficient of T-P02 under different test load

It can be seen that shaft resistance is substantially mobilised for the portion embedded in Colluvium (Zone A). The test results of T-P01 also indicated that the shaft resistance at Colluvium was almost fully mobilised at 4.6N. The upper CDG portion (Zone B) of T-P01 and T-P02 were also substantially mobilised to 4.1N and 3.4N. However the trend shown in Figure 13 and Figure 14 illustrates that the shaft resistance of the shaft grouted bored pile was not fully mobilised.

For the lower portion of both trial piles embedded in CDG with higher SPT-N values, the shaft resistance was mobilised to a limited extent as indicated by the dotted lines. This implies that extra shaft resistance could be mobilised if the applied load was further increased. The designed friction coefficient and the test results are summarised in Table 6.

Table 6: Summary of Designed Friction Coefficient and mobilised Friction Coefficient

	Friction coefficient			Capping Ultimate Friction
	Designed	Mobilised		
		T-P01	T-P02	
Colluvium	3.6**	4.6	8.3*	140kPa
CDG	2.4**	4.1*	3.4*	140kPa (SPT-N value capped at 58.3)

* The shaft resistance of the trial piles was not fully mobilised
** A FOS of 2.0 is adopted for estimating pile working load capacity

It seems reasonable to review the values of friction coefficient under plain and post shaft-grouted conditions. The test results of T-P01 and T-P02 are compared with the data extracted from a literature by Ng et. al (2000), and also with the test results of a plain frictional bored pile of the Robinson Road development mentioned previously in section 2.3.2. The comparison is shown in Figure 13

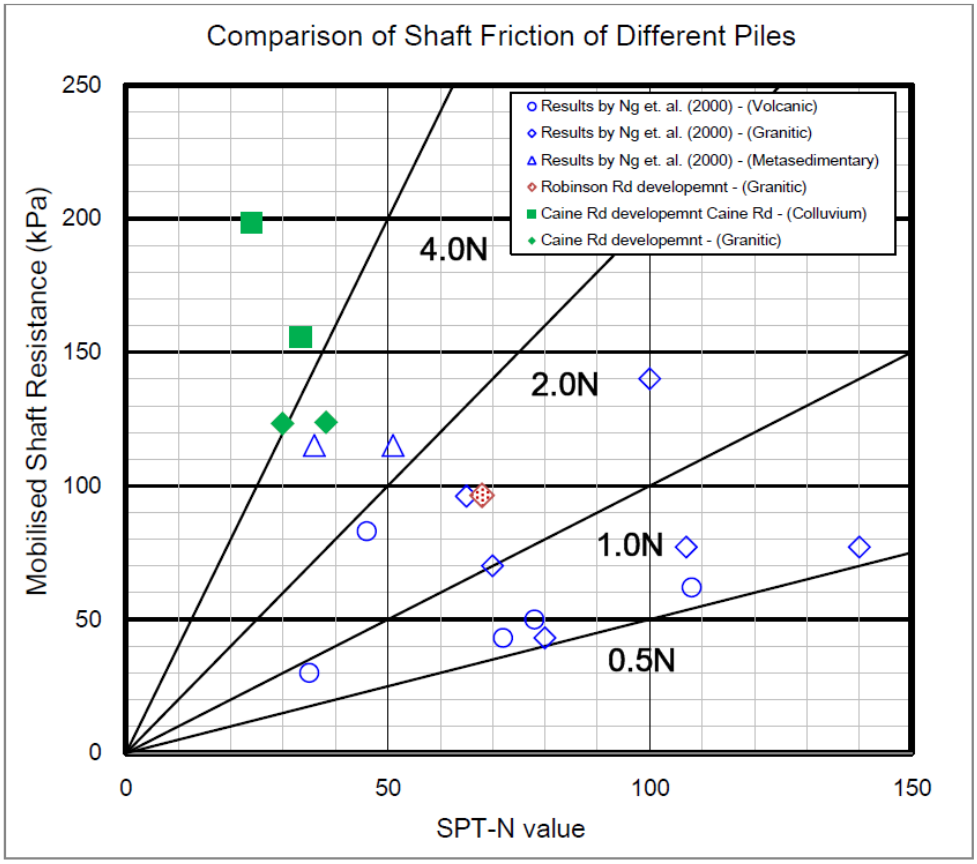

Figure 13: Comparison of shaft resistance of shaft grouted piles and plain frictional bored piles

As shown in Figure 15, the friction coefficient with the average SPT-N value of metasedimentary , granitic and volcanic saprolites were reviewed by Ng et. al (2000). The friction coefficient of the plain friction bored piles embedded in both granitic and volcanic saprolites mainly lies between 0.5N and 2.0N, as reported by Ng et. al, while the shaft resistance mobilised in metasedimentary saprolites is relatively greater. The results from the shaft grouted bored piles embedded in CDG, with N value less than 40, at Caine Road (T-P01 and T-P02)

are approximate 3.5N - 4.0N. This illustrates that shaft resistance of shaft grouted piles can be few times greater than that of plain frictional piles embedded in saprolite, not to mention that the shaft resistance had not been fully mobilised. For the portion of pile which is embedded in CDG with higher N values, the shaft resistance is mobilised to a very small extent.

3 SMALL REPLACEMENT PILES

3.1 Mini piles

The construction of mini piles only requires relatively small mechanical plants. This provides a solution to construction works for sites in hilly terrain with restricted working space or accessibility difficulties. It also minimises the environmental disturbance. In cases of hilly terrain, the drilling equipment can be hung from the end of jib with main body of the crane at level area.

Minipiles have been in use in Hong Kong since 1970's and the most common mini-pile in Hong Kong nowadays is the 219mm diameter hollow section with four numbers of T-50 reinforcement bars. This arrangement provides an allowable working load of approximately 1400kN. In recent years, the loading capacity were increased to 2350kN by using 3 numbers of 63.5mm diameter high yield thread bar (grade 555/700 i.e. fy = 520MPa) in a 273mm casing. The configuration of this minipile is shown in Figure 14.

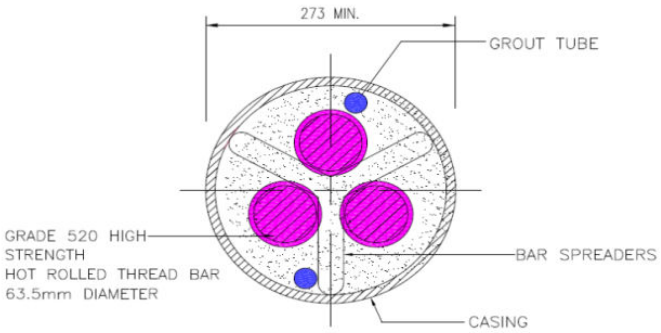

Figure 14: Configuration of a minipile with 63.5mm diameter high strength threadbars

Conventionally, minipiles are not designed to resist bending moments in view of the limited bending capacity of the reinforcement bars. To resist lateral loads, they normally have to be raked so that their own axial load capacity can be utilised. Nonetheless, approval from Buildings Department has been given to a development in Central to allow the casing to provide the bending resistance in SEC 2/2008 (BD 2008).

3.2 Prebored H Piles

Conventional driven H piles could be damaged by underground boulders and generates significant nuisance to the neighbourhood. Prebored H Piles were therefore introduced in the 1980s to overcome these problems. The pile shaft is formed by boring and steel H section is inserted afterwards. Better than minipiles and similar to driven H-piles, prebored H-piles possess higher axial load capacity and bending resistance.

Overburden Drilling with EXcentric bit (ODEX) method was widely adopted for shaft boring works. The Odex system consists of a bottom pilot bit and an eccentric "swing out" reamer bit which rides along its shaft. The bottom pilot bit and the eccentric reamer are connected with a casing shoe with guide device ahead of the casing tubes bottom. The eccentric reamer swings out and drills a hole slightly larger to allow the progression of the casing by gravity. ODEX uses compressive air as flushing medium. Exhaust air from the hammer is blown directly into the ground at the centre of the cutting head, which may bring excessive cuttings as well as loose soils to the ground surface, causing ground loss or wash out zone around the drill bit. It is sometimes unavoidable that some cuttings would be flushed up outside the casing as the drillhole is made slightly larger

than the casing.

In 2008, two serious incidents of ground movement occurred during the preboring works. Significant ground subsidence occurred next to a construction site at Queen's Road, Central. Another incident happened in Sheung Wan - "A multi-storey crack up to 15cm wide opened up on Tuesday between the Lee Hing Building at 98 Connaught Road West and a taller structure, standing wall-to-wall with it next door." (SCMP 2008).

Since 2008, the ODEX method is generally not allowed in urban areas, especially near old buildings. In order to minimise ground loss and the risk of overbreaking, the concentric drilling system is often adopted. It creates less disruption to the ground and greatly reduces ground loss.

Concentric drilling system consists of a hammer operating inside a steel casing, a centre bit and a ring bit. The hammer is driven by high pressure air, usually at 7 to 18 bars. With the rotary motor and hammer in action, the drill bit advances simultaneously and drives the steel casing downwards. High pressure air vents out through an orifice in the drill bit to air-lift the soil and rock cuttings out of the bored hole, usually through gap between the hammer and the steel casing. The return flushing air is guaranteed to be forced up within the casing pipe immediately after exiting the pilot bit. This made concentric drilling better at minimising the disturbance to the surrounding ground during the drilling process (Wong et. al. 2011b). However, the ring bit is left in place and sacrificial.

The ODEX and Concentric drilling system (Robit) are shown in the schematic diagrams in Plate 12 and Figure 15 respectively.

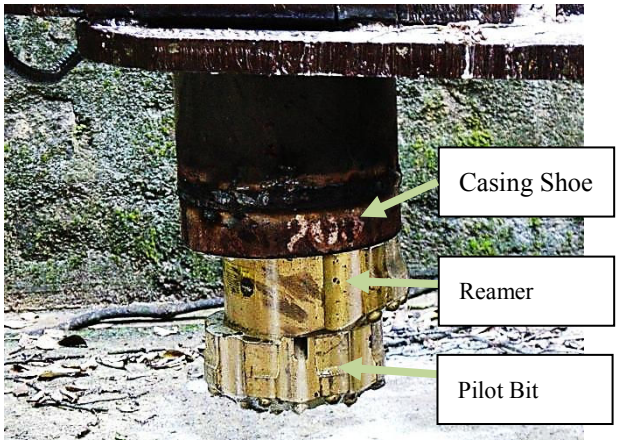

Plate 12: Annotated photo of ODEX system

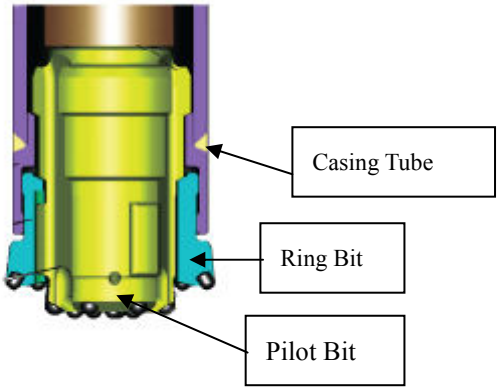

Figure 15 : Schematic diagram of Robit system (with courtesy of www.holeproduct.com)

3.3 Shaft grouted prebored H-piles

Prebored H-piles are conventionally socketed in bedrock and their loading capacities are mainly derived from rock socket friction. However, for developments in area with extremely deep rockhead, construction of pile to reach bedrock is impractical, such as a development project within the Central - Sheung Wan Strip mentioned in section 2.3.1.

The development for a 25-storey residential tower is located in the Mid-levels where bedrock is over 80m below ground level. The layout plan and geological profile of the site is shown in Figure 16 and Figure 17. The restricted site access and limited working space inhibits the use of large diameter bored piles. Conventional small diameter friction piles do not have the necessary capacity to support the building. In view of this, shaft grouted frictional pre-bored steel H-piles were adopted. The configuration of the Shaft grouted prebored H-pile is shown in Plate 13 and Figure 18.

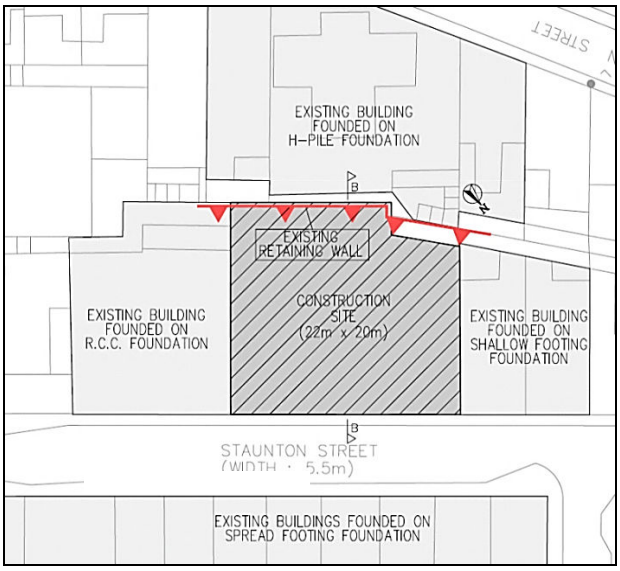

Figure 16: Site layout plan

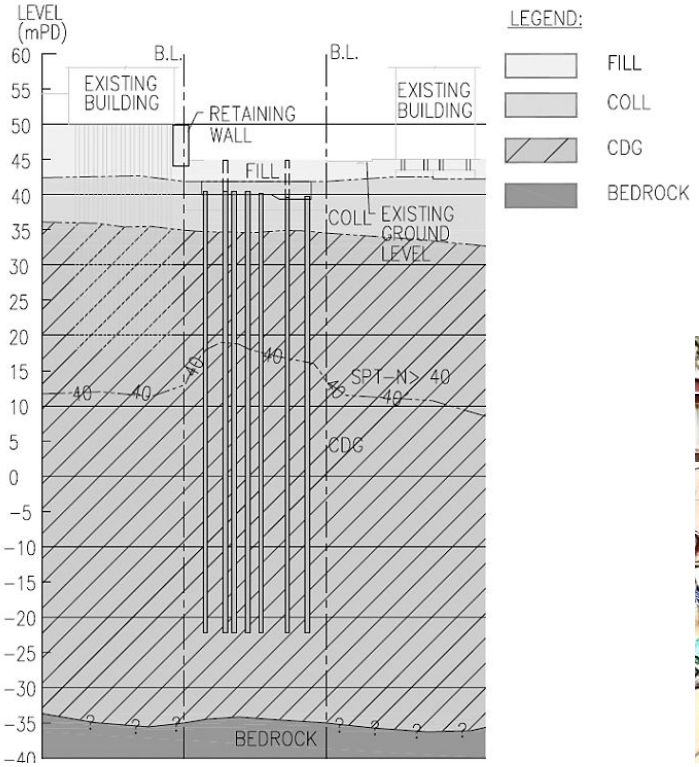

Figure 17: Geological profile of the site

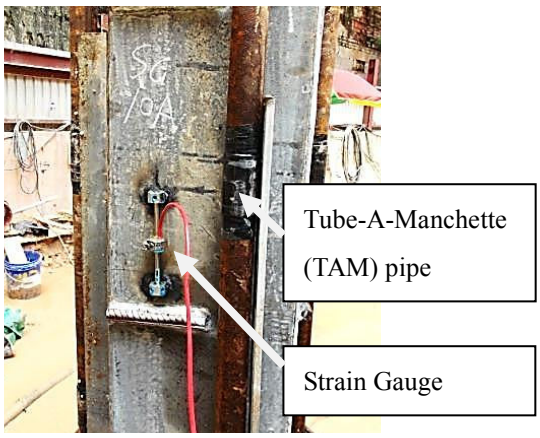

Plate 13: Details of Trial Pile TP2

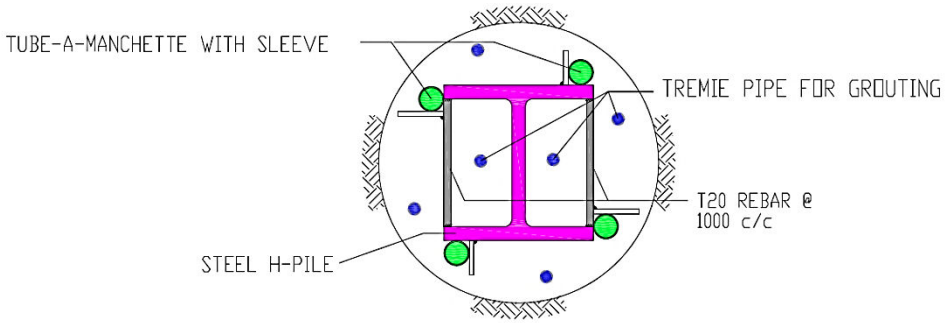

Figure 18: Typical section of a shaft grouted frictional pre-bored steel H-pile

Shaft grouted frictional prebored steel H-pile is not a recognised foundation under the current list of Recognised Types of Piles in Buildings Department. Loading test on 2 full scale instrumented trial piles were carried out to determine the shaft resistance and verify the design assumptions. The pile load profile of the two trial piles are shown in Figure 19 and Figure 20.

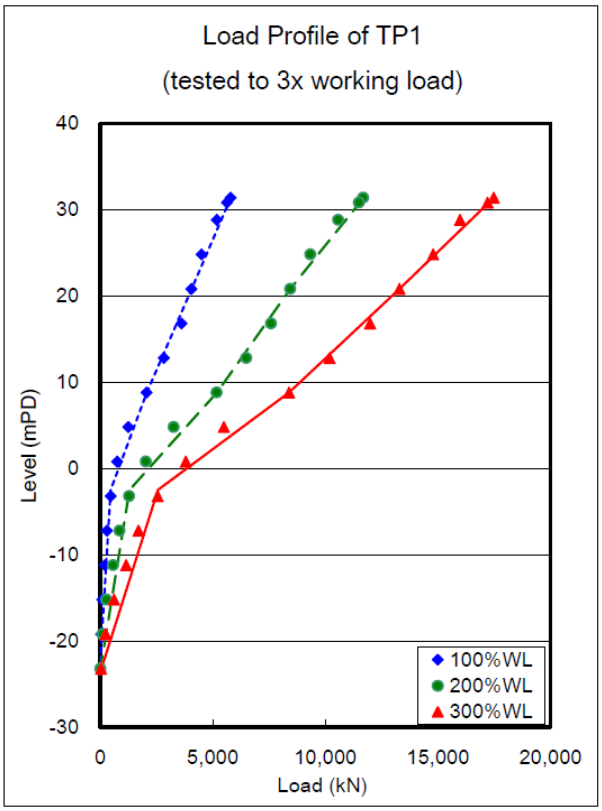

Figure 19: Pile load profile of TP1

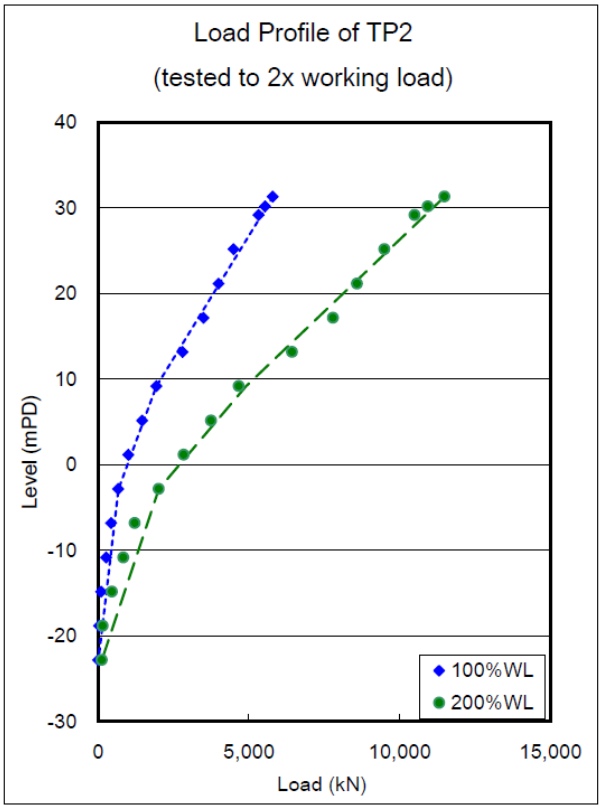

Figure 20: Pile load profile of TP2

The results are divided into 8 groups (Zone A – Zone H) according to the SPT-N value. The shaft resistance of the bottom portion (Zone E - H) of the trial piles was mobilised to a very limited extent and therefore not shown for clarity. The depths and the corresponding N values of Zone A - D are shown in Table 7.

Table 7: The depth and the corresponding N values of different zones

T-P01	Level (mPD)		Average	T-P02	Level (mPD)		Average
	From	To	N value		From	To	N value
Zone A	32.4	28.8	26	Zone A	32.4	29.2	19.5
Zone B	28.8	20.8	14.3	Zone B	29.2	21.2	23.3
Zone C	20.8	12.8	40	Zone C	21.2	13.2	36
Zone D	12.8	4.8	61	Zone D	13.2	9.2	50.5

The trial piles TP1 and TP2 have achieved shaft resistance up to 12.3N kPa and 12.6N kPa respectively under 300% and 200% working load, as shown in Figure 21 and Figure 22. The trial piles show consistent results. The shaft resistance contributed by the colluvium layer was not taken into account in the design. In order to determine the friction value without the influence of the colluvium layer, the corresponding portion was sleeved.

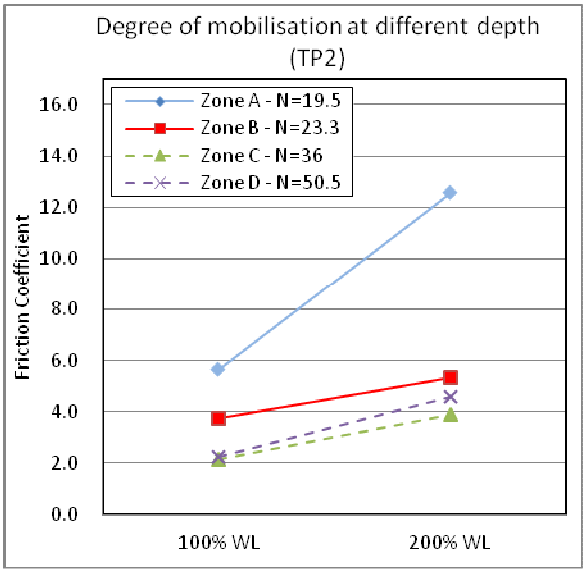

Figure 21 : Summary of frictional coefficient among different zone for TP1

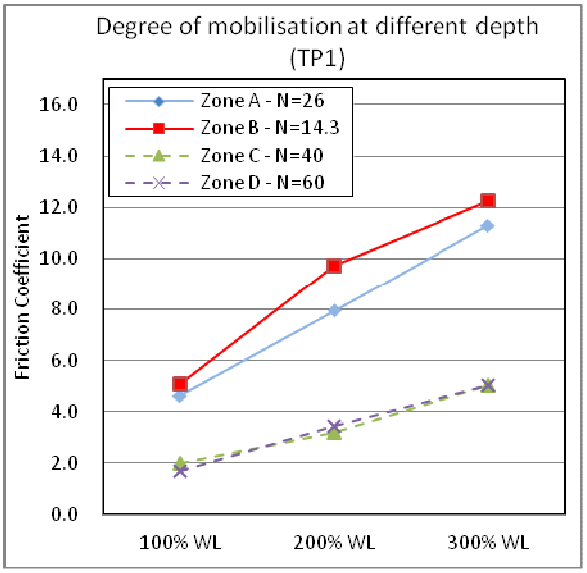

Figure 22 : Summary of frictional coefficient among different zone for TP2

Similar to the shaft grouted bored piles mentioned previously, the trend in Figure 21 is linear, which suggests that the shaft resistance of the piles was not fully mobilised.

The settlement of the piles is shown in Table 8. The actual settlement of the trial pile TP1 at 300%WL (18,000kN) is less than a quarter of the allowable.

Table 8: Actual settlement at100%, 200% and 300%WL for TP1 & TP2

Pile Mark	Pile Head Settlement			Allowable Settlement under Peak Load
	1x WL (6,000kN)	2x WL (12,000kN)	3x WL (18,000kN)	
TP1	5.5mm	10.8mm	16.8mm	71.9mm
TP2	10.5mm	21.0mm	--	92.3mm

The designed friction coefficient and the test results are summarised in Table 9.

Table 9: Summary of Designed Friction Coefficient and mobilised Friction Coefficient

	Friction Coefficient			Capping Ultimate Friction
	Designed	Mobilised		
		T-P01	T-P02	
CDG	5N**	12.3N*	12.6N*	200kPa (SPT-N value capped at 40)

* The shaft resistance of pile was not fully mobilised
** A FOS of 3.0 was adopted for estimating the working load capacity

The actual shaft resistance of T-P01 mobilised under 300% working load is shown in Table 10. Although the pile capacity was not fully mobilised, the shaft resistance is mobilised up to around 300kPa, which is significantly greater than the approved ultimate frictional force of 200kN. This suggests that there should be room for increasing the allowable friction.

Table 10: The mobilised shaft resistance of the trial piles (T-P01)

Zone	Mobilised Shaft Resistance (kPa)	SPT-N value	Friction Coefficient
A	293.5	26.0	11.3
B	176.0	14.3	12.3
C	202.1	40.0	5.1
D	306.6	61.0	5.0

4 DISPLACEMENT PILES

4.1 Percussive piles

Before the 1970s, displacement piles, such as Precast Reinforced Concrete Piles, Precast Prestressed Spun Concrete Piles and Driven Cast-in-place Concrete Piles were widely used in Hong Kong. However, due to various reasons, they have phased out. Nowadays, only Driven H Piles are still in common use.

The major drawback of percussive piles is the noise and vibration during percussion, as well as the emission of excessive black smoke, which lead to neighbourhood's resistance. The use of diesel hammers is restricted by the Noise Control Ordinance (EPD 2006). Nowadays, displacement piles are often driven by hydraulic hammers (shown in Plate 14).

Plate 14: Photo of a hydraulic hammer

4.2 Jacked piles

Jacked piles have been widely used in China and Southeast Asia, but it is relatively new to Hong Kong. Jacked piles were first officially used in Hong Kong in 2000 as part of the foundation strengthening works of two existing building blocks in Tin Shui Wai.

Jacked piles are installed into the ground by hydraulic pressure. As shown in Plate 15, the steel H-pile was being pressed into ground by hydraulic jacks with kentledge as counterweight. The jacking process is quiet and vibration-free. Virtually no nuisance would be made during the jacking process. This makes jacked piles particularly suitable for noise and vibration sensitive areas.

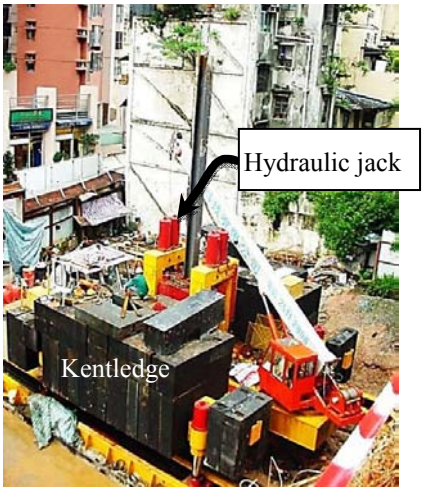

Plate 15: Pile jacking machine at Hollywood Road Site

Jacked piles are not common in Hong Kong as the size of the jacking machine has limited its use in urban area. It might be difficult to install the piles near site boundary. Moreover, underground obstructions could cause serious problems to the jacking process if they are deep under the ground.

Following jacked piling in Tin Shui Wan, a private residential development in Hollywood Road also adopted jacked piles in the foundation system. The area became very vulnerable to any drilling or vibrating operation after significant ground settlement and horizontal movement had been recorded during foundation works at a site opposite the road. Therefore, the jacking technique was adopted in order to reduce the vibration and minimise the adverse effects on the surrounding structures. Steel H-piles were jacked to the approximate founding level using a jacking machine. However, the final set was still done by drop hammers to fulfil the statutory requirements.

Since 2000 to 2003, jacked piles were used in several private and HKHA developments (Chan, 2005). The construction methods of jacked piles in these projects were similar to that adopted in the Hollywood Rd project. Pile buckling was also reported by Chan (2005). This was caused by the formation of voids around the H-pile during pile jacking. This can be solved by filling the voids with sand during the jacking process.

From the basics of soil mechanics, pre-loading is an effective way of reducing the creep settlement as the settlement during reloading would be much smaller. Li and Lam (2011) reported that, in the Lee On Estate project, a preloading force of 2.3WL had significantly reduced the residual/creep settlement of jacked piles during static load test under 2WL. The results satisfied both the total pile head settlement and residual settlement criteria. With the development of the pre-loading technique, jacked piles that are solely installed by jacking, without involving drop hammers in the final set, were successfully installed in ArchSD and HKHA projects.

Recently, jacked piles without final set by drop hammer were also adopted in a private development at Tai Po (BD 2011). The termination criteria for jacking were slightly different from that stipulated in the particular specification for Jacked Steel H-piles of ArchSD (ArchSD, 2008). The termination criteria of jacked piles set

out by the particular specification for Jacked steel H-piles (ArchSD 2008) and the summary decisions of the Structural Engineering Committee SEC 02/2011 (BD 2011) are summarised in Table 11.

Table 11: Comparison of termination criteria of jacked piles

Criteria	Architect Services Department - Particular Specification	Buildings Department (BD) - SEC 02/2011
Preloading	Stage 1: 2.3WL Stage 2: 2.2WL	3.05WL
Holding time	Stage 1: Suitable hold time determined by the Contractor Stage 2: Hold until the rate of settlement is less than 5mm in 15 minutes	Hold until the rate of settlement is less than 5mm in 15 minutes (minimum 30 seconds)

Despite the fact that fully jacked piles had been approved by the Buildings Department in a private development project, jacked pile remains unlisted in the recognised pile type under the central data bank of the Buildings Department. The acceptance of jacked pile is still considered on a case by case basis.

5 SHALLOW FOUNDATION

5.1 Project description

In recent years, there have been more heritage conservation projects. The Urban Renewal Authority (URA) project at Mallory Street, Wan Chai, was a Grade II Historic Building, also known as the "Green House". It was originally a series of four-storey pre-war tenement buildings with timber flooring and load bearing brick walls. Desk study revealed that the existing site was reclaimed in 1863 and that the existing buildings were built in 1910s. A typical geological section is shown in Figure 23.

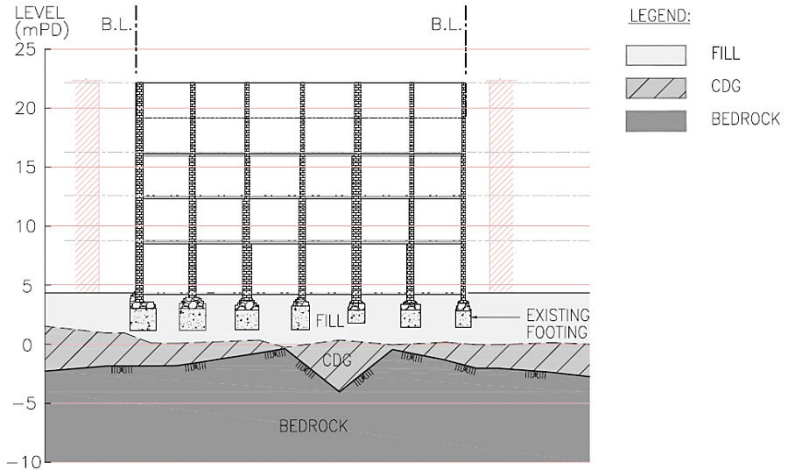

Figure 23: Ground profile underneath the "Green House"

The revitalisation project involved the change of usage from residential to cultural/commercial. The increase in imposed load, together with the structural strengthening works, would cause the soil bearing pressure underneath the strip footings to double to nearly 200kPa. Since the footing are resting on reclaimed fill (SPT-N = 4-8), strengthening works have to be carried out.

Conventional foundation strengthening works, such as underpinning using mini-piles, was considered to be too risky as the old brittle structure could be damaged during the invasive pile installation. The low headroom would also impose restrictions on the pile installation.

Ground improvement by grouting was adopted to increase the bearing capacity of the founding stratum of the footings and to reduce the total and differential settlement of existing footings under the additional loading (Wong & Leung 2010). This was the first of its kind for which the approval of the Buildings Department was sought.

5.2 Grouting

In order to have better penetration into the soil, fine milled Portland cement (Micro-fine cement) was chosen for this project. The grain size of this micro-fine cement is 98% passing 20 μm sieve, which is 4.5 times smaller than ordinary Poland Cement. The comparison in grain size of Ordinary Poland Cement and Micro-fine cement is shown in Table 12.

Table 12 : comparison of Ordinary Poland Cement and Micro-fine cement

Type of Cement	Grain Size	Specific Surface Area (m^2/kg)
Ordinary Poland Cement	98% (<90μm)	320 – 380
Micro-fine cement	98% (<20μm)	450 – 650

The grouting pressure adopted was the effective overburden pressure, σ_v', allowing for the effect of bearing pressure from the existing building. The comparison between designed grouting pressure and actual grouting pressure are shown in Figure 24. It can be seen that the actual grouting pressure was larger than the calculated effective overburden pressure. This was to cater for the head loss during the grouting process and to increase the penetration effectiveness of the grout into the soil underneath the existing footing.

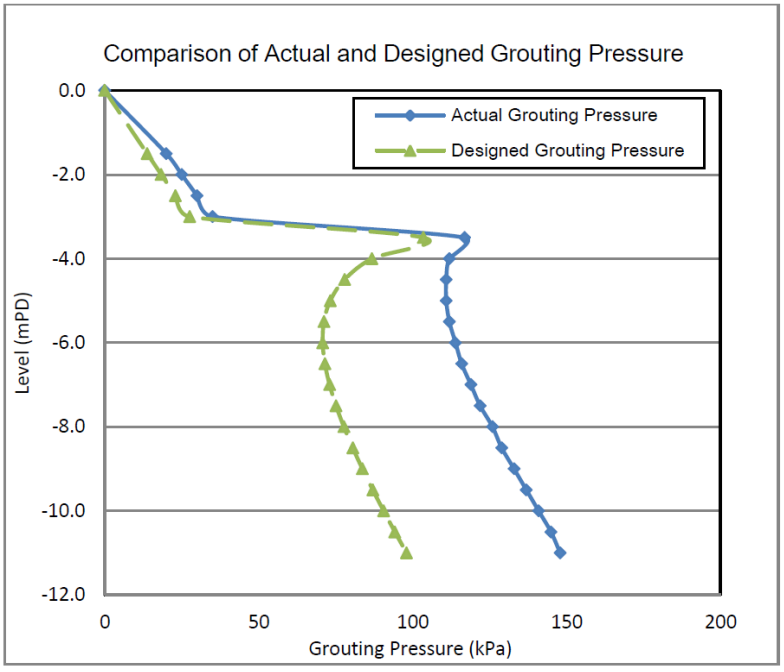

Figure 24 : Comparison between designed grouting pressure and actual grouting pressure

5.3 Preloading

After completion of grouting works, loading tests were carried out concurrently on all strip footings. The arrangement is shown in Figure 25. The loading test was effectively a full scale preloading to the existing footings to verify the effectiveness of the grouting works. Less than 1mm settlement was recorded in the loading test, which confirms the effectiveness of the strengthening works.

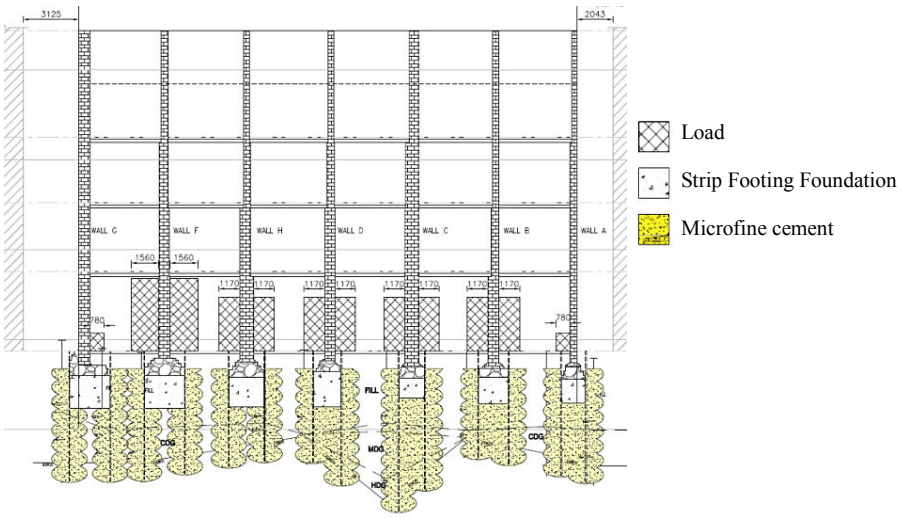

Figure 25: The arrangement of preloading

The foundation strengthening works was successfully completed and the revitalised building is now in use. The comparison of the building before and after the revitalisation works is shown in Plate 16.

Before After

Plate 16: Comparison of the building before and after the revitalisation works

6 CONCLUSION

Owing to the increasing site constraints, more difficult ground conditions, less public resilience to nuisance caused by constructions and more stringent statutory control, the foundation works have advanced in both design approach and installation techniques. Friction piles, plain or shaft-grouted, or whether it be barrettes, small or large replacement piles, are gathering more popularity. When more test data become available, the friction values can be reviewed and adjusted to achieve more cost efficient design. Jacked piles can provide a relatively quiet environment during its installation process. In light of the higher public demand for a quieter environment, there may be room for further exploring the use of this type of piles.

REFERENCES

Architectural Services Department 2008. Particular Specification for Jacked steel H-piles. *Available at http://www.archsd.gov.hk/media/11320/e146.pdf* (accessed on 10 May 2014)
Buildings Department. 1990. *Practice Note for Authorised Persons and Registered Structural Engineers 141 (1990)* Buildings Dept., Hong Kong.
Buildings Department. 2000. *Practice Note for Authorised Persons and Registered Structural Engineers 66 (June 2000) Buildings Dept*., Hong Kong.
Buildings Department. 2004. *Code of Practice for Foundations*. Buildings Dept., Hong Kong.
Buildings Department. 2008. The summary of decisions of the structure engineering committee SEC 02/2008. Available at http://www.bd.gov.hk/english/inform/BC/SEC08-02.pdf (accessed on 10 May 2014)
Buildings Department. 2011. The summary of decisions of the structure engineering committee SEC 02/2011. Available at http://www.bd.gov.hk/english/inform/BC/SEC11-02.pdf (accessed on 10 May 2014)
Chan, F. 2005. Termination Criteria for and Behaviour of Jacked Piles in Completely Decomposed Granite, *MPhil Thesis, HKUST*
Chan, S.T., Wong, F. C.C. & Tsoi, M.W.T. 2002. Trial of jack piling in a Housing Authority Foundation Project. Jack Piling in Hong Kong. *Centre for Research & Professional Development:* 15-20
Choy, K.K. & Wong, C.M. 2007. Development and Statutory Control of Pile Foundations for Private Buildings in Hong Kong since the Seventies. *Proceedings of the 27th Annual Seminar of the Geotech. Div. of the Hong Kong Instn. Engrs*, Hong Kong: 119-124.
Environmental Protection Department. 2006. *A Concise Guide to the Noise Control Ordinance*. Ninth edition.
Hong Kong Government. 1975. Building (Construction) Regulations. *Laws of Hong Kong*, Chapter 123. Hong Kong Government.
Li, V. & Lam, J. 2011. Development of Jacked Piling in Hong Kong, *The 2nd VLA Seminar, "New Development in Jacked Piling"*: 88-116.
Ng, C.W.W., Rigby, D.B., Li, J.H.M., Yau, T.L.Y., Lee, S.C. & Calton. C. 2000. Side Resistance of Large Diameter Bored Piles Constructed Under Water in Saprolites.
Proceedings of the 19th Annual Seminar of the Geotech. Div. of the Hong Kong Instn. Engrs, Hong Kong: 137-144.
Plumbridge, G.D., Littlechild, B.D., Hill, S.J. & Pratt, M. 2000. Full scale shaft grouted piles and barrettes in Hong Kong – A first. *Proceedings of the 19th Annual Seminar of the Geotech. Div. of the Hong Kong Instn. Engrs*, Hong Kong: 157-166.
SCMP. 1996. Death site contractors accused of breaches. *South China Morning Post*, 3rd September, 1996.
SCMP. 2008. Residents evacuated as building tilts. *South China Morning Post*, 10th July 2008.
Sze, J.W.C., Lam, A.K.M., Pappin, J.W. & Chan, K.M. 2007. Design & construction of shaft-grouted friction barrette in Tung Chung Designated Area. *Proceedings of the 27th Annual Seminar of the Geotech. Div. of the Hong Kong Instn. Engrs*, Hong Kong: 299-304.
Wong, C.M., Lee, C.T.L. & Ting, R.C.M. 2011a. Construction of Hand-dug Caissons for Slope Stabilization near the Peak Lookout. *Proceedings of the 31st Annual Seminar of the Geotech. Div. of the Hong Kong Instn. Engrs*, Hong Kong: 100-107
Wong, C.M., Lee, C.T.L. & Ting, R.C.M. 2011b. Innovative Materials and Drilling Method adopted for Soil Nailing Works at Po Shan Road. *Proceedings of the 31st Annual Seminar of the Geotech. Div. of the Hong Kong Instn. Engrs*, Hong Kong: 108-113

Wong, C.M. & Leung B.C.H. 2010. Structural Assessment of Century-old Tenement for Revitalization Purpose. *Proceedings of HKIE/IstructE Joint Struct. Div. Annual Seminar 2010*.

Modelling of Combined Piled-Raft Foundations using 3-D FEM

William W.L. Cheang
Plaxis AsiaPac, Singapore

Noppadol Pien-wej
Asian Institute of Technology, Thailand

Harry S.A. Tan
National University of Singapore

Kamol Almornfa
Kasetsart University at Kampangsaen

ABSTRACT

Piled raft foundations have been recognised as an economical method of supporting top super-structures without compromising the safety and performance. The challenge in piled-raft foundation design and analysis is simulating all the necessary feature of interactions of such foundation system. Piled-raft foundations has proven to be a viable and cheaper alternative to conventional pile foundation. The strategy of using piled raft foundation is that the coupled response of raft, piles and supporting soil are taken into account directly.

Three dimensional finite element analyses, which falls under the rigorous computer-based methods, are normally performed to ascertain the complete response of the piled-raft. In principle, the use of 3-D FEM removes the need for approximations and assumptions. With advancements in computer science, pre/post-processing and kernel code-line configurations complex piled-raft foundation boundary value problems can be solved within a reasonable analysis-design turnaround time.

In this paper, a benchmark analysis (Section 2: Numerical Experiments 1) is first performed to test the validity of the finite element code in modelling a single pile. Subsequently, a series of finite element experiments (Section 3: Numerical Experiments 2) were conducted to investigate the performance of various analytical methods on the modelling of pile and piled-raft foundations (Simple to Rigorous methods) on pile load sharing, bending moments and deflection across the raft. The experiments also investigate the influence of reducing of the number of piles on settlement and factor-of-safety. In the final study (Section 4: Case History), the authors will highlight a case where a piled-raft foundation in Bangkok subsoil were optimised to obtain the best economy. The number of piles, size and thickness of the raft were reduced to a point where they obtained factor-of-safety and deflection is within engineering tolerance.

1 INTRODUCTION

In the conventional design of pile foundations, the piles are designed to share the load at ultimate state and the pile cap would be designed to link the piles together. The contribution of the pile cap to bearing capacity is not included in the design. A piled raft is a raft foundation that has piles to reduce the amount of settlement. The raft foundation and the piles would be designed to act together to ensure the required settlement is not exceeded. A significant part of the bearing capacity comes from the raft and piles. This later method is also known as the Combined Pile-Raft Foundation (Katzenbach and Deepankar, 2013).

The authors will highlight a case where a piled-raft foundation in Bangkok subsoil were optimised to obtain an economical design. The number of piles, size and thickness of the raft were optimised to the required engineering tolerance and factor-of-safety. This paper shows that the usage of advanced 3-D finite element analysis can be routinely applied in the design of Piled-raft foundations. The concept of Piled Raft foundation

will not be illustrated in detail here as various research and workers have worked on this for the past two decades (Poulos, 2001A, Poulos 2001B, Reul & Randolph, 2003, Lee at.al, 2010).

2 NUMERICAL EXPERIMENTS NO.1

2.1 Single Pile Models

In any complex soil-structure-interaction problems it is essential that the main components of the model are validated individually (i.e. single pile response) prior to its incorporation into the global geotechnical FE model (Tan, 2014). An overview of the approaches suitable for validation and calibration are given in the following subsections.

2.2 Axi-symmetric Single Pile model.

Modelling a single vertical pile in axi-symmetric space is the most simple. It can be used to study the capacity of the pile and also shear stress transfer along the pile. The axi-symmetric 2D model is always used as a first approach to evaluate the FE model and back-analysis of in-situ pile load test. The later is useful for the purpose of calibrating model parameters for subsequent global FE model.

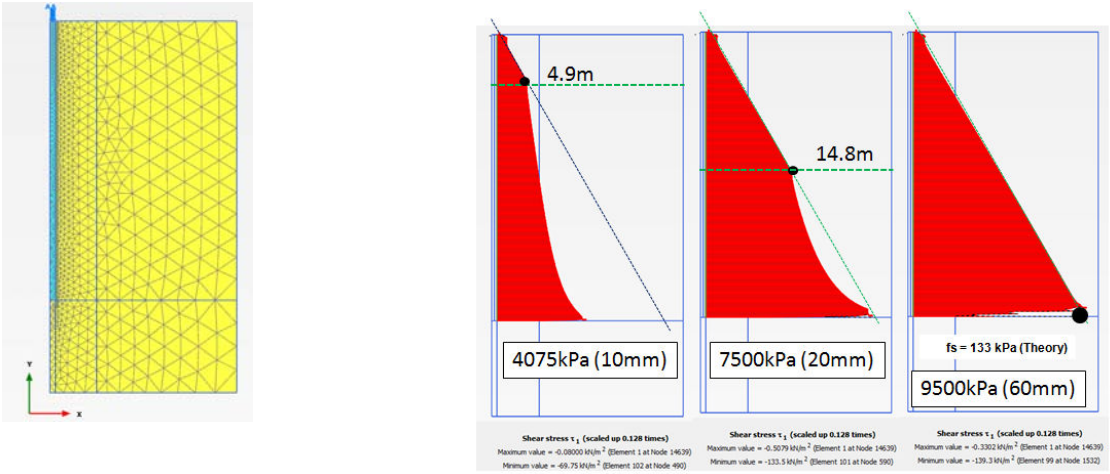

A) Numerical Pile Load Test: 2-D Axi-symmetry Model

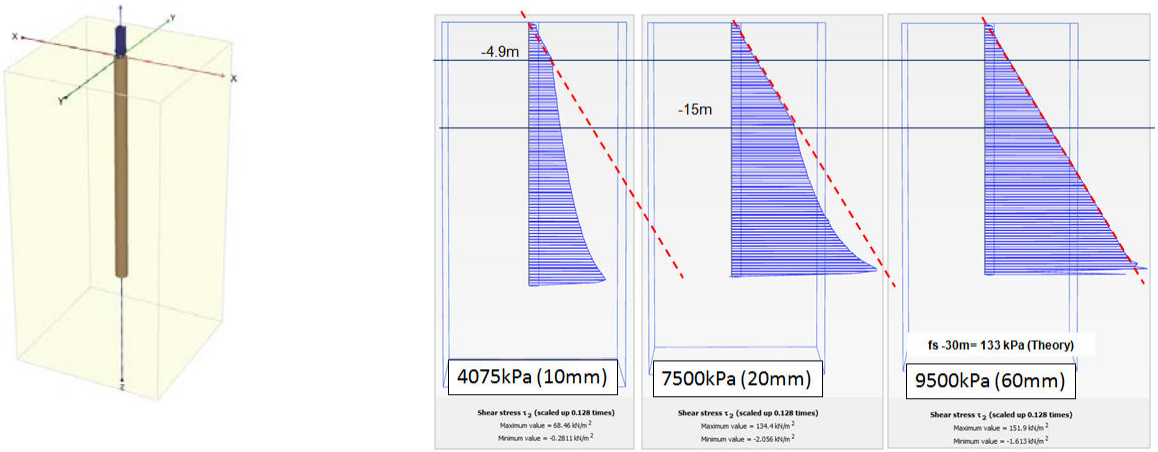

B) Numerical Pile Load Test: 3-D Solid (Continuum) Model

Figure 1: Numerical pile load test in 2-D and 3-D space

2.3 3-D Single Pile model

In this work all the bored piles were modelled using the continuum (solid pile) approach which means the geometry of the pile is explicitly included and descretised. To ensure correctness we suggest that a simple calibration and "confidence" analysis is made to compare a 3D-Solid pile model with a 2D Axi-symmetry pile model. These two models were then benchmarked against the theoretical ultimate shaft and end bearing capacity for generalised cohesive and sandy soil. In Figure 1 we compare the distribution of skin resistance along the pile shaft for a non-cohesive soil material. The theoretical ultimate pile capacity can be easily hand-calculated. The 2D-Axisymmetry and 3D Solid models were set up to test against this theory. Results are comparable and correct. In these two models the ultimate shaft and toe resistance is an outcome of the analysis. However if the pile is modelled as "embedded" (Embedded Pile is a type of structural element in PLAXIS 3D) the ultimate pile resistance can be prescribed as an input parameter or calculated as an outcome of the analysis. For the former (input) the authors suggest that the response from the Embedded Pile model should be checked and calibrated against an actual in-situ pile load test for foundation engineering projects. For numerical experiments, embedded piles should be checked and calibrated against its equivalent in 2D axi-symmetry or 3D model space.

3 NUMERICAL EXPERIMENTS NO.2

3.1 Typical condition of Bangkok Sub-soil

In Bangkok, the subsoil is normally consists of thick deposit of clays and tall buildings for many decades are designed and founded on pile foundation concept. A raft is of course included in this concept but seldom utilised in carrying part of the total weight of the superstructure. Application of a piled raft foundation in Bangkok is still very much in its infancy. Figure 2 shows a typical situation of superstructures resting on piled foundations located in Bangkok subsoil condition. The stratification of the layers are also illustrated in the aforementioned figure.

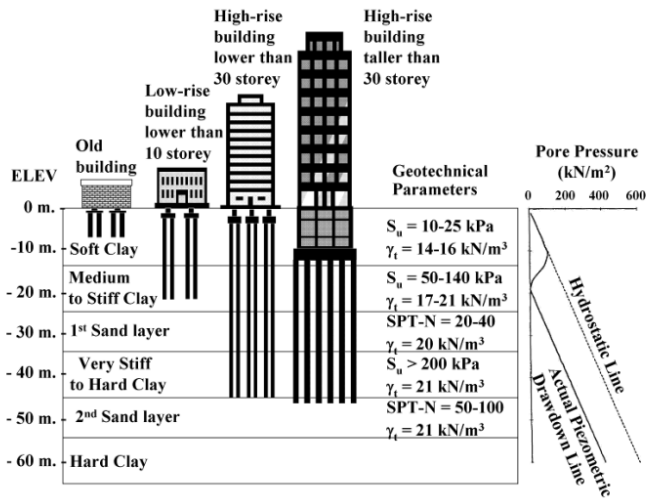

Figure 2: Typical design of superstructure using Piled Foundation concept in Bangkok subsoil

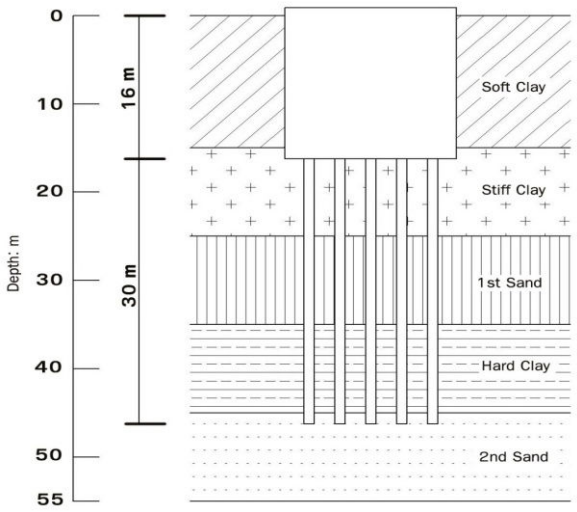

Figure 3: Configuration of Model 1 for numerical experiment

3.2 Comparison of methods

In this section the authors will highlight numerical experiments carried out to investigate the potential of using 3-D FEM for a hypothetical foundation located in Bangkok subsoil condition. The conditions of the numerical experiments are:

1. The raft is supported on 25 bored piles on Bangkok subsoil.
2. The raft has a thickness of 1 meter and located at a depth of 16 m.
3. The diameter of the bored piles is 1 m and the toe set at 46 m. This ensures the pile is 30 m in length.
4. The configuration of the problem is shown in Figure 3.

This exercise aims to show the differences and advantages of using 3D-FEM approach in comparison with some conventional analytical methods such as:

1. Combined Stress Method (M1)
2. Plate on Pile Springs Method (M2)
3. 3-D Finite Element Method where the raft is not in contact with soil (M3)
4. Plate on both pile and soil springs method (M4)
5. 3-D Finite Element Method where raft is in contact with soil (M5)

The methods are graphically illustrated in Figure 4.Using methods M1, M2 and M3 the foundation system was analysed as conventional piled foundation system where the geotechnical contribution of the raft is neglected. In M4 and M5 the foundation was analysed as piled-raft foundation system. In piled-raft foundation analysis all features of pile, soil and raft are taken into account. All these five methods were applied on the same model which is introduced in the following section.

In this series of numerical experiments the loads acting on the foundation were analysed with uniform and lines-points approach. In this paper only the uniform loading condition will be reported. The setup of the this load type is shown in Figure 5. In this section the focus is on the investigation of using M5 for Bangkok subsoil condition and the setup of M5 will be described herein.

In M5 the finite element model in three dimension is shown. The element type is 15-node wedge elements. Plate structural elements are used to model the raft. The raft is located at a depth of 16 m and in the M5 model the 16 m thick soil is not explicitly modelled but transferred as an equivalent surcharge load and the initial stresses are setup based on this. The boundaries of the model is illustrated in Figure 6. Approximately 20,000 elements were used in this experiment.

In this experiment the simple Mohr-Coulomb model (linear elastic perfect plastic model) was applied as the interest was on investigating the ultimate strength. Using approach “Undrained C” in Plaxis this invariably switches the MC model to a TRESCA model. The raft and bored piles were modelled as linear elastic material model. The soil parameters are illustrated in Table 1.

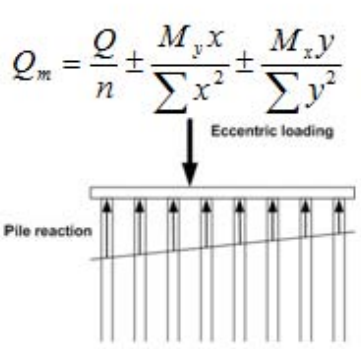

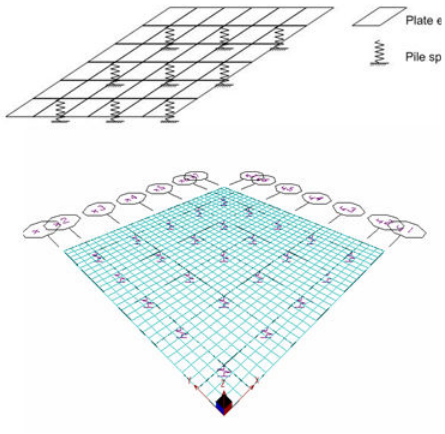

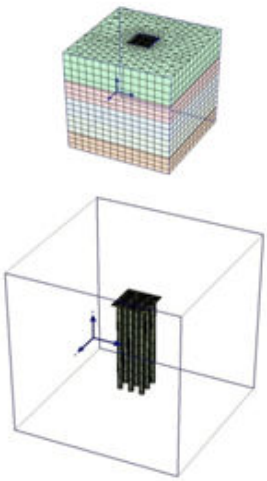

M1: Combined Stress

M2: Plate on Pile-Spring

M3: 3-D FEM (Raft-No Soil Contact)

Pile Foundation Analyses

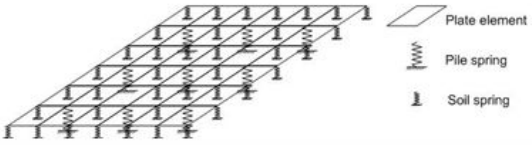

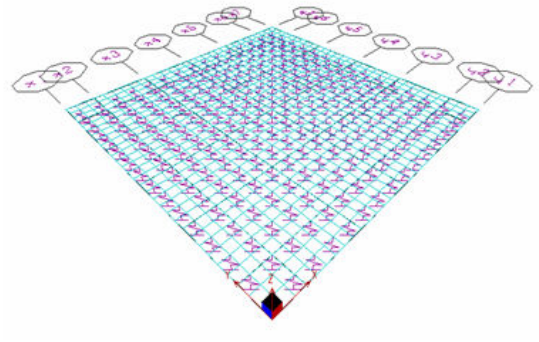

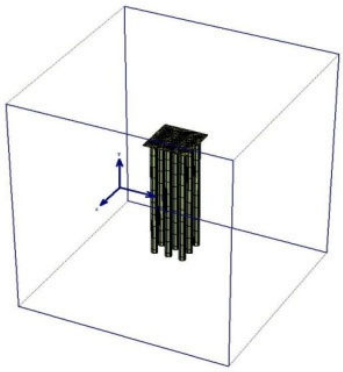

M4:Plate on both pile-soil-springs

M5: 3-D Fem (Raft in contact with soil)

Piled-Raft Foundation Analyses

Figure 4: Illustration of the five methods used in the numerical experiments.

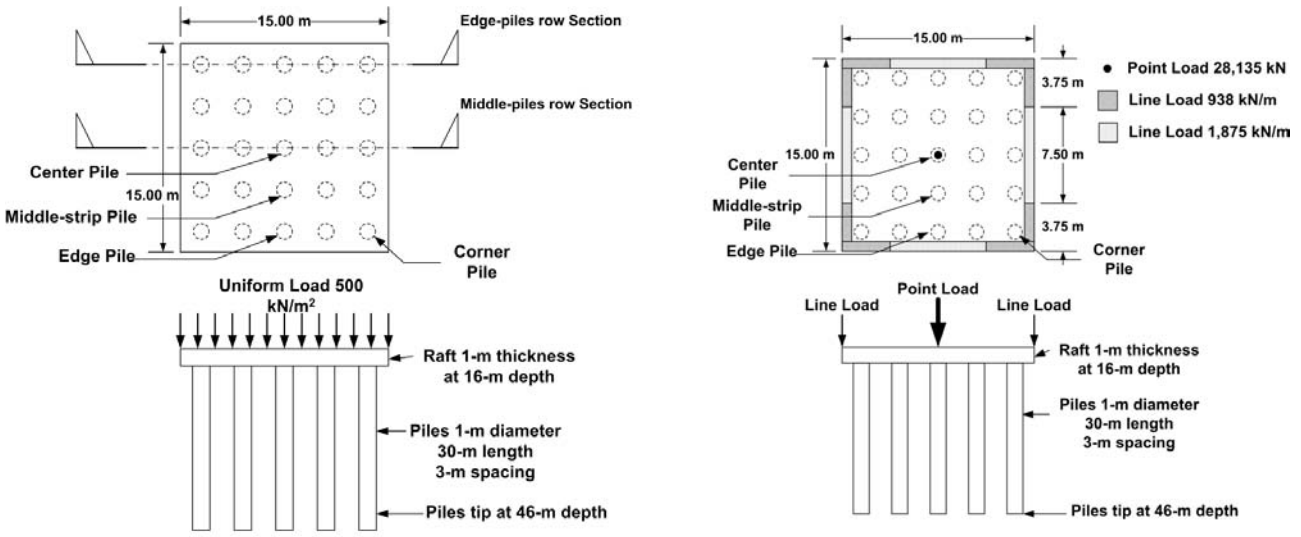

Figure 5: Uniform and Lines-Points Loading Conditions

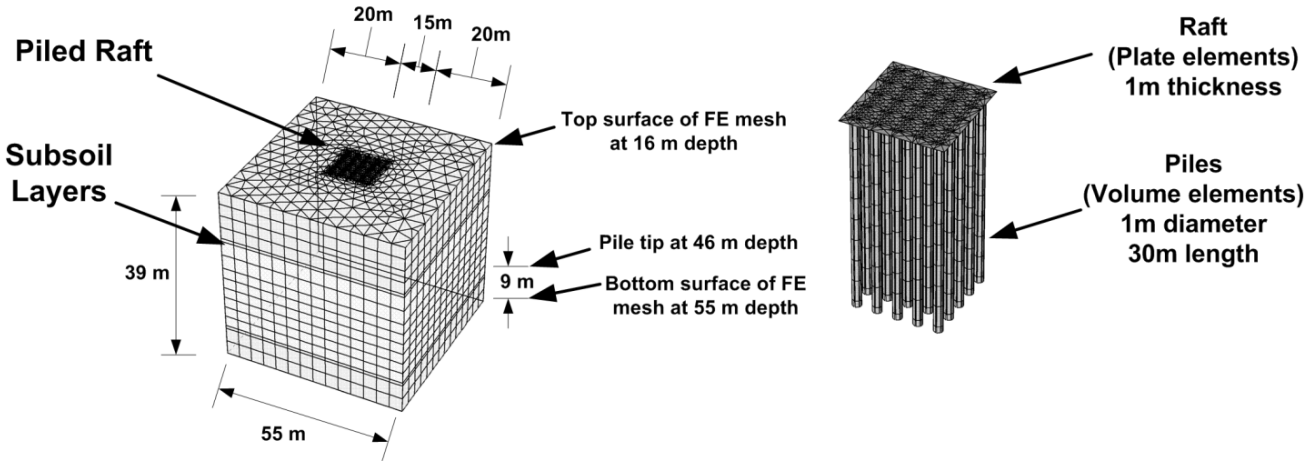

Figure 6: Model 5 (Descretisation, Elements and Geometry)

Table 1: Soil layering and parameters

Material	Depth	Young's modulus	Poisson ratio	Unit weight	Friction Angle	Cohesion	Interface parameters
	(m)	(kN/m²)		(kN/m³)	(degree)	(kN/m²)	
Soft clay	0-15	3 000	0.495	15.2	-	20	0.9
Stiff clay	15-25	40 500	0.495	18.4	-	90	0.5
1st sand	25-35	80 000	0.3	19.4	35.8	1	0.6
Hard clay	35-45	150 000	0.495	19.8	-	300	0.3
2nd sand	45-55	200 000	0.25	20.1	36.2	1	0.6

3.3 Results from method of analysis

Under uniform loading conditions the response based on the five methods are given in Figure 7 to 10. In Figure 7 it can be seen that methods 1 to 3 rely on the piles alone for foundation capacity. The variation of percentage of load sharing in M4 and M5 is due to the analytical approach.

In Figure 8 the loading of the corner, edge and center piles are shown. In M1 the variation is not seen as this method do allow such detail. In M1 to M3 the influence of raft is not taken into account therefore the magnitude of loading on the piles are higher that M4 and M5.

Figure 9 illustrate the development of bending moments along the raft. Method M2 and M4 provide larger maximum negative bending moments when compared to 3-D FEM approaches like in M3 and M5.

The factor-of-safety for all the piles (centre, edge and corner) are shown in Figure 10 comparing the various safety factors. The foundation system was designed base on piled foundation concept. In this concept the contribution of the raft is neglected. Analysing this proposed design again via "Pile Raft Foundation" concept yielded higher factor-of-safety values as the contribution of the raft is taken into account.

3.4 Results from optimising pile numbers

In a subsequent set of analysis a parametric run was conducted where the number of piles were reduced. In all practicalities this is also the target of most optimisation exercises in real analysis and design schemes. The parametric analysis is illustrated in Figure 11.

The aim of this optimisation scheme is to reduced the number of piles and the outcome of the optimised configuration gave acceptable factor-of-safety. In Figure 7 the percentage of load shared by the piles calculated using M5 is 77% based on conventional pile design concept. The target is to achieve a load share of 40 and 60 percent for the raft and piles respectively. The F.O.S can be as low as 1.5. Reducing the number of piles will increase raft settlement, but this situation is controlled by re-arranging the position of the piles to reduce differential settlements. In essence absolute overall settlement can increase but differential settlement is controlled. The differential settlement of the raft after optimisation 1 and 2 is shown in Figure 12.

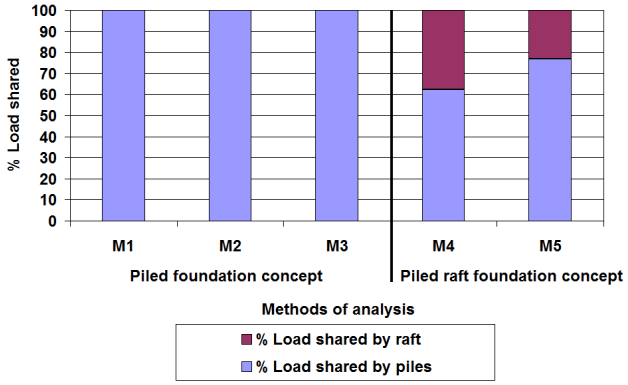

Figure 7: Load percentage between piles and raft

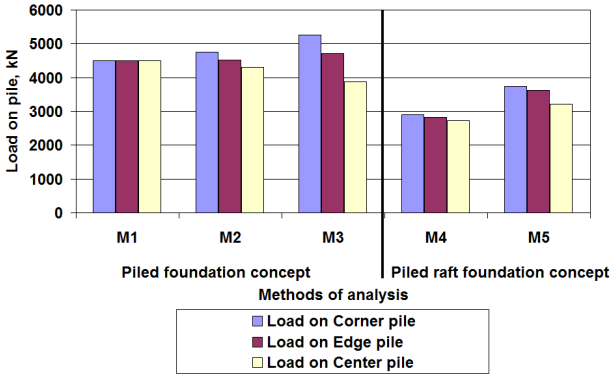

Figure 8: Loading on Piles

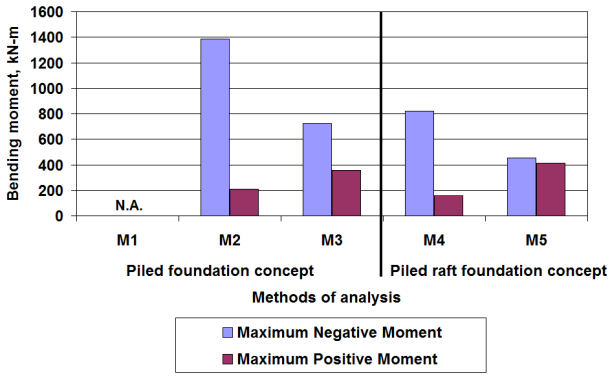

Figure 9: Bending Moments on Raft

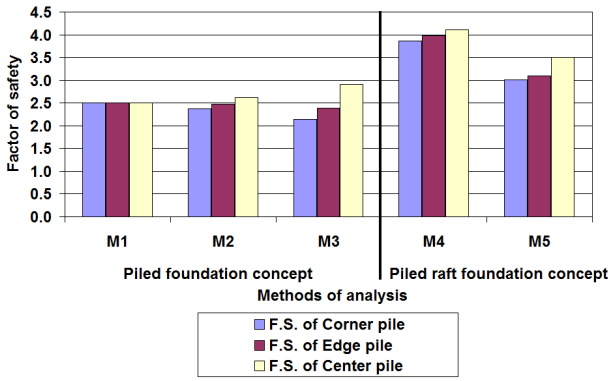

Figure 10: F.O.S of Piles

4 CASE History

The selected case is a high-rise building situated on the west bank of the Chao Phraya River in the prime business zone in Central Bangkok. The building has 51 floors and a relatively small foot print area. Thus, the foundation of the building was designed as a single raft on piles. The initial analysis and design followed the conventional approach (ignore contribution of raft). A 3.5-m-thick concrete raft was supported by 110 number of 1.8-m-diameter bored piles and 18 barrette piles (1.5m x 3m in size). Barrette piles were used in zones of higher concentrated column loads and a large number of bored piles were required with spacing of 2.5 times of pile diameter. Raft width extends beyond building footprint to accommodate all piles. Details on the actual and adjusted design is given in Table 2.

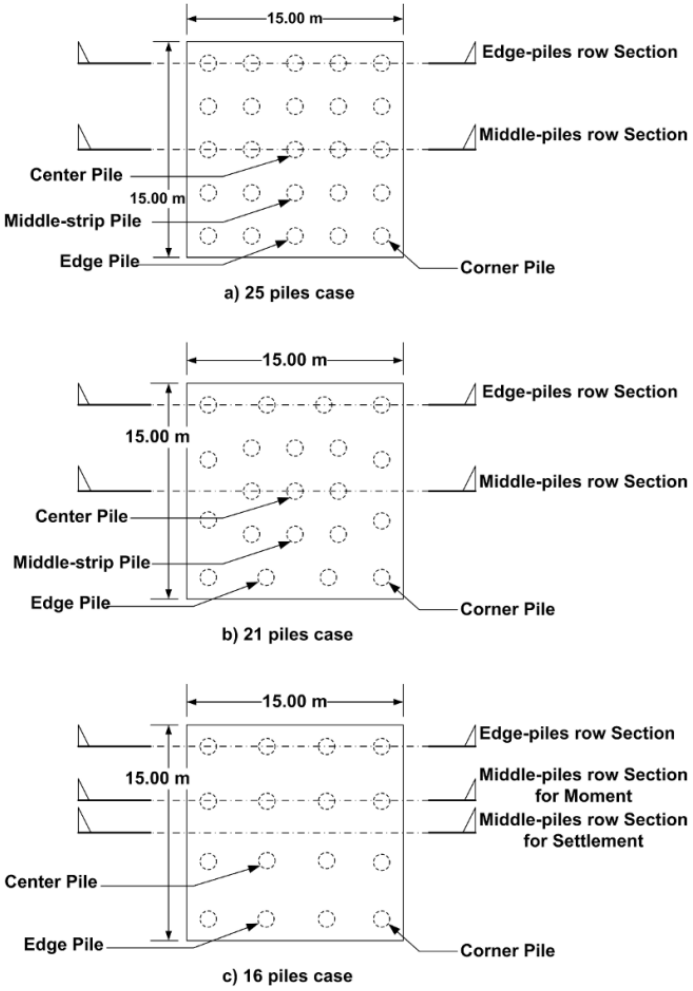

Original
(Piled Foundation Concept)
- Piles: 25 nos.
- Overall F.O.S = 2.5

Optimisation 1
(Piled Raft Foundation Concept)
- Pile: 21 nos.
- Overall F.O.S = 2.1

Optimisation 2
(Piled Raft Foundation Concept)
- Piles: 16 nos.
- Overall F.O.S = 1.6

Figure 11: Optimisation of number of piles.

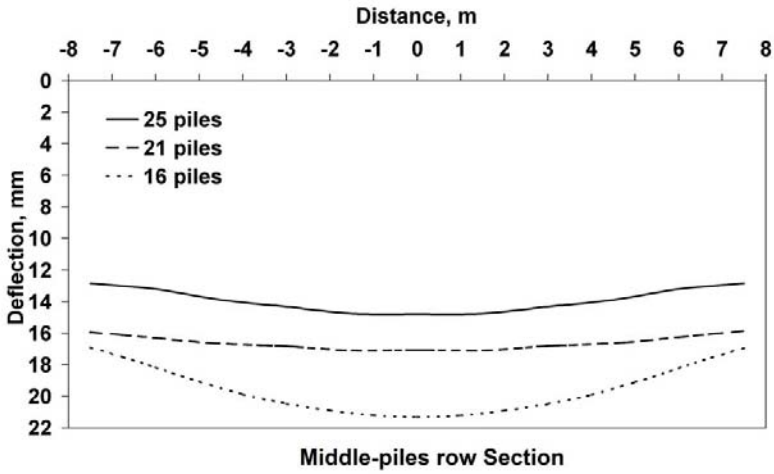

Figure 12: Differential settlement of the raft at 25, 21 and 16 number of piles

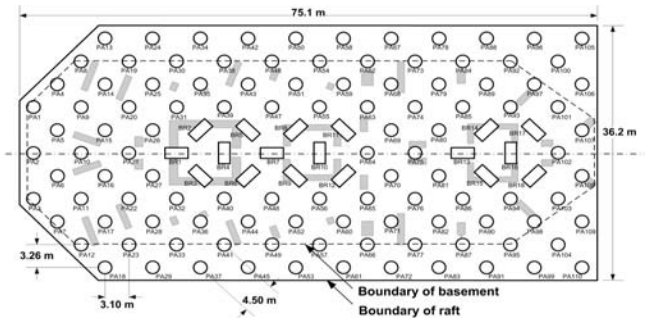

a. Initial design

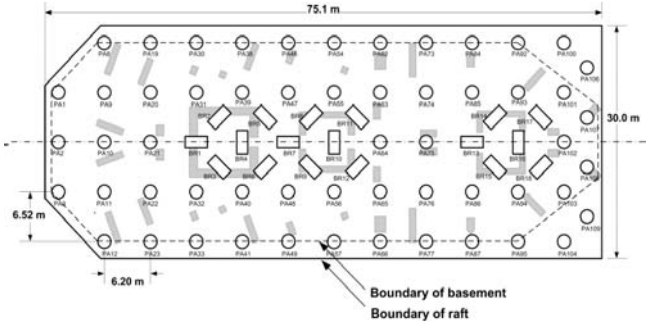

b. Optimise raft size and pile nos.

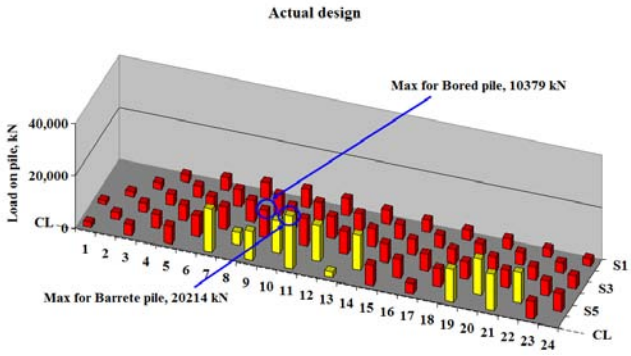

c. Load on each pile due to original design

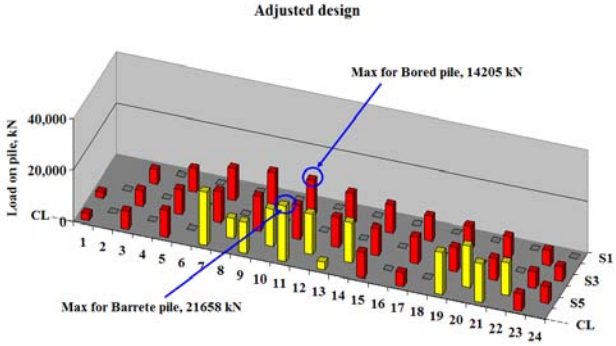

d. Load on each pile after adjustment

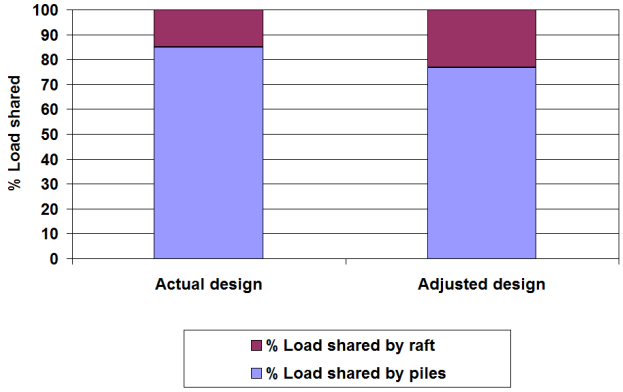

e. Percentage of load shared

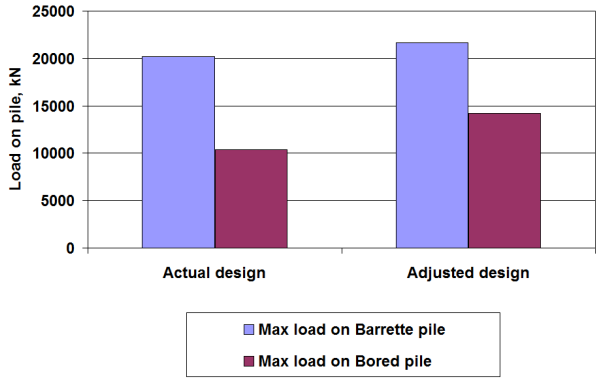

f. Development of max load in original and adjusted design

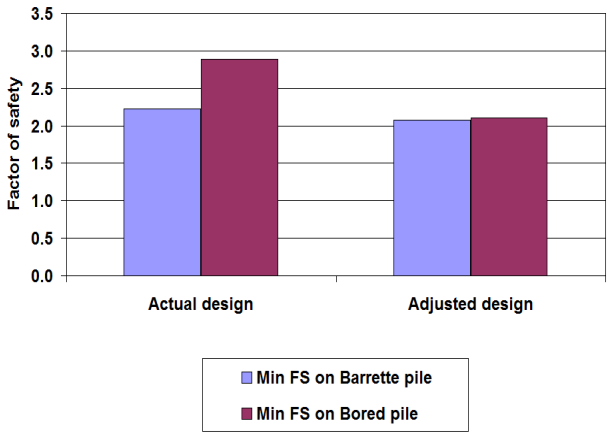

g. Factor of safety before and after adjustment

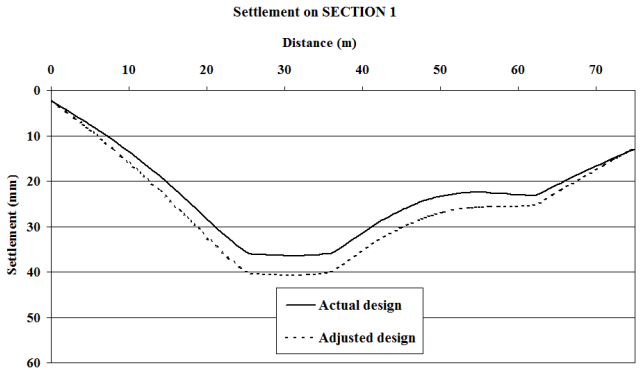

h. Settlement of raft

Figure 13: Results comparing "Adjusted" with "Actual" design

Table 2: Information comparing two different design schemes

INITIAL	ADJUSTED
• Raft size of 75.1m x 36.2m • 110 Bored piles • 18 Barrette piles • Overall F.S of 4.09	• Raft size of 75.1m x 30m • 56 Bored piles • 18 Barrette piles • Overall F.S. of 2.48

Figures 13a and b show the layout of the piles of the initial and optimised designs. In Figures 13c and d illustrate the distribution of pile forces across the raft. It can be seen that difference of maximum and minimum pile loads were reduced. Piles at the corner and perimeter areas are now taking large loads utilising them much further in the whole foundation scheme.

Figure 13e illustrates load shared between the raft and pile. In the actual design the percentage of load sharing was 15% and 85% for the raft and piles respectively. When the foundation scheme was analysed as pile-raft concept the percentage of load sharing between the raft and piles were 25% and 75% respectively. In true physical sense the later results are true and closer to reality as the raft is physically in contact with soil are taken into account.

Figure 13f illustrates the overall pile loads being shared between the barrettes and bored piles. In both cases the number of bored piles were reduced and position shifted. Figure 13g show the factor-of-safety of the actual and adjusted design. It is obvious that the adjusted design is still above the contractually agreed value of 1.5 set by a local agency. It can be said that in the adjusted design the piles were engineered to carry a larger magnitude of foundation loads and hence maximising as far as possible its geotechnical and structural capacities.

Figure 13h shows that based on 3-D finite element analysis of the adjusted design, overall settlement increased by 14% at the most significant section which is beneath the core of the building. Differential settlement was also slightly increased. This is expected as reducing the number of piles and changing centre-to-centre spacing will increase foundation settlement but still within the accepted engineering tolerance. The adjusted design provided a more economical solution as the raft size and pile numbers were significantly reduced.

5 CONCLUSIONS

In this paper we have highlighted the possibility of performing complex piled raft analysis in routine geotechnical works. In this paper we have reported a case where a simple quadratic piled raft foundation located in typical Bangkok subsoil was analysed via conventional and finite element method. The results are indicated that conventional design approach is conservative and can be grossly expensive.

This numerical experiment was conducted at the initial stages of a project. In part the idea is to obtain some form of experience and calibration. Lessons learned from this experiment was eventually transferred to a real project located in Bangkok.

Real load distribution among the piles beneath the raft can be very different depending on the approach and analysis method. Surely by adopting M5, which is a 3-D FEM analysis, a more realistic response and results will be obtained as all elements of soil-pile-raft interaction were taken into account. The experiments in this paper indicated that the piles were loaded to a percentage range of 70 to 80%. Using the conventional method the resulting design is too conservative and expensive as the raft was not accounted for. By rearranging the number of piles and position the piles were engineered to carry larger loads. The percentage of load taken by the raft was transformed from 15% to 25%. In Bangkok subsoil the most basements are 4 to 6 levels below ground. The raft is located close to stiff clay layer . This layer is over-consolidated and rafts located on and within this layer should be utilised as part of the load carrying system in this case.

REFERENCES

Katzenbach., & Choudhury, D. (2013). ISSMGE Combined Pile-Raft Foundation Guideline, *ISSMGE Technical Committee TC 212 – Deep Foundations.*

Lee, J.H.,Kim Y.H.& Jeong, S.,S., (2010).Three dimensional analysis of bearing behaviour of piled raft on soft clay, *Computer and Geotechnics*, 37, p.p.103-114.

Poulos, H.G., (2001A). Piled-raft foundation: Design and application, *Geotechnique* 51, No.2, p.p.95-113

Poulos, H.G, (2001B). Methods of Analysis of Piled Raft Foundations, *A Report Prepared on Behalf of Technical Committee TC18 on Piled Foundations ISSMGE*.

Reul, O. & Randolph, M.F.,(2003). Piled raft in over consolidated clay: comparison of in-situ measurements and numerical analysis, *Geotechnique* 53, No.3 p.p.301-31

Tan, S.A., (2014). *Study of PLAXIS 2D vs 3D Single Pile models, CE5107*, Department of Civil & Environmental Engineering, University of Singapore, Singapore.

The Capacity of Driven Steel H-Piles

Leonard John Endicott
AECOM Asia Company Ltd, Hong Kong
Xu Zhang & Limin Zhang
The Hong Kong University of Science and Technology, Hong Kong

ABSTRACT

The Hiley formula, which is fundamentally based on transfer of energy during the impact of a hammer onto a pile, has been used for estimating the capacity of driven piles for decades. In the early years the formula gave reasonable results, notably for short piles. However as piles have become longer and of higher capacity and as new techniques have developed, the formula has become less reasonable and some users have modified the formula. Pile Dynamic Analysis (PDA) was devised as a means of numerically modelling the dynamic effects of pile driving. Instrumentation for PDA provides a direct measurement of the forces transferred to the top of the piles during driving. Comparison between results of many static load tests with PDA has validated the PDA method of determining the capacity of the piles. As a consequence PDA is now widely adopted as the method for acceptance of capacity of driven piles in Hong Kong. In addition to dozens of results of static load tests, results of many hundreds of PDA tests are available. These results provide the opportunity to examine some long held concepts such as "the smaller the final set, the higher is the capacity of the pile". By contrast there is substantial evidence that in many cases the driving force in the piles can be independent of their final set over quite a wide range of values of final set. Based on a study of the test results for many piles it is proposed that it is time to change methods of determining capacity of piles by using modified versions of the Hiley formula and to use the PDA method. Moreover the PDA method can be used to determine maximum stresses in piles and thereby establish criteria to prevent damage to piles during driving.

1 INTRODUCTION

Pile Dynamic Analysis (PDA) testing has been in use for several decades to check the integrity of piles (Goble & Likins 1996). As the result of comparison between hundreds of static load tests with PDA test analyses during the last decade it has been observed that wave analysis is a fairly accurate method for pile capacity prediction (Fung et al. 2004; Li et al. 2011). It has become a common practice in Hong Kong to adopt PDA testing for checking the ultimate capacity of driven piles and it is quite common nowadays for contracts whereby a large portion of production piles are subjected to PDA testing. As a consequence there are many hundreds of PDA testing results at a job site.

PDA testing involves instrumentation with strain gauges and accelerometers attached to the top of each pile such that during the fractions of a second whilst the hammer strikes the pile the driving force in the pile can be deduced from the strain gauges and the acceleration can be measured and the velocity and displacement can be computed (Pile Dynamics Inc. 2000). From this data, the maximum driving force, FMx, at the top of the pile can be determined. The analysis is configured in order to estimate the frictional forces that are developed down the shaft of the pile and the reaction at the toe, for which the maximum force at the toe is RMx. The analysis requires estimates of dynamic properties of the ground to be input and trials are carried out to match the relationship of FMx vs. time that is recorded at the top of the pile. In the past calibration of the PDA analysis was carried out by comparison with static load tests. Comparison of PDA results with static load tests has identified dynamic properties of the ground which give good agreement with the static load test results and now fewer static load tests are carried out (Fung et al. 2004).

Notwithstanding the use of PDA testing to prove the capacity of driven piles, many contracts require the use of the Hiley formula, or similar, to estimate the final set for driving according to the size of pile, length of

the pile, size of hammer and the stroke of the hammer to be used.

This paper makes use of PDA test data from three sites in Hong Kong where steel H-piles of 305 mm x 305 mm x180 kg/m size were driven to depths generally in the range of 20 m to 60 m using hydraulic hammers ranging from 16 tonnes to 25 tonnes and with strokes of 0.4 m to 4 m. Test results are available for driven piles with a set of the order of 400 mm per 10 blows down to less than 10 mm per 10 blows.

2 MODIFIED HILEY FORMULA

The Hiley formula has been used for decades to estimate the capacity of driven piles. It considers the energy of WH from a hammer of weight W and stroke or drop height of H, transmitted to a pile of weight P, with a coefficient of restitution of e and a hammer efficiency of E_h. It also considers the absorption of the energy by the set s, and by half of the temporary compression of the cushion C_c, and the temporary compression of the pile C_p and of the soil C_s. The energy transmitted divided by the absorption gives the driving resistance R which is taken to be the capacity of the pile. The Hiley formula can be stated as follows:

$$R = \frac{E_h\left[\frac{W+Pe^2}{W+P}\right]WH}{s+\frac{1}{2}(C_c+C_p+C_s)} \quad (1)$$

By inspection of this formula, the set, s, is in the denominator and therefore R, the driving resistance or capacity, is inversely proportional to the magnitude of the set.

It is common to estimate the temporary compression of the pile by computing the elastic compression under the imposition of the driving force as follows:

$$C_p = \frac{R\,L}{E\,A} \quad (2)$$

where L is the length of the pile, E is the elastic modulus of the pile and A is the cross sectional area of the pile. C_p is proportional to L and appears in the denominator of the Hiley formula and therefore R, the computed driving resistance, is related inversely to the length of the pile.

It is a common practice to determine the set to which a pile shall be driven to achieve a specified capacity and to produce a table with values of set decreasing for increased lengths of pile for different weights and drop distances of the hammer.

3 PDA TEST RESULTS

Instrumentation data from the PDA tests include values for FMx. This is the measured driving force at the top of the pile. According to the Hiley formula, FMx should be inversely related to the set. This conception has been examined by combining the data from all three sites and including the results from 496 PDA tests. Figure 1 shows a plot of values of FMx vs. set (mm/10 blows) for a 16-tonne hammer.

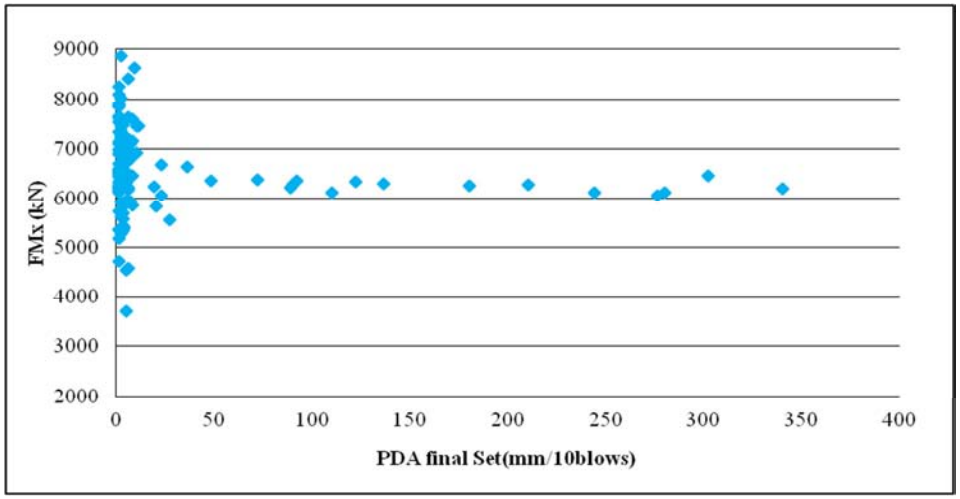

Figure 1: FMx vs. set utilizing a 16-t hammer

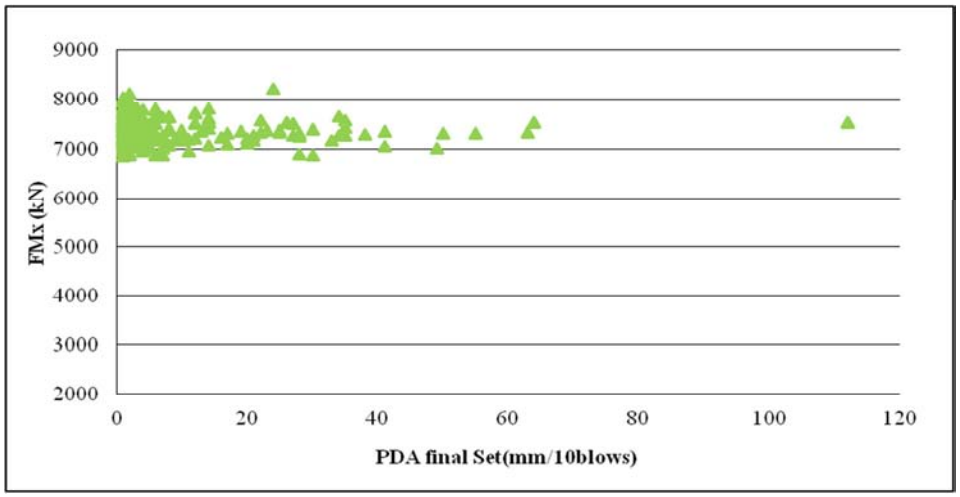

Figure 2: FMx vs. set utilizing a 25-t hammer

It is evident that, for sets in the range of about 50 mm/10 blows to nearly 400 mm /10 blows, the driving capacity is very close to 6000 kN. This result is contrary to the conception that the driving force is inversely related to the set. A similar plot for the use of a 25-tonne hammer is shown in Figure 2, which also shows that, for a considerable range of final set values the driving force is close to, and more than, 7000 kN. This data also does not reflect an inverse relationship between the set and the driving force that is assumed in the Hiley formula.

Both sets of data show significantly increased forces as the set is reduced below about 10 mm/10 blows. This set is defined as refusal (Buildings Department 2004). Such hard driving normally is associated with end bearing on very hard materials such as rock whereby the compression wave in the pile is reflected at the toe and travels up the pile and thereby increases the maximum force at the top of the pile. Based on this interpretation, the basic driving force in a pile with little or no reflection from the base might be considered to be of the order of about 6000 kN for the 16-tonne hammer and about 7000 to 7300 kN when using a 25-tonne hammer. It may also be considered that when driving to refusal, reflection from the base increases the maximum force at the top of the pile to more than 8000 kN in these two cases.

Another consideration is that, according to the Hiley formula, the driving force is proportional to the mass of the hammer and the stroke. Figure 3 and Figure 4 show plots of FMx vs. stroke for the 16-tonne hammer and 25-tonne hammer respectively from the data with final set over 25 mm/10 blows. These plots show a trend of increasing maximum driving force with increasing stroke. However it is evident that FMx is not

proportional to stroke as adopted in the Hiley formula.

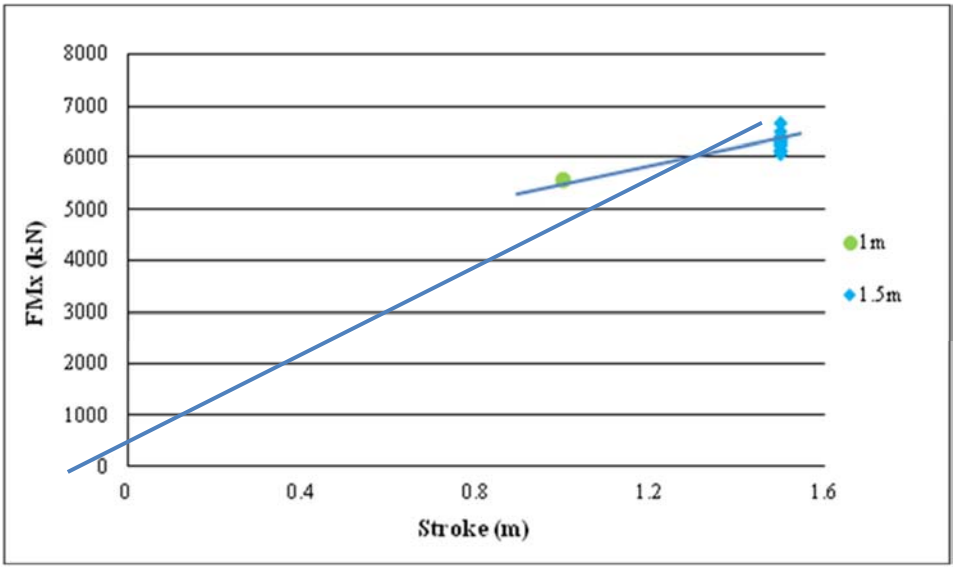

Figure 3: FMx vs. stroke of 16-t hammer

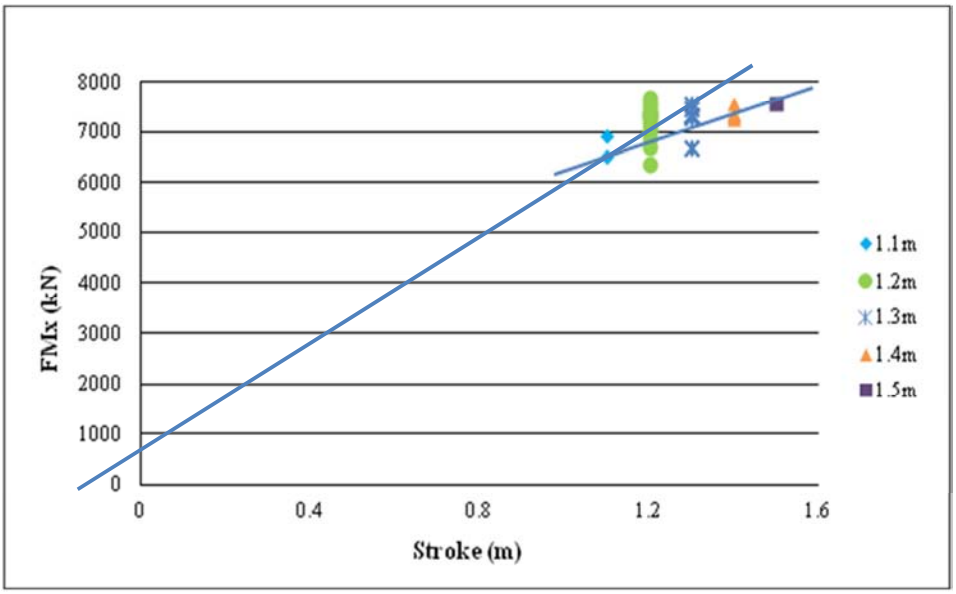

Figure 4: FMx vs. stroke of 25-t hammer

The maximum force at the base of a pile is not measured directly. It is computed by a process of estimation by a trial shaft friction distribution and matching the measured force/time/deflection relationships measured at the top of the pile. However a comparison of PDA test results with static load tests indicates that the computations are generally reasonably good (Fung et al. 2004). Figure 5 shows a plot of RMx vs. set for the 16-tonne hammer. The results are similar to the values of FMx with some differences. For sets greater than refusal (10 mm/10 blows), some values of FMx are less than 6000 kN, the value for FMx at the top of the pile, and this may be attributed to a reduction of force in the piles due to shaft friction. Likewise, when driving to refusal (less than 10 mm/10 blows) the RMx is increased with values generally similar to those recorded at the top of the pile but marginally greater.

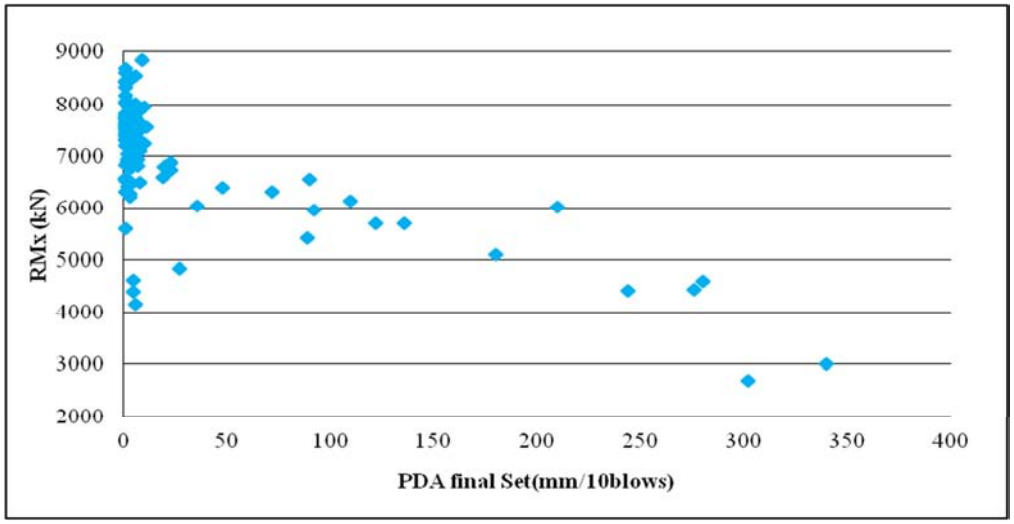

Figure 5: RMx vs. set for 16-t hammer

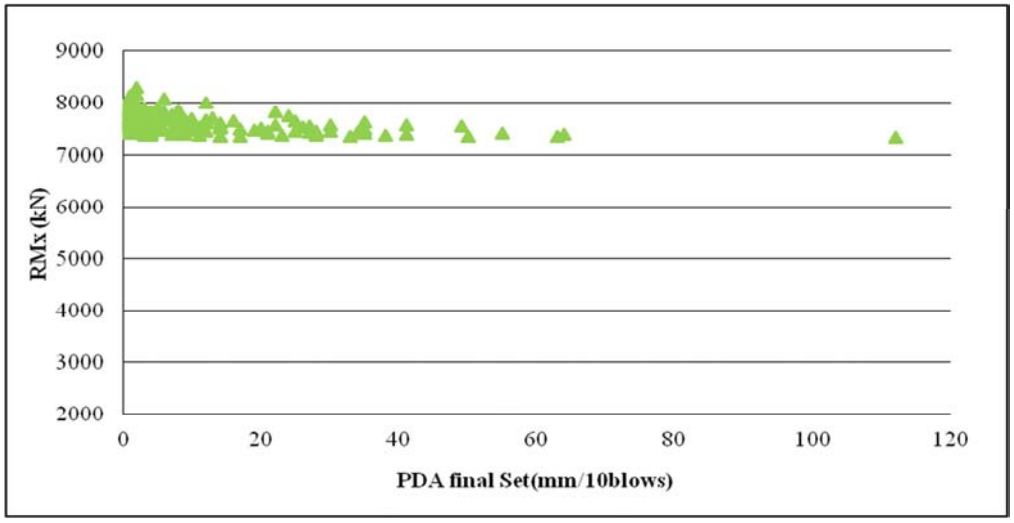

Figure 6: RMx vs. set for 25-t hammer

Likewise Figure 6 shows a plot of RMx vs. set for the 25-tonne hammer. In this plot there is a tend with a lot of results lying above the value of RMx = 7200 kN and when driving to refusal the maximum values rise to about 8500 kN, which is marginally more than is recorded for the FMx in Figure 2.

Pile length varies in the studied areas, Figure 7 shows the differences between RMx and FMx values at different pile lengths. The plot shows that RMx and FMx are virtually independent of the length of the piles.

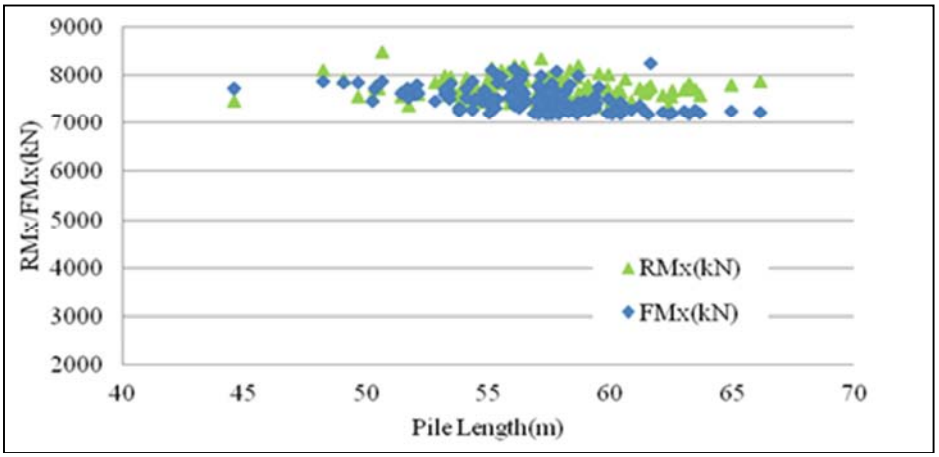

Figure 7: RMx and FMx vs. pile length

4 CONCLUSIONS

Based on this study, it can be concluded that 305 mm x 305 mm x180 kg/m H-piles driven by 16-tonne and 25-tonne hammers can achieve a capacity of 6000 kN to about 7200 kN without driving to refusal for a range of set values from 10 mm/10 blows to as much a 120 mm or even 350 mm (the range of data available). Importantly the driving force is almost constant, unrelated to the set, until refusal is achieved and reflection from the toe increases both the driving force and the bearing capacity. The actual driving force and capacity can be increased by increasing the stroke, but the force and capacity are not directly proportional to the stroke, and are not related to the length of the pile, as adopted in the Hiley formula.

By driving to refusal, i.e. to sets of 10 mm/10 blows or less, the forces in the piles are computed to increase by as much as 2000 kN. Such hard driving runs the risk of damage to the tips of the piles unless they are reinforced.

It is considered that, with the continued use of PDA testing for driven piles, the selection of weight of hammer and stroke could be determined empirically from previous PDA data and that the Hiley formula, even with modifications, is no longer a useful predictor.

REFERENCES

Buildings Department 2004. *Code of Practice for Foundations.* Buildings Department, the Government of the HKSAR, Hong Kong.

Fung, W.K., Wong, M.K. & Wong, C.T. 2004. A study on capacity predictions for driven piles. *HKIE Transactions,* 11(3): 10-16.

Goble, G.G. & Likins, G.E. 1996. On the application of PDA dynamic pile testing. *Proceedings of the Fifth International Conference on the Application of Stress-wave Theory to Piles 1996.* Orlando, Florida, 263-273.

Li, W.W., Wong, M.K. & Chan, Y.K. 2011. The application of PDA/CAPWAP to ensure quality and capacity in driving long steel H-piles. *HKIE Transactions*, 18(2): 10-16.

Pile Dynamics Inc. 2000. *Pile Driving Analyser Manual.* 4535 Emery Industrial Parkway, Cleveland, OH 44128.

Feasibility of Bored Pile Foundation Modification in Hong Kong

Edmond K.L. Fung
AECOM

ABSTRACT

Pile foundation is a significant structural element in many structures. Selection of suitable pile type for different ground conditions is the most fundamental decision to be made by foundation designers. It is no doubt that minimizing the pile numbers under a given design loading is the prime goal of an ideal foundation design in terms of economics. The reduction of pile numbers and quantities also shortens the construction time and enhances sustainability, as well as improves safety during construction, especially in the case of complex underground conditions with construction constraints in a well-developed dense populated city like Hong Kong.

To achieve an economical foundation design, it is important to explore and develop innovative ideas, which may involve modifications from traditional foundation types and construction techniques. Foundation design in Hong Kong is required to comply with the standard design codes or specifications set out by different government authorities. The most optimized foundation layout may therefore be different, even under the same loading condition, if design requirements by different authorities are to be satisfied. This paper will focus on the discussion on current bored pile foundation design criteria under different design codes and specifications of different government authorities for private and public housing developments such as Buildings Department (BD), Hong Kong Housing Authority (HKHA), Architectural Services Department (ASD) and Highways Department (HyD). Further discussion on the feasibility of bored pile foundation modification satisfying different design standard is presented.

1 INTRODUCTION

The prime objective of pile foundation design is to ensure that the foundation system would have sufficient capacity to withstand the loading originated from the superstructure. Such support elements act as a medium to transfer the loading from the superstructure through a structural pile cap down to the ground by end bearing and/or skin friction resistance of the piles. Besides the consideration of resisting the combination of vertical and lateral loading in general, structure stability under the action of wind loading and/or uplift loading and avoidance of excessive settlement should also be considered during the foundation design process. Well-established design methods are available and have been used in practice. These methods are generally accepted by checking authorities in Hong Kong. However different authorities may have different design standard and specifications, the most optimized foundation types, layout and quantities may therefore be different dependent on the design standard and specifications being adopted. Apart from the design requirements clearly stated on the standards, there are some other common practices which are not specified on the standards clearly. These will affect the effectiveness of the foundation design.

Bored pile foundation is one of the most common and cost-effective pile types being adopted in Hong Kong. In order to optimize the foundation design in terms of economics, viz. enhance the pile capacity and minimize the quantities of construction materials and construction time, some modifications to the foundation system may be needed. However, most of the time, these modifications are not guided by fundamental design principles or theories. They are needed to meet different design criteria under different standards.

2 CURRENT DESIGN CRITERIA FOR BORED PILE FOUNDATION

Circular concrete bored piles are usually installed by boring down to the required founding level and forming a certain rock socket into sound rock by chiseling method or a reverse circulation drill (RCD) rig to achieve

the end-bearing capacity and bond friction between rock and concrete. Pile shaft capacity is achieved by reinforced concrete pile shaft with steel cage.

2.1 Buildings Department (BD)

In Hong Kong, private developments need to be approved by the Buildings Department and the associated bored pile foundation design should comply with "Code of Practice for Foundation 2004 (COP Foundation 2004)" in general.

Some of the major current design criteria specified in COP Foundation 2004 are listed below:

- Allowable end-bearing capacity achieved by rock socket diameter or enlarge base (bell-out) diameter. Size of bell-out cannot exceed 1.5 times the pile shaft diameter.
- Allowable bond or friction capacity between rock and concrete. Design bond length for frictional resistance cannot exceed 2 times pile shaft diameter or 6.0m whichever is smaller.
- Minimum clear horizontal spacing of 500mm between shaft surfaces or edge of bell-outs should be provided.
- Adequate horizontal restraints in at least 2 directions shall be provided to individual piles or pile cap.
- Pile and pile cap should not be used together to resist lateral forces.
- Either rigid cap or flexible cap design assumption can be adopted specified in COP Concrete 2004.

Some design criteria commonly adopted in practice but not specified in the standard very clearly are as follows:

- Minimum steel ratio for both shear links and vertical bars for pile shaft.
- Compression steel can be adopted for enhanced the pile shaft capacity.

2.2 Hong Kong Housing Authority (HKHA)

Most public housing developments are approved by Housing Department and their Independent Checking Unit (ICU), the associated bored pile (Type 3) foundation design should comply with "General Specification (GS) HKHA" in general. Most of design criteria comply with BS8004 and BS8110, but "Code of Practice for Foundations" published by BD has been adopted as a common standard nowadays except for the aspects discussed below.

Some of the major design criteria specified in GS which are not specified in COP Foundation 2004 are listed below:

- Allow only one type of pile in each pile cap.
- Maximum design displacement of pile caps and piles is 25 mm
- If the center to center spacing of two adjacent Type 3 piles is less than 2.5 times the diameter of the larger pile base and the difference in founding levels of these two piles is greater than the clear distance between their bases on plan, justification is necessary.

Some design criteria commonly adopted in practice but not specified in GS clearly are as follows:

- Bond strength in type 3 piles is not specified.

2.3 Architectural Services Department (ASD)

Most government developments are approved by ASD and the associated bored pile foundation design comply with "ASD General Specification for Building 2007 (GS)" in general.

Some of the major current design criteria specified in the GS are described as follows:

- Do not use piles with enlarged bases unless specified otherwise. Allowable end-bearing capacity achieved by rock socket diameter or permitted enlarged base (bell-out) diameter. Size of permitted bell-out cannot exceed 1.5 times the shaft diameter.

- Minimum center to center spacing shall be 750mm or 2.0 times the least width whichever is the greater.
- Combination of load elements supported by one large pile cap shall not be allowed. (i.e. single column or wall support by a single pile cap only.)
- Piles shall not be positioned directly under any wall opening.
- Tension piles shall not be permitted.
- Maximum design concrete strength shall not exceed 7.5MPa.
- Minimum pile length shall be 5.0m.
- Founding levels of adjacent piles shall not differ by more than the clear distance between the pile bases.
- 0.4% of cross sectional area of bored pile as the nominal steel for bored pile.
- Either rigid cap or flexible cap design assumption can be adopted specified in COP Concrete 2004.

Some design criteria commonly adopted in practice but not specified in the GS clearly are as follows:

- Bond stress between concrete and rock can be adopted for allowable pile capacity.
- Compression steel can be adopted for enhanced the pile shaft capacity.
- Pile and pile cap should not be used together to resist lateral forces.

2.4 Highways Department (HyD)

Most government developments in major highways, roads and bridges should be approved by HyD and the associated bored pile foundation design should comply with "Structures Design Manual for Highways and Railways (SDM)" in general. SDM has specified that the foundation design should comply with BS5400 and it also specifies that foundation design should comply with BS8004, and the associated reinforcement design should comply with BS8110. Since the mentioned BS standards just describe the design principles instead of very detailed design criteria as in documents issued BD, ASD and HKHA as mentioned above, therefore foundation design in HyD's project are very flexible and very much rely on the discussion between foundation designers and authority.

3 DISCUSSION

Typical design criteria for bored pile foundation under different authorities has been briefly introduced in the above sections and the summary that may influence the piling layout are listed in Table 1.

According to Table 1, different numbers of piles may be required to satisfy different authority's criteria even though the magnitude of loading and ground conditions are exactly the same. These criteria are the main factors which will influence the pile numbers.

Consider the minimum design pile center to center spacing, for a group of 3.0m diameter bored piles, minimum pile spacing is 3.50m under COP Foundation 2004, but 6.0m is required under ASD.

Allowable bearing capacity for a bored pile with 3.0m shaft diameter and a maximum 4.50m bell-out diameter resting on grade III/II rock (5.0MPa) is 79,521kN under COP Foundation 2004, but due to the limitation of no bell-out diameter is allowed under ASD, the allowable bearing capacity is just 35,342kN. This means that only 44% of BD's criteria can be achieved. Allowable bond strength between rock and concrete per meter rock socket length for a 3.0m shaft diameter bored pile resting on grade III/II rock (5.0MPa) is 6,597kN under COP Foundation 2004, but NIL is allowed under ASD. Therefore, allowable design pile capacity by end bearing plus bond strength between rock and concrete for a 3.0m shaft diameter with maximum 4.50m bell-out diameter bored pile resting on grade III/II rock (5.0MPa) is 86,118kN under COP Foundation 2004, but due to the limitation under ASD, it is just 35,342kN, that is only 41% of BD's criteria can be achieved.

Table 1: Major Design Criteria for Bored Pile Foundation

Authority	Pile Spacing	Size of Enlarged Bell-out	Allowance to Adopt Bond Strength between Rock & Concrete	Maximum Design Concrete Strength	Piling Layout Restraint
BD (COP Foundation 2004)	500mm between shaft surfaces or edge of bell-outs	cannot exceed 1.5 times the shaft diameter	700kPa; bond length to be 2 pile shaft diameters or 6.0m whichever is smaller	Not specified	at least 2 directions shall be provided to individual piles or pile cap
ASD (General Specification for Building 2007)	750mm or 2 times the least width whichever is the greater	enlarged base is not allowed unless specified	Not specified	shall not exceed 7.5MPa	a. Single column or wall support by single pile cap only b. piles shall be positioned under wall opening c. Tension pile is not allowed
HKHA (General Specification)	Same as BD	Same as BD	Not specified	Same as BD	a. Allow only one pile type in one pile cap b. Maximum horizontal displacement of 25mm
HyD (SDM, BS8004)	Not specified	Not specified	Not specified	Not specified	Not specified

Concrete strength for 45D concrete is 9.0MPa under COP Foundation 2004 that is 63,617kN in terms of pile shaft capacity for a 3.0m diameter bored pile. But the maximum concrete strength under general specification ASD is 7.5MPa only. This implies 53,014kN in a 3.0m diameter pile shaft capacity, and just 83% of BD's criteria can be achieved.

Based on the explanation of above selective items extracted from Table 1, it seems that bored pile capacity cannot be fully utilized and it will affect the piling layout in terms of minimum pile spacing and pile numbers as well which are summarized as shown in Table 2.

Table 2: Comparison of Bored Pile Capacity Between ASD and BD

Authority*	Shaft Dia. / Bell-out Dia. (m)	Max. Concrete Strength For 45D (MPa)	Founding Criteria (MPa)	Pile Shaft Capacity (kN)	Bell-out Capacity (kN)	Bond Strength between Rock & Concrete per meter (kN)	Design Pile Capacity (Bearing + Friction) (kN)	Min. Pile Spacing (m)
ASD	3.0 / 3.0	7.50	5.0	53,014	35,342	0	35,342	6.00
BD	3.0 / 4.5	9.00	5.0	63,617	79,521	6,597	86,118	5.00

According to Table 2, it can be seen that the piling layout including pile numbers would be significant different under different requirements even when the magnitude loading of the superstructure are exactly the same. Apart from pile capacity, piling layout restraint as mentioned in Table 1 is also a factor that influences pile numbers, for instance SDM does not describe the foundation design very specifically, and therefore preparation of initial proposal for HyD's projects may involve a lot of assumptions made by the designer instead of following very clear guidelines. For example at least 2 directions shall be provided to individual piles or pile cap is a design criteria under BD, but it seems not appropriate to apply under bridge structure since a certain length distance between bridge piers, and therefore long tie beam or strap beam between two piers is not effective, and to fulfill BD's design criteria, 3 piles group must be adopted instead of 2 piles

group, and as a result leading to over design. According to the above discussion, it is highly desirable to reappraise piling design by unifying design standards to achieve the best economy.

4 RECOMMENDATION

Apart from unifying design standards as described above, practical operation and site considerations are also important factors that need to be taken into account. According to common practice in Hong Kong, due to mechanical restriction, maximum 3.0m shaft diameter of bored pile can be constructed normally. In order to enhance the bored pile capacity based on fundamental design principle, enlarging shaft diameter by rolling a larger steel casing is the most ideal direction, pile capacity will be increased about 7.0% by increasing every 100mm diameter in general. But a chain consideration from construction point of view is that a bigger lifting crane and RCD would require extra working area and headroom for the new machinery, and therefore should be a bigger concern in comparison with design considerations (see Plates 1, 2 & 3 below).

Plate 1: Steel casing for bored pile

Plate 2: Reverse circulation drill rig (RCD)

Plate 3: Reverse circulation drill rig (RCD)

Maximum design bell-out diameter as 1.5 times bored pile shaft diameter is commonly adopted in Hong Kong practice, which limits the maximum diameter of the bell-out to 4.50m for a pile with 3.0m shaft diameter. But bell-out bit or trimming cutter currently used in Hong Kong can achieve more than 4.50m

diameter of bell-out, and the bearing capacity can be increased about 4.5% by increasing every 100mm diameter in general.

Allowable vertical bearing pressure could be higher than the presumed values suggested by COP Foundation 2004 by demonstration under a trial pile test. This approach has been adopted in a current project C801 Express Rail Line – Detailed Design for West Kowloon Terminus and the advantage is upgrading the allowable bearing capacity for grade III rock from 5.0MPa to 7.5MPa, representing an increase of allowable bearing capacity for bored pile by 50%.

5 CONCLUSIONS

The conclusion of this paper can be drawn as follows:

- Bored pile foundation is a common and effective foundation type in Hong Kong.
- Bored pile foundation design in Hong Kong requires to comply with standard design codes or specifications set out by different government authorities, and the most optimized foundation layout may therefore be different, even under the same loading condition.
- It is high time to reappraise the overall design approach for achieving the prime goal of an ideal foundation design in terms of economics by minimizing the amount of piles numbers, and reducing pile numbers through maximising the pile capacity.
- Recommend to unify various standards in order to prevent any unnecessary conservative design.
- Innovative idea of enhancing bored pile capacity by rolling larger steel casing diameter (larger than 3.0m) should be considered.
- Innovative idea of relaxing the design requirement of limiting the maximum bell-out diameter to 1.5 times shaft diameter should be considered.
- Innovative idea of enhancing the allowable bearing pressure for rock category by trial pile test should be encouraged.

REFERENCES

Buildings Department 2004. *Code of Practice for Foundations*. Building Department, HKSAR Government, Hong Kong.

Architectural Services Department 2007. *General Specification for Building 2007 Edition.* Architectural Services Department, HKSAR Government, Hong Kong.

Highways Department, *Structures Design Manual for Highways and Railways*. Highways Department, Government of the Hong Kong Special Administrative Region.

Hong Kong Housing Authority 2008, *General Specification 2008 Edition.* Hong Kong Housing Authority, HKSAR Government, Hong Kong.

Civil Engineering and Building Structures Standards Committee. *BS8004: 1986 Code of Practice For Foundations,* Board of BSI

Civil Engineering and Building Structures Standards Committee. *BS8110: 1997 Structural Use of Concrete,* Board of BSI

Civil Engineering and Building Structures Standards Committee. *BS5400: 1998 Steel, Concrete and Composite Bridges,* Board of BSI

Chris Cheung, John Mennis, Keith Chong. *Proposed Site Specific Allowable Vertical Bearing Pressure of Bedrock in project C801 Express Rail Line – Detailed Design for West Kowloon Terminus.* AECOM

Recent Development of Shaft-grouted Piles in Hong Kong

A.K.M. Lam, G.K.F. Yam & A.Y.T. Liu
Ove Arup and Partners Hong Kong Limited

ABSTRACT

The use of shaft-grouting technique to enhance the pile shaft friction has been applied to the pile design and construction in Hong Kong since 1990s. This technique has been used for large diameter friction bored piles and friction barrettes for sites with weak saprolites and extra-ordinary deep bedrocks where the installation of the conventional driven piles and end bearing piles were found to be technically challenging. Recently, this technique has been applied to small diameter piles such as friction mini-piles and friction pre-bored H-piles at urban sites with access constraints and extended to areas with the geology dominated by the meta-siltstone/sandstone formation underlying by the marble bedrock. This paper gives a brief account of the development history and reviews the recent development of the shaft-grouting technique in Hong Kong. The design approaches and parameters for different soil strata verified by instrumented test piles subject to static load tests are discussed. Some observations and experience during construction of shaft-grouted piles are also summarized and discussed in this paper.

1 INTRODUCTION

The geology of Hong Kong Special Administrative Region (Hong Kong) is dominated by fill, marine deposit, colluvium and alluvium underlain by completely decomposed saprolites and solid granitic and volcanic bedrock. In some areas, an extra-ordinary deep bedrock poses a construction challenge to the conventional large diameter bored pile bearing on the rock and the pre-bored H-piles socketed into rock to support high-rise structures. The alternative is to use friction piles. However, in view of the limited shaft capacity of plain piles, the concept of shaft-grouting to enhance the shaft frictional capacity has been introduced to Hong Kong since 1990s and has been applied to friction bored piles and barrettes for site with weak saprolites. This technique has recently been extended to areas with the geology dominated by meta-siltstone/sandstone formation underlying by marble bedrock beyond 150m below ground. In recent years, the urban redevelopment has rapidly expanded in Hong Kong to satisfy the local demand and progressively more high-rise buildings are built within congested urban sites with works area and access constraints. In this regard, small diameter friction piles enhanced by the shaft-grouting become viable foundation options for sites characterized by extra-ordinary deep bedrocks.

2 A REVIEW OF SHAFT-GROUTING EXPERIENCE

The shaft-grouting technique was traditionally used for large diameter friction bored piles and friction barrettes for sites with weak saprolites and extra-ordinary deep bedrocks where the installation of the conventional driven piles and end bearing piles were found to be technically challenging. There were a few reported cases of using shaft-grouted piles in Hong Kong. The full-scale load testing programme for the KCRC West Rail Phase I reported by Plumbridge et al (2000) demonstrated that the shaft friction capacities measured for shaft-grouted barrettes and bored piles in completely decomposed granite (CDG) and volcanic (CDV) achieved up to a two or three fold increase in comparison with those without shaft-grouting. The use of shaft-grouted barrette in MTRC Kowloon Station Mega Tower Development reported by Chan et al (2004b) and the private residential developments at Tung Chung Designated Area reported by Sze et al (2007) also demonstrated the enhancement of shaft friction by shaft-grouting technique in sandy alluvium, completely decomposed rhyolite (CDR), CDG and diamict deposit (DD).

The shaft-grouting technique was also expanded to small diameter piles. In traditional design of small

diameter piles involving pressure grouting or pressurizing the concrete in Hong Kong such as Pakt-in-Place (PIP) pile, the ultimate shaft friction followed the empirical relationship of 4.8 x N where N is the Standard Penetration Test (SPT) 'N' value. Using the same empirical relationship, Lui et al (1993) reported the results of the three proof load tests on friction mini-piles consisting of 3T50 rebars showing a significant improvement of shaft resistance by shaft grouting the CDG layer.

3 RECENT SHAFT-GROUTING EXPERIENCE

Recently, the shaft-grouting technique has been extended to areas with site geology dominated by meta-siltstone/sandstone formation underlying by the marble bedrock. The experience in Yuen Long site is one of the successful examples. This technique also becomes more common for small diameter piles such as friction mini-piles and friction pre-bored H-piles at urban sites with access and works area constraints these days. The experience at sites near Hollywood Road, Seymour Road and Wong Nai Chung Road in urban areas of Hong Kong are discussed in the paper.

Yuen Long Site (YL): The site falls within the Scheduled Area of Northwest New Territories (Schedule Area No.2) with ground level at about +4.2mPD underlain by completely decomposed metamorphosed siltstone (CDMS). As revealed from the ground investigation (GI) records, the geology of the site mainly consists of about 4m think of fill overlaying about 4m to 18m thick of alluvium followed by a thick layer of completely to moderately decomposed metamorphosed siltstone. Cavity pockets are found in sound marble in various boreholes. Sound marble bedrock is encountered at depth of approximately 130m to deeper than 160m below the existing ground and no bedrock is found at some boreholes sunk to depth of greater than 180m. It was proposed to construct high-rise tower blocks within the site. In view of the geological setting, shaft-grouted barrettes with a size of 2.8m x 0.8m and a working capacity of 15.5MN were adopted.

Hollywood Road Site (HWR): The site is underlain successively by about 2m to 7m thick fill, about 6m to 9m thick bouldery colluvium, about 3m to 6m thick colluvium and more than 30m thick decomposed granite. Soil stratum of SPT 'N' value greater than 200 is encountered about 30m to 40m below ground. No bedrock is encountered at depth of 75m or greater. Two new buildings were proposed to construct within the site surrounded by existing historical buildings. In view of the limited site access, shaft-grouted friction pre-bored H-piles with a pile diameter of 610mm were proposed to support the new buildings with a working capacity upto 6MN. The existing historical buildings to be conserved were underpinned by shaft-grouted friction mini-piles consisting of 4T50 deformed bars with a pile diameter of 323mm and a working capacity of 1.57MN.

Seymour Road Site (SMR): The site falls within the Mid-Levels Scheduled Area (Scheduled Area No.1) over an existing slope and surrounded by existing geotechnical features and existing buildings. The ground investigation revealed that the site is composed of 1 to 6m thick of fill, 10 to 20m thick of colluvium, which is then underlain by a thick layer of medium dense to very dense completely to highly decomposed granite (C/HDG) to an average depth of 110m below the existing ground. The bedrock is found at depth of 115m to beyond 130m below the existing ground. A high-rise residential tower with a podium structure was proposed. In view of the site topography, shaft-grouted friction mini-piles comprising 4T50 deformed bars with a pile diameter of 323mm and a working capacity of 1.57MN were proposed to support the vertical load of the podium.

Wong Nai Chung Road Site (WNC): The ground investigation revealed that the site is underlain successively by about 5m thick of fill, about 7m to 15m thick of alluvial sand and more than 54m thick of CDG. No bedrock is encountered at depth of 70m or greater. A high-rise tower was proposed for the development. Due to the limited width of the site, the use of the large diameter bored piles became infeasible. In view of the geological condition, shaft-grouted friction pre-bored H-piles with a pile diameter of 610mm and a working capacity up to 6MN were proposed

4 DESIGN PARAMETERS AND CAPACITY

The compressive capacity of the shaft-grouted pile is mainly derived from the mobilized shaft friction in soil enhanced by shaft grouting. The shaft capacity was estimated with direct correlation with SPT 'N' values as given in the equation below.

$$\tau = f_s \times N \tag{1}$$

where τ = ultimate skin friction (kPa), f_s = correlation factor with SPT N-value and N = mean SPT values.

The ultimate skin friction was limited based on the previous load test results. The adopted design parameters for different sites are summarized in Table 1. A global factor of safety (FOS) is applied to the ultimate shaft resistance to derive the allowable pile capacity.

Table 1: Summary of Foundation Design Parameters

Site	Pile type with shaft-grouting	Pile size	Soil type	Approx. depth of stratum (m)	SPT 'N' range	Design shaft friction with correlation with SPT 'N'	Design limiting friction (kPa)	Design FOS
YL	Barrette	2.8m x 0.8m	Alluvium	4 – 18	4 – 113	4.5	180	2.0
			CDMS	18 – 54	10 – 200+	2.0	140	2.0
HWR	Mini-pile	323mm dia.	CDG	14 – 38	37 – 200+	4.8	240	3.0
	Pre-bored H	610mm dia.	CDG	9 – 51	30 – 200+	4.8	192	3.0
SMR	Mini-pile	323mm dia.	CDG	12 – 57	13 – 63	4.8	240	3.0
WNC	Pre-bored H	610mm dia.	Alluvium	5 – 18	21 – 39	4.5	180	3.0
			CDG	18 – 65	18 – 200+	4.8	192	3.0

5 PILE CONSTRUCTION

For shaft-grouted barrettes, the trench excavation was carried out using a mechanical grab for the upper portion of approximately 15 to 20m and the remaining trench excavation was carried out using a hydromill. The trench stability was maintained by bentonite slurry. When the trench excavation was completed and prior to the installation of the reinforcement cage, a scraping tool was lowered to the trench to remove the soft deposit or bentonite cake sticking on the soil faces. The soft deposit that had accumulated at the base of the trench was then removed using a suction pump. Mild steel tube-a-manchette (TAM) grout pipes of 48mm diameter, with prefabricated holes covered by rubble sleeves spaced at typical 0.33m intervals, were attached to the external face of the reinforcement cage, on four sides of the barrette. In total, eight shaft grouting pipes were installed around the perimeter of the barrette; three on each long side and one on each short side. The arrangement of the shaft grouting pipes around the barrette is shown in Figure 1.

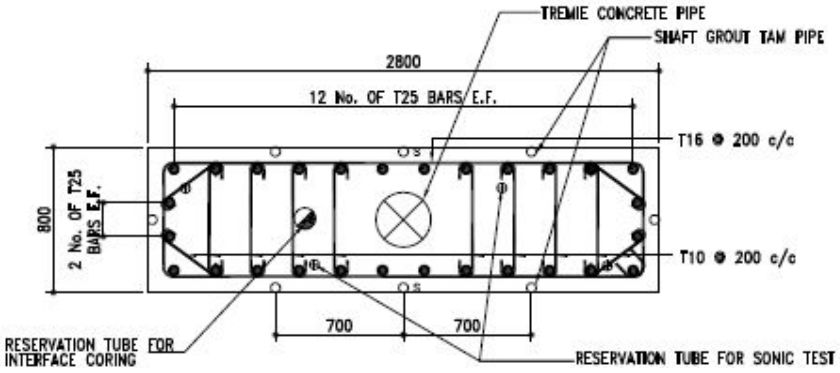

Figure 1: Typical grout pipe arrangement of shaft-grouted barrette

For shaft-grouted mini-piles and pre-bored H-piles, a pre-bored hole was formed by concentric drilling method. A temporary steel casing was provided during the pile boring to prevent the hole from collapse. After reaching the design founding level, a bundle of reinforcement or steel section with TAM pipes will be placed centrally into the completed hole. For test piles, sleeve casing with 2mm thick bitumen coating with slightly smaller diameter than the temporary steel casing was installed to eliminate the shaft resistance contributed by the superficial layers such as fill and colluvium. The pile was then grouted under water to the ground level in one continuous operation followed by the extraction of the temporary steel casing. The construction details for shaft-grouted mini-pile and pre-bored H-pile are illustrated in Figures 2 and 3 respectively.

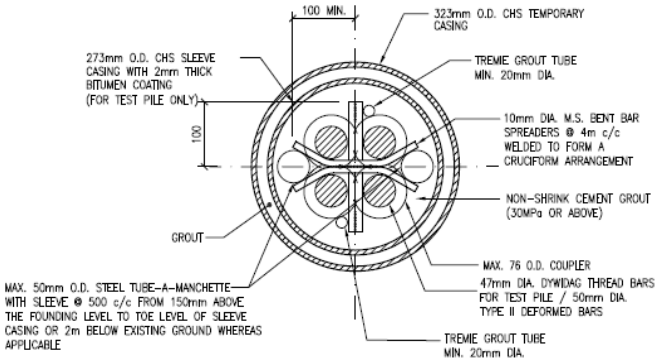

Figure 2: Typical grout pipe arrangement of shaft-grouted mini-pile

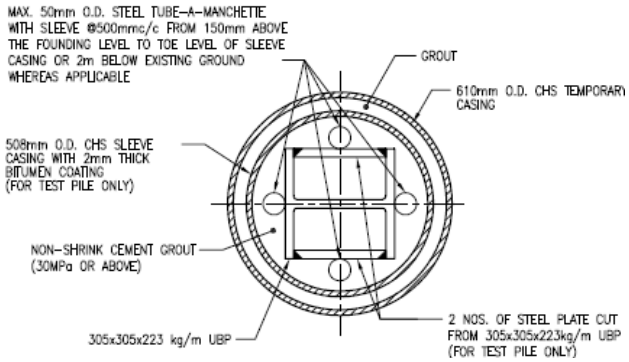

Figure 3: Typical grout pipe arrangement of shaft-grouted pre-bored H-pile

When the piles were constructed, the water cracking were usually carried out between 12 and 24 hours after grouting or concreting. The rubble sleeves were first cracked under a water pressure of 20-40 bar using a small diameter flexible double end packer system. Cement grout was then injected from the lowest sleeve in each grout tubes at regular interval (i.e. usually 1m for barrette/bored pile and closer spacing for small diameter piles) and carried out in a bottom up sequence. The grouting operation was usually real-time monitored and controlled by an electronic system. The primary criterion is to achieve the target grout volume of 35 litre per surface area of the pile aiming to restore any inward soil displacement during the trench excavation or pile bore. Other criteria include the achievement of the target grout pressure of 2 times the effective overburden pressure and the average grout intake over a designated grouting depth.

Based on the site observations, occasional blockage of the rubble sleeves and low grout intake at certain levels were reported. These may be attributed to the presence of hard layers, upward flow of grout blocking the flow path of sleeves above, decrease of grout viscosity with time, poor quality rubble sleeves, etc. This can be improved by prolonged injection of water during the water cracking operation, avoid over-grouting at lower sleeves, regular check on the flowability of grout and compensation of grout take from adjacent sleeves.

6 TEST PILE

Test piles were proposed for all sites prior to the commencement of the working piles. Most of the test piles were instrumented over their full depth to measure the load shed to the ground and the pile displacement along the pile depth. Strain gauges were installed at regularly interval from the pile cut-off to 1m above pile base. For barrettes, four sets of strain gauges were usually installed at each level while for mini-piles and pre-bored H-piles, two sets of strain gauges were normally installed. For barrettes, because of the larger pile sectional area, rod extensometers were also installed to the interface of different soil stratum and to the pile base to counter-check the measurement from the strain gauge readings. During the loading tests, the vertical displacement of the head of the pile was measured directly using Linear Variable Differential Transformers (LVDT) and cross-checked by dial gauges mounted on the reference beam.

For barrette, the test load was applied in two loading and unloading cycles to maximum 2 times of the design working capacity while for mini-piles and pre-bored H-piles, the test load was applied in three cycles to 3 times of the design working capacity. In view of the high test load, high strength thread bars for mini-pile and built up H-section with additional stiffening plates for pre-bored H-pile were commonly adopted for test piles. A 72-hour hold was carried out at the maximum test load in order to fulfill the statutory requirement. The acceptance criteria of proof test for barrettes can make reference to Sze et al (2007) while that for mini-piles and pre-bored H-piles follow the criteria stipulated under BD (2004).

7 RESULTS AND INTERPRETATIONS

The pile head settlements and residual settlements of the test piles at maximum test load for different sites are summarized in Table 2. They are well within the acceptance criteria. The strain gauges readings were analyzed to interpret the load distribution along the test piles. At each level, the strain values were averaged and any isolated gauges giving anomalous readings were excluded. The mobilized shaft friction and the correlation factor with SPT N-value are summarized in Table 3.

Table 2: Summary of Test Pile Settlement

Site	Test pile reference	Pile type	Maximum test load (kN)	Pile length below ground (m)	Pile head settlement (mm)		Residual settlement (mm)	
					Measured	Allowable	Measured	Allowable
YL	BR-1	Barrette	31,000	50.9	26.0	66.1	5.4	33.8
	BR-2	Barrette	31,000	50.4	22.2	66.1	7.4	33.8
HWR	TP-M2	Mini-pile	4,710	38.2	28.6	59.6	6.1	6.7
	TP-M3	Mini-pile	4,710	34.1	20.2	53.9	4.1	6.7
	TP-H1	Pre-bored H	18,000	53.5	28.1	89.9	5.4	22.5
	TP-H2	Pre-bored H	18,000	57.5	47.4	91.0	9.5	22.8
SMR	TPA1	Mini-pile	4,710	54.6	37.6	104.4	3.7	9.4
	TPA2	Mini-pile	4,710	47.2	32.6	85.6	3.0	8.1
WNC	TP-1	Pre-bored H	18,000	63.4	11.9	58.7	0.2	6.7
	TP-2	Pre-bored H	18,000	64.9	16.1	59.8	0.7	6.7

It can be seen that the test barrettes at YL site showed that the correlation factor with SPT N-value in the alluvium could be up to 13.5N while the maximum mobilized shaft friction was only about 138kPa. This is due to the fact that the loose alluvial deposit with low SPT N-value in the range of 4 to 15 shows a greater improvement in load transfer at the pile soil interface after shaft-grouting. However, because of its low SPT N-value, the shear resistance is limited. Comparing with the CDMS with SPT N-value ranging from 17 to

greater than 200, the test pile BR-1 demonstrated that the maximum mobilized shaft friction was as high as 167kPa while the test pile BR-2 verified that the correlation factor with SPT N-value could be up to 3.1N. The test mini-piles and pre-bored H-piles with mean SPT N-values ranging from 14 to 110 in CDG generally showed that the correlation factors varying from 2.6N to as high as 24.4N. The mobilized shaft friction was generally greater than 240kPa except for test pile TPA1 with relatively low mean SPT N-value of 14.

Table 3: Summary of Mobilized Shaft Friction for Instrumented Piles

Site	Test Pile Reference	Pile Type	Soil Type	Mean SPT 'N'	Mobilized shaft friction, fs	fs/N
YL	BR-1	Barrette	Alluvium	9	121	13.5
			Alluvium	6	73	12.1
			CDMS	96	167	1.7
			CDMS	200	143	0.7
	BR-2	Barrette	Alluvium	10	138	13.5
			CDMS	42	106	2.5
			CDMS	26	81*	3.1
HWR	TP-M2	Mini-pile	CDG	43	275	6.4
	TP-M3	Mini-pile	CDG	78	248	3.2
			CDG	95	243	2.6
			CDG	110	298	2.7
	TP-H1	Pre-bored H	CDG	78	264	3.4
	TP-H2	Pre-bored H	CDG	49	284	5.8
SMR	TPA1	Mini-pile	Residual soil	14	277	19.4
			CDG	14	127	9.4
	TPA2	Mini-pile	CDG	22	427	19.2
			CDG	19	353	18.6
WNC	TP-1	Pre-bored H	Alluvium	31	482	15.5
			CDG	18	438	24.4

* Denotes the shaft friction has not been fully mobilized

8 COMPARISON WITH PUBLISHED TESTS

Figure 4 compares the recent shaft-grouted barrette and bored pile test results with the data from previous projects reported by Plumbridge et al (2000), Chan et al (2004b), Sze et al (2007) & GEO (2006). Given the available test data, a lower bound value of 5N with a limiting shaft friction of 200kPa for sandy alluvium and 2.4N with a limiting shaft friction of 140kPa for weak saprolites and CDMS can be established. Figure 5 presents the relationship between the shaft friction and the mean SPT N-value for mini-pile and pre-bored H-piles for the alluvium and CDG. Because of the size effect, both test mini-piles and pre-bored H-piles show a substantially greater mobilized shaft friction as well as the correlation factor with SPT 'N' value than barrettes and bored piles. Based on the data from different sites, a lower bound value of 4.8N with a limiting shaft friction of 240kPa for CDG and alluvium is established. These lower bound values may be used for preliminary design of shaft-grouted piles. However, they may vary slightly with different geological

formations, soil permeabilities, soil stiffnesses, pile installation methods, contractor's experiences and equipment, etc. Site specific pile load tests are therefore suggested to ensure satisfactory pile performance.

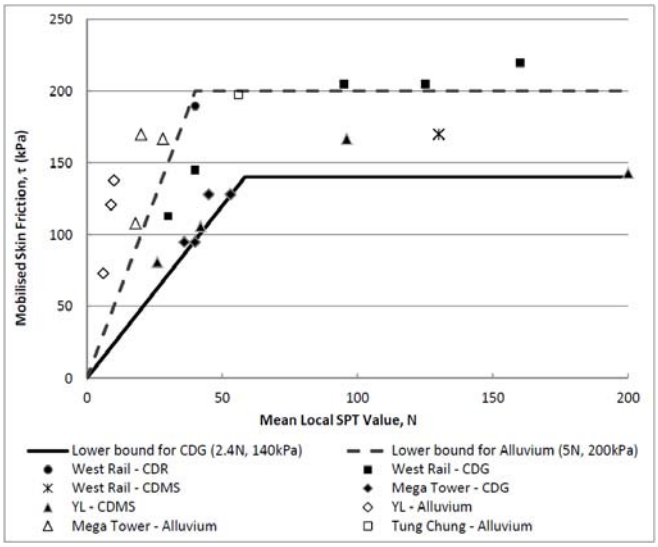

Figure 4: Shaft friction in alluvium, CDG & CDMS for barrette and bored pile tests in Hong Kong

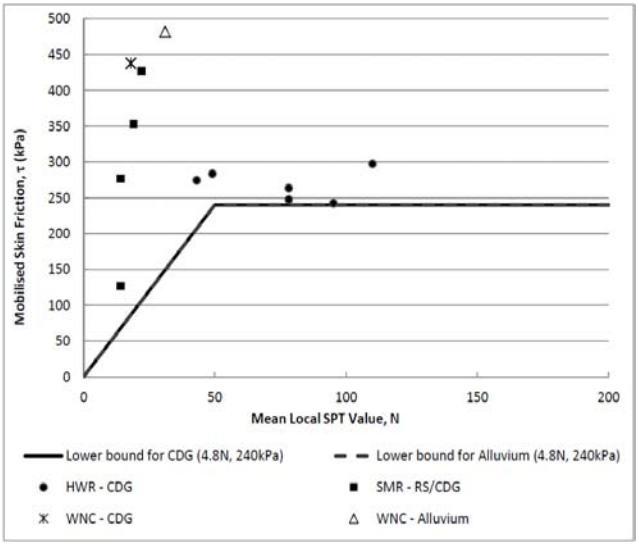

Figure 5: Shaft friction in alluvium & CDG for mini-pile and pre-bored H-pile tests in Hong Kong

9 CONCLUSIONS

The use of the shaft-grouting technique has traditionally been applied for friction barrettes and bored piles in the alluvium and weak saprolites. The application of shaft-grouted barrettes at Tung Chug reported by Sze et al (2007) and at Yuen Long have demonstrated that this technique can be extended to areas with the geology dominated by diamict deposit and meta-siltstone/sandstone underlying by marble formation in Hong Kong. In recent years, more urban sites are redeveloped within congested areas into high-rise structures. Given the works area and site access constraints, friction mini-piles and pre-bored H-piles enhanced by shaft-grouting are the viable foundation solution for sites characterized by extra-ordinary deep bedrocks. A couple of projects in Hong Kong presented in the paper has proven the mobilized shaft frictions in alluvium and completely decomposed granite for these small diameter piles.

REFERENCES

BD (2004), Code of Practice for Foundations, Buildings Department, HKSAR, 57p.

Chan, G., Lui, J.Y.H., Lam, K., Yin, K.K., Law, C.W., Lau, R., Chan, A., & Hasle, R. (2004b), Shaft Grouted Friction Barrette Piles For A Super High-rise Building, *Proceedings, New Perspectives in the Design and Construction of Foundation Structures, HKIE*, 83-98.

GEO (2006), *Foundation design and construction publication No. 1/2006*, CEDD, HKSAR

Lui, S.P.Y., Cheung, S.P.Y. & Chan, A.K.C. (1993), Pressure grouted minipiles for a 12-storey residential building at the mid-levels scheduled area in Hong Kong, *Proceedings Second International Conference on Soft Soil Engineering, Guangzhou*, 419-424.

Plumbridge, G.D., Littlechild, B.D., Hill, S.J. & Pratt, M. (2000). Full scale shaft grouted piles and barrettes in Hong Kong – A first. *Proceedings of the Nineteen Annual Seminar of the Geotechnical Division of the HKIE, Hong Kong,* 157-166.

Sze, J.W.C., Lam, A.K.M., Pappin, J.W. & Chan, K.M. (2007), Design and construction of shaft-grouted friction barrette in Tung Chung Designated Area, *Proceedings of the HKIE Geotechnical Division Annual Seminar 2007, HKIE,* 299-304.

Pile Settlement Induced by Diaphragm Wall Installation

I.S. Haryono
Golder Associates (HK) Ltd., Hong Kong
M. Korff
Deltares, Delft, The Netherlands

ABSTRACT

The influence of diaphragm wall installation to the surrounding soil has been analysed earlier by many researchers. However, soil – structure interaction during the installation process has not received many attentions. The analysis of field monitoring data of North – South Line project in Amsterdam indicates that the installation process of the diaphragm wall has a significant influence on the adjacent piled buildings. Three-dimensional finite element analysis is carried out to back analyse the installation process of the diaphragm wall panels. The calculated settlements of the piles and the soils are verified against the monitored settlement of the soils and the buildings. Based on the calculation results, the axial force in the piles is reduced after the installation of the panels. Stress relief in the soil and the influence of relative pile – soil settlement have been found as the main triggering factors. Moreover, the results indicate that pile settlement has a close relationship to the neutral plane in the piles and therefore, this could be a basis for the assessment of pile settlement in an excavation project.

1 INTRODUCTION

It is well understood that construction of diaphragm wall installation always induces disturbance to the adjacent soils and the importance of the modelling of the construction process has been well recognized. Ng et al (1995) with pseudo three-dimensional numerical analysis and subsequently, Ng & Yan (1999) with full three-dimensional model showed the effect of horizontal arching and downward load transfer mechanisms in the diaphragm wall installation sequence. Some observations were also made on the deformation, but it was only limited to surface settlement. In other result, based on centrifuge result in overconsolidated clay, Powrie and Kantartzi (1996) investigated the effect of panel length to the settlement after the construction of diaphragm wall. The results indicated that the longer the panel, the larger the settlement of the adjacent soil. Gourvernec and Powrie (1999) emphasized based on comparison between analysis using plain-strain model and full three-dimensional model that diaphragm wall installation is indeed a three-dimensional phenomenon.

However, the results of these studies are only limited to the influence on the soils. The influence of diaphragm wall installation on the adjacent piles has not received many attentions. Many construction sites are situated in a densely populated urban area and hence, the distance between the diaphragm wall alignment and the adjacent existing buildings is very close. In this condition, the installation potentially affects the adjacent pile foundations.

This paper will discuss the results of back analysis carried to simulate the pile – soil interaction during diaphragm wall installation in the North-South Line project, Amsterdam, The Netherlands. Using the results, observation on the pile behaviour affected by diaphragm wall installation will be presented. Moreover, some correlation between pile settlement and the neutral plane, as the effect of negative skin friction, will be discussed.

2 NORTH-SOUTH LINE PROJECT, AMSTERDAM

2.1 Introduction

North – South Line project is constructed to expand the existing subway system in Amsterdam. This project passed through the historic centre of Amsterdam. The old buildings in the region were constructed in the late 1800s and founded on driven timber piles. In total, 8 underground stations were constructed but the focus of this paper is set on Ceintuurbaan station, particularly on cross section 13110E, which is situated at the east part of Eerste jan van der Heijdenstraat.

Figure 1 shows the plan view of the Ceintuurbaan Station with the building and ground deformation monitoring points. Ceintuurbaan station is the deepest underground station built among other stations built in this project. The final excavation level is NAP -30.9 m and the level of the surface is NAP +0.4 m (NAP is Dutch reference level). Moreover, this is also the narrowest station, 12.8 to 13.8 m wide and the length of the station is approximately 210m. The cross section No. 13110E showing the station is presented in Figure 2. The diaphragm wall is 1.2 m thick and it is constructed to NAP -45 m. In general, the length of each diaphragm panel varies from 2.6 m to 5.8 m. There are 7 levels of struts, including concrete roof, 2 floor slabs, 2 levels of 1000 mm hollow-circular steel struts, and jet grout layer which is constructed below the base slab.

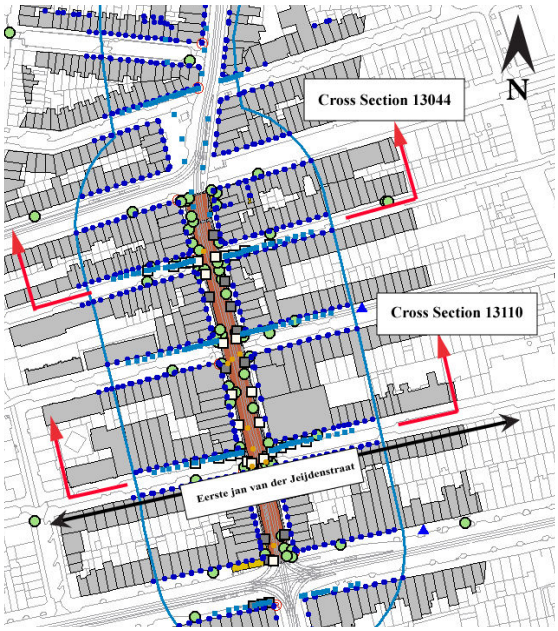

Figure 1: Plan view of Ceintuurbaan station

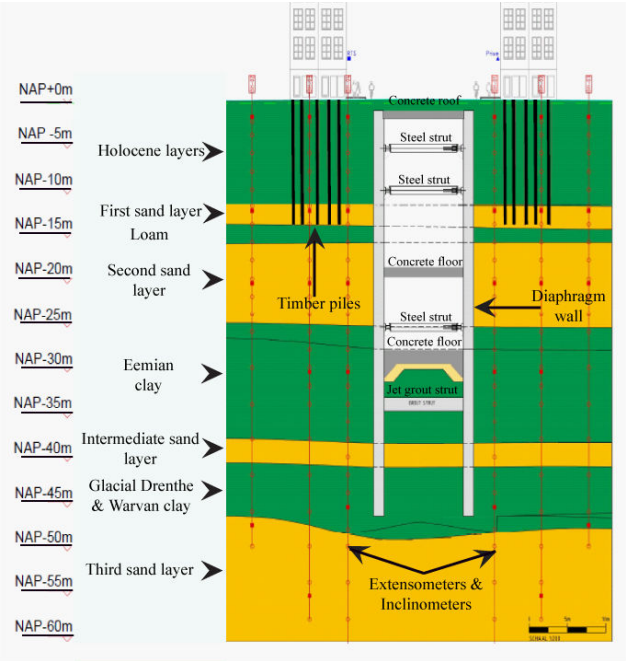

Figure 2: Cross section of Ceintuurbaan Station at 13110E

2.2 Subsurface condition

Figure 2 illustrates the cross section No. 13110E and also the typical subsurface condition found in the region. Table 1 lists the subsurface materials and the associated phreatic levels of each material.

It is commonly understood that Amsterdam surface experiences long term and continuous settlement (Hogenes, 1998). The settlement rate is approximately 2.2-3.5 mm/year at the ground surface. This is caused by the polder conditions in combination with the fact that the government gradually increases the road level which triggers the occurrence of consolidation and creep settlement.

2.3 Pile condition

The typical foundation for old buildings in Amsterdam is illustrated in Figure 3. A row of twin driven timber piles were installed underneath the masonry walls of the buildings. The horizontal distance between each group of piles is approximately 80 cm centre to centre. Each pile has 180-200 mm diameter at the top and normally, it is tapered with gradient of 8 mm/m, resulting in smaller tip diameter. It is found that the minimum tip diameter is about 80 mm to 85 mm. The tip of the pile is generally driven into the First sand layer, which is at approximately NAP -12 m to -13 m. No records of working load of the piles are found, however, Korff (2013) suggested that the minimum and maximum working load for each pile is between 70 kN and 140 kN, and the most likely case is between 70 kN and 100 kN.

Table 1: Soil layers and phreatic levels

Geomaterials	Top Level [NAP]	Phreatic Level [NAP]	Geomaterials	Top Level [NAP]	Phreatic Level [NAP]
Sandfill*	+0.4m	-0.5m	Loam	-14.0m	-3.0m
Holland peat*	-3.0m	-0.5m	Second sand layer	-16.0m	-3.0m
Old sea clay*	-5.0m	-0.5m	Eemian clay	-25.0m	-3.0m
Waddeposit*	-6.4m	-0.5m	Intermediate sand layer	-38.0m	-3.0m
Hydrobia clay*	-10.5m	-0.5m	Glacial Drenthe clay	-42.0m	-3.0m
Basis peat*	-11.0m	-0.5m	Glacial Warvan clay	-45.0m	-3.0m
First sand layer	-11.5m	-3.0m	Third sand layer	-50.0m	-3.0m
**Members of Holocene layers*					

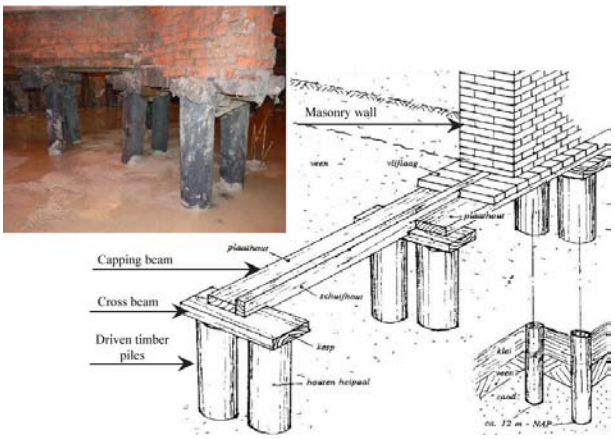

Figure 3: Typical Amsterdam foundation (Zantkuijl 1993)

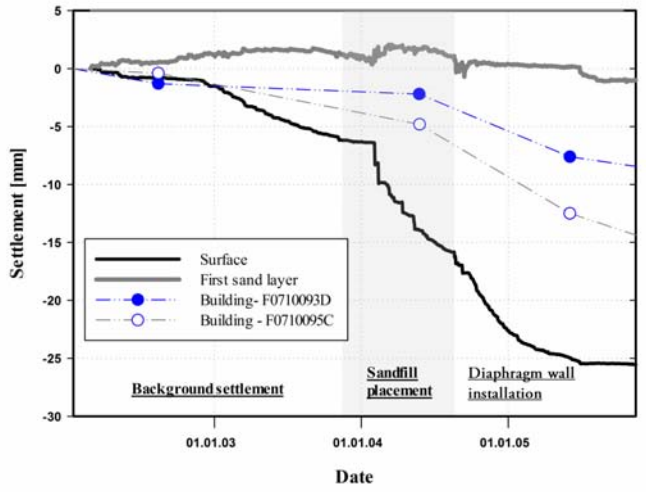

Figure 4: Results from monitoring points situated 3 m from diaphragm wall

2.5 Construction sequence

The construction of the Ceintuurbaan station actually consists of several phases. However, the focus of this study is on the initial phases carried out prior to the bulk excavation. The first phase is the placement of 70 cm thick sand layers on top of the station box as a working platform to construct the diaphragm wall panels. After this phase, diaphragm panels were immediately constructed. The distance between the outer perimeter of the diaphragm wall and the adjacent buildings is approximately 3 m.

2.6 Discussion on the monitoring results

Figure 4 shows the monitoring results of the cumulative settlement of the ground surface, First Sand layer, and the adjacent building measured from monitoring points located approximately 3 m from the edge of the

diaphragm wall. The plots indicate that the building settles 7 to 13 mm, notwithstanding the first sand layer does not show any notable settlement. Moreover, the settlement value of the building is generally less than the settlement of the ground surface.

This phenomenon is normally found in piles experiencing negative skin friction, one of the triggering factor of settlement for pile affected by deep excavation (Korff 2013). Figure 5 illustrates the distribution of soil and pile settlement in the downdrag event is illustrated in Figure 5. Assuming that the elastic compression of the pile is negligible, then the settlement of the pile subjected to downdrag is governed by the position where the relative soil and pile displacement is zero. This position is normally called neutral plane. In this location, negative and positive skin friction will be balanced.

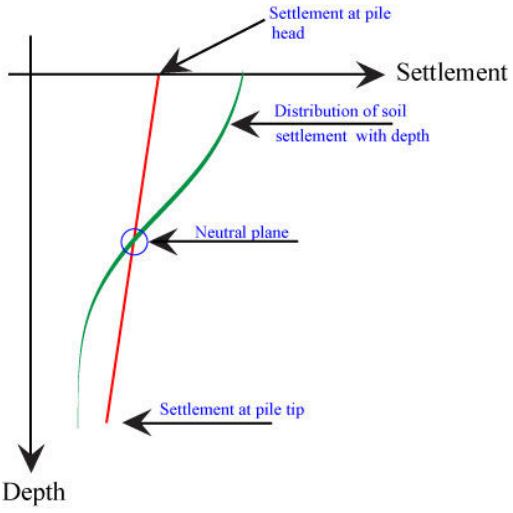

Figure 5: Illustration of relative pile – soil displacement due to downdrag

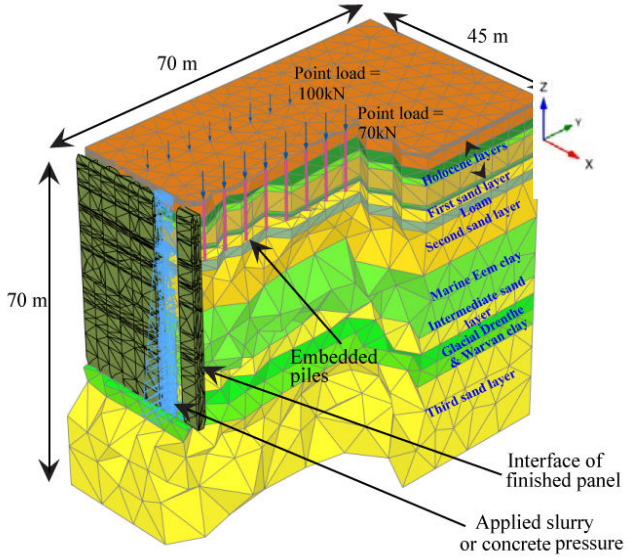

Figure 6: 3D model of panels installation

3 NUMERICAL MODEL OF DIAPHRAGM WALL INSTALLATION

3.1 General

Three – dimensional analysis is carried out to simulate the installation process using PLAXIS3D software. The analysis consists of 3 main stages; simulation of 100 years of long term settlement, sandfill placement, and the construction of diaphragm wall panels. It is believed that the long term settlement has mobilized negative skin friction in the pile, therefore, this step is deemed to be significant to model the piles as this step will give the correct initial condition of the piles. Figure 6 shows the plan view of the model. Two rows of piles are modelled in the analysis and the locations of these rows are placed at the footprint of the actual buildings. Haryono (2013) learned that the response of the soil in cross section 13110E is influenced utmost by the installation of 5 adjacent panels. However, to consider the response of the adjacent piles groups, the analysis will simulate the installation of 9 panels. The length of these panels varies between 2.6 m to 3.8 m.

3.2 Soil constitutive model and analysis sequence

Considering the insitu condition, there are 2 distinct events that will influence the decision of the constitutive model used in the analysis, which are the long term settlement and the diaphragm wall installation. Consequently, 2 different sets of soil constitutive models are used in the analysis. To model the consolidation and creep, the Soft Soil Creep (SSC) Model is adopted, while for the sandfill placement and diaphragm wall installation phase, the soils are modelled using Hardening Soil Model. The complete soil parameters used in this study are summarized in Table 2 and Table 3. The analysis consists of 3 main stages; (1) simulation of

100 years autonomous settlement, (2) sand fill placement period, and (3) the construction of diaphragm wall panels at 13110E.

Table 2: Adopted soft soil creep parameters during the simulation of 100 years of autonomous settlement (adopted R_{int} = 0.7 for all soil layers)

Material	γ_{unsat} [kN/m^3]	γ_{sat} [kN/m^3]	c' [kPa]	ϕ [^{0}]	e_o	C_c [kPa]	C_s [kPa]	C_α [kPa]	k_x, k_y, k_z [m/day]	POP [kPa] Or OCR
Sandfill	Modelled as Hardening Soil Model (see table 3)									POP = 0
Holland peat	10.5	10.5	5	20	7.78	2.644	0.24	0.023	$8.64x10^{-4}$	POP = 10
Old sea clay	11	16.5	7	33	1.35	0.606	0.086	0.049	$1.29x10^{-4}$	POP = 10
Waddeposit	Modelled as Hardening Soil Model (see table 2)									POP = 0
Hydrobia clay	13	15.2	8	34	1.73	0.880	0.1	0.0063	$8.64x10^{-5}$	POP = 10
Basis peat	11.7	11.7	6	21	3.63	2.104	0.2	0.0123	$8.64x10^{-4}$	POP = 10
1st sand layer	Modelled as Hardening Soil Model (see table 3)									POP = 0
Loam										POP = 0
2nd sand layer										POP = 0
Eemian clay	13.1	17.9	20	32	0.99	0.358	0.033	0.0044	$1.73x10^{-4}$	OCR = 2.0
Intermediate sand layer	Modelled as Hardening Soil Model (see table 3)									POP = 0
Glacial Drenthe clay	15.9	19.7	15	34	0.64	0.143	0.014	0.0018	$8.64x10^{-3}$	OCR = 1.5
Glacial Warvan clay	15	18.5	5	32	0.32	0.143	0.014	0.0018	$8.64x10^{-3}$	OCR = 1.5
3rd sand layer	Modelled as Hardening Soil Model (see table 3)									POP = 0

Table 3: Adopted hardening soil parameters during construction (Adopted R_{int} = 0.7 for all soil layers)

Material	γ_{unsat} [kN/m^3]	γ_{sat} [kN/m^3]	c' [kPa]	ϕ [^{0}]	E'_{50ref} [kPa]	E'_{50ref} [kPa]	E'_{50ref} [kPa]	k_x, k_y, k_z [m/day]	m	R_{int}
Sandfill	15	15	0.1	25	10000	8000	30000	$8.64x10^{-2}$	0.8	0.7
Holland peat	10.5	10.5	5	20	2000	1000	10000	$8.64x10^{-4}$	0.8	0.7
Old sea clay	11	16.5	7	33	9000	3000	25000	$1.29x10^{-4}$	0.8	0.7
Waddeposit	13.3	17.9	2	35	12000	6000	33000	$8.64x10^{-3}$	0.5	0.7
Hydrobia clay	13	15.2	8	34	9000	5000	15000	$8.64x10^{-5}$	0.8	0.7
Basis peat	11.7	11.7	6	21	2000	1000	10000	$8.64x10^{-4}$	0.8	0.7
1st sand layer	16.8	19.8	0.1	33	40000	30000	200000	12.96	0.5	0.7
Loam	14.4	18.5	0.1	33	17000	13000	45000	2.592	0.5	0.7
2nd sand layer	15	19	0.1	35	35000	35000	190000	8.64	0.5	0.7
Eemian clay	13.1	17.9	20	32	11000	5500	50000	$1.73x10^{-4}$	0.8	0.7
Intermediate sand layer	16	19.4	0.1	33	2500	15000	140000	$8.64x10^{-1}$	0.5	0.7
Glacial Drenthe clay	15.9	19.7	15	34	15000	5000	75000	$8.64x10^{-3}$	0.8	0.7
Glacial Warvan clay	15	18.5	5	32	15000	4000	58000	$8.64x10^{-3}$	0.8	0.7
3rd sand layer	17	19.6	0.1	35	35000	40000	200000	8.64	0.5	0.7

3.3 Pile model

In this study, it is assumed that the buildings are sufficiently flexible to follow settlement of the piles. The following analysis will model the buildings as a row of piles with a point load applied on top of the pile to simulate the working load imposed by the superstructure. The presence of the twin piles is simplified and hence, it is represented by a single pile. Two rows of piles are modelled in the analysis and the locations of these rows are placed at the footprint of the masonry walls, as shown in Figure 6. The tip of the piles is set at NAP -12 m (First Sand layer) and the diameter of the piles is assumed as 180 mm. Due to the uncertainties in the actual working load, two different loads are applied, i.e 100 kN and 70 kN. The piles are modelled using the embedded pile model available in PLAXIS3D. The calculation of the maximum tip resistance and shaft resistance of the pile adopts the CPT-based method as indicated in Eurocode 7 with Dutch guideline (NEN9997-1+C1). Table 4 summarizes the maximum shaft resistance (T_{max}), calculated based on the cone resistance of each layer (q_c) and the shaft friction factor (α_s). Furthermore, the maximum tip resistance is 78 kN; assuming the pile class factor (α_p), factor of pile base shape (β), and factor of the cross section of the pile base is 1. The elastic stiffness of the timber pile is assumed a 15 x 10^6 kPa.

Table 4: Shaft resistance of the embedded pile model

Materials	α_s	q_c [MPa]	T_{max} [kN/m]
Sandfill	0.01	2.0	11.3
Holland peat	0.00	0.5	0.0
Old sea clay	0.02	1.0	11.3
Waddeposit	0.01	1.0	5.7
Hydrobia clay	0.02	1.0	11.3
Basis peat	0.00	0.5	0.0
First sand layer	0.01	Varies between 1 &18	56.55

3.4 Diaphragm wall installation

The simulation of the diaphragm wall consists of 2 stages, i.e trenching and concreting phase. In the trenching period, hydrostatic pressure envelope is applied in a certain time span according to the actual trenching period in the construction schedule. There has been no measurement on the unit weight of the bentonite, however based on the back analyses, a best fit of the soil and pile displacement can be obtained using unit weight of 12 kN/m^3. During concreting period, different pressure envelope is applied. Bilinear pressure envelope suggested by Lings et at (1994) has been adopted in this study. Back analyses by Wit & Lengkeek (2002) in Amsterdam case study and Schad et al (2007) in Rotterdam case study prove that the suggested pressure envelope by Lings et al is feasible to be applied. During the back analysis in this study, it was found that a critical depth of 1/5 of total depth leads the results to a good agreement with the measured soil settlement. This is comparable to the measured critical depth in an Amsterdam field test as presented by Wit & Lengkeek (2002).

4 ANALYSIS RESULTS

4.1 Comparison between calculated and monitored soil and pile settlement

Figure 7 shows the settlement of the ground surface, First Sand layer, and adjacent buildings along the cross section 13110E. In the figure, pile 70 refers to pile loaded by 70 kN and pile 100 refers to pile loaded by 100 kN. The plots indicate that the calculated settlement is comparable to the measurement data. Furthermore, it suggests that the settlement of pile 70 is generally closer to the measured buildings settlement. It can be concluded that the actual working load of the pile is possibly close to 70 kN. The difference in the settlement of pile 70 and 100 can be explained by the difference in the neutral plane position, which will be discussed further in the next chapter.

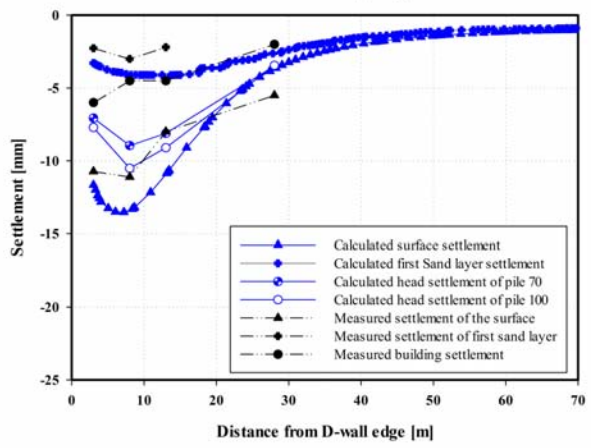

Figure 7: Calculated and measured soil and building settlement

The discrepancy between the settlement of pile 70 and the measured building settlement might be caused by the limitation of embedded pile model. This model is originally intended to model soil – replacement pile, e.g bored pile. Therefore, specific feature in driven pile such as densification at the pile tip cannot be fully included resulting in softer behaviour.

4.2 Change in piles axial force.

Some changes in the axial force profile of pile 70 and 100 could be observed. Figure 8 and 9 presents the changes of the axial force in the piles located 3 m away from diaphragm wall, indicated as pile 70-3 and pile 100-3. Due to the installation of diaphragm wall panels, the axial force in the piles is slightly reduced. The reduction in the load distribution of the pile is mainly controlled by the stress relaxation in the soil during the trenching and concreting period. In this period, the difference between the slurry or concreting pressure and the insitu stress leads to the reduction in normal stress acting on the pile, in which the pile relies on to gain its capacity.

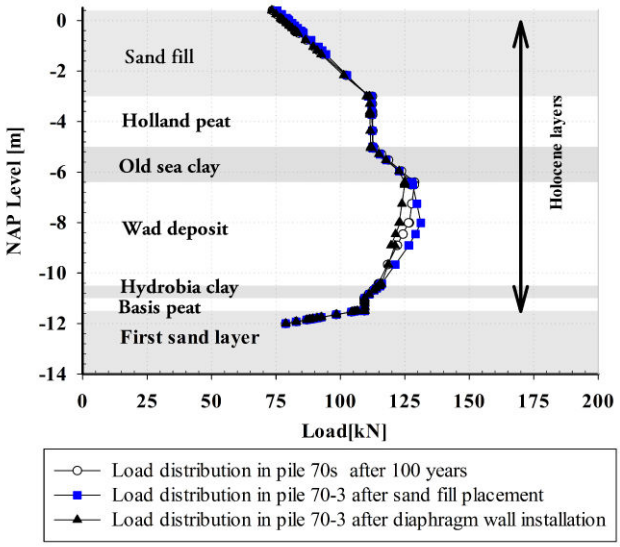

Figure 8: Calculated axial force in pile 70-3

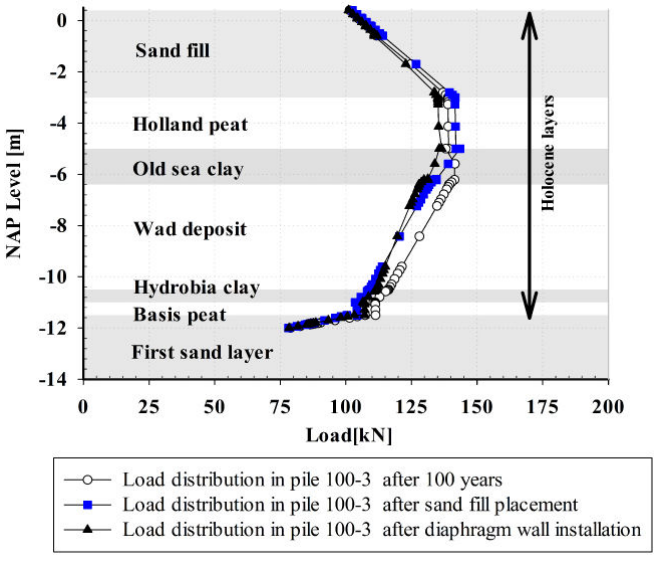

Figure 9: Calculated axial force in pile 100-3

It can be observed that in both piles, negative skin friction has been developed after 100 years of long term settlement. Moreover, it should be noted that maximum shaft and tip resistance has been achieved prior to the commencement of the project. Based on the observation on the axial force in the piles, different neutral plane is found. In the initial condition, the neutral plane of piles loaded by 70 kN is located at NAP -8 m, while for piles loaded by 100 kN, the neutral plane is higher at NAP -6 m. As described by Korff (2013), the neutral plane and the settlement of the pile subjected to drag load is influenced by the external load. Larger load will potentially induce higher neutral plane position and eventually, it leads to larger settlement. Figure 10 illustrates the changes of the neutral planes from both piles as the construction proceeds. The plots show that the trend of the ratio of the measured building settlement to the ground surface and foundation layer settlement matches with the trend of the neutral plane location in each construction stage, particularly with the neutral plane location from piles loaded with 70 kN of working load. This reasonable agreement shows that that pile settlement is closely related to the position of the neutral plane and hence, the approximate settlement of the pile could be predicted by understanding the position of neutral plane of the pile.

On the other hand, it can be observed that the neutral plane location of pile 100-3 is higher than the neutral plane location observed in pile 70-3. This observation explains larger load is normally associated with higher neutral plane position and therefore, it could be expected that piles with larger load will experience larger settlement.

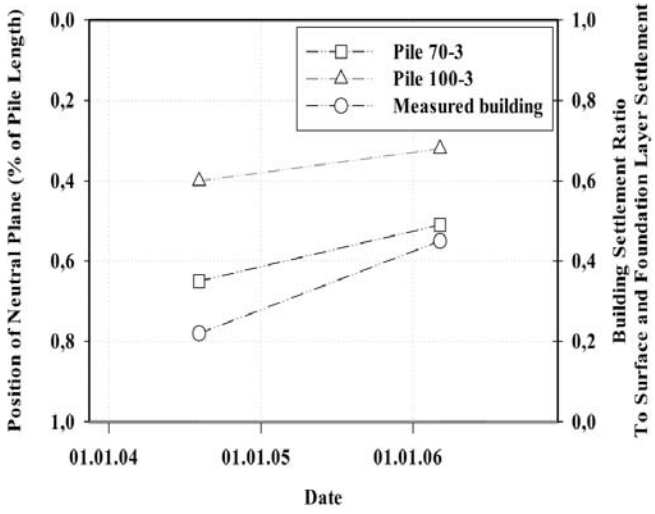

Figure 10: Comparison between position of neutral plane and building settlement ratio to surface settlement

5 CONCLUSIONS

The results of the study show that due to the installation of diaphragm wall, the axial force in the piles has been reduced and it is mainly caused by the stress relief in the soil which further leads to the reduction in normal stress acting on the pile. Moreover, it can be observed that the settlement of the pile could be related to the position of the neutral plane. Therefore, position of neutral plane could be a first order guidance in predicting pile settlement. However, this conclusion needs to be confirmed in other situation when the pile tip capacity is significantly disturbed or there are some traces of notable stress reduction in the surrounding area.

REFERENCES

Brinkgreve, R. B. & P. A. Vermeer. 2012. PLAXIS 3D-Finite Element Code for Soil and Rocks Analysis.

Gourvenec, S. M. & W. Powrie. 1999. Three-dimensional finite-element analysis of diaphragm wall installation. *Geotechnique* 49(6): 801-823.

Haryono, I.S. 2013. *Pile foundation and soil response to deep excavation*. MSc. Thesis, Delft University of Technology.

Hogenes, C.A.G. 1998. Meetboutennet Amsterdam (NAP-hoogtemerken). 7 August 1998. Omegam.

Korff, M. 2013. *Response of piled buildings to the construction of deep excavations*. Diss. IOS Press.

Lings, M. L., C. W. W. Ng, & D. F. T. Nash. 1994. The lateral pressure of wet concrete in diaphragm wall panels cast under bentonite. *Proceedings of the ICE-Geotechnical Engineering* 107(3): 163-172.

NEN 9997-1+C1. 2012. *Nederlandse Norm,Geotechnisch ontwerpen van constructies – Deel 1, Algemene Regels*. Netherlands Normalisatie Instituut, Delft.

Ng, C. W., Lings, M. L., Simpson, B., & Nash, D. F. T. 1995. An approximate analysis of the three-dimensional effects of diaphragm wall installation. *Geotechnique* 45(3): 497-507.

Ng, C. W. W. & R. W. M. Yan. (1999). Three-dimensional modelling of a diaphragm wall construction sequence. *Géotechnique* 49(6): 825-834.

Powrie, W. & C. Kantartzi. 1996. Ground response during diaphragm wall installation in clay: centrifuge model tests. *Geotechnique* 46(4): 725-739.

Poulos, H. G. 2008. A practical design approach for piles with negative skin friction. *Proceedings of Institute of Civil Engineers, Geotechnical Engineering* 161: 19-27.

Schad, H, Vermeer P.A., & Lächler, A.. 2007. Fresh concrete pressure in diaphragm wall panels and resulting deformations. *Advances in Construction Materials 2007*: 505-512. Springer Berlin Heidelberg.

Schanz, T., Vermeer, P. A, & Bonnier, P. G. 1999. The hardening soil model : formulation and verification. *Beyond 2000 in Computational Geotechnics; Proceedings of the International Symposium*: 281-296.

Shen, R. F. 2008. *Negative skin friction on single pile and pile groups*. PhD Thesis. National University of Singapore.

Vermeer, P. A. & Neher, H. P. 1999. A soft soil model that accounts for creep. *Beyond 2000 in Computational Geotechnics; Proceedings of the International Symposium:* 249-261.

De Wit, J.C.W.M & Lengkeek, H.K. 2002. Full scale test on environmental impact of diaphragm wall trench installation in Amsterdam. *Proceedings of the International Symposium on Geotechnical Aspects of Underground Construction in Soft Ground.*

Zantkuijl, H.J. 1993. *Bouwen in Amsterdam – Het Woonhuis in de stad* (Building in Amsterdam). Amsterdam, Architectura & Natura.

Some Suggestions for Updating the Foundation Code

Victor Li
Victor Li & Associates Ltd.

ABSTRACT

The Buildings Department (BD) issued the Code of Practice for Foundations (CoPF) in 2004 with input from other government departments, representatives of the professional bodies, the construction association and the academics. Currently, the BD has established a Technical Committee, with input from the profession, to review the code in an attempt to issue a new edition of it. This paper discusses some suggestion for updating the foundation code. Aspects discussed include presumed bearing capacity of soil and rock, interpretation of plate loading test, acceptance criteria for pile loading test, formulation of final set table for driven piles and proposal for streamlining the approval process of new foundation technology.

1 INTRODUCTION

All private development projects in Hong Kong are subject to the control of the Buildings Ordinance and prior approval of foundation design by the Buildings Department (BD) is needed before foundation works can be implemented. Although the Code of Practice for Foundations (CoPF) published by the BD in 2004 (BD, 2004) is aimed at controlling the design and construction of foundation works for private development projects, some government departments including the Housing Department and the Architectural Services Department (ASD) have also adopted this code for public works projects. Therefore, the CoPF has influence on the practice of foundation works in Hong Kong beyond private development projects.

The practices for design and construction of foundations evolve with time. Foundation codes should preferably be updated from time to time to cope with the latest advances in design methods and technological development of foundation equipment. The BD has set up the Technical Committee for Code of Practice for Foundations in 2008. One of the terms of reference of the Committee is to review the CoPF. This paper discusses some suggestions for updating the CoPF.

2 PRESUMED BEARING CAPACITY FOR SOILS AND ROCK

In the current CoPF, values of presumed allowable bearing pressure are specified in Table 2.1 of the code for various category of soils and rocks, ranging from highest value of 10000kPa for Grade I rock with no weathered joints (i.e. Category 1(a) material) to the lowest value of less than 50kPa for loose submerged sand (i.e. Category 3(d) material). This set of presumed bearing capacity values are perhaps the most important guidelines among other provisions of the code which dictate the foundation practice in Hong Kong. However, there are problems or difficulties in implementing these guidelines.

2.1 Presumed bearing capacity for rock

For rocks (i.e. Category 1(a) to 1(c) founding materials), the presumed bearing capacity is conservative in terms of the stipulated allowable value and stringent in terms of the qualifying criteria for founding material.

Category 1(a) with a specified presumed allowable bearing pressure of 10000kPa is applicable only for Grade I granitic or volcanic rocks with 100% total core recovery (TCR) and no weathered joints. Such materials are virtually non-existent in this world. Grade I rock is difficult to come by and even if it existed, the rockmass bounds to have some small weathered joints. It is risky for engineers or contractors to design the foundation based on Category 1(a) rock. Even if they are lucky enough to find no weathered joints in the predrill holes, the remedial works for the completed foundations will be disastrous when the post-construction drillholes do unfortunately intercept a few weathered joints. The designers will need to use a lower design bearing capacity value in the end for formulating the remedial proposal for the unacceptable piles. For this

reason, the author is not aware of any foundation works in Hong Kong designed based on this category of founding material. A similar predicament occurs for Category 1(b) rock as it is difficult to obtain over 5m of Grade II rock in the predrill holes and post-construction drillholes. Foundation designers often have no choice but to design foundation based on Category 1(c) rock with a lower presumed bearing capacity of 5000kPa.

The qualifying criteria for founding materials are also difficult to fulfill and often cause problems to the designers/contractors. Take Category 1(b) rock as an example, the founding material has to be "fresh to slightly decomposed strong rock of material weathering grade II or better, with a TCR of more than 95% of the **grade** ..". This statement is often interpreted in the design checking process as implying that all materials in the core run have to be materials of the same **grade** (i.e. Grade II) and no poorer materials can appear in the core. If a 1.5m core run is retrieved, for instance, the founding material is deemed to satisfy the criteria for Category 1(b) rock if it contains at least $1.5 \times 0.95 = 1.425$m of Grade II rock. If one interprets the qualifying criteria in the strictest sense of the English words, the remaining $1.5 \times 0.05 = 0.075$m of the core run can be void, but it cannot be soils or Grade III rock even if they are intuitively better than an empty void. This sounds an unreasonable interpretation, but unfortunately it is often the case in the current practice. Foundation contractors in Hong Kong often needs to excavate long lengths of hard rocks (in the geological sense) to reach the "design" rock which can meet the qualifying criteria. There is often a sad joke amongst foundation designers/contractors in Hong Kong that it is better to use wash boring for retrieving the rock cores such that the soils in the joints can be completely washed away and hence can be interpreted as voids than to use good quality sampler to recover everything in the core.

2.2 Presumed bearing capacity for soils

For rock, it is perhaps acceptable to adopt a specified bearing capacity value because the actual ultimate bearing capacity of rock will be too much to be usable for practical design. However, specifying constant presumed bearing capacity values for soils are not reasonable from a theoretical standpoint. It is well known from textbook bearing capacity theory that the bearing capacity of soils depends on embedment depth and size of footing. Specifying a presumed bearing capacity value simply based on the qualifying criteria for the founding materials can lead to both conservative and unsafe designs depending on the situation. This can be explained using a worked example in Table 1 (Li 2007).

Table 1: A worked example for bearing capacity calculations (Li 2007)

Footing size, B (m)	Ultimate bearing capacity (kPa)
0.6	173
1	288
3	865
5	1441
10	2882
Design parameters/assumptions: - cohesion, $c' = 0$; angle of shearing resistance, $\phi' = 35^o$; unit weight, $\gamma = 20$ kN/m^3; - footing is a square footing, with level base resting on level ground surface dry soils without embedment - foundation load acts at centre of footing without eccentricity	

Suppose that the soils under consideration is dry medium dense sands classified as Category 3(b) materials under the current CoPF. The presumed bearing capacity will be 100kPa according to the code. According to Table 1, this presumed bearing capacity is unsafe for small footings with dimension less than about 1m and too conservative for large raft footings.

In the current CoPF, presumed bearing capacity values of 3000 kPa and 1000 kPa are specified for Category 1(d) (i.e. material of weathering grade better than IV with TCR $\leq$ 50%) and Category 2 material (i.e. highly to completely weathered soils with SPT $\geq$ 200). It is debatable whether Category 1(d) materials should be more correctly treated as soils if such materials can contain as low as 50% rock. In current practice, the

presumed bearing capacity values for Category 1(d) and 2 materials are used for design of pile foundations. According to the results of Table 1, this can be unsafe if the pile length is short.

In the current practice, the presumed bearing capacity value applies to the design total pressure. This will lead to the following mind-boggling situation. Suppose the founding material is dry soil classified as Category 3(c) material with a unit weight of 20kN/m^3. According to the current CoPF, the soils have a presumed bearing capacity of 100kPa. If one digs a 5m deep pit, construct a footing and backfill the pit with soils, the footing cannot no longer take up any additional load because the self-weight of the footing and the backfilled soils will have caused a bearing pressure of 100kPa. However, if one constructs a surface footing, it can be designed to have an allowable bearing capacity of 100kPa. This is an interesting conclusion from a theoretical point of view because the bearing capacity of a footing with embedment is always higher than that of a surface footing according to soil mechanics principles.

2.3 Suggestions for change

a. Increase the presume bearing capacity for rock

As explained above, foundation designers and contractors in Hong Kong often design the foundations based on Category 1(c) founding material because the chance of fulfilling the qualifying criteria for this category of founding materials is higher. However, this will limit the bearing capacity to 5000kPa. To increase the bearing capacity, bellout is commonly used in Hong Kong for piles founding on hard rocks.

There is a wealth of experience to confirm that the granitic and volcanic rocks in Hong Kong are strong materials that can attain a much higher bearing capacity. The evidences include:

- Full-scale loading tests (e.g. Hope et al. 2000; Plumbridge et al. 2000) indicate that an allowable bearing capacity of 10MPa is easily achievable for granitic and volcanic rocks and also for the softer rock of marble formation (Holmes et al. 1990)

- There are numerous successfully completed buildings with foundations founded on marble formation and highly fractured metasedimentary rocks in Hong Kong with a design bearing capacity of 5000kPa. If buildings founded on such softer or fractured rocks have performed satisfactorily for decades in the past, there is certainly room for increasing the bearing capacity for the stronger granitic and volcanic rocks.

- Founding materials will be subjected to stress induced confinement when the foundation is loaded. The confinement will in turn increases the bearing capacity of founding material. Li & Lau (2012) has recently reported a case study for bored piles and diaphragm walls founding on micro-fractured granite with a design bearing capacity of 5000kPa. The materials behave like a weak rock which can be easily broken by hands. Laboratory tests confirmed that the weak rock can fail at a vertical applied stress of 40MPa, well above the design bearing capacity value of 5MPa, when the deep foundation is subjected to stress induced confinement.

In Macao, piles founding at igneous rocks are often designed to have an allowable bearing capacity higher than that adopted in Hong Kong. It is common to adopt a design bearing capacity of 7500kPa for Category 1(c) rock (Yeung 2014). In view of the above discussions, there is room for increasing the presumed bearing capacity values for rocks. There are several ways to achieve it directly or indirectly.

- *Directly increase presumed bearing capacity values*:
  It is the most direct method although the author foresees that it is unlikely to happen. Given the long history of the current presumed bearing capacity values used in Hong Kong, one will doubt if the CoPF will be updated to relax the design values.

- *Increase the end-bearing capacity according to the rock socket length*:
  In other countries, bellout are usually used for stiff soils or weak rocks to increase the end-bearing resistance of piles. In Hong Kong, bellout are used for the same purpose even if the founding materials are strong igneous rock with compressive strength usually much higher than plain concrete.

The bell is unreinforced. A finite element study by Sheikh & O'Neill (1988) indicates that tensile stress sufficient to cause rupture of the unreinforced concrete may develop in the bell. One should therefore doubt the usefulness of bellout in strong rock. Bellout can perhaps be treated as a practical trick to achieve a higher pile capacity without relaxing the presumed allowable bearing values through the following indirect means.

i. The bearing area is increased and hence a higher calculated pile capacity can be achieved even if the designer is not convinced that the unreinforced bell is effective in resisting the vertical load.

ii. The construction of bellout requires a certain minimum embedment in rock to be provided. This will enhance the bearing capacity of rock due to enhanced confinement by the rockmass. The confinement offered by the rockmass is more effective than the bellout in enhancing the pile capacity. If one ignores the contribution of the bell given its uncertain performance, the effective bearing pressure of a bored pile is summarized in Table 2. This is based on the assumption that the bored pile is subjected to limitations specified in the current CoPF (i.e. bellout limited to 1.5 times the shaft diameter and the maximum gradient of the bellout is 30^o from vertical) and that the adopted presumed allowable bearing pressure 5000kPa for Category 1(c) rock.

Table 2: presumed bearing capacity of Category 1(c) rock

Pile diameter	Bellout diameter	Minimum embedment length of bellout	Design presumed allowable bearing stress assuming bellout effective	Effective allowable bearing stress assuming bellout **not** effective
2m	3m	0.866m	5000 kPa	11250 kPa
2.5m	3.75m	1.083m		
3.0m	4.5m	1.299m		

According to Table 2, the provision of bellout is equivalent to elevating the design bearing capacity to over 10MPa by providing a minimum embedment of about 1m.

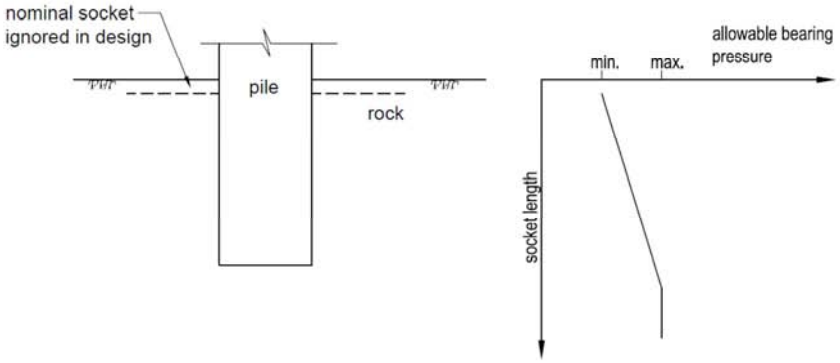

Figure 1: Proposed for presumed allowable bearing capacity

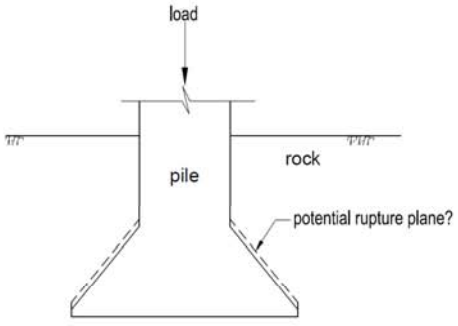

Figure 2: Pile with bellout under loading

It is well established that the bearing capacity of geomaterials increase with embedment and confinement. If one accepts the ineffectiveness of bellout as a reality and the primary benefit of the bellout is to force designers/contractors to provide a minimum embedment length in rock in return for a higher pile capacity, a more direct way for increasing the pile capacity is to set the presumed allowable bearing pressure according to embedment depth as depicted in Figure 1. The minimum value is applicable when only a nominal rock socket length is provided. It then increases with embedment up to a threshold maximum value when a sufficient rock socket length is provided. The extra embedment length in rock is the insurance premium paid for achieving a more economic design. The contractor should be willing to provide an additional embedment

length in rock indicated in Table 2 if a comparable increase in bearing capacity can be accepted in return. The time in drilling an extra length of rock may be less than the total time required for setting up the bellout drillbit and constructing the bellout.

Increasing the bearing capacity according the embedment depth in rock is a more robust way for foundation design than unconditional increase in presumed bearing capacity values. If the foundation designer or contractor is prepared to spend the effort in increasing the socket length of the piles, he can be rewarded by a higher bearing capacity.

In the current practice, it is acceptable to consider both the rock socket resistance of the pile shaft and the end bearing resistance of the bellout when assessing the total capacity of the pile. When the pile settles under loading, the bell may separate from the rockmass and one would doubt if the rock socket resistance above the bellout can still be developed (see Figure 2). With the proposal of described in Figure 1, no bellout may be necessary to attain the same pile capacity and the combined use of rock socket and end bearing resistance will become more technically sound.

b. Relax the qualifying criteria for founding materials:

Since Category 1(a) materials seldom exist in reality, it is suggested to relax the qualifying criteria for Category 1(a) materials to allow Grade II rock with weathered joints to be accepted. It will slightly increase the chance of encountering rockmass meeting the qualifying criteria.

As weathered joints bound to occur for naturally weathered rock, it is unreasonable not to accent weathered materials poorer than the specified material grade. For Category 1(c) founding materials, for instance, 85% of the core run should be Grade III or better rock according the qualifying criteria in CoPF. It is considered reasonable to allow the remaining 15% of core run to be voids, un-retrieved rock fragments or weathering materials of poorer weathering grade.

Psychologically, it may be more comforting to require the base of the bored piles to be in direct contact with the rock of the design material grade. If so, it is suggested that the founding materials over a depth of 600mm below the founding level should be rock of the specified weathering grade with TCR of 100%. Currently, the largest bellout diameter of bored piles commonly used in Hong Kong is 4.5m. The bearing area for a 4.5m diameter bellout will be increased to a circular area of 5.7m in diameter at a depth of 0.6m below the founding level assuming a spread angle of 45^{o} for stress dispersion. If the bored piles is designed to be founded on Category 1(c) with a presumed allowable bearing stress of 5000kPa, as is normally the case for bored pile foundations in Hong Kong, the bearing stress will be reduced to approximately 3000kPa at a depth of 600mm below the founding level. This is commensurate with the presumed allowable bearing pressure of 3000kPa for Category 1(d) materials which can contain as low as 50% rock.

c. Relax the limit on bellout size:

If the suggestion of increasing the pile capacity according to embedment depth according to Figure 1 is too drastic to be acceptable, another way to achieve a more economic design with the same pile capacity is to relax the limit on the size of bellout. This will reduce the total duration of rock excavation.

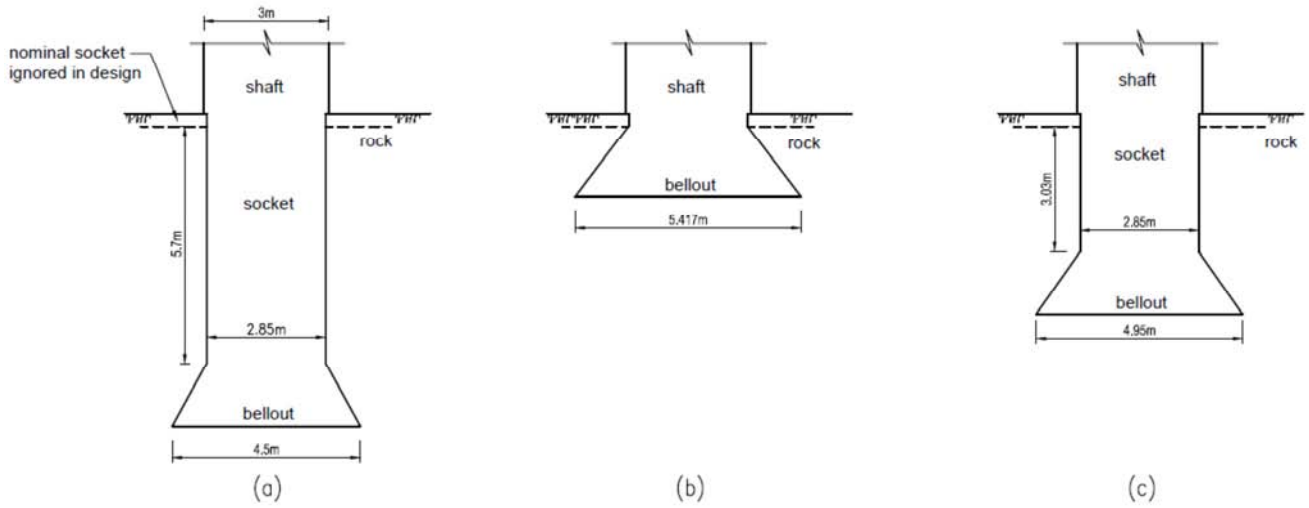

Figure 3: (a) Current practice (b) Fully end-bearing pile (c) Enlarged bellout with reduced socket length

Figure 3(a) shows the minimum embedment depth required to achieve the maximum pile capacity for a 3m diameter bored pile designed to be founded on Category 1(c) materials. For piles constructed using 3m diameter steel casing, the diameter of the rock socket that can be provided is usually limited to 2.85m. The maximum pile capacity of a 3m diameter piles is assessed to be 115246kN according to current design rules. If we are to achieve the same pile capacity without the contribution of rock socket resistance, the bellout size needs to be increased to 5.417m or 1.8 times the pile shaft diameter. Based on the author's discussion with major foundation contractors in Hong Kong, it may be difficult to construct bellout drillbits that can achieve a bellout diameter equal to 1.8 times the shaft diameter. A more practical ratio will be 1.65. In this case, a rock socket equal to 3.036m or 1.065 times the rock socket diameter needs to be provided to achieve the same maximum pile capacity of a 3m diameter pile.

d. Abandon presumed bearing capacity materials for soils

As discussed earlier, it is not rational to specify constant presumed allowable bearing capacity values for soils. It is logical to abandon the presumed allowable bearing capacity of soils and adopt the principles of soil mechanics for estimating the allowable bearing capacity of soils. Guidelines for calculating the bearing capacity of shallow and deep foundations founding on soils are given in Geoguide 1 (GEO 1993) and GEO Publication No. 1/2006 (GEO 2006).

For pile foundation founding on soils, the ultimate end-bearing capacity q_u can be estimated by the relation of:

$$q_u = N_q \, \sigma'_v, \tag{1}$$

where N_q is the bearing capacity factor and σ'_v is the effective overburden pressure at the founding level (GEO 2006).

For dense soils, the bearing capacity factor N_q is about 100 corresponding to an angle of shear resistance of $\phi = 37^o$. For a pile embedded in fully submerged soils with an effective unit weight of 9kN/m^3, the minimum pile length to achieve an allowable bearing capacity of 3000kPa with a factor of safety of 3 will be of the order of 10m. If Category 1(d) material is treated as soils rather than rock, it is advisable to provide a minimum pile length of 10m when using the presumed allowable bearing capacity of 3000kPa for design.

e. Revise definition of allowable bearing capacity for soils

As discussed above, the current interpretation of allowable bearing pressure based on total applied stress is not logical. This is because the factor of safety is also applied implicitly to the overburden pressure. A more rational definition for defining the allowable bearing capacity, q_{all}, is given below:

$$q_{all} = \frac{q_{ult} - q_o}{F} + q_o \quad (2)$$

where q_{ult} is the ultimate bearing capacity which can be estimated using bearing capacity equations for soils, q_o is the overburden pressure expected to exist throughout the design life of the footing and F is the factor of safety, which is specified to be 3 in the CoPF.

Bearing capacity equations published in the literature are generally developed for rectangular or circular footings. The bearing capacity of soils increases with the footing size. It is therefore conservative to use the largest inscribed rectangle or circle within the irregular shape as the design footprint of the footing when estimating its bearing capacity.

3 INTERPRATION OF PLATE LOADING TEST

When the design bearing capacity of soils is large, structural engineers usually look for plate loading test(s) to verify the design bearing capacity. Under the current practice, the maximum test load is equivalent to an applied pressure equal to three times the design allowable bearing pressure. The plate settlement at maximum test load should comply with an acceptance criterion specified in the CoPF. Although the acceptance criterion in CoPF resembles that described in Terzaghi and Peck (1968 Eq.54.1), it is different and the actual source of this criterion remains an enigma.

The current practice for plate loading test is not reasonable. It is against the principles of soil mechanics because the bearing capacity of a shallow footing depends on footing size amongst factors. Using the result of Table 1 as an example. A footing with a design allowable pressure of 300kPa is conservative for a 5m square footing, but is definitively too large for a 0.6m square test plate. If one applies a maximum test pressure of 900kPa to a small test plate, failure is doomed to occur. This perhaps explains why shallow footings are seldom in Hong Kong used for supporting tall building despite the good conditions of saprolitic soils because the chance of passing the plate loading test is small. Tall buildings supported by footings on soils are common outside Hong Kong (such as the 26-storey Henderson Centre in Beijing), but rarely seen in Hong Kong although they do exist in Hong Kong (such as the over 40-year old 24-storey Garfield Mansion in the Mid-Levels).

There is a need to rationalize the acceptance criteria for plate loading test. The ultimate capacity of a test plate resting on a dry sandy soil on a level ground can be expressed as follows based on the bearing capacity equation:

$$q_{ult} = ½\ \gamma B\ N_\gamma s_\gamma \quad (3)$$

where B is the size of the test plate, N_γ a bearing capacity factor, γ the unit of soils and s_γ the shape factor equal to 0.6 for a square plate or circular plate.

For a uniform soil, the bearing capacity factor N_γ for the test plate and the prototype footing are the same, but the ultimate bearing capacity value changes with size of the bearing area. When verifying the adequacy of the footing design in terms of bearing capacity, the plate loading test should aim at confirming the adequacy of the design bearing capacity factor N_γ.

If the ultimate bearing pressure depends on bearing area, the maximum test load P_{max} should be adjusted according to the size of the test plate. For a square plate, the following equation is obtained:

$$P_{max} = q_{ult} B^2 = ½\ \gamma B^3 N_\gamma s_\gamma = 0.3\ \gamma B^3 N_\gamma \quad (4)$$

Ultimate failure of the test plate can be interpreted as the load corresponding to a settlement equal to 15% of the plate size according to the recommendation of the British Standard BS1377 for testing of soils. By

measuring the failure load, one can back-calculate the bearing capacity factor N_γ to ascertain if it is higher than the design value for the footing.

When designing a footing founding on soils, it is important to check whether settlement is within acceptable limits. The prediction of settlement requires information of the soil modulus. Treating the test plate as a rigid footing, the Young's modulus of soil, *E*, is related to the plate settlement by the following equation for a square plate.

$$\mathrm{E} = \frac{P(1-v^2)}{\alpha\, s\, B} \tag{5}$$

where *P* is the applied load, ν is the Poisson's ratio, *s* the measured settlement at loading *P* and α is a coefficient.

Slightly different values of α have been reported by different researchers in the literature, but the value is generally of the order 1.0. Barkan (1962) reported a value of α = 1.08 quoting the result obtained by a Russian researcher. The same value has later been reported in the publication by Whitman & Richart (1967). The plate loading test can be used as a tool for back-calculating the field modulus of soils. As the performance of a structure supported by the footings is controlled by the settlement under working load conditions, it is considered reasonable to perform the back-analysis using the results at a test load corresponding to the design allowable pressure and not that at maximum test load.

The corresponding results for a circular test plate are:

$$P_{max} = \frac{3\pi}{40}\gamma B N_\gamma \tag{6}$$

$$\mathrm{E} = \frac{P(1-v^2)}{s\, B} \tag{7}$$

The Poisson's ratio of soils is usually the range of 0.2 to 0.3. For practical purpose, a design value of 0.2 may be adopted without significantly affecting the accuracy of the back-analysis.

4 ACCEPTANCE CRITERIA FOR PILE LOADING TEST

The acceptance criteria for pile loading test comprise an allowable total settlement at maximum test load and an allowable residual settlement upon full release of test load on completion of loading test. The pile acceptance criteria adopted in the CoPF differs in two major aspects from those commonly used outside Hong Kong. Firstly, it is not common to specify a residual settlement criterion in other parts of the world. Secondly, the duration of maintained loading at maximum test load is very long in Hong Kong (72 hours). In other regions, the maximum test load is usually maintained for a period of 24 hours or less.

As argued by the Li et al. (2003a), full unloading of piles will only occur when the structure they support is demolished. If a structure performs satisfactorily under larger pile settlements when the structure is constructed or later occupied, the residual settlement becomes irrelevant in assessing its performance. The residual settlement criterion can therefore be dropped.

The duration of 72 hours for maintained loading at maximum test loads is exceedingly long as compared with that implemented in other regions outside Hong Kong. Creep settlement of the test pile occurs during maintained loading. Li et al. (2003b) observed that the creep settlement of jacked steel H-piles tend to follow a rectangular hyperbolic trend. A significant portion of the creep settlement will occur in the initial period of maintained loading. Similar behaviours are expected to occur for driven piles or rock-socketed piles. The performance of piles under creep movement can be assessed by observing, say, the initial 24 hours of maintained loading. There is room for reducing the duration of the maintained loading for loading test in Hong Kong.

Hundreds of loading tests of piles are conducted in Hong Kong every year. There should be a wealth of data to compare the cumulative creep settlement at 24 hours and 72 hours. If necessary, the criterion for total settlement can be slightly tightened to compensate for the reduced duration of maintained loading. This will have beneficial effect of shortening the construction programme of foundation projects in Hong Kong.

5 DESIGN AND QUALTY CONTROL OF DRIVEN H-PILES

Pile Driving Analyzer (PDA) tests are becoming more popular as a tool for controlling the pile driving process and as a means for predicting the capacity of driven piles. An elaborate system based on PDA testing for controlling the installation of driven steel H-piles by hydraulic hammers has been promulgated in the General Specification for Building (GSB) issued by ASD. The author supports wider use of PDA testing in Hong Kong for better quality control of driven piles and complete replacement of drop hammers by hydraulic hammers for pile installation. However, care must be exercised when incorporating the current ASD approach in the CoPF.

In the ASD approach, the final set table is formulated using the results of CAPWAP analysis processed using data obtained from PDA testing. The procedures as described in the latest version of GSB are briefly described as follows:

a. Carry out PDA tests for at least 5 piles and obtain the predicted pile capacity using CAPWAP analysis. The pile capacity so predicted is named hereafter the CAPWAP capacity.

b. Using the same information of pitched length, hammer weight, drop height, measured elastic compression of soil and pile ($C_p + C_q$) and etc for the 5 PDA-tested piles, one can also predict the pile capacities of the 5 piles using the Hiley formula based on selected input parameters of hammer efficiency E_h and coefficient of restitution e. Although the elastic compression of the pile cushion C_c is also a parameter in the Hiley formula, it is assigned a constant value of 5mm for simplicity because the magnitude of C_c is usually small and will not significantly affect prediction of pile capacity. The pile capacity predicted by the Hiley formula is named hereafter as the Hiley capacity.

c. Calculate the average CAPWAP capacity and average Hiley capacity. Adjust the two parameters E_h and e until the following equality is met.

   $$\lambda \times \text{average CAPWAP capacity} = \text{average Hiley capacity} \quad (8)$$

   Theoretically, $\lambda = 1$ if CAPWAP analysis and the Hiley formula are both accurate in predicting the pile capacity. A value of $\lambda = 0.85$ is used to be conservative and the value of e is capped at 0.65 as stipulated in ASD's GSB.

d. The combination of E_h and e so obtained can then be used to as back-calculated design parameters for input to the Hiley formula in formulating the final set table.

When adopting this ASD approach to in the CoPF in its present or modified form, one must be aware of the following fundamental issues:

a. The validity of the above approach hinges on the accuracy of CAPWAP analysis in predicting the pile capacity. The author has some reservation on accuracy of the CAPWAP analysis as discussed in Li & Lam (2006). CAPWAP analysis may under-predict the pile capacity for higher-capacity piles driven to a small final set. If so, introducing the reduction factor of 0.85 in the procedure of back-analysis will make the derived parameters overly conservative, rendering the final set table unworkable.

b. In the current CoPF, the lower and upper envelopes of the final set table values are set at 25mm and 50mm per 10 blows respectively. This will result in a very narrow band of final set values in the final set table as explained by Li & Lam (2007, 2012). If the ASD approach for back-analyzing the input parameters of the Hiley formula is too conservative, the final set table so obtained may not be workable and the observed $C_p + C_q$ values will lie outside the acceptable envelopes of the final set table.

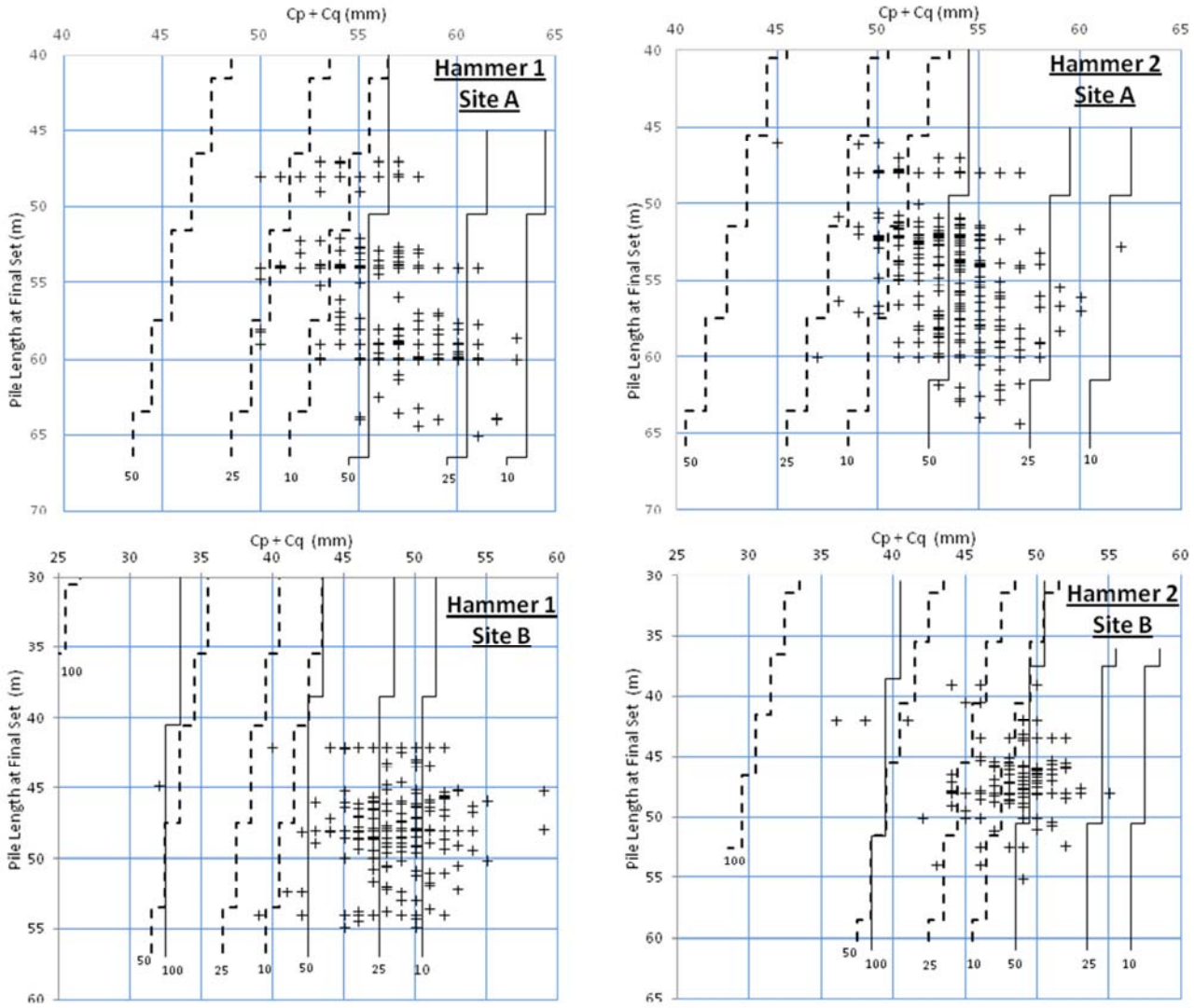

Figure 4: C_p+C_q values at final set for two sites

Figure 4 shows the actual results of $C_p + C_q$ value obtained from two foundation projects (named Site A and Site B) where a total of over one thousand driven H-piles have been installed using hydraulic hammers. Various envelopes of the final set values have been obtained for two different values of $\lambda = 0.85$ and 1.0. When $\lambda = 1$ is used, the restriction of capping $e = 0.65$ has been relaxed. Otherwise, the back-analysis may yield $E_h > 1$, which is not reasonable. The dotted lines and solid lines in Figure 4 represent the envelope for $\lambda = 0.85$ (the ASD approach) and $\lambda = 1$ respectively. An envelope marked by a number 10 is the envelope corresponding to 10mm/10 blows and etc.

It can be observed that almost all the observed C_p+C_q values lie outside the envelope corresponding to 25mm/10 blows if the current ASD approach is adopted. In Hong Kong, a final set of 10mm/10 blows is commonly adopted as the criteria for hard driving. This may be regarded as a practical limit on the lower envelope of the final set table. Lowering the final set value further for this lower envelope implies that the piles have to be driven practically to refusal before achieving a satisfactory final set. This will risk damaging the piles and hence it is not recommended to shift the lower envelope below 10mm/10 blows. Even if the lower envelope based on the ASD approach is relaxed to 10mm/10 blows, the majority of observed C_p+C_q values are still outside the lower envelope. This implies that the current ASD approach is likely to be too conservative by setting $\lambda = 0.85$ or may be the CAPWAP analysis is too conservative in predicting the actual pile capacity. The author has discussed this observation with some piling contractors in Hong Kong and they do confirm this finding when implementing the ASD approach. At present, the ASD allows contractors to

verify the capacity of a pile by CAPWAP analysis if the observed C_p+C_q value of the pile falls outside the envelope of the final set table. This explains why it is commonplace for contractors to conduct PDA tests and CAPWAP analyses for almost 100% of the driven steel piles in ASD foundation projects, as in the case for Site A and Site B. If so, the final set table will become a somewhat redundant tool for control of pile installation.

Adopting a less conservative value of $\lambda = 1$ will improve the situation. The percentage of data falling outside the lower envelope is reduced as summarized in Table 3. However, the percentage is still high for Site B Hammer 1.

Table 3: Percentage of data outside lower envelope (for final set table obtained based on $\lambda = 1$)

Site	Hammer no.	Lower envelope	% of results outside lower envelope
A	1	25mm/10 blows	0
A	1	10mm/10 blows	2.9%
A	2	25mm/10 blows	0.3%
A	2	10mm/10 blows	1.7%
B	1	25mm/10 blows	41.7%
B	1	10mm/10 blows	16.2%
B	2	25mm/10 blows	0
B	2	10mm/10 blows	0.6%

Increasing the value of λ to 1.0 is equivalent to shifting all the envelopes of the final set table to the right. It reduces the percentage of data falling outside the lower envelope, but may increase the chance of data falling outside the upper envelope. For Site A Hammer 2, the percentage of data outside the upper envelope corresponding to 50mm/10 blows is significant. In all cases, the percentage of data points falling the upper envelope corresponding to 100mm/10 blows is small.

If the ASD approach is to be incorporated in the CoPF to encourage wider use of hydraulic hammers for final setting of piles and better control of the foundation works using PDA testing, some of the provisions in the code and/or current design practice as well as the checking approach have to be modified. Otherwise, it is foreseen that a significant percentage of the completed piles will be condemned as unacceptable piles purely because of the inherent limitations of method of formulating final set table. The following are suggested.

a. The value of λ should be increased. A value of $\lambda = 1$ is suggested.

b. The limitation of capping the value of $e = 0.65$ should be removed.

c. The lower and upper envelop be relaxed to 10mm/10 blows and 100mm/10 blows respectively as suggested by Li & Lam (2007). As discussed in Li & Lam (2007), there is no sound technical reason to restrict these two envelopes to 25mm and 50mm/10 blows in the current CoPF.

d. Even if λ is relaxed to 1.0 as suggested, a certain percentage of the piles may still have C_p+C_q values falling outside the envelopes of the final set table as evidenced by the results for Site B Hammer 1 in Table 4. If the observed C_p+C_q value of a completed pile falls outside the envelopes of the final set table, it is allowed to use CAPWAP analysis to verify its pile capacity, in line with the current ASD practice.

When making a recommendation for the value of λ to be adopted, one should strike a balance between conservatism and practicality. If the value of λ is set too low, the contractor will continue to use the drop hammer for final setting of piles.

6 STREAMLINING THE PROCESS OF FOUNDATION APPROVAL

There are conflicting requirements when preparing a foundation code. From a viewpoint of statutory control under the Buildings Ordinance, the CoPF should be simple, rigid and conservative to make the approval of foundation plans a simpler task. From a technical point of view, rigid procedures and conservative guidelines

will stifle the advancement of foundation technology. In particular, the duration needed for obtaining approval of new foundation techniques is often too long to be acceptable to the developers or contractors.

The slow development of jacked piling is a good example to illustrate this point. 900-ton pile jacking machines with servo-control, which were perhaps the heaviest and most advanced pile jacking machine in the world at that time, were used in Hong Kong in 2001 for installation of jacked H-piles. A larger, 1050-ton pile jacking machine, again possibly the world record at the time, was introduced to Hong Kong in 2011 for installing jacked H-piles for a private residential development in Tai Po. After some initial teething problems, the technology for installation of jacked piles is now fairly mature (Li & Lam 2011). Jacked H-piles have been used successfully for the foundations at 8 sites in Hong Kong (Li & Lam 2011). Trial jacked H-piles with very satisfactory performance have also been constructed recently in 2012 at a site in Yuen Long. Hong Kong had perhaps led the advancement of jacked H-piles in the past because jacked H-piles with such a design high capacity were seldom if ever installed in other countries. Unfortunately, jacked H-piles are still not regarded as a recognized conventional pile type in the checking process by BD. If the developer/designer/contractor wants to adopt jacked piling for private development projects, the additional time required to be spent before consent for working piles can be granted can easily be 5 months or longer. Few developers can tolerate such a delay in their development. This has a significant deferent effect on advancing the foundation technology. In Macao, the approval time for accepting a new foundation technology is much shorter. The technology of jacked piling developed in Hong Kong has been "exported" to Macao in recent years and quickly become more advanced there, with high-capacity jacked spun piles also used for supporting tall buildings (Yeung 2013).

Streamlining the approval process to reduce the additional time needed for obtaining consent for working piles will provide a greater incentive for developer/designer/contractor to use newer technologies. Some suggestions for streamlining the process are:

a. Local experiences gained from public works projects can also be considered in assessing the need for trial piles. If there are sufficient experiences gained for the new technology in Hong Kong from other government buildings or civil engineering projects, waiving the requirement for trial piles or granting of consent of working piles and trial piles at the same time may be considered.

b. Foundations completed using new technologies can be abandoned if they fail to achieve the expected performance. The consequence of allowing new foundation types to be installed is not great from a view point of public safety as long as the developer/designer/contractor are well aware of the risk and prepared to replace the unsatisfactory piles if necessary. If so, the granting of consent for trial pile installation and partial if not full consent for the working piles at the same time may be a viable way to encourage the use of new foundation technologies.

7 CONCLUSIONS

Some guidelines in the current CoPF have weakness which may not be defensible under the scrutiny of soil mechanics principles. Some suggestions for updating the foundation codes are given in the paper. It is hoped that the paper can encourage further discussions by fellow engineers in Hong Kong to make the revised foundation code a document that is simple, suitably conservative and sufficient flexible to encourage wider use of new foundation technology.

REFERENCES

Barkan, D.D. 1962. *Dynamics of Bases and Foundations.* McGraw-Hill Book Company.

Buildings Dpeartment (BD) 2004. *Code of Practice for Foundations*.

Geotechnical Engineering Office (GEO) 1993. *Geoguide 1 – Guide to Retaining Wall Design.*

Geotechnical Engineering Office (GEO) 2006. *GEO Publication no. 1/2006 - Foundation Design and Construction.*

Holmes, D.G., Keung, C.P.Y. and Li, K.S. 1990. Heavy foundations in karstic limestone. *Proc. Conference on Deep Foundation Practice*, Singapore, 105-110.

Hope, S., Young, S. and Dauncey, P. 2000. Airport railway pile tests. *Proc. HKIE Annual Seminar – Foundations*, 145-155.

Hill, S.J., Littlechild, B.D., Plumbridge, G.D. and Lee, S.C. 2000. End bearing and socket design for foundations in Hong Kong. *Proc. HKIE Annual Seminar – Foundations*, 167-178.

Li, V. 2007. Use of plate load test for design of shallow foundations – a suggested alternative practice. *Bridging Research & Practice – the VLA experience*, Centre for Research & Professional Development, 191-199.

Li, V. and Lam, J. 2011. Development of jacked piling in Hong Kong. *The 2nd VLA Seminar – New Developments in Jacked Piling*, Centre for Research & Professional Development, 88-116.

Li, V. and Lam, J. 2006. Discussion on Observations on using the energy obtained from stress-wave measurements in the Hiley formula. *HKIE Transactions*, 13(2), June, 63-64.

Li, V. and Lam, J. 2007. New criteria for formulating final set table for high-capacity steel H-piles. *Bridging Research & Practice – the VLA Experience*. Centre for Research & Professional Development, 213-237.

Li, V. and Lam, J. 2012. When can we stop using drop hammers for driven piles?. *Bridging Research & Practice – the VLA Experience: Volume 2*, Centre for Research & Professional Development, 75-95.

Li, K.S., Lam, J. and Lee, P.K.K. 2003a. *Design and Construction of Driven and Jacked Piles - Chapter 1: General Principles*, Centre for Research & Professional Development, 1-22.

Li, K.S., Lam, J. and Lee, P.K.K. 2003b. *Design and Construction of Driven and Jacked Piles - Chapter 2: Jacked Piles*. Centre for Research & Professional Development, 23-50.

Li, Victor & Lau, C.K. 2012. Some new developments in foundation design and construction in Hong Kong. *Proc. HKIE Joint Structural Division Seminar*, 63-79.

Shiekh, S.A. and O'Neill, M.W. 1988. Structural behavior of 45-degree underreamed footings. *Transportation Research Record*, Vol.1119, 83-90.

Terzaghi, K. and Peck, R.B. 1968. *Soil Mechanics in Engineering Practice*, 2nd Edition, John Wiley & Sons.

Whitman, R.W. and Richart, F.E. 1967. *Design Procedures for Dynamically Loaded Foundations*. Research Report, The University of Michigan.

Yeung, A.T. 2013. Non-percussive installation methods for precast prestressed concrete spun piles. *Proc. Conference on Foundations: State-of-the-Practice*, 143-157.

Yeung, A.T. 2014. Personal communication.

Installation of Prestressed Spun High Strength Concrete Piles by Hydraulic Jacking

Albert T. Yeung

University of Hong Kong, Hong Kong Special Administrative Region, China

ABSTRACT

The technique of hydraulic jacking has been applied to install prestressed spun high strength concrete PHC) piles in Macau. It should be noted that PHC piles are significantly cheaper than steel H-piles of comparable load-carrying capacities. PHC piles also have a lower carbon footprint than steel H-piles. The Macau experience will be presented in detail in this paper to introduce this pile installation technique, and to demonstrate how this technique can reduce material and construction costs, reduce construction time, increase environmental friendliness, improve site quality control and reduce construction risk. The limitations of the technique will also be presented. Moreover, the engineering performance of PHC piles installed by this technique deduced from full-scale maintained pile load tests will be presented. Lastly, the obstacles to the introduction of this cost-effective, efficient and environmentally friendly pile installation technique to Hong Kong will be discussed.

1 INTRODUCTION

Pile foundations are often required to support tall buildings and heavy infrastructures necessary to accommodate the rapid economic and population growth of Hong Kong. The common types of piles being used in Hong Kong include large-diameter bored piles, barrettes, steel H-piles, prestressed spun high strength concrete pipe piles (PHC piles) and mini-piles. The construction of large-diameter bored piles, barrettes and mini-piles requires excavation, installation of a reinforcement cage and *in-situ* concreting or grouting. The construction process is thus quite involved. Prefabricated piles, such as steel H-piles and PHC piles, are typically installed by preboring or percussion. The construction of a prebored socketed steel H-pile requires preboring, insertion of a steel H-pile, grouting and removal of casing. PHC piles are seldom installed by preboring in Hong Kong. Again, the construction process is quite involved. Installation of these prefabricated piles by percussion is most economical if the geological conditions are favorable. However, the construction method inevitably induces vibration, noise and air pollution problems despite of the stringent environmental requirements promulgated by the Hong Kong SAR Government. The limits on pile driving hours promulgated by the noise permit system operated by the Environmental Protection Department may reduce the adverse noise impact to sensitive receivers. The use of hydraulic hammer may alleviate the air pollution problem. However, the vibration problem remains. From a geotechnical standpoint, the founding conditions of a driven pile are not fully revealed. Although every driven pile is accepted using the Hiley formula in Hong Kong, there is no guarantee on its engineering performance, in particular its load-carrying capacity and the load-settlement characteristics. In fact, the engineering performance of a driven pile has to be evaluated by a pile integrity test, a pile dynamic analysis and/or a full-scale pile load test. Because of cost and time implications, these tests cannot be applied to every pile in a project. The energy impacted on a pile by the pile integrity test is probably inadequate to penetrate the full length of the pile. Therefore, the test is probably inappropriate for the evaluation of the founding conditions of the pile. Typically, pile dynamic analyses are performed on approximately 10% of the piles installed and full-scale pile load tests are performed on 1% of the piles installed. Therefore, there is a significant possibility that defective piles are not identified. The technique of hydraulic jacking can rectify most of these environmental problems and quality control problems. In this paper, the background of jacked piles is given. The experience of installing PHC piles by hydraulic jacking in Macau is also presented.

2 JACKED PILES

The technique of jacked piles was developed in the U.S., primarily for underpinning of existing structures (White 1975). The technique was later developed in China, Japan, Singapore, Malaysia and Australia as a pile installation method (Lam & Li 2003; Li 2011; Li et al. 2003). On February 16, 2007, the International Press-in Association, an academic organization with support from Giken Seisakusho Co., Ltd. of Japan, was established in Cambridge, England to explicate the underground phenomena and mechanisms encountered by the press-in technology in close collaboration with various technical fields such as civil, construction, environmental, geotechnical, instrumentation and mechanical engineering. Research awards are being granted to researchers worldwide to develop a better understanding of the technology. However, the progress on wide application of the technique in Hong Kong is extremely slow (Li & Lam 2011). Although the technique has been adopted for the successful installation of steel H-piles in a few public projects, the Buildings Department, i.e. BD, has approved only one private project at Fung Yuen, Tai Po using thirty-one (31) jacked steel H-piles to date (Li et al. 2011; Yeung & Li 2012). Moreover, the procedures approved for the quality control of the installed piles are extremely stringent, making the installation technique not very efficient or cost-effective. The approved design load-carrying capacity of these steel H-piles is similar to that of driven steel H-piles even the piles are not driven, rendering the installation method economically less attractive (Li & Lam 2011).

The installation technique has been applied to install PHC piles in Macau. It should be noted that the material cost of PHC piles is significantly cheaper than that of steel H-piles of comparable load-carrying capacities. PHC piles also have a lower carbon footprint than steel H-piles The Macau experience will be presented in detail in this paper to introduce this pile installation technique, and to demonstrate how this technique can reduce material and construction costs, reduce construction time, increase environmental friendliness, improve site quality control and reduce construction risk. The limitations of the technique will also be presented. Moreover, the engineering performance of PHC piles installed by this technique deduced from full-scale maintained pile load tests will be presented. Lastly, the obstacles to the introduction of this cost-effective, efficient and environmentally friendly pile installation technique to Hong Kong will be discussed.

3 STEEL H-PILES VERSUS HIGH STRENGTH CONCRETE PIPE PILES

Both steel H-piles and PHC piles are commonly used in Hong Kong while PHC piles are commonly used in Macau. A brief comparison of these two types of piles is given to facilitate further discussion.

3.1 Steel H-piles

Steel H-piles commonly used in Hong Kong are Grade 55C 305×305×149 kg/m, 305×305×180 kg/m or 305×305×223 kg/m and their design load-carrying capacities are 2,451 kN, 2,958 kN and 3,677 kN, respectively, as the design compressive stress of the steel H-piles is limited to 30% of the yield stress of steel to control the driving stress during percussion.

3.2 PHC piles

PHC piles are historically known as Daido piles in Hong Kong although the nomenclature may be technically incorrect. The original Daido piles were made in Japan where they are installed as replacement piles, as they are placed into prebored holes followed by grouting of the annular void space between the pile and the cylindrical vertical walls of the prebored hole. However, Daido piles are installed by percussion in Hong Kong. Since the installation method of Daido piles has been changed, construction problems, such as damage of pile shoe, crushing of concrete near the pile tip, damage of pile head, development of tensile cracks in the pile etc., occur in Hong Kong. Daido piles were later manufactured in Hong Kong and manufacturers of piles of lower quality from mainland China also enter the Hong Kong market, resulting in more construction problems unforeseen by the original Daido pile designers.

Although BD enlists approved manufacturers, the quality of piles is only evaluated during the application process for inclusion on the list but not on a regular basis afterwards. Any subsequent deterioration of manufacturing quality has never been monitored. The loop hole has been manipulated by some unethical

mainland China pile manufacturers. Some of these enlisted manufacturers have already closed their business for years but they maintain their presence in the market as BD enlisted manufacturers, resulting in market monopoly by a few dominating market players who may not be able to produce high-quality PHC. As a result, PHC piles have become less popular for more than a decade in Hong Kong due to a series of unfortunate events in construction sites in Tin Shui Wai, Tung Chung etc. However, the use of PHC piles in Hong Kong has been rejuvenated recently.

Precast prestressed concrete piles are manufactured in different shapes and sizes. The most common type being used in Hong Kong and Macau is the tubular PHC pile as shown in Figure 1. They are manufactured by spinning wet concrete in a formwork with pre-tensioned wires installed. The compressive strength of the concrete and the tensile strength of the pre-tensioned wires are approximately 80 MPa and 1,420 MPa, respectively. The outer diameter of the pile D varies from 300 mm to 600 mm and the thickness T varies from 70 mm to 130 mm. The design load-carrying capacity of the pile is thus ranging from 900 kN to 3,500 kN.

3.3 Material cost

An accurate comparison on the material costs of different types of piles can only be made on piles of similar design load-carrying capacities. The comparison is thus made on Grade 55C 305×305×223 kg/m steel H-pile and Type AB-130 PHC pile with D = 600 mm and T = 130 mm to Chinese Standard GB13476-2009. The design load-carrying capacities of the two types of piles are both approximately 3,500 kN.

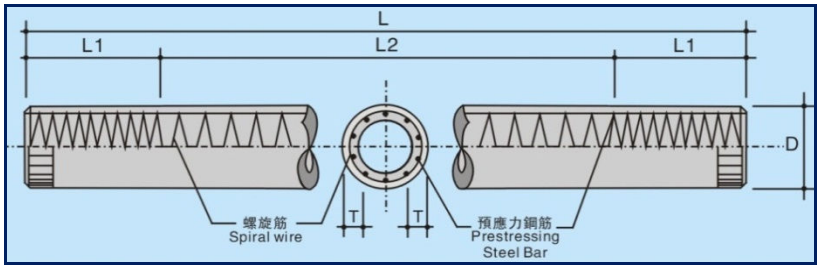

(a) Pile details

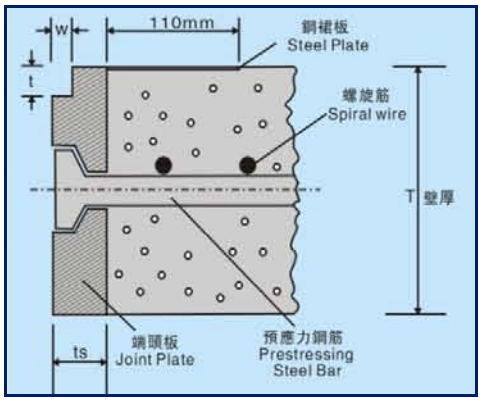

(b) Joint details

Figure 1: Details of the PHC pile

The unit material costs of the steel H-pile and the PHC pile are approximately HK$1,200/m and HK$600/m, respectively. If the required lengths of the piles are similar, the cost/tonne of support load of the PHC pile is thus approximately a half that of the steel H-pile. The length required to achieve the same design load-carrying capacity for the PHC pile is in general shorter than that for the steel H-pile, as the side resistance developed along the length of the PHC pile is normally higher than that of the steel H-pile. The PHC pile is thus particularly useful in karst formation areas of Hong Kong to reduce foundation stress exerting on the marble rockhead. However, it should be noted that the masses per unit length of the PHC pile and the steel H-pile are 0.499 and 0.223 tonne/m, respectively. The transportation cost of the PHC pile is thus approximately twice that of the steel H-pile and the transportation logistics are more complicated.

3.4 Carbon footprint

Taking a carbon footprint of 0.76 tonne CO_2 per tonne of structural steel, the carbon footprint of the Grade 55C 305×305×223 kg/m steel H-pile is thus

0.76 x 0.223 = 0.17 tonne of CO_2 per m of steel H-pile (1)

Similarly, taking a carbon footprint of 0.155 tonne CO_2 per tonne of reinforced concrete, the carbon footprint of the Type AB-130 PHC pile of D = 600 mm and T = 130 mm is thus

0.155 x 0.499 = 0.077 tonne of CO_2 per m of PHC pile (2)

It is demonstrated that the use of more PHC piles can be a significant contribution by the construction industry towards a cleaner and more sustainable environment.

3.5 Proximate availability of PHC piles

There are many high quality PHC pile manufacturers in the vicinity of Hong Kong. It is much easier to satisfy the material requirements of LEED or BEAM by the use of PHC piles than that of steel H-piles in terms of carbon footprint and transport distance of construction materials. Shortening of transport distance contributes directly to the reduction of transportation costs and indirectly to the reduction of fossil fuels and air pollution.

4 INSTALLATION OF PHC PILES BY HYDRAULIC JACKING

4.1 Advantages and disadvantages

As piles are jacked into the ground continuously by a hydraulic jacking system without percussion, no noise or vibration is thus generated. As a result, there is practically no limitation on the operation hours. The hydraulic system is powered by electricity and no black smoke resulting from incomplete combustion of diesel is generated. Most adverse impacts of pile installation on the nearby environment or sensitive receivers are thus eliminated. The technique makes it possible to install piles in close proximity of existing buildings or sensitive areas such as underground structures of the subway system. Piles are hydraulically jacked to the target load-carrying capacity with no unnecessary extra penetration, resulting in considerable savings in material, labor costs and construction time. More importantly, every jacked pile is fully load-tested during construction for better quality assurance. The daily production rate of jacked piles is considerably higher than that of driven piles, as there is no restriction on operation hour. As no tension is generated in the concrete pile during jacking, potential tensile damage to the pile induced by percussion is eliminated.

As the design load-carrying capacity of the pile is increased, the reaction required for jacking is increased proportionally. As a result, the dead weight of the pile jacking machine for the installation of piles of design load-carrying capacity of 3,500 kN is approximately 10,000 kN. It is very difficult to maneuver such a large and heavy pile jacking machine in construction sites of small footprints and/or steep terrain. As jacked piles are displacement piles, particularly for PHC piles, all the potential disadvantages of displacement piles have to be carefully considered and necessary precautions for proper installation of piles have to be taken.

4.2 Pile jacking machine

The pile jacking machine for the installation of PHC piles used in Macau as shown in Figure 2 is imported from mainland China together with the skilled laborers employed to operate the machine. The machine has a rated jacking capacity of approximately 10,000 kN. The pile jacking machine is equipped with a built-in crane for the lifting of PHC piles. It should be noted that the transportation of pile jacking machines to site is not an easy task. It takes seventeen (17) 70-tonne trucks to transport all the components of a single pile jacking machine to site for re-assembly. Moreover, the maneuverability of 70-ton trucks on a construction site is also limited by site conditions. Temporary access roads are often required to support these heavy trucks.

4.3 Clamping device

There is need for a specially designed clamp for the jacking of PHC piles. The design adopted in Macau is shown in Figure 3. It consists of several small clamps installed concentrically. The design enables the exertion of a uniform hoop stress on the pile so as to minimize the possibility of pile crushing. The stroke of each jacking operation is between 1.5 m to 2 m. Two simultaneous clamping devices are used in some pile jacking

machines manufactured in mainland China for the installation of PHC piles to reduce the risk of pile crushing.

4.4 Termination criteria

The termination criteria to be adopted for the jacked pile should be such that the pile would satisfy the requirements of the static load test. The load-carrying capacity of most PHC piles in Macau is designed to the structural capacity of the PHC pile, i.e. 3,500 kN. Therefore, the ultimate load to be imposed on these piles in the static load tests would be 7,000 kN. The termination criteria for pile jacking adopted are: the pile is subjected to: (a) at least two cycles of sustained load of 2.2 times the design load-carrying capacity, i.e. 7,700 kN, for 30 seconds each to stabilize the pile settlement; and then (b) a sustained jacking load of 7,700 kN for 15 minutes and the rate of settlement does not exceed 5 mm/15 minutes. Unlike the jacking of steel H-piles, the criterion of settlement rate of less than 5 mm/15 minutes under the ultimate jacking load is normally satisfied during the first 15 minutes of sustained ultimate jacking load for most PHC piles, resulting in a much less tedious acceptance jacking process for PHC piles than that for steel H-piles.

Figure 2: Pile jacking machine for PHC piles

Figure 3: Clamping of PHC pile

4.5 Pile connections

Unlike driven piles, the pile jacking machine remains in place during the welding process, as the pile remains at the center of the machine and sticking approximately 1 m above ground. The welding process is thus always on the critical path of the pile jacking process. Gas metal arc welding using CO_2 as the shielding gas is used for connection of PHC piles in Macau. It is a welding process which joins metals by heating the metals to their melting point using an electric arc. The arc is between a continuous, consumable electrode wire and the metal being welded. The arc is shielded from contaminants in the atmosphere by a shielding gas, i.e. CO_2. A semi-automatic welding process is normally adopted, i.e. automatic electrode wire feeding by the equipment and manual handling of the welding gun by the welder. It is learnt from site experience that it takes approximately 15 minutes for two welders working simultaneously to complete the welding for a pile connection, an obvious expedient when compared to electric arc welding.

4.6 Results of the static load test

Every jacked pile has been preloaded to 2.2 times the design load-carrying capacity before the static load test. Therefore, the loading exerted on the pile during the static load test, i.e. 2 times the design load-carrying capacity, is practically a re-loading with the magnitude smaller than the maximum load that the pile has experienced. Using the same loading sequence and acceptance criteria adopted in the Hong Kong, all the test piles satisfy the requirements of the static load test. A typical load-settlement curve is shown in Figure 4.

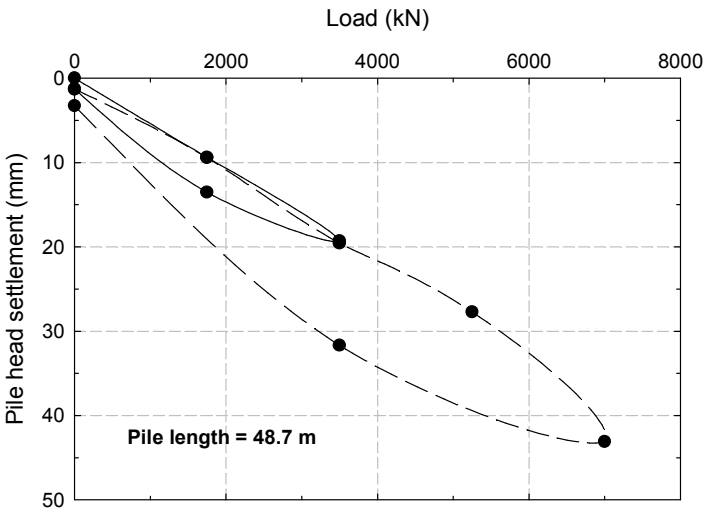

Figure 4: Load-settlement curve during static load test

5 OBSTACLES FOR THE IMPLEMENTATION OF THE TECHNOLOGY IN HONG KONG

As remarked by Li et al. (2000), the foundation construction equipment used in Hong Kong is the state-of-the-art but the construction technology adopted is very out-of-date. One of the major obstacles for the implementation of the hydraulic jacking of PHC piles in Hong Kong is probably the unnecessary, over-restrictive, bureaucratic and inappropriate government control. Jacked pile is still not a pile type recognized by BD. As a result, its design has to be approved on a project-by-project basis. The approval procedure is thus lengthy and the requirements are excessively restrictive, as demonstrated by the Fung Yuen Project (Li et al. 2011). In view of financial costs, developers and foundation designers will be reluctant to implement the technology.

The soil conditions in Hong Kong may make it difficult to install PHC piles of D = 600 mm and T = 130 mm. The typical size of PHC piles being used in Hong Kong is D = 500 mm and T = 125 mm, resulting in a design load-carrying capacity of 2,700 kN. The number of piles has to be increased by approximately 30% in comparison to Grade 55C 305×305×223 kg/m steel H-piles. However, the obstacle can be eliminated by the use of concrete of compressive strength of 105 MPa which is a mature technology in Japan.

Quality control and assurance of PHC piles is an important issue, as there are too many manufacturers of variable quality in the market. It is not an easy task to confirm all the PHC piles in a particular lot are from the same manufacturer as a result of the complicated transportation logistics. However, the problem can be easily solved by tracking each pile by the use of a RFID in conjunction with a GPS.

The supply of PHC piles in Hong Kong is practically a closed market as controlled by the listing system of BD. The system may function as a quality control and assurance system if the pile quality is being monitored regularly. Unfortunately this is not the situation now. Moreover, the increase in concrete strength or pile diameter may require another round of bureaucratic approval procedure which is a deterrent in the development of new technology or new material.

6 CONCLUSIONS

Installation of PHC piles by hydraulic jacking has been successfully implemented in Macau for many projects. It is evident from these successful case histories that there are no insurmountable technical obstacles. There are some solvable technical issues to be overcome for its implementation in Hong Kong. However, most obstacles arise from administrative issues imposed by the Hong Kong SAR Government. Therefore, it is a matter of the determination of the Hong Kong SAR Government to implement this cost-effective, efficient and environmentally friendly pile installation technique in Hong Kong.

REFERENCES

Lam, J. & Li, K.S. 2003. Introduction. In K.S. Li, N.C.L. Ho, L.G. Tham & P.K.K. Lee (ed.), *Case histories of jacked piling in Hong Kong*. Hong Kong, Centre for Research & Professional Development, 1-35.

Li, V. (ed.) 2011. *New developments in jacked piling*. Centre for Research & Professional Development, Hong Kong.

Li, K.S., Ho, N.C.L., Lee, P.K.K., Tham, L.G. & Lam, J. 2003. Jacked piles. In K.S. Li (ed.), *Design and construction of driven and jacked piles*. Hong Kong, Centre for Research & Professional Development, 23-50.

Li, K.S., Lo, S.-C.R. & Lam, J. 2000. Design of pile foundation in Hong Kong – Time for change? In *Proc., Foundations – 20th HKIE Geotechnical Division Annual Seminar*, Hong Kong, 77-86.

Li, V. & Lam, J. 2011. Development of jacked piling in Hong Kong. In V. Li (ed.), *New developments in jacked piling*. Hong Kong, Centre for Research & Professional Development, 88-116.

Li, V., Lam, J. & Ho, N. 2011. *Techniques for installation of jacked H-piles*. Centre for Research & Professional Development, Hong Kong.

White, E.E. 1975. Underpinning. In H.F. Winterkorn & H.Y. Fang (ed.), *Foundation engineering handbook*. New York, New York, Van Nostrand Reinhold, 626-638.

Yeung, A.T. & Li, V. 2012. Recent case studies of jacked piles in Hong Kong and Macau. In V. Li (ed.), *Bridge research and practice – the VLA Experience*, Vol. 2. Hong Kong. Centre for Research and Professional Development, 97-120.

Is My Geotechnical Modelling Conservative or Aggressive? – A Challenge in the Design of a Deep Foundation Excavation

Gavin S.H. Toh
Lambeth Associates Limited, Hong Kong
(A Member of Gammon Group)

ABSTRACT

The design of deep excavation in Hong Kong has often focus on the soil model such as the shear strength and stiffness of geological material. Back-analyses of these parameters were often carried out and results published indicating the conservatism of the typical adopted values and deriving a higher parameters to fit the measured ground movement. With the advancement of loading jack system, high magnitude of preloading the excavation lateral strutting support was commonly adopted in the deep excavation design. In the project presented in this paper, the measured forces of some struts were up to 100% of the predicted value. However, the measured ground movement was smaller in magnitude than those predicted in the design. Is the geotechnical modeling conservative or aggressive?

1 DEEP EXCAVATION DESIGN

In an urban society such as Hong Kong, it is not uncommon to see that underground structures such as building basements, foundation and tunnels for mass transportation are going deeper into the ground. In these deep excavation work, it is important to address the geotechnical challenges in the design with considerations of public and construction safety.

1.1 The "puzzle" in the geotechnical model

In the design of excavation work, the ground condition is generally derived from the ground investigation borehole log. The correctness of the geological profile is subject to the numbers, extent and spacing of the boreholes. The ground water level (GWL) is estimated from measured standpipes or piezometers readings with additional 1m to 2m to accommodate the raining season. At areas where the site is susceptible to flooding, higher GWL may be considered in the design.

The soil model in the design requires soil parameters that are derived from laboratory and field tests. Typical design parameters for the different soil material in Hong Kong have been well documented. Back-analyses of completed projects deriving the parameters are well recognized in Hong Kong. For example, A Chan (2003) has published the values of Young Modulus (E) that can be directly correlated to SPT N-values.

The surrounding condition, such as existing pavement/road and buildings, are considered in the design. Magnitude of typical pavement/road surcharge is well established and accepted in Hong Kong. Where required surcharge of adjacent building foundation is estimated and taken account.

The structures to support the excavation such as the cofferdam vertical wall and lateral support strutting system are specified by designer. The structural stiffness and capacity of these elements are incorporated in the design and in general constructed on site accordingly.

Figure 1 present a "puzzle" illustration covering the four different pieces in deep excavation design: Ground condition; Soil Model; Surrounding condition; and Specified Structures.

Figure 1: The "Puzzle" in deep excavation design

To verify the design and better manage and control buildings damage, instrumentations are set up to measure movement such as ground settlement and cofferdam wall deflection, GWL, and forces in the lateral support struts.

1.2 Are we being conservative?

Pan et al. (2001) reported the measured deflection was about 50% of the predicted values for a diaphragm wall used in the excavation for the Tseung Kwan O station and tunnel. The ground consisted of 15-18m of reclaimed fill with 8m of soft marine clay.

In a deep basement design for a project in Central where the ground comprises 8-10m of Fill and 8m of Alluvium/Marine Deport, the measured deflection was about 53% of the value predicted for a diaphragm wall cofferdam (Sze and Young (2003)).

A Chan (2003) has published, based on back analyses of deep excavation works of past projects, the values of Young Modulus (E) that can be directly correlated to SPT N-values. The paper reported that an E/N value of 1.5 (MPa) for Fill, Alluvium and Marine Deposit and an E/N value of 2 (MPa) for CDG are considered a reasonable and conservative estimation of lateral displacement of deep excavation.

Askew el al. (2006) reported that the maximum measured wall deflection was 74% of the predicted magnitude of strutted pipe pile wall for the East Rail tunnel project. The measured strut forces were 42% to 67% of the predicted values. Another pipe pile wall cofferdam for a Youth Centre in Chai Wan recorded strut loads measuring between 26% and 60% of those predicted.

The project examples indicate measured wall deflection and ground responses are consistently smaller in magnitude than predicted in the original design. The suggestion is to optimize the excavation design using an improved empirical E/N value correlation. However, this optimization should be applied without compromising public safety and safety in construction. The consequence is high if any failure of excavation in a typical Hong Kong building site, which is normally in close proximity to existing properties and dense population.

2 THE EXCAVATION DESIGN OF TUNG YING BUILDING

This paper presents the foundation excavation design for the redevelopment of the old Tung Ying Building along Nathan Road in Tsim Sha Tsui. The design adopted the E/N value correlation. With the advancement of loading jacking system, the struts were preloaded to a predetermined value up to 60% of the maximum design load of the struts to control cofferdam wall deflection and ground response. The measured movement and strut forces and comparison with the predicted magnitude are discussed.

In the previous paper on the same project, G Toh (2010) has presented the excavation designs with emphasis on the constructability and safety where potential hazards in the excavation works such as restricted headroom for construction plant, complicated sequence of works and type of strutting system were designed out in the design stage. The paper further highlighted the important of building damage control mechanism from instrumentation and design verification to works control and risk assessment management system for the success of the entire excavation works.

The background of the project and geotechnical design considerations are briefly discussed in the following paragraphs.

2.1 Site location and adjacent sensitive structures/utilities

The old Tung Ying Building located in the urban and busy district of Tsim Sha Tsui, was redeveloped and the new commercial building is known as "The ONE." The redevelopment includes a 5-level basement that required excavation up to 30m deep. The site is approximately 110m in length and 26m wide, and in close proximity to existing buildings/utilities. The existing operating MTRC tunnel about 20m below ground beneath Nathan Road has a minimum clear distance of only 3.8m from the site boundary. Site layout plan is shown in Figure 2.

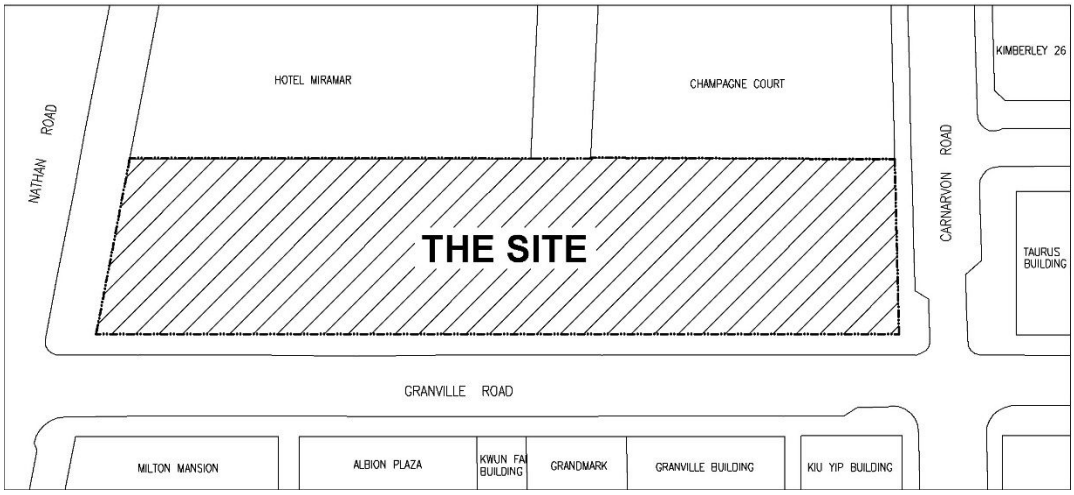

Figure 2: Site location plan

2.2 Excavation and lateral support design

In the excavation and lateral support (ELS) design, the temporary cofferdam wall consisted of pipe pile with grout curtain to provide water cut-off to the excavation. Five layers of struts were adopted to provide the required lateral support and stability to the excavation cofferdam.

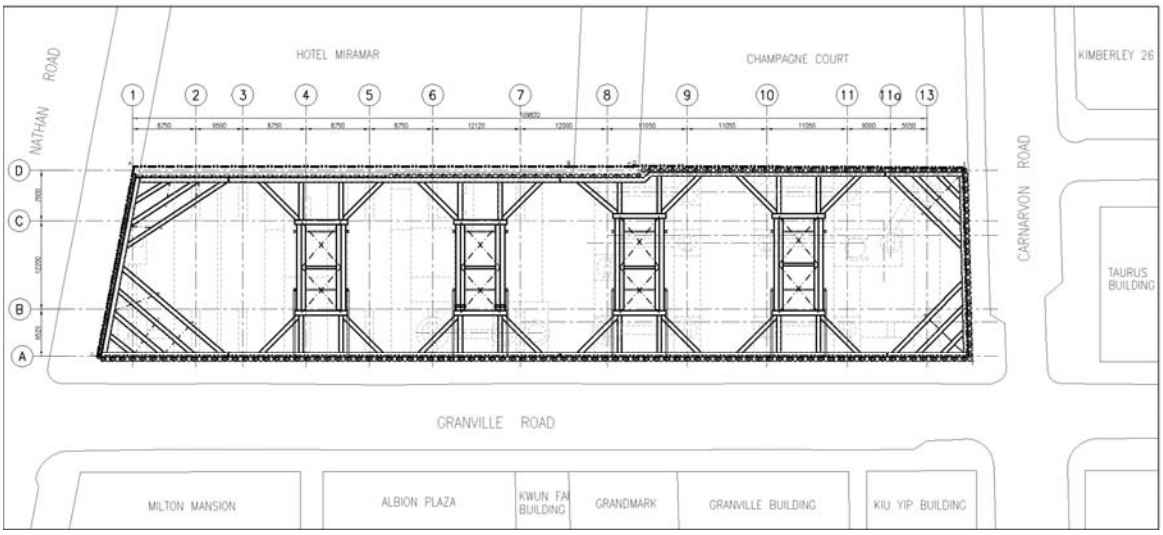

Figure 3: Strutting arrangement layout plan

The layout plan showing the strutting arrangement and section showing the strutting levels and geological conditions are shown in Figure 3 and 4 respectively.

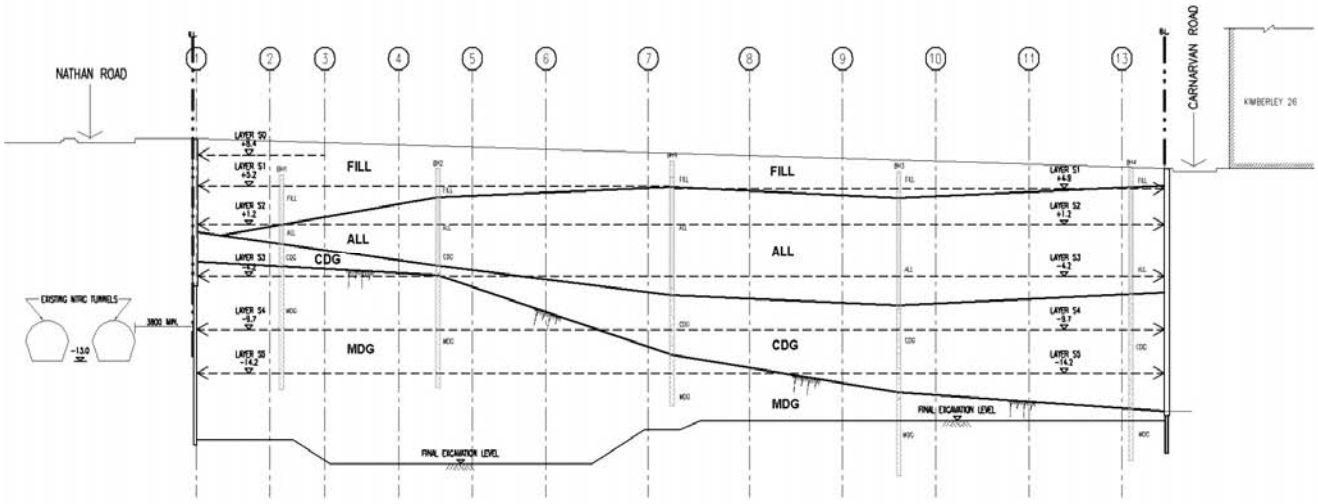

Figure 4: Geological section and strutting levels

2.3 Geological parameters

Ground strata comprising approximately 2 to 5m of sand fill, underlain by 2 to 11m of Alluvium. Beneath the Alluvium layer is the Grade V completed decomposed granite (CDG). A zone of Grade V/IV granite with SPT N value greater than 200 was presence above the bedrock. Bedrock of moderately strong to strong granite was encountered at approximately 10m below ground at the Nathan Road side and dipped to about 30m below ground at the Carnarvon Road side. Ground water level (GWL) measured from standpipe/piezometer was around 3.0m to 3.5m below ground.

The design soil parameters for the Fill, Alluvium and CDG were determined from the laboratory tri-axial tests with CDG separated into two classes, one with SPT N<200 and the other with SPT N>200. The Young Modulus of the soil adopted the E/N correlation where E/N of 2.0 for CDG and 1.0 for Fill and Alluvium.

3 MEASURED VERSUS PREDICTED VALUES

A comprehensive system of instrumentation monitoring system was set up on the surrounding pavement, road and nearby existing buildings and utilities. Three inclinometers were installed along Nathan Road in view of the displacement sensitivity of the existing MTR tunnel. The struts were preloaded to predetermined value, and the loading on the struts was essential to the cofferdam movement and ground responses. Strain gauges were therefore installed on the struts, and the readings were monitor "real-time" using the GEOMON system developed in-house by the Contractor.

3.1 Is the geotechnical model conservative?

Comparison of the predicted and measured magnitude of the maximum lateral displacement of the wall and ground vertical settlement along Nathan Road are summarized in Table 1.

From Table 1, the result indicates that for rock head at 16.5m depth the measured maximum lateral wall displacement of 10mm at inclinometer I2 is only 28% of the predicted magnitude. Inclinometer I1 located at the corner of the cofferdam measured deflection of 7mm. The readings of I3 was abnormal and suspected to be damage. For the ground settlement the maximum measured magnitude was 10mm along Nathan Rd, which is about 52% of the magnitude estimated in the geotechnical model. Along Granville Rd, the measured settlement 15mm is about 70% of the predicted value.

Table 1: Summary of wall lateral displacement and ground vertical settlement

	Prediction	Measured	Location of instrumentation
Wall Deflection	46mm (RH @ 22m)	10mm	I2 – at middle portion of the cofferdam wall & rock head at 16.5m below ground
	36mm (RH @ 16.5m)	7mm	I1 – at the corner of the cofferdam wall & rock head at 12.5m below ground
Ground Settlement	19mm	10mm	Maximum measured ground settlement along Nathan Road
	21mm	15mm	Maximum measured ground settlement along Granville Rd

The wall deflection profiles measured by the inclinometer and the predicted curve are shown in Figure 5. The comparison may suggest that in the original design the soil model, such as the ratio of the E/N correlation adopted errs on the conservative side. A higher E/N correlation may be considered a reasonable prediction of the lateral displacement of the wall.

In view of the different rock head levels considered in the predicted model and actual inclinometers location, normalized deflection (with maximum value) and normalized depth (with respective rock head depth) are included in Figure 5. The lateral wall deflection profile in I2 matches the predicted curve at the lower portion, whereas in the upper portion the measure lateral wall deflection is lower than the predicted value at the initial cantilever stage. From the profile of I1 the corner effect is apparent where maximum deflection occurs at the top of the wall, during the initial cantilever stage, and further movement during excavation is

minimal.

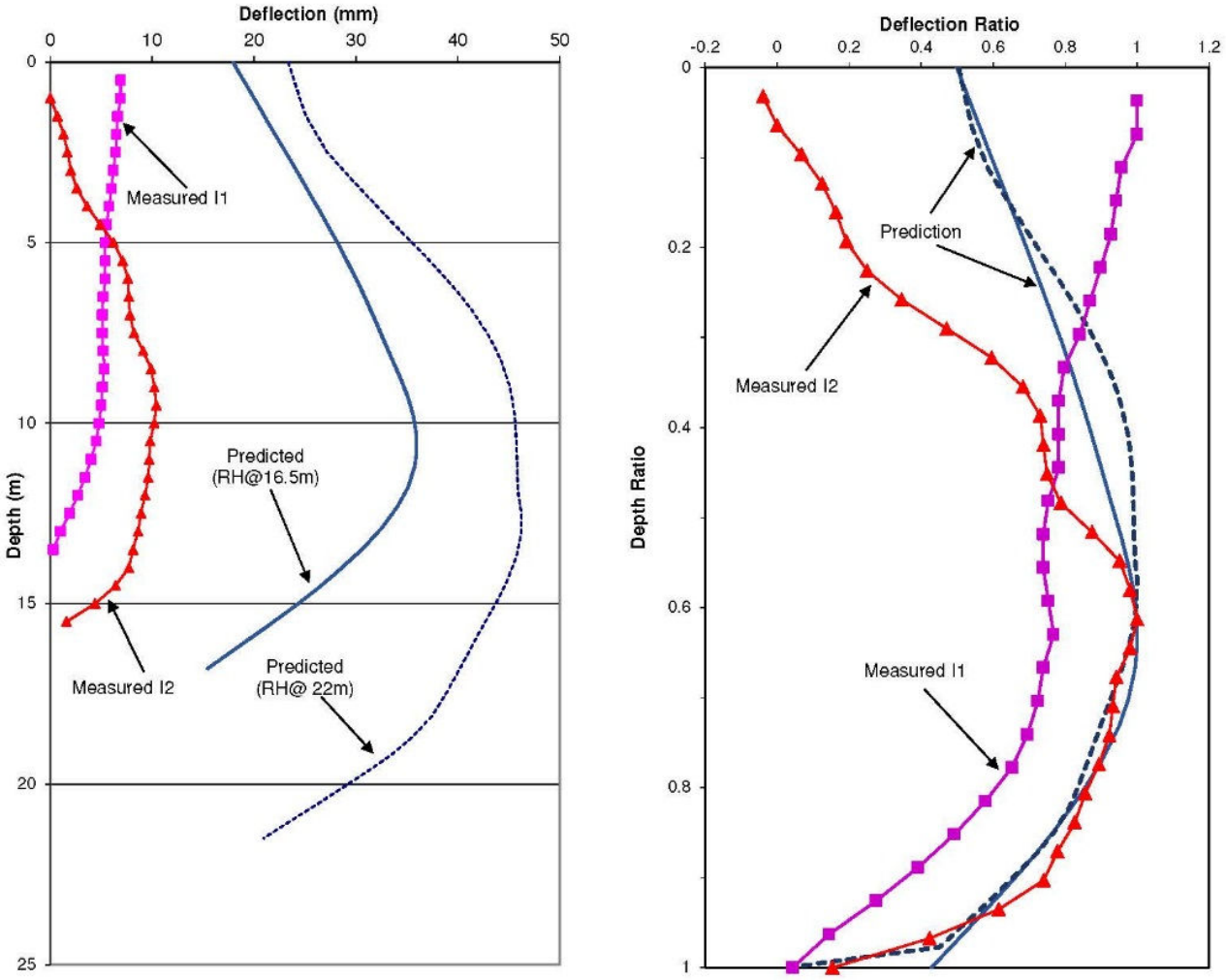

Figure 5: Predicted and measured wall lateral displacement

3.2 Is the geotechnical model aggressive?

The comparison of the struts forces between the measured strain gauges readings and the predicted values from the original design using FREW analyses are plotted in Figure 6. In the excavation design all the strut layers were preloaded except the first strut layer S1. Strain gauges were installed at the second (S2) to the fifth (S5) layers. For the purpose of this paper, PLAXIS analyses are carried out to compare with the results.

Figures 6 plots the changes of the strut forces in S2, S3, S4 and S5 with construction stages from excavation to removal of the struts. The preloading stage of each strut layer is shown in the plots. From the plots the behavior of the forces on the struts are apparent. The strut force increases when excavation proceeds to the next strut layer. A reduction of strut force occurs when the lower layer of strut is preloaded. An increase of strut force happens when the lower layer of strut is removed.

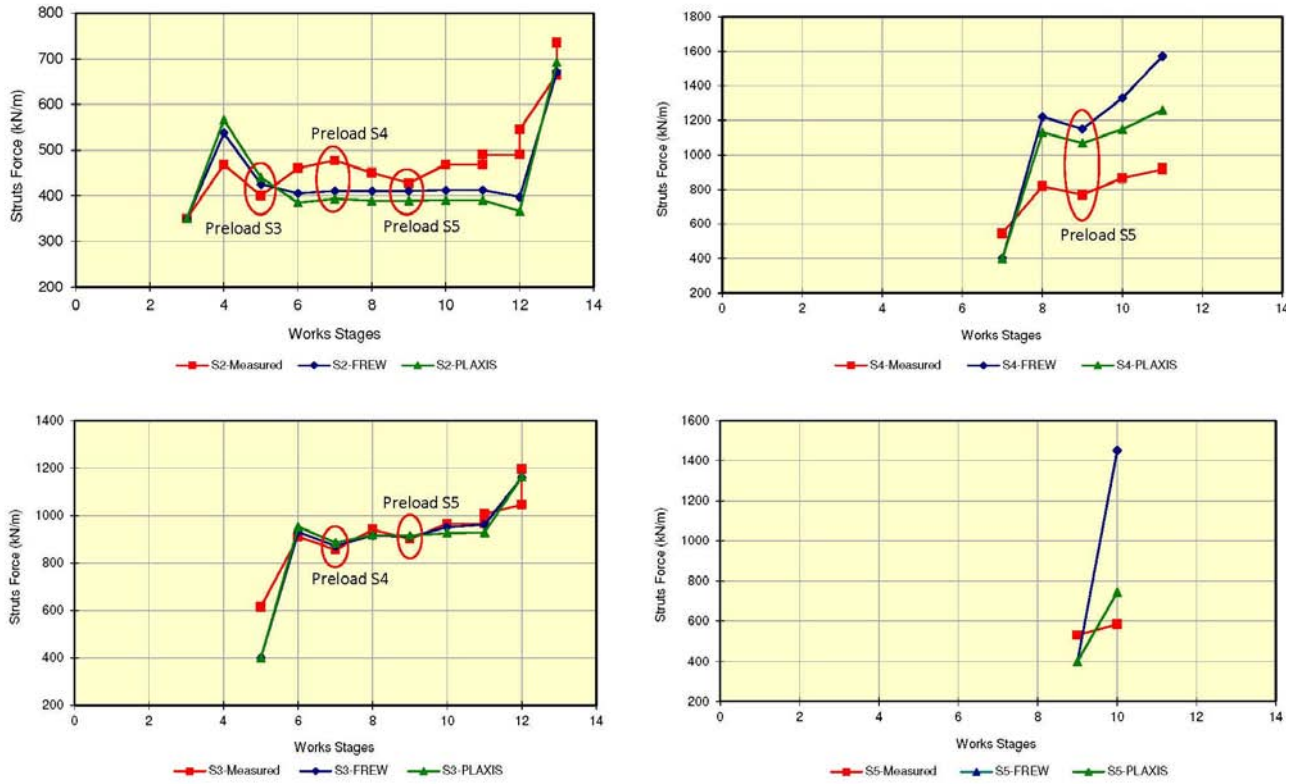

Figure 6: Measured and predicted strut forces (layer S2 to S5)

From the plots, the measured strut force in S2 are up to 20% higher than the predicted value. For S3 the measured value matches with the predicted forces from both the FREW and PLAXIS models. Whereas the measured force in S4 and S5 is lower, around 40% to 70% of the predicted forces depending on which numerical models. The PLAXIS model gives a lower S4 and S5 forces than the FREW results. This is likely due to the effect of higher rock head towards the Hotel Miramar side modeled in PLAXIS. The design section of the cofferdam model of FREW and PLAXIS is illustrated in Figure 7. Summary of the percentage difference between measured and predicted strut forces is presented in Table 2.

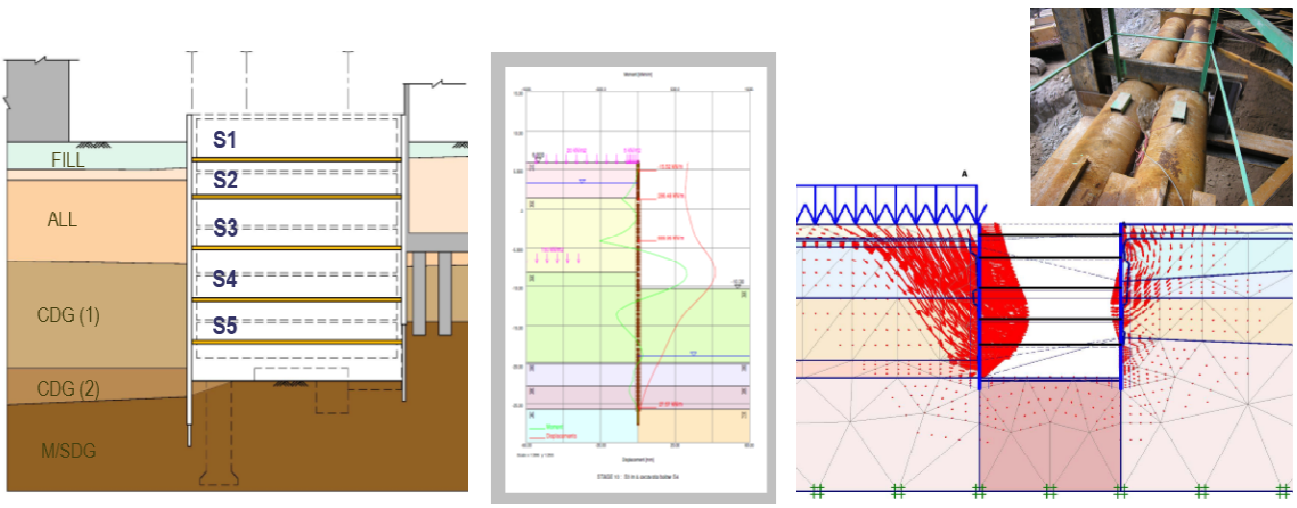

Figure 7: The section of cofferdam in this study

Table 2: Difference between measured and predicted strut forces

Strut Layer	% Difference (Measured/FREW)	% Difference (Measured/PLAXIS)
S2	±15%	±20%
S3	±5%	±4%
S4	64%	73%
S5	40%	79%

In view of the results in S2 and S3, one may deem that the original design has underestimated the forces in the strut and the soil model adopted may be aggressive if not the entire depth of the cofferdam at least for the top portion of the design model.

4 CONCLUSIONS

The ground response measured was smaller in magnitude than those predicted in the original design. This appears to be consistent with the findings of other experiences in Hong Kong discussed earlier. Apart from the E/N correlation the soil parameters derived from laboratory test may reflect more adverse parameters than exist insitu due to sampling disturbance in the ground investigation. The presence of the existing old piled foundations within the site may stiffen the ground, which has not been considered in the design model. In additional the existing piled foundation of the surrounding existing buildings could have provided a stiffer ground strength. These factors are related to three pieces of the "puzzle" – Ground condition; Soil Model; and Surrounding condition – which are often either deduced from tests or assumed based on recognized parameter in a conservative manner in the geotechnical model for deep excavation design.

The measured forces at the top layers of the strutting system matches the magnitude predicted in the original design. The ratio of the measured and predicted values decreases for the lower strut layers that are within the stiffer CDG and rock head as compared with the top layers within the less dense Alluvium and Fill. It is worthy of note the preload magnitude in S2 and S3 was up to 40% to 60% of the maximum calculated strut forces in the original design, whereas the preload in S4 and S5 was 30% or less. The lateral strutting system including the vertical cofferdam wall is the last piece of the "puzzle" – Specified Structure – which the designer defines in the excavation design model.

Is my geotechnical model conservative or aggressive? The conclusion from comparison of the measured and the predicted value does not appear to answer this question. Perhaps the focus is not on the geotechnical model but on the deep excavation work itself – whether the work is a success or a failure. Therefore the right question to ask: "Is the excavation work a success or a failure?"

What constitutes success or failure in excavation work? It is not about collapse or zero movement of the excavation cofferdam. In the paper, G Toh (2010) illustrated a successful excavation work for the Tung Ying redevelopment where constructability and safety were achieved. Potential hazards in the excavation works such as restricted headroom for construction plant, complicated sequence of works and type of strutting system were taken into account in the geotechnical modelling.

ACKNOWLEDGEMENTS

This paper is published with the permission of The Chinese Estate (Tung Ying Building) Limited and Gammon Construction Limited.

REFERENCES

Askew, I., Sein, D., Frame, A. 2006. Improving design efficiency and safety in substructure building works in Hong Kong through observational method design. *Proceedings of the Seminar on The Observational Method and It's Application in Hong Kong, HKIE-HKGES-AGS(HK)*

Chan, A. 2003. Observations from excavations – A reflection. *Proceedings of the Seminar on Case Histories in Geotechnical Engineering in Hong Kong, HKIE Geotechnical Division*

Pan, J.K.L., Pappin, J.W., Cowan S., and Lam L.W.Y. 2001. An application of the observational method at Tsueng Kwan O Station and Tunnels. *Proceedings of the Seminar on Geotechnical Deformation and Movement, HKIE Geotechnical Division*

Sze, J.W.C. and Young, S.T.M. 2003. Design and construction of a deep basement through an existing basement at Central. *Proceedings of the Seminar on Case Histories in Geotechnical Engineering in Hong Kong, HKIE Geotechnical Division*

Toh, G.S.H. 2010 Constructability and Safety Perspective in Design of a Deep Basement Excavation in the Urban District of Tsim Sha Tsui. *Proceedings of the Seminar on Geotechnical Aspects of Deep Excavation, HKIE Geotechnical Division*

The Adoption of Rock-head Level for Foundation Design and Construction in Hong Kong

N.R. Wightman
Jacobs SKM, Hong Kong
A.D. Mackay
Nishimatsu Construction Company, Hong Kong

ABSTRACT

To ensure the safe design and construction of foundations in the Hong Kong Special Administrative Region (HKSAR) high quality and stringent standards are set out in the HKSAR Government Building Ordinance (BO). In particular areas of relatively complicated ground conditions which need to be addressed when planning foundation installations are referred to as "Scheduled Areas", in the fifth schedule of the BO, and "Designated areas" in documentation providing guidance to the BO. This paper provides an overview of the engineering geological characteristics which form the basis of these foundation requirements. An appreciation is given of the characteristics for the main geological groups encountered in the HKSAR, ranging from plutonic, volcanic, dyke intrusions, marble, sedimentary and metamorphic rocks. As considerable experience has been gained in the foundation installation into granite it is commented that the documentation tends to base its requirements on these characteristics with specific reference emphasized for the difficulties associated with marble. The paper summarizes considerations that should be addressed for other rock types, which may need more specific consideration during the site investigation, design and construction phases of foundation installations. It is also notes that the application of more commonly adopted and recognized rock-head definitions for foundations is being applied to other construction applications, such as sub-surface and bulk excavations, which may lead to inappropriate design and construction assumptions.

1. INTRODUCTION

The HKSAR Government BO standards set out a safe, high quality engineering standard for foundation design and construction. In particular the Code of Practice for foundations published by the Building Authority (BA, 2004a) allocates suitable presumed allowable bearing capacities for piled installations founded in rock, typically adopting the "Category 1(b)" definition of 5000kPa for piles, which requires verification from a minimum Total Core Recovery (TCR) of 85% moderately decomposed rock or better over a 5m length from a borehole". The basis for this is from the "traditional GI practice in the HKSAR to prove boulders are not present" (GEO, 1996). These "boulders" are often defined as corestones formed during the Partial Weathering (PW) process typical of granitic rocks (GEO, 1992). As part of this weathering process sub-horizontal, relatively weak discontinuities are formed, termed sheeting joints, which potentially impact the foundation bearing capacity (Fletcher, 2004). Whilst the presence of these discontinuities is characteristic of some types of granite and coarse grained volcanic rock in the HKSAR, they are not typical of many other rock types of rock which exhibit different weathering fronts (GEO, 1996 & 2007). An example is marble, which has a rock-head founding criteria based on the presence of sound marble with no cavities over a TCR of 20m from a drillhole (Chan, 1994). This paper provides an overview of rock-head definitions for foundations and its relevance for the different rock types typically encountered in the HKSAR.

2. ROCKHEAD REQUIREMENTS FOR FOUNDATIONS IN THE HKSAR

"Rockhead can be one of the most critical issues for construction purposes" (GEO, 2007). For foundations the design criteria founded into rock are outlined in BA, 2004, which is "deemed to satisfy the Building (Construction) Regulations" set out to support the BO. A summary of the presumed bearing capacity values and ground investigation (GI) verification requirements for pile installations founded on rock are summarized in Table 1 (BA, 2004). Additional specific requirements for foundation installations set out in documentation providing guidance to the BO are summarized in Table 2.

Table 1: Presumed Bearing Capacity

Presumed bearing capacity	Verification criteria
Category 1(a) – 10,000kPa	Fresh, very strong rock, 100% Total Core Recovery (TCR), minimum Unconfined Compressive Strength (UCS) of 75MPa
Category 1(b) – 7,500kPa	Fresh to slightly decomposed, very strong to strong rock, 95% TCR, minimum UCS of 50MPa
Category 1(c) – 5,000kPa	Slightly to Moderately decomposed, moderately strong rock, 85% TCR, minimum UCS of 25MPa
Category 1(d) – 3,000kPa	Moderately decomposed, moderately strong to moderately weak, 50% TCR

Table 2: Presumed Bearing Capacity

Reference	Location	Ground conditions	Verification criteria
Fifth Schedule, BO (BD, 2005 & BD, 2004)	Ma On Shan and North West New Territories	Metasediments, caviatious marble and deep level superficial deposits	20m TCR into "sound" marble
Designated Area (BD, 2006 & GEO, 2004)	Northshore Lantau		

As part of the requirements for foundation installation a rockhead contour plan is required for approval prior to commencing the works (BA, 2012). Relatively complicated ground conditions, often present in sedimentary, marble, marble bearing and metamorphic rock conditions, as summarized in the documentation referencing the designated area, northshore Lantau and the Scheduled Areas may result in localized deep weathering fronts (BA, 2005 & 2006; GEO, 2004; Chan, 1994, Fletcher et al, 2000 and Wightman & Lai, 2006).

3. ROCKHEAD CONSIDERATIONS FOR FOUNDATIONS IN HONG KONG

3.1 Rockhead characteristics

Rockhead is typically defined as the uppermost level of solid rock and can vary considerably over relatively short distances as a result of geological variations. An example of this effect is the presence of PW in granite and the effects of faulting, which may have localized deep weathering effects position different rock types in close proximity (Figure 1 and Figure 2).

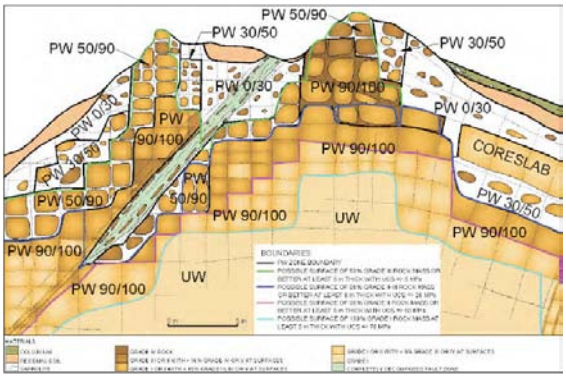

Figure 1: Schematic PW weathering scheme indicating variability of rockhead (GEO, 2007)

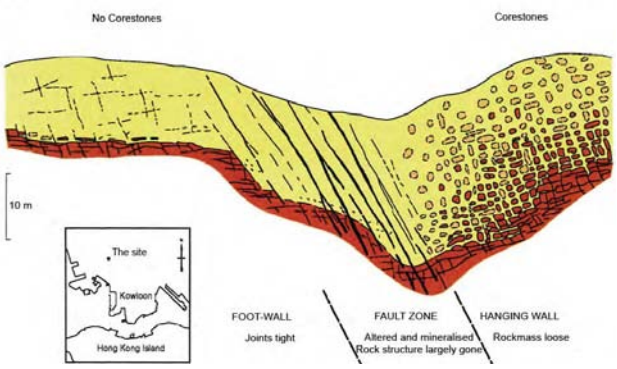

Figure 2: PW weathering zone located in close proximity to a zone with no corestones (Whiteside, 1988)

Rockhead is defined by the weathering effects, typically based on the decomposition grade being Grade III or better rock (GEO, 1992), notwithstanding "weathering has a significant effect on the engineering properties of rock", and as a result requires "careful description" (GEO, 1992). Weathering effects are defined as either disintegration (mechanical) and / or decomposition (chemical). Although the rocks in the HKSAR are largely influenced by decomposition, disintegration processes typically effect and may often have a major influence on the strength (GEO, 2007). Important weathering influences are summarized in Table 3.

Table 3: Weathering effects

Processes	Relevant descriptions and / or effects (GEO, 2007)
MECHNICAL - water absorption and release; stress and temperature changes	Micro-fracture growth. Typically resulting from de-stressing from the decomposition of quartz and feldspar components in the rock, becoming more obvious in coarse-grained granite.
DECOMPOSITION - breakdown of minerals to a more stable chemical state	Variable weathering front with associated permeability variation.

3.2 Examples of rock-head definition difficulties applied to foundations

In general the "Category 1(b)" definition for foundation installation is adopted in the HKSAR and requires verification by proving a minimum TCR of 85% moderately decomposed rock or better along a 5m length from a borehole" (BA, 2004). To satisfy this the rock coring can either be triple or double coring methods using foam or similar flushing method (GEO, 2000). The advantage of the triple core and a foaming agent is an improved TCR, particularly in fractured rock and rock with relatively closely spaced discontinuities, more typical of pyroclastic rocks, and rock with weak infill along the discontinuities. Notwithstanding the use of double coring methods is cheaper. This typically leads to significant cost and time increases when the TCR is reduced leading to an increase in the depth of pile installation accordingly.

The basis of the 85% TCR requirement is "to prove that corestones are not present" (GEO, 1996). Whilst this criterion is applicable for some granites and coarse grained pyroclastics (GEO, 2007) it is often broadly applied to other geological groups, for which it may not be applicable. At best this may lead to an over-robust design and construction approach. The negative aspect is insufficient attention given to the specific considerations for the foundation design and construction, such as abrupt changes in rock-head elevation over relatively short distances and the effect of adversely orientated discontinuities with respect to foundation installations; as outlined below.

3.2.1 Abrupt changes in geological conditions

During pile installation corestones, associated with loosening and opening of joints caused by inclined faulting, were encountered, refer to Figure 2 (Whiteside, 1988). This caused difficulties verifying toe pile toe levels and increased difficulty of installation during construction. This resulted in the rockhead being far lower than required when the contour plan for foundation level was produced. Rockhead depth in the Designated

area of Northshore Lantau has also referenced rockhead exceeding 160m below ground level (m bgl) within deep zones of preferential weathering along steeply dipping feldsparphyric rhyolite dykes.

The adoption of the rockhead contour plan for approval prior to commencing the works (BA, 2012) can often result in localized low elevations in the rockhead level which are often a result of a borehole intercepting a relatively thin zone of preferential weathering. This can be associated with faulting or rock with greater susceptibility to weathering, such as intrusions. It is considered that the plan should either be adjusted to coincide with the orientation of the depression or suitable supplementary geological modelling be provided.

3.2.2 Pyroclastics

Pyroclastic rocks in the HKSAR exhibit considerable lithological variation, such as re-crystallization, welding and flow texture. Many have a sedimentary origin, termed "eutaxites", and have often undergone re-orientation from the effects of regional faulting and intrusions. This leads to the re-orientation and nature of the bedding structure, often exhibiting a very close spacing and a sub-vertical orientation with an associated preferential weathering along the exposed planes of weakness causing abrupt changes in the weathering front. As referenced in GEO, 1996, "generalisation about piling in volcanic rocks is inadvisable".

3.2.3 Weathering Effects other than Decomposition

The effects of mechanical weathering in the HKSAR is documented for slope instability associated with rapid infiltration of surface water into the groundwater system during periods of intense rainfall, leading to rapid increases in groundwater pressures. For PW zones this has often led to rapid saturation of the relatively permeable saprolite surrounding core-stones, disintegrating the saprolites and opening discontinuities (Buttling, 1986 & Mackay et al, 2008). In the HKSAR, as the vegetation canopy has been removed and replaced with exposed surfaces over the last few decades, and leaking utilities are commonly present in urban environments the effects of mechanical weathering from rapid groundwater fluctuations should be considered.

Alteration has a significant effect on the engineering properties of rock. This occurs when gases and fluids infiltrate existing rock during subsequent geological intrusions, resulting in mineral alteration, typically the feldspars, within the original rock. The resulting change in engineering properties can be similar to those occurring from decomposition.

3.2.4 Weathering Effects on different Geological Groups

Weathering for different geological groups often differs from the standard "decomposition" characteristics set out in GEO, 1992. As plutonic and pyroclastic rocks have similar strengths in a fresh condition the adoption of the decomposition grading classification is applicable. However other rocks in the HKSAR, particularly sedimentary and metamorphic rocks may be weaker in the fresh condition (Beggs et al, 1985). As a result the adoption of a more specific weathering grade is needed, however to date a suitable classification is not available for the adoption of a more specific and suitable weathering grade (GEO, 2007)

3.3 Rock-head definition for foundations used in other applications

As clear definitions for rock-head are often lacking for other engineering works in the HKSAR there is a tendency to adopt the rockhead definition set out for foundations. Applications typically include bulk and / or sub-surface excavations. A typical problem is the adjustment of data based on the TCR requirement, which is a linear measurement, to that obtained from 2 or 3 dimensional records obtained during exposure. A schematic representation adjusting the linear measurements to 2 and 3 dimensions is presented in Figure 3 (GEO, 2007).

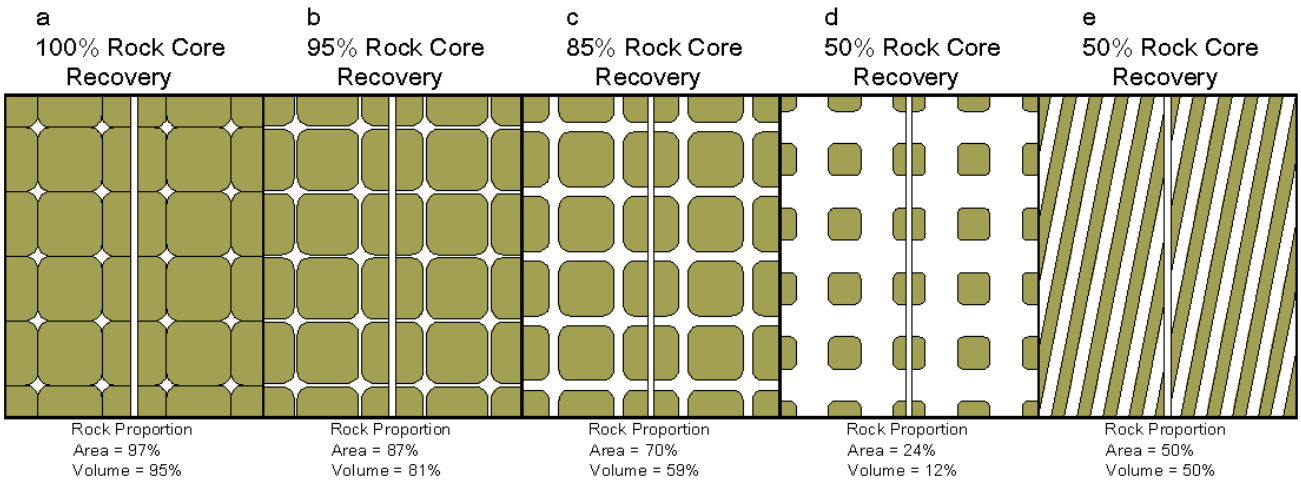

Figure 3: Schematic depiction of rock percentage and correlation with rock core recovery (assuming 100% recovery of the rock material), after GEO, 2007

4 MASS CHARACTERISTICS

4.1 Weathering profiles in rock

A PW range from 0/30 to 90/100 is adopted for granitic and pyroclastic geological groups (GEO, 1992) and can extend to significant depths (see Figure 4), referenced to be 20m for coarse grained pyroclastic rocks (GEO, 2007). Given this variability, the rock-head definition based on borehole data can be misleading in defining rock mass quality. An example is shown in Figure 5, which represents a tunnel which may encounter rock of poor quality requiring mining methods instead of drill and blast methods depending on the Q-value estimation.

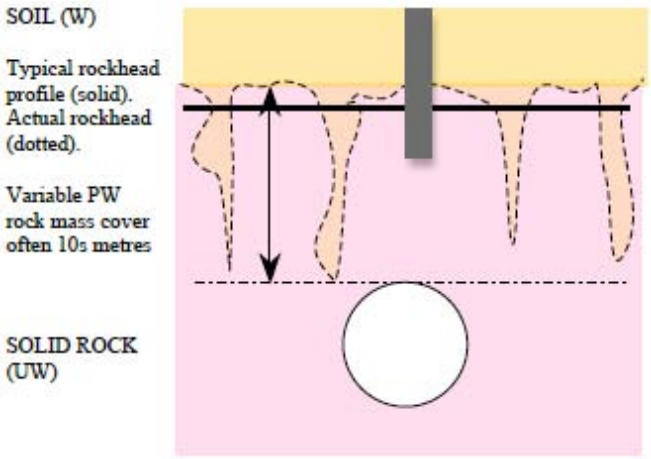

Figure 4: Idealised rockhead for piles with variable rock mass cover to tunnel (10's metres)

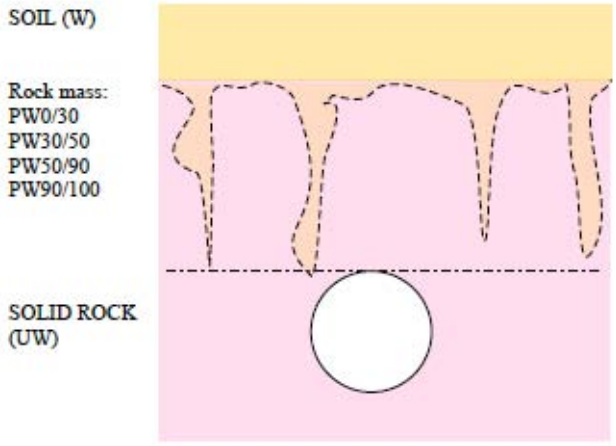

Figure 5: Partially weathered rock mass better indicates rock conditions with Q-system used for solid rock (UW).

Discontinuities determine the behaviour of rock masses, the development of conceptual engineering geological models are required to provide an interpretation of the variability in the ground (Jack et al, 2012). An example is the Sha Tin Strategic Cavern Area (Figure 6), which has various engineering properties compared to the 'rockhead' definition, which only described the engineering properties of one weathered rock

profile. Tattersall et al (2012) raised the importance of providing a good geological model as being essential prior to the geotechnical assessment of any construction project.

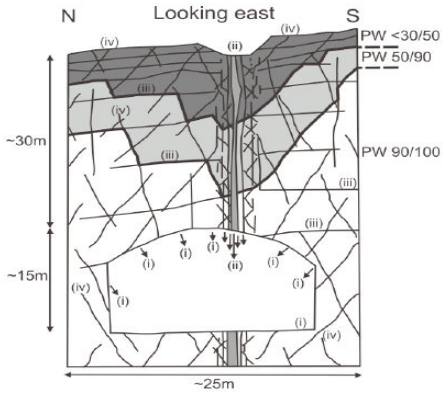

Figure 6: Conceptual engineering geological model of cavern excavation

Geoguide 3 - GCO (1988a)				GCO (1984) – based on Ruxton & Berry (1957)	
Description		Symbol	Characteristics	Zone	Characteristics
Residual Soil		RS	Residual soil derived from insitu weathering; mass structure and material texture/fabric completely destroyed.	A	Structureless sand, silt and clay. May have boulder concentration at the surface.
Partially Weathered Rock	0 / 30% Rock	PW 0 / 30	Less than 30% rock. Soil retains original mass structure and material texture/fabric (i.e. saprolite). Rock content does not affect shear behaviour of mass, but relict discontinuities in soil may do so.	B	Residual material with corestones. Rock percentage is less than 50% corestones are rounded and not interlocked.
	30 / 50% Rock	PW 30 / 50	30% to 50% rock. Both rock content and relict discontinuities may affect shear behaviour of mass.		
	50/ 90% Rock	PW 50 / 90	50% to 90% rock. Interlocked structure.	C	Corestones with residual material. Rock percentage is 50% to 90% and corestones are rectangular and interlocked.
	90 / 100% Rock	PW 90 / 100	Greater than 90%. rock Small amount of the material converted to soil along discontinuities.	D	More than 90% rock. Minor residual material along major discontinuities which may be considerably iron stained.
Unweathered Rock		UW	100% rock. May show slight discolouration along discontinuities.		

Figure 7: Geoguide 3 classifications of partially weathered rock with earlier GCO definitions (Tattersall et al, 2012).

Understanding previous records and knowledge of existing structural geological information is essential for ground characterisation. Although the term 'rockhead' is used as one of these definitions, Figure 7 indicates that other factors need consideration, such as rock mass classification based on the Q-system to describe rock (grade III or better). This approach allows a wider set of engineering geological considerations, accounting for structural geology and allowing for the presence of weathered horizons, either less or more weathered than that described by the rock-head definition.

3.2 Producing engineering geological models

Interpretation of the geological data is required to produce geological models (Figure 9).

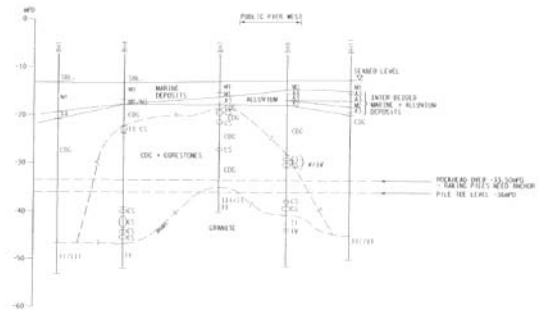

Figure 8: Geological section indicting deep zone of partially weathered granite in Victoria Harbour

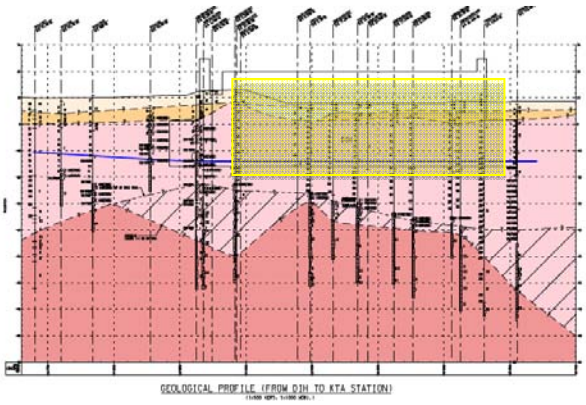

Figure 9: Partially weathered zone (hatched) indicated between completely decomposed granite and rockhead.

The development of geological models rests needs to be provided to enable initial geological block diagrams to be completed for conceptual engineering purposes and more detailed geological profiles produced allowing for initial design considerations to be discussed or detailed designs to be completed while minimising construction risks through risk control in the design phase.

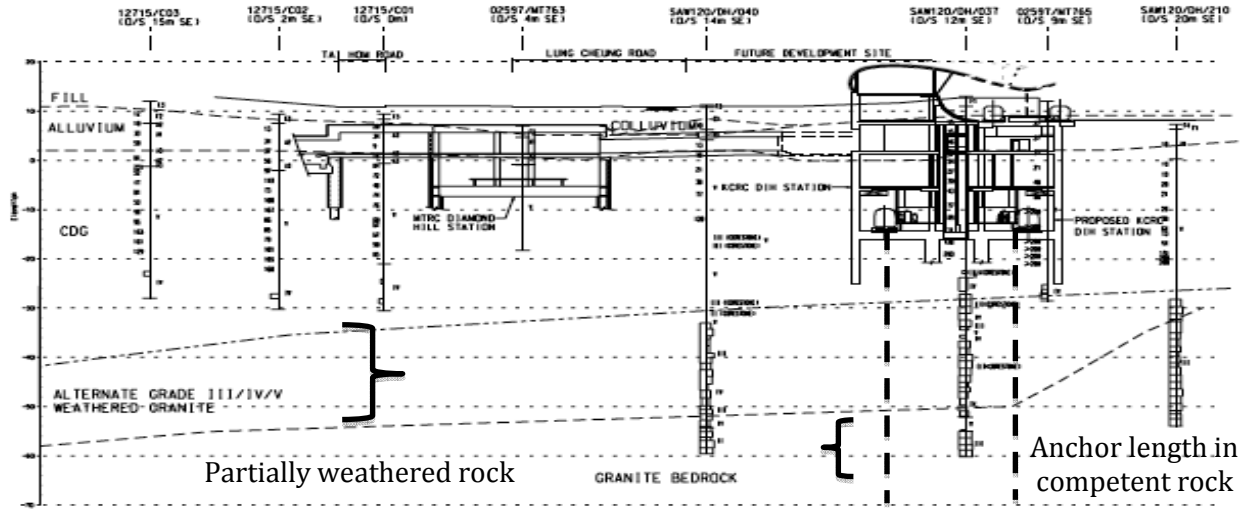

Figure 10: Partially weathered zone indicated as alternate grade III/IV/V weathered granite and impact of PW zone has on depth and anchorage of tension piles.

Examples of the PW zone presentation is shown in Figure 8, for a marine driven piling project which had limited data on PW rock, but later found the area to have a significant depth of corestones, and Figure 9 for a station box where the partially weathered zone (hatched area) impacted on the potential construction of diaphragm wall panels with significant chiseling being required to cut through corestones. The rockhead indicated in Figure 9 (top of the pink shaded area) would have not given much information on the presence or thickness of corestones, which would be encountered giving good reason to apply a thorough engineering geological approach to producing the geological models.

Other engineering aspects to consider are tension piles performance, which must interact with competent rock (Figure 10) in order to obtain adequate bond strength and pull out resistance. Drilling programme considerations depend on the expected presence of corestones in the partially weathered zone. With cost implications it would possibly be more cost effective to propose other means of preventing flotation of buried structures. Further details should be presented to enable these types of conclusions to be made by more detailed geological features presented on the geological profiles.

4. CONCLUSIONS

The definition of 'rockhead' used for foundation design and construction is set out in the guidance documentation for the BO of the HKSAR government. The requirements are typically based on a decomposition weathering classification, accounting for PW effects in the TCR retrieved from boreholes during the GI phase. Areas of more complicated ground conditions, such as the "Scheduled" and "Designated" Areas are also accounted for in the documentation. Although attention is given to achieving a safe design and construction standard, site specific engineering geological characteristics, which may have a major influence on the works, should always be recognized. This includes the effects of different weathering classifications applicable to different geological groups, specific engineering properties of pyroclastic rocks, suitable geological modelling representation particularly in the rockhead contour plan preparation and suitable GI techniques to provide accurate data for the geological model preparation and improve the TCR in more sensitive ground conditions. The use of the rockhead definition is suitable for foundations and should not be applied to other engineering works, such as sub-surface and bulk excavations, which require specific rockhead definitions applicable to their design and construction requirements.

REFERENCES

BA, 2004a. *Code of Practice for Pile Design and Construction.* BD, HKSAR Government.
BA, 2005. *Development in Area Numbers 2 and 4 of the Scheduled Areas* (APP 61), PNAP, 161, BD, HKSAR.
BA, 2006. *Development in the Designated Area of North shore Lantau* (APP 134), PNAP 283, BD, HKSAR.

BA, 2012. PNAP 66, *Piled Foundations* (APP 18), Buildings Department (BD), HKSAR.

Beggs, C.J. & Tonks, D.M. (1985). *Engineering Geology of the Yuen Long basin.* Hong Kong Engineer, Vol. 13, No. 3, pp 33-41.

Buttling, S. (1986). Remedial works to a major rock slope in Hong Kong. Proceedings of the International Conference on Rock Engineering and Excavation in an Urban Environment, Hong Kong, pp 41-48. (Discussion, pp 480-481).

Chan, Y.C. 1994. Classification and Zoning of Marble Sites. GEO Report No. 29, GEO, CEDD, HKSAR Government, 49p.

Fletcher, C.J.N., Wightman, N.R., & Goodwin, C.R. 2000. *Karst - related deposits beneath Tung Chung New Town, Hong Kong: implications for deep foundations*. Proc. Conf. Eng. Geology, IOM3 HK, pp139-149.

Fletcher, C.J.N. 2004. *Geology of Site Investigation Boreholes from Hong Kong*. Applied Geoscience Centre, Department of Earth Sciences, The University of Hong Kong, 132p.

GEO, 1992. *Guide to Rock and Soil Description,* Geoguide 3. GEO, CEDD, HKSAR Government.

GEO, 1996. *Pile Design and Construction.* GEO Publication No. 1/96, GEO, CEDD, HKSAR Government.

GEO, 2000. *Guide to Site Investigation (Geoguide 2)*. GEO, CEDD, HKSAR Government.

GEO, 2004. *The Designated Area of Northshore Lantau.* GEO Technical Guidance Note No. 12, GEO, CEDD, HKSAR Government.

GEO, 2007. *Engineering Geological Practice in Hong Kong*. GEO No. 1/2007, GEO, CEDD, HKSAR Government, 278p.

Jack, C.D., Parry, S & Hart, J.R. 2012. *Structural geological input for a potential cavern project in Hong Kong.* Proceeding of 32nd Annual Seminar Geotechnical Division, HKIE, 25th May 2012, HK, 347p.

Mackay, A.D. & Leung S., 2008. Site Investigation for Cut Slope Stability in an Area of Complicated Groundwater Conditions, Kwai Fong, HK. Slope Mitigation and Protection: Int. Conf. on Slopes, Kuala Lumpar (KL), Malaysia; pp 243-262.

Tattersall, J.W., Tam, J.K.W. & Garshol, K.F. 2012. *Engineering geological approach for assessment of quantities and programme for deep tunnels in Hong Kong.* Proceeding of 32nd Annual Seminar Geotechnical Division, HKIE, 25th May 2012, Hong Kong, 347p.

Whiteside, P.G.D. 1988. *Structural control in the development of granitic corestones.* Geological Society of Hong Kong Newsletter, Vol. 6, pp4-10.

Wightman, N.R. & Lai, A. 2006. *Investigation and Foundation Design in Marble / Karst Designated Areas of Tung Chung and Ma On Shan*. Proc. Seminar in HK Geot. Works in Karst in SE Asia, HKIE, pp109-140.

Impact of Changing Geological Conditions for Foundation Design and Construction in Tung Chung New Town Area

N.R. Wightman & J.F. Benson
Jacobs SKM Limited, Hong Kong

ABSTRACT

The Tung Chung New Town will be undergoing further infrastructure expansion over the next decade (2012 onwards) with proposed developments being planned to the East and West. The areas demarcated for these new town developments coincide with the designated area of Northshore Lantau, established in 2004, with the geological complexities highlighted on geological survey sheet report indicating the potential for rapidly changing geological conditions below the ground surface, particularly with deep dolines complicating the development of new infrastructure with deep foundations. The resulting difficulties in selecting geotechnical design parameters in highly variable ground and deep rock causes construction problems. Through careful construction site selection and geological investigations, these difficulties may be overcome provided attention is paid to using comprehensive risk mitigation procedures. This paper provides insight to future town planning and ground investigation needs for structural foundation design and construction, and highlights the techniques to achieve a comprehensive understanding of the geology. The investigations required for long-term infrastructure in Tung Chung and the recommended risk management procedures for a successful outcome at all project stages. Through this process, infrastructure planning has direct beneficial contribution to the development of Tung Chung, by avoiding construction delays or high foundation costs associated with excessively complicated geology.

1 INTRODUCTION

1.1 Tung Chung New Town Expansion

The future development of Tung Chung New Town was outlined by the Town Planning Board (2012) indicating the zones being considered for buildings and structures to the east and west of the existing infrastructure (Figure 1). The development will include residential high-rise buildings, roads with bridges and low-rise shopping, sports and leisure complexes. The main constraints to the development were shown to be predominantly from the existing Chek Lap Kok airport with height restrictions related to airport operations. Other important considerations will include examining in detail, the geology and the further existence of the Tung Chung Formation and or deep or rapidly changing rock levels, and changes to geological conditions in these areas. In terms of planning and estimating the cost of the proposed construction costs, the potential risk for excessively high costs for foundations must be considered with mitigation measures including the careful selection of appropriate, lower risk construction sites in advance, in order to reduce the depth of foundations.

One such development, Tower 5 on Site 3 in Tung Chung New Town (Plate 1), now called 'Seaview Crecent', inadvertently was positioned immediately above a doline, in 1999, with related very steep and very deep rockhead to over 150m below ground level. The cost and time for foundation construction was found to be excessive and the site for tower block 5 was eventually abandoned even though adjacent blocks were successfully constructed on shorter bored or driven piles (Plate 2). Tung Chung was included into the designated area of the Northshore of Lantau Island (GEO, 2004) requiring special measures to be implemented for ground investigation and design for all developments. The comprehensive risk mitigation process requires an understanding of the limitations associated with piling equipment for bored piles sunk deep into the Tung Chung Formation, and methods of placement of very long heavy reinforcement cages.

2 TUNG CHUNG NEW TOWN PLANNING

2.1 Designated area of Tung Chung

The Town Planning board (2012) has produced plans (Figure 1) showing yellow shaded zones depicting areas for development in Tung Chung New Town. These zones coincide with the 'Designated Area of Northshore Lantau' (GEO, 2004) shown in Figure 2, which are areas likely to be underlain by the Tung Chung Formation and locally comprise complex geological conditions requiring special attention to avoid problems for deep foundations relating to high-rise buildings and structures. These geological structures require additional ground investigation procedures to be carefully considered as solid rock or rock head is often deeper than 130 m increasing in some areas to over 200 m. At these depths, ground investigation becomes particularly difficult with rarely used ground investigation techniques being recommended (Wightman *et al*, 2001).

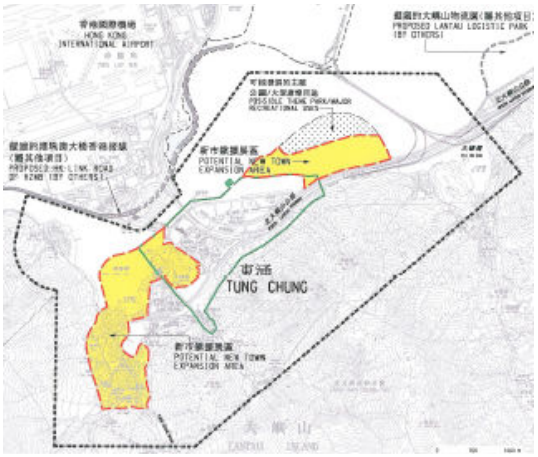

Figure 1: Development plan of Tung Chung New Town (Town Planning Board, 2012)

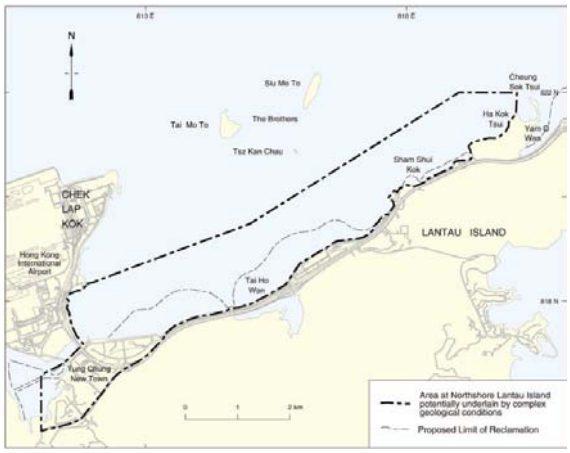

Figure 2: Designated area of Tung Chung (GEO, 2004)

2.2 Geology of Tung Chung

The Tung Chung Formation was first discovered in 1991 and reported by the Geotechnical Engineering Office (GEO) and the British Geological Survey (BGS) (Gillespie *et al*, 1998). The data was further collated and geological profiles of the Tung Chung Formation presented by Kirk (2000) from the BGS data and Fletcher *et al* (2000) included data from extensive advanced ground investigations, Wightman *et al* (2001) and Figure 3, completed at the site of Tower 5 on Site 3 (Seaview Crescent), Plate 1.

Plate 1: Tower 5 (Site 3) in Tung Chung reclamation area.

Plate 2: Tung Chung with undeveloped areas (2012).

The GEO published details in Geological Map Sheet No. 6 (Sewell & Kirk, 2002) and GEO (2007) as a result of these investigations and findings. A Tung Chung Geological model was developed including data from Site 3 of Tung Chung New Town. Findings from geophysical surveys (Kirk *et al*, 2000) were used to help assess the rapidly changing nature of the ground between boreholes indicating deep rock contours (Figure 7) allowing better engineering judgments to be made with respect to either use of end bearing piles or areas requiring adequate soil-structure support.

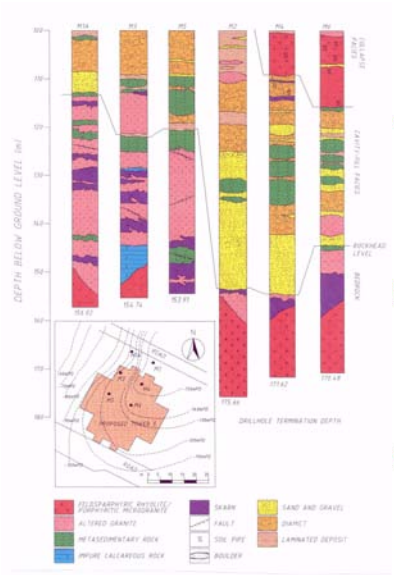

Figure 3: Advance GI schematic logs indicating changeable conditions. (After Fletcher *et al*, 2000)

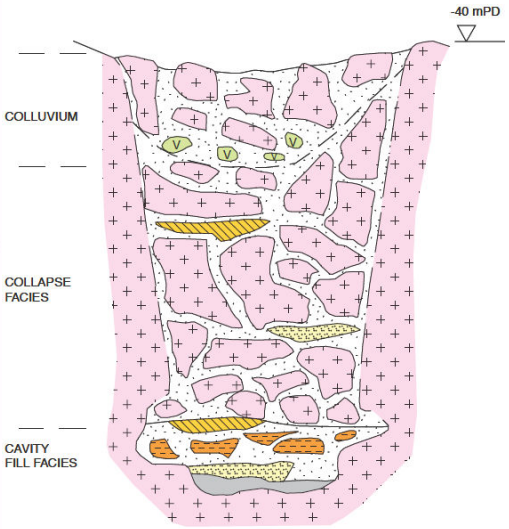

Figure 4: Schematic section of doline to 155 m deep. (After Fletcher *et al*, 2000)

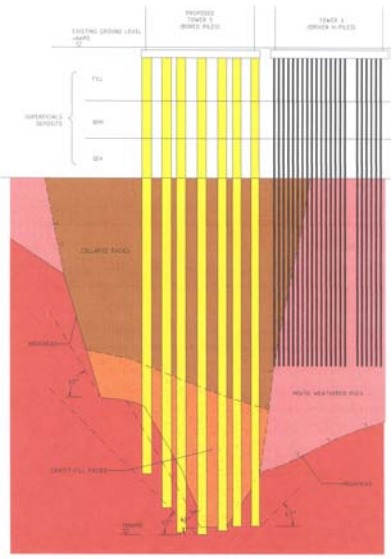

Figure 5: Tower 5 bored piles in doline feature adjacent Tower 6 driven piles in CDG. (After Fletcher *et al*, 2000)

The geological process that led to the Tung Chung Formation occurred during mass granitic intrusions into the existing marble formation, which surrounded large monolithic marble blocks called xenoliths.

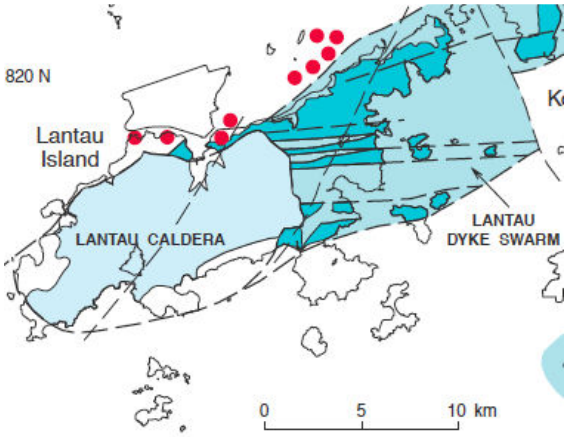

Figure 6: Marble / Skarn zones of Tung Chung (after GEO, 2002)

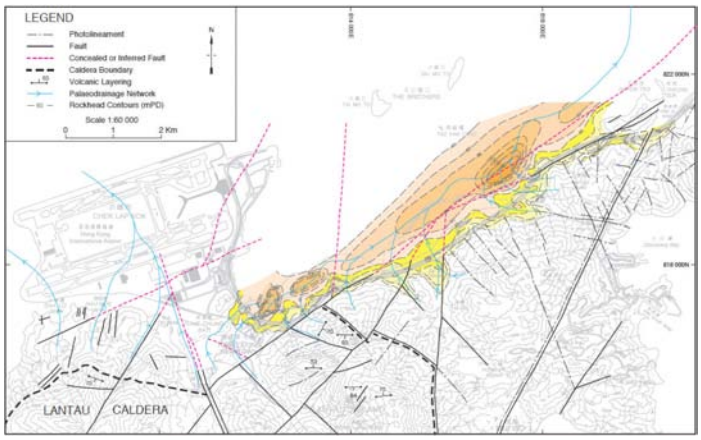

Figure 7: Deep rockhead contours (orange shading) in Tung Chung (after GEO, 2002)

The xenoliths in the granitic rock mass subsequently dissolved forming cavities that become filled with sediments and enabling collapse features called 'dolines', to form (Figure 4) when weathered overlying material filled the cavity voids, Figure 3 and Fletcher *et al*, 2000. The findings indicated that dolines existed with marble /skarn (Figure 6) being indicative of the granite to marble contact surfaces (Fletcher *et al*, 2000 & Fletcher, 2004) with the collapse facies of overburden strata propagating downwards. Dolines are associated with deep depressions in rock level with the insitu rock mass giving minimal indication of collapse movement except for telltale sand filled injection features and occasional foreign inflow material such as volcanic gravel from adjacent hillsides.

2.3 Advanced ground investigation techniques

It is important to recognise the different geological features that overlie deep rock due to the presence of other adverse geological strata such as filled cavities of the Tung Chung Formation (Figures 3 and 4). Aids for logging boreholes have been developed during Tung Chung's first phase of development by GEO (1998). Glossary of terms for the geological features encountered is provided by Wightman & Lai (2006) with reference to photographs of the recovered soils shown by Fletcher (2004).

Geophysical investigation methods such as microgravity, gamma density and both surface and downhole seismic survey gave images of rapidly changing levels of rockhead exceeding 160 m below the surface. Combined with advanced drilling techniques using state of the art drilling mud and carefully controlled drilling operations, difficult sample recovery was achieved with samples recovered from the deep weathered and cavity filled zones which helped provide new data in supplementing the geological model.

3 PILE DESIGN AND CONSTRUCTION CONSIDERATIONS

3.1 Foundation at Tower 5, Site 3 (Seaview Crescent) Tung Chung

It is important to recognise and identify these complex geological features initially during the town planning stage in order to make some provision for building layouts to avoid or effectively manage the associated risks of the most difficult areas for construction. Later foundation design will need to consider the geotechnical properties of the geological features present. Tower 5 at Seaview Crecent (Figure 3) was one such development where the decision to abandon Tower 5 avoided both excessive time delays and a large extra budget, but only after difficulties in construction of the development had commenced. Situations may arise for a site covering just one building footprint, which then leads to these problematic delays and cost over-runs. Typical ground investigation logging guidelines (GEO, 1998) provide assistance to practitioners particularly in describing the different types of soil / rock materials found in Tung Chung but within the Northshore Lantau Designated Area more specific guidelines are recommended to understand the complex interaction of risks associated with complicated geology with a glossary of terms provided by Wightman & Lai (2006).

The usual ground investigation techniques of regular sequences of undisturbed sampling and in-situ testing (SPT) was also modified with boreholes providing continuous sampling with Mazier sample tubes recovered for splitting to enable detailed geological inspection particularly to recognise the diamict deposits and cavity infill materials, which have an effect on the soil-structure interaction and pile behaviour. Other boreholes are used to recover mazier / U100 samples for geotechnical purposes and enable insitu testing to be carried out for SPT and say self-boring pressuremeter testing. SPT N-values from 140 m deep were indicated as zero due to the failing of the soil under the load applied by the drill string, which were later confirmed to be easily disturbed coarsely bedded, rounded sand deposits filling a cavity 12 m thick.

A further improvement to obtaining high quality samples is by using Gel Push Samples (Silva *et al* 2010), which are similar to mazier samples but with a gel intruded to externally coat the sample to provide support and a frictionless recovery into the sample tube.

3.2 Geological & Geotechnical issues

With changing geological conditions and possibility of encountering different formations across the footprint of a building, the geotechnical issues are greatly increased (Table 1). TGN No. 12 (GEO, 2004) points out the need for experienced geologists to be involved in logging boreholes and focus on obtaining both the geotechnical parameters and a reliable ground model is essential. Generally the ground behaviour of the Tung Chung Formation is changeable with depth depending on the depth cavities are encountered.

Table 1: Geotechnical issues relating to encountering geological features and expected findings.

Geological Features	**Expected Geological Findings**	**Geotechnical Issues**
Collapse feature (doline) [Tung Chung Formation]	• Depression in strata horizons • Collapse facies heterogeneous • 'In-situ' rock displaced • Soil pipes present • Cavities present (filled)	• Rapid geological changes. • Rapid changing of parameters. • Continuous sample recovery needed to examine changeability. • Hydrogeological flows different.
Cavity fill	• Interbedded clays, silts and sands • Uniform rounded sands at depth • Clay deposits (halite)	• Rounded sand non-interlocking • Low strength / micro-faulted • Parameters not yet measured
Deep rock head	• Steep rock surface • Solid rock over 160m deep • Weathered rock not in-situ	• Competent rock issues • Strength profile variable • GI difficulties – mud drilling
Other geological formations: • Chek Lap Kok Granite • Lantau Granite • East Lantau Rhyodacite	• Granitic and rhyolitic intrusions • Volcanic formations • Marble xenoliths / karst • Complete weathering of rock	• More reliable ground conditions • Solid rock shallower • Presences of marble, karst and skarn in contact with granite

3.3 Design Risks & Mitigation

The design of foundations for structures in the Tung Chung area requires extra care to avoid future construction difficulties or building foundation performance problems (Table 2). This is particularly important in offshore areas where limited previous ground investigation has been carried out. Risk mitigation at the conceptual design stage is highly recommended, and is possible by employing advanced ground investigation techniques incorporating splitting and logging of continuous sampling tubes to rock in areas where ground conditions indicate the presence of cavity fill or very deep solid rock.

Table 2: Design issues relating to encountering geological features and expected design risk

Geological Feature	**Design Risk**	**Design Risk Mitigation**
Collapse feature (doline) with cavity fill [Tung Chung Formation]	• Geotechnical parameters unknown • Inappropriate geotechnical assumptions • Very weak clay / silt materials • Rounded sand	• Prior site selection for structures • Advanced ground investigation • Splitting Mazier tubes for logging • Better recovery of samples (>140m) • Alternative foundation solutions • Avoid site location
Deep solid rock (100m to over 200m)	• Large diameter bored piles to rock	

	• Piles encounter weak layers	• Reduce excessive pile boring to rock • Reduce settlement of friction piles
Steep solid rock (>60m to over 150m)	• Uneven end bearing distribution • Building tilt possible at completion	

3.4 Pile construction issues

The construction of end bearing piles to depths greater than130m are of particular concern and likely to be at the thresh hold of current capability of piling plant (Table 3). The extreme depths for the construction of the single trial pile for Tower 5, Site 3 foundation construction, caused several months delay to the programme with excessively high cost overruns. The 155m long reinforcement cage broke numerous times prior to concreting. The RCD piling plant was working at capacity and with the head jamming on encountering weak cavity fill. The tower was eventually abandoned due to the excessive difficulties encountered (Wightman & Lai, 2006). The trial pile was noted as the world's longest pile on completion. The bridge connecting Towers 3 and 6 is located at the footprint of Tower 5 (near Seaview Crescent). To reduce the potential for large settlements, the bridge foundation used a floating box foundation with a very low net load increase on the underlying soils. Site 4 in Tung Chung used shaft grouted friction barrettes using average SPT values obtained from the variable soils and conditions (Sze *et al*, 2007).

Table 3: Construction issues relating to encountered geological features and expected construction risk.

Geological Feature	**Foundation Type**	**Construction Risk & Issues**
Collapse feature (doline) with cavity fill [Tung Chung Formation]	• Shaft grouted barrettes • Friction piles (Driven H) • Bored piles to rock (end bearing)	• Bored piles over 2.5m diameter need 3 or more nested casings. • Cost and time (ref: Tower 5, Site 3) • Jamming of pile drill head • Piling plant deflected from vertical • Excessive over break during boring • Excessive settlements • Plant working at maximum capacity • Long-term pile creep / settlement
Deep rock head (Steep rock)	• Shaft grouted friction barrettes, (Sze *et al*, 2007) • Friction piles • Compensated/ floating foundations • Lightly loaded raft foundations	

3.5 Risk mitigation

To obtain better cost effectiveness via risk management techniques for the design and construction of infrastructure at Tung Chung, advanced ground investigation programmes are suggested to allow town planning aspects to take into account, the early issues with respect to the complex geology and ground conditions. Very experienced engineering geologists who have previously dealt with the Tung Chung Formation are recommended to be involved with any advance investigations, with added value provided by geophysical survey methods to derive geological models being developed. Both time and cost implications for foundation construction is a prime consideration for the future infrastructure design of deep foundations in the Tung Chung area.

4 CONCLUSIONS

During the infrastructure and town planning conceptual design phase, the location of structures should avoid areas of very deep inconsistent solid rock due to the problems associated with steep rockhead and or deep rock cavities. Alternative foundations design solutions should be considered where dolines are encountered to reduce the potential for excessive time and cost over runs.

Risk mitigation processes should be considered at the initial phases of the planning process to avoid issues with deep rock and rapid changes in geology across sites to be used for infrastructure. Geotechnical engineers and geologists should pay special attention to the ground investigation design and procedure. The logging of boreholes would greatly benefit the splitting of Mazier tube samples for observation of geological anomalies and features such as cavity deposits or diamict / collapse facies. The scrutiny of very experienced engineering geologists are considered essential for accurate geological models to be developed.

REFERENCES

Geotechnical Engineering Office, 1998. *Lexicon of terms used for drillcore logging and surface mapping at Tung Chung, Lantau Island, Hong Kong.* Geotechnical Engineering Office, CED, HKSAR.

Geotechnical Engineering Office. 2004. *The Designated Area of Northshore Lantau.* GEO Technical Guidance Note No. 12 (TGN 12 – Revision A). Geotechnical Engineering Office, CEDD, HKSAR, p4.

Geotechnical Engineering Office. 2007. *Engineering Geological Practice in Hong Kong.* Publication No. 1/2007. Geotechnical Engineering Office, CEDD, HKSAR, p278.

Gillespie, M R, Humpage, A J & Ellison, R A. 1998. *The Geology of Tung Chung New Town*. Report by the British Geological Survey (BGS) for the Geotechnical Engineering Office, CED, HKSAR.

Fletcher, C.J.N., Wightman, N.R., & Goodwin, C.R. 2000. Karst - related deposits beneath Tung Chung New Town, Hong Kong: implications for deep foundations. *Proceedings of the Conf. on Engineering Geology HK 2000, 11 November 2000, Institution of Mining and Metallurgy, Hong Kong Branch*, pp139-149.

Fletcher, C.J.N. 2004. *Geology of Site Investigation Boreholes in Hong Kong.* Applied Geoscience Centre (DES HKU), Hong Kong Construction Association (SI Contractors Committee) and AGS (HK), p132.

Kirk, P.A., Brown, C. & Collar, F. 2000. Use of gravity surveys in preliminary and detailed site investigation at North Lantau. *Proceedings of 19th Annual Seminar, Geotechnical Division HKIE*, May 2000.

Kirk, P. A. 2000. Adverse ground conditions at Tung Chung New Town. In A. Page and J Reels (eds.) *The Urban Geology of Hong Kong*. Geological Society of Hong Kong, Bulletin No. 6.

Sewell, R.J., and Kirk, P.A. 2002. *Geology of Tung Chung and Northshore Lantau Island*. Hong Kong Geological Survey Sheet Report No. 6. Geotechnical Engineering Office, CED, HKSAR, p91.

Silva, S.D., Wightman, N. & Kamruzzaman, M. 2010. Geotechnical ground investigation of the Padma Main Bridge. *Proceedings of Bangladesh Geotechnical Conference 2010: Natural Hazards and Countermeasures in Geotechnical Engineering, ISSMGE, November 4-5, 2010, Dhaka, Bangladesh*, pp181-188.

Sze, J W C, Lam, A K M, Pappin, J W, & Chan, K M. 2007. Design and construction of shaft-grouted friction barrette in Tung Chung Designated Area. *Proc. of 27th Annual Seminar, Geot. Div. HKIE,* May 2000

Town Planning Board. 2012. *Tung Chung New Town Development Extension: Stage One Public Engagement*, TPB Paper No. 9111, HKSAR, p12.

Wightman, N R, Hitchcock, B K, Burbidge, H T, Frappin, P & Goodwin, C R. 2001. Advances in Site Investigation Practice for Deep Foundations, Tung Chung New Town, Lantau Island, Hong Kong. *Proceedings of the International Conference on Insitu Measurement of Soil Properties and Case Histories: IN-SITU 2001, 21 May 2001, Bali, Indonesia*, pp511-519.

Wightman, N.R. & Lai, A. 2006. Investigation and Foundation Design in Marble / Karst Designated Areas of Tung Chung and Ma On Shan. *Proceedings of the One Day Seminar in Hong Kong on Geotechnical Works in Karst in South-East Asia, 26 July 2006, HKIE*, pp109-140.

Foundation Design for a Residential Development in Adverse Ground Condition at Designated Area of Northshore Lantau

J.W.C. Sze & J.C.Y. Li
Ove Arup and Partners Hong Kong Limited
C.K. Lau
Sun Hung Kai Architects and Engineers Limited

ABSTRACT

A development site falls within the Designated Area of Northshore Lantau where is underlain by adverse ground condition characterized by extra-ordinary deep rockhead, weak in-situ soils and the presence of loose materials at great depth as revealed from the site specific ground investigation. Various conventional and non-conventional pile foundation options were studied, designed and approved to support the five blocks of high-rise residential buildings. The final adopted foundation scheme was around 500 nos. of conventional driven steel H-piles and around 1,700 nos. of small diameter large displacement steel tubular piles. While being uncommon in residential projects, the steel tubular piles proved to be a cost-effective and fast track foundation solution in the given ground conditions. This is a useful precedent case for the new developments within this Designated Area and other adverse geotechnical condition sites. The Paper discusses the development of the foundation scheme, the trial pile programme, observations during the driving process, Pile Driving Analyzer (PDA) tests, CAPWAP analyses and the performance of the as-constructed piles as revealed from the static load tests.

1 INTRODUCTION

The site is located at Tung Chung Town Lot No. 36 (TCTL36) which is bounded to the south by Ying Hei Road, to the north by the future promenade, to the east by TCTL37 (another residential development site) and to the west by a future road. The existing average ground level is around +5.5mPD. The dog-leg shaped site has an area of 25,400m^2 with a width about 80m, as shown in Figure 1. It is proposed to construct five 33-storey residential buildings, several low-rise houses and a retail complex sitting over a common one-level car-park basement structure, as shown in Figure 2.

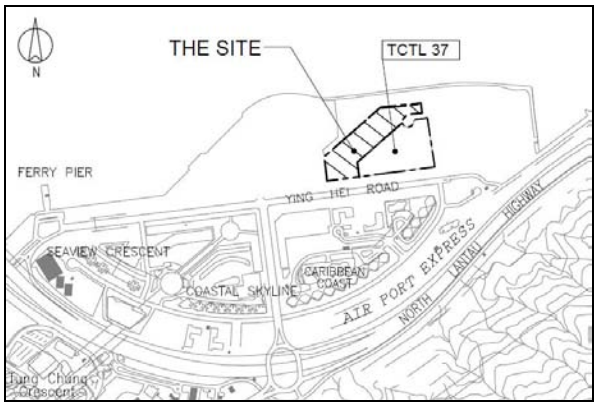

Figure 1: Site Location Plan

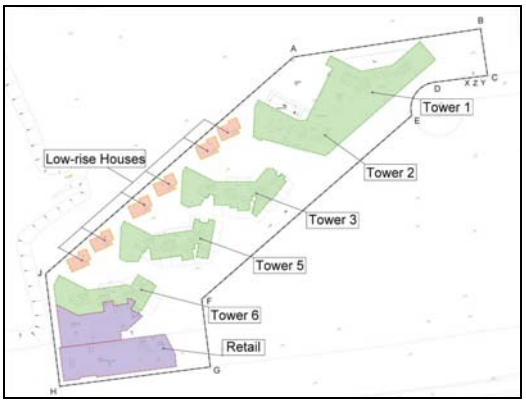

Figure 2: Proposed Building Plan

2 GROUND CONDITIONS

Fletcher (2004) summarised the complexity of the ground condition at the Northshore Lantau Island. The site was reclaimed by 2003 as part of the Phase 3A Tung Chung Development to the north of Ying Hei Road using conventional band drain and surcharging method. Based on the site specific staged ground investigation with several boreholes having continuous Standard Penetration Test (SPT) and Mazier sampling, the soil stratigraphy comprised fill, marine deposit, alluvium, decomposed rocks and granitic bedrock. The Fill has a thickness of 16 to 26m deep and generally comprises coarse to very coarse soils, from sand to cobble, occasionally boulder. Upto 9m thick marine deposit was revealed except at the southern and northern ends of the site in the proximity of seawalls for different phases of reclamation. The marine deposit is a slightly sandy clayey silt. The alluvial layer has a thickness of 15m to 22m and consists of interbedded silt and sand materials, and upto 6m thickness of gravel/cobble. These superficial deposits were underlain by unsorted in-situ weathered silty/sandy granite with feldsparphyric rhyolite dykes (diamict deposits) of variable thickness. All boreholes were terminated 5m into the granitic bedrock and the Grade III rockhead level ranged from -41mPD to -146mPD. A typical geological section in SW-NE direction is presented in Figure 3.

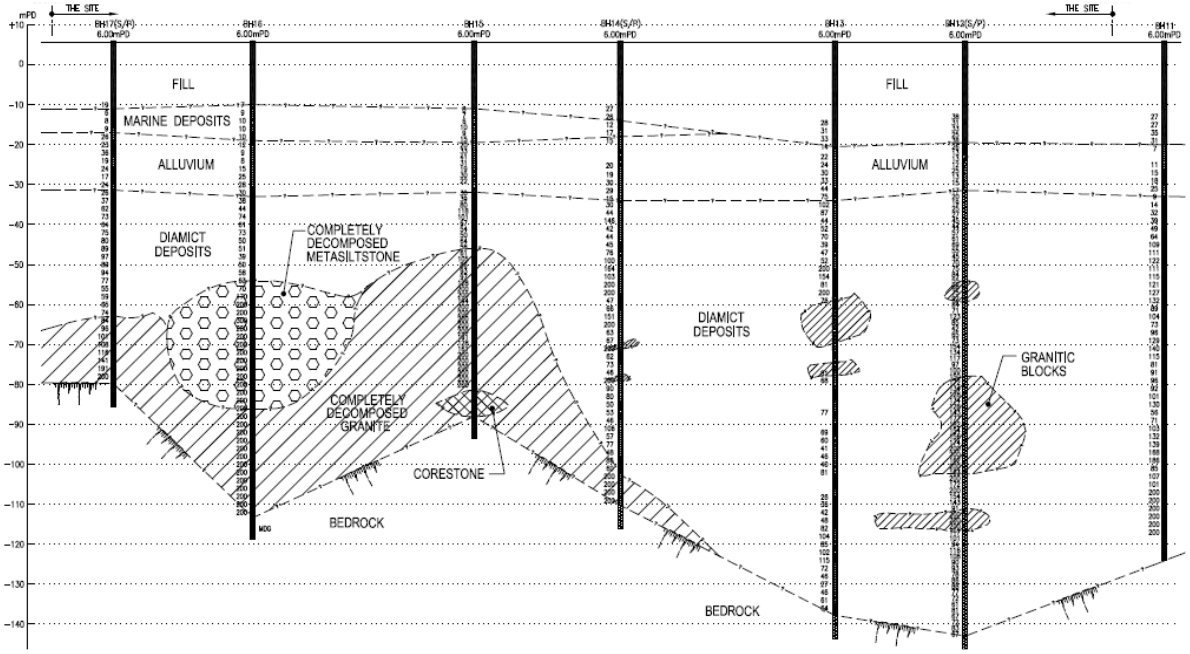

Figure 3: Typical Geological Section

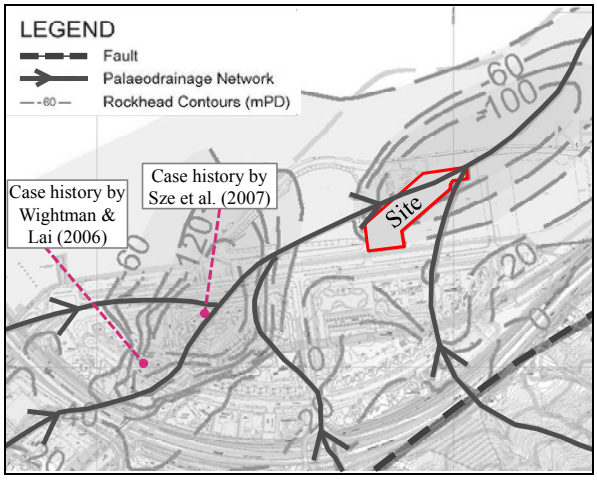

Figure 4: Site in related to Underground Palaeodrainage Network

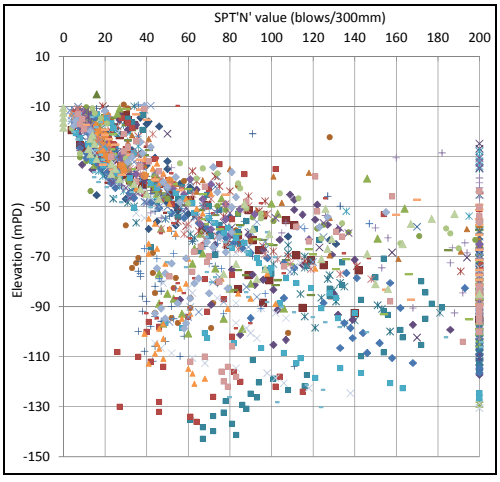

Figure 5: SPT'N' profile

The findings from the site specific boreholes generally tallied with the ground condition inferred by Sewell & Kirk (2002) which suggested that north-eastern portion of the site is likely to be affected by marble-related rocks and the inferred underground palaeodrainage network in related to carbonate rock. The relationship of the site and the inferred palaeodrainage network by Sewell & Kirk (2002) is shown in Figure 4. Solution of the carbonate rock occurred predominately in these underground water channels resulting in decomposition of the overlying granite and rendering in a collapsed structure above the previous caverns where the marble developed in places. This feature was revealed in some of the boreholes at where a reversal of SPT'N' profile was observed, as shown in Figure 5, in associated with a depressed rockhead level.

3 CONSIDERATIONS AND EVOLUATION OF FOUNDATION DESIGN

The complex ground condition at the Designated Area of Northshore Lantau inevitably posed great challenges to foundation designs. Wightman & Lai (2006) presented a case of adverse ground condition at a tower block within a development nearby which demanded the end-bearing bored pile scheme to be sunk to a maximum of 165m below ground. A trial 2.5m diameter bored pile using telescopic temporary casing method was constructed in late 1996/early 1997 down to 155m and concluded the option to be nonviable, and the tower was finally abandoned. Sze et al. (2007) also presented a case history of a successful use of unconventional shaft grouted barrettes in lieu of conforming ultra-long driven H-pile scheme in the vicinity, where weak soils were revealed and the rockhead was unidentified with boreholes sunk to -195mPD. Trial barrettes with static load test upto 45MN were required to demonstrate the adopted frictional parameters which took a substantial time to construct and test. Interestingly the TCTL36 site is situated along the same palaeodrainage line that runs underneath these two projects, as shown in Figure 4, and is facing similar adverse ground conditions.

3.1 Foundation Design at Southern Portion of the Site

At the southern portion of the site which occupies around 25% of the total footprint, the ground appeared to be "normal" and little affected by the marble xenolith. A normal increasing trend of SPT'N' value with depth was revealed with a rockhead level of -42mPD to -110mPD. Conventional large diameter end-bearing bored piles and driven steel H-piles were considered to be feasible. Driven steel H-piles of S450J0 305x305x223kg/m Universal Bearing Pile (UBP) section with an allowable capacity of 3,600kN were adopted in this area in view of the cost effectiveness and the potential ground risk in associated with end-bearing bored pile option.

3.2 Foundation Design at Northern Portion of the Site

Foundation design for the remaining 75% site footprint, where is severely affected by the marble xenolith, was far more challenging. Conventional end-bearing bored pile option was considered nonviable in view of the extraordinary deep rockhead, in excess of 150m below ground. Due to substantial thickness of weak soil, driven steel H-pile if adopted might also result in very long piles, in the order of 90m, even with a relaxed final set criterion. Verticality control of such long pile was another concern. The reversal of SPT'N' profile may also result in abrupt change of as-built pile lengths in the vicinity, which may subsequently affect the load distribution and differential settlement. This option was also considered not preferable.

Replacement piles such as friction bored pile and barrette were considered. Due to larger perimeter, shaft grouted barrette was considered to be more cost effective in terms of reduced pile length. A 2.8mx0.8m, 75m deep shaft grouted barrette should be able to provide an allowable capacity of 22,000kN. The use of this unconventional type of pile in similar ground conditions was also proven, see Sze et al. (2007). For this option raft cap/tie beam is required to transfer the column loads into the barrettes in order to minimise the total number of barrettes.

Given the substantial depth of weak deposit, large displacement piles were also considered since they have potential to terminate at much higher levels than steel H-piles and are able to address part of the concerns related to steel H-piles as mentioned above. The applicability of Precast Prestressed Concrete (PPC) Pile was reviewed but considered nonviable in view of its ability to sustain high impact forces (both compressive and tensile stresses) to terminate at great depth and overcome hard pans, potential obstructions in fill and alluvial layers, and available space for replacement piles in case of damage.

In view of the concerns over steel H-piles and PPC piles, a driven steel tubular pile scheme was developed. While driven steel tubular piles are common for offshore and near-shore structures such as piers or ports with

its advantage of having high lateral stiffness in resisting environmental loads in any directions, the use of tubular piles in residential developments by the local industry was uncommon. Grade S355J0 508mmOD 20mm thick steel tubular pile having an allowable capacity of 3,170kN was adopted. The tube is formed by bend-rolling of hot rolled steel plate into circular hollow section and joined by electrical resistance weld. The steel grade and thickness were chosen due to the manufacturing limitation. The estimated average pile length at the design stage was 64m. Given a steel weight of 241kg/m but difference in pile lengths, the tubular pile option in effect was able to provide the same gross capacity to steel H-pile scheme with 12% less steel weight.

Both shaft grouted barrette and steel tubular pile options were designed, submitted and approved. Steel tubular pile was subsequently chosen in view of the cost effectiveness, enhanced construction programme, plant availability and the workmanship of installing the tubular pile was envisaged to be easier to manage.

3.3 Adopted Foundation Scheme

The final adopted foundation scheme comprised 503 nos. of S450J0 305x305x223kg/m steel H-piles and 1,700 nos. of S355J0 508mmOD 20mm thick steel tubular piles. The working pile installation was carried out between October 2012 and March 2013. With the sensitive receivers such as the school located to the opposite side of Ying Hei Road, the noise permit stipulated 3 hours per working day for percussive works with a maximum 10 piling rigs. This gave an average production rate of around 1,000m/day. No compliant from the neighbours was received. An aerial view of the site during pile installation is shown in Plate 1.

Plate 1: Pile Installation in Progress (adjacent construction site in background)

4 OBSERVATIONS & DISCUSSIONS ON DRIVEN STEEL TUBULAR PILES

4.1 Close-ended Pile Detail

For an open-ended tubular pile, Paikowsky & Whitman (1990) pointed out that full plugging will be formed if the depth/diameter ratio exceeds 35 in dense sand. In that case, the resulting static capacity has no difference from a close-ended one. With the estimated pile depth in this site, this condition could easily be satisfied. Nevertheless, close-ended detail with crossed-blades, as shown in Plate 2, was adopted to protect the pile tip from potential damage when penetrating through the cobble rich fill and alluvial layers. It also allowed tape/dip meter measurements within the pile shaft to be conducted on every pile which gives a quick pile integrity check by measuring the pile length as well as the groundwater level within the shaft as a reflection of the condition of the welded joints. More interesting is that visual inspection over the entire internal shaft became possible by lowering a CCTV camera into the selected piles. No integrity issue was revealed from these tests.

Plate 2: Pile Shoe Detail

4.2 Trial Piles

In view of the variability of ground condition and large quantity of steel tubular piles required, a trial pile programme was initiated concurrent with finalisation of the building layout plan in mid 2012 to ascertain its drivability, pile response, quality control process, order of pile length when driven to set and pile performance. In this regard, three trial piles with static load test were assigned at three different locations over the site. Another four test piles were driven adjacent to one of the trial piles to study the potential influence from pitching piles in its vicinity and necessity for pre-boring. The trial pile programme confirmed the applicability of the scheme and the estimated tentative founding levels. It also provided useful reference for the contractors who were interested in bidding the working pile contract, who can appreciate the ground risk when entering into a lump sum foundation contract in this kind of ground condition.

4.3 Piles as Temporary Vertical Support

Without using a follower, the temporary pile cut-off levels were close to the existing ground which was lowered by 1m prior commencement of the piling works. Some piles were designed to support the permanent ground floor slab around the towers prior to the bulk excavation in order to eliminate the need of a temporary traffic deck and to enable a semi top-down construction of the basement under a fast track programme. These piles were then to be encased in reinforced concrete to form composite permanent columns.

Bending stiffness of the tubular pile is 1.7 and 5.2 times that of H-pile in major and minor axes respectively. Such high rigidity is advantageous in positioning and verticality control. A view of steel fixing for the composite column is shown in Plate 3.

Plate 3 : Steel Fixing for Column

4.4 Observed Range of C_p+C_q values

The recorded temporary compression of pile and soil, $C_p + C_q$, values of the tubular piles ranged from 39mm to 50mm. The normalised values of ($C_p + C_q$)/embedded pile length against pile length are shown in Figure 6. It can be seen that the values ranged from 0.6mm/m to 1.0mm/m. These are slightly lower than those of H-piles after considering the difference in pile driving stress. This may be due to the tubular piles have a shorter effective length due to a higher shaft friction as result of the large displacement nature.

The range of the observed $C_p + C_q$ values, accompanied by the observed pile capacity, formed a guideline on the desirable range as a site control to ensure sufficient hammer energy is adopted.

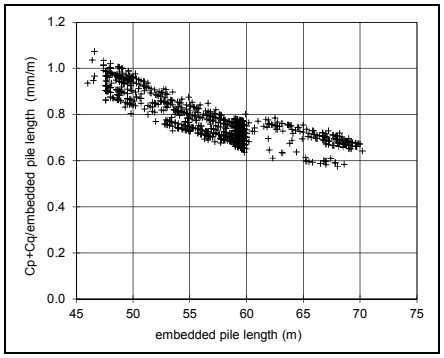

Figure 6 : Recorded $C_p + C_q$ ratio

4.5 Set-up Phenomenon and Quality Control

The tentative founding levels of the driven tubular piles were established based on a combination of SPT'N'≥ 80 contour and a minimum pile length estimated by the static equation of allowable frictional resistance equals to 1.5x'N' (kPa) and an allowable base resistance of 5MPa when driven to final set.

High degree of set-up phenomenon was observed during the driving process of these tubular piles in contrast to the H-piles within this site. A normalised hammer blowcount record from one of the trial tubular piles is plotted as Figure 7, which showed a significant increase in hammer blowcount after resuming pile pitching upon temporary ceases for pile extension and associated weld test. This raised a concern over early termination of these piles during installation of the working piles.

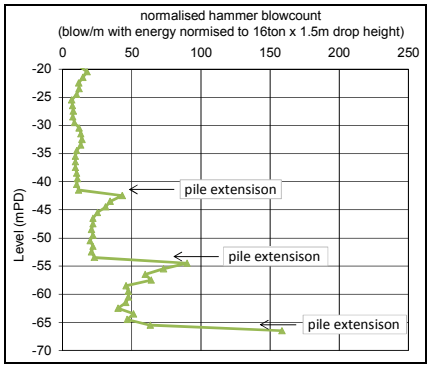

Figure 7 : Hammer Blowcounts

To avoid a "false set" of these piles and to ensure the robustness of the foundation system, the working piles were designed to satisfy the minimum length requirement as well as to achieve a final set of not more than 10 mm/10 blows. A total of 5% PDA tests were carried out on the tubular piles to monitor the driving stress and pile integrity. CAPWAP analyses were also carried out to infer the static pile capacity.

The average as-built pile length was found to be 59m which is 5m shorter than the tentative ones. 50 nos. of post-construction drillholes with SPT at 1.5m c/c were sunk to provide further confidence on the founding levels of these tubular piles being appropriate. Out of 1,700 working tubular piles, only two piles were found to be distorted due to the obstructions and were subsequently extracted for repair and re-drive.

4.6 Pile performance

Including trial piles, there were 25 nos. of static load tests carried out for the tubular piles. The measured pile head settlements at the peak test load of two times the pile capacity were found to be 30% to 50% of the allowable settlement corresponding to the Davisson Criterion. The residual settlements were found to be minimal. This has proven that the applied load was dissipated via shaft friction and minimal load was transferred to the pile base. This is somewhat consistent with the observation from over 90 nos. of CAPWAP results which revealed an average of 95% applied load being carried by the shaft during these re-strike tests. These observations implied that the ultimate capacity had not been fully mobilised.

Figure 8 shows a plot of the capacity ratio, which is defined as the activated static capacity from CAPWAP/required ultimate pile resistance Ru, versus the maximum pile driving stress. At 200MPa (0.6fy), the lower bound capacity ratio is 1.1 and increased linearly with the driving stress. This further affirmed the adopted final set criterion and hence the final pile lengths were erred on conservative side and had enhanced the robustness of the foundation system.

Given the differences in working stress and pile spacing between the tubular pile and H-pile options, the resulting pile stiffness of tubular piles is around 60% higher than that of H-pile option to support the same tower load. This helps to offset a portion of the foundation settlement due to thick and weak underlying soils.

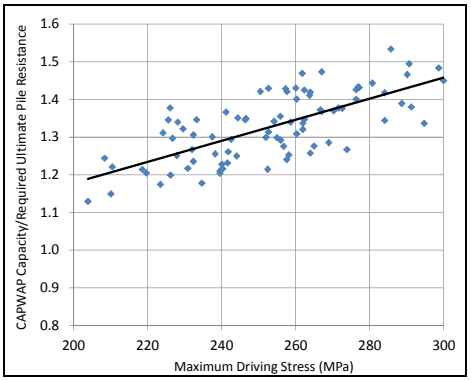

Figure 8 : Capacity Ratio vs Driving Stress

5 CONCLUSIONS

Unconventional S355J0 508mmOD 20mm thick steel tubular pile foundation was developed for the residential development where is underlain by adverse ground condition characterized by extra-ordinary deep rockhead, weak in-situ soils and the presence of loose materials at great depth.

The use of the steel tubular piles was proven to be a cost-effective and fast track foundation solution in the given ground condition. The quality control process and observations were discussed. This project could be a useful precedent case for the new developments in the vicinity within this Designated Area and other sites with similar adverse geotechnical condition.

REFERENCES

Fletcher, C.J.N. 2004. *Geology of Site investigation boreholes from Hong Kong*. 109-113.

Paikowsky, S. G., & Whitman, R. V. 1990. The effect of plugging on pile performance and design. *Canadian Geotechnical Journal*, Vol 27(4), 429-440.

Sewell, R.J. & Kirk, P.A. 2002. *Hong Kong Geological Survey Sheet Report No.6 - Geology of Tung Chung and Northshore Lantau Island*. Geotechnical Engineering Office, Civil Engineering Department, HKSAR

Sze J.W.C., Lam, A.K.M., Pappin, J.W. & Chan, K.M. 2007. Design and Construction of Shaft-Grouted Friction Barrette in Tung Chung Designated Area, Hong Kong. *Proc of Geotechnical Advancements in Hong Kong since 1970s*, *HKIE, Hong Kong*: 299-304.

Wightman, N.R. & Lai, A. 2006. Investigation and Foundation Design in Marble/karst Designated Areas of Tung Chung and Ma On Shan. *Proc of Seminar on Geotechnical Works in Karst in South-East Asia*, *HKIE, Hong Kong*: 106-139.

Design Principles for Soil Friction Pile Derived from Fundamental Theories & Field Data

H.Y. Wong
Geotech Eng Ltd, Hong Kong
C.Y. Kan, C.T. Wong & M.K. Leung
Architectural Services Department, Hong Kong

ABSTRACT

Traditional replacement non-percussion piles (e.g. pre-bored rock-socketted steel H-piles/ mini-piles, or large diameter bored piles) usually derive the resistance from end-bearing on hard stratum only. However, on some sites in Hong Kong (e.g. in Mid-Levels) sound bedrock can only be found at very deep level, and a cost effective solution is to adopt displacement or replacement piles relying on the shaft friction component ("friction piles"). In this paper, the fundamental theories governing the forces acting on the pile/soil system and the actual soil stress-strain relationship are firstly considered. In order to develop from fundamental theories the general principles for friction pile design, Architectural Services Department ("ArchSD") has been carrying out since the mid 1990s analyzing/loading tests on 12 nos. meticulously instrumented friction piles. With the loading and deformation at various depths measured for each loading stage, the relative shear displacement and axial load profiles can be established for each instrumented pile. These together with the SPT-N value (which is a measure of the shearing resistance that is available in the soil) can then establish at various depths the ratio of shearing strength to SPT-N value thus mobilized and finally a more workable friction pile design equation.

1 INTRODUCTION

Piles supporting foundations can be classified in accordance with the following two basic approaches:

Approach (1): To classify piles in accordance with construction method, i.e. either displacement piles, or replacement piles.
Approach (2): To classify piles in accordance with the design mode, i.e. either friction piles, or end-bearing piles.

However, the following points should be noted in the design of any of these pile types:

(1) some pile types can be a mixture of displacement and replacement piles. In the same manner, some of them can be a mixture of friction and end-bearing piles; and
(2) a friction pile can be installed by either the displacement or the replacement method or by a combination of both. The same applies to end-bearing piles.

The design of end bearing piles in Hong Kong is relatively simple as in most cases these will be bearing on intact rock. On the other hand, the design of friction piles will be much more involved as these will not only be affected by the soil properties, the ground and groundwater conditions as well as the construction method, in particular the latter (Brown *et al* 2007). The purpose of this paper is therefore to propose a rational method of designing friction piles by firstly going through the fundamental soil mechanics theories. This is followed by processing the data of a series of well planned and meticulously executed field works carried out in ArchSD since the mid 1990s. These comprise analyzing/loading tests on 12 nos. of fully instrumented piles.

2 FRICTION AT PILE AND SOIL INTERFACE

2.1 Fundamental soil mechanics theories

Consider, as in Figure 1a, the forces acting on the pile/soil interface and the immediately adjacent elementary volume of soil. Adopt the fundamental theories to forces operating in this system:

$$\tau_s = c_a + \sigma_h \tan\delta \quad (1a)$$

$$\sigma_h = K\sigma_v' \quad (1b)$$

where c_a= adhesion between pile/soil interface, τ_s= frictional shear stress acting along the vertical pile/soil interface, σ_h= horizontal earth stress acting on the vertical pile/soil interface, δ= friction angle at pile/soil interface or friction angle of soil immediately adjacent to pile/soil interface (whichever is smaller), K= horizontal earth pressure coefficient, and σ_v'= effective vertical soil stress immediately adjacent to pile/soil interface.

c_a will be ignored, as its value will be considerably reduced during pile installation, and hence its effect on the results of the back analysis and proposed design equation will be quite minimal. With this conservative assumption, combining Eqs (1a) & (1b) will yield:

$$\tau_s = K\sigma_v' \tan\delta \quad (2)$$

Integrating Eq (2) with respect to the depth z along the complete pile/soil interface will then yield

$$P_f = \int_0^H \tau_s \pi D dz = \pi D \int_0^H K\sigma_v' \tan\delta \, dz \quad (3)$$

where P_f= total soil frictional resistance acting over the pile/soil interface, D= pile nominal diameter (assuming to be constant along the whole length), and H = total pile length.

It can be seen from Eq (3) that P_f depends on three soil/site parameters, namely, K, σ_v' and δ, as well as their variation with depth z, in particular δ.

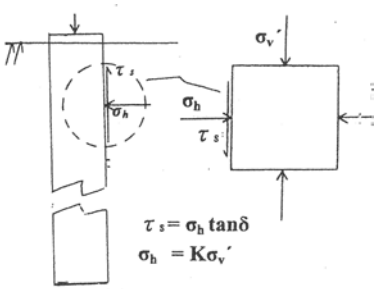

(a) Forces acting on pile/soil system

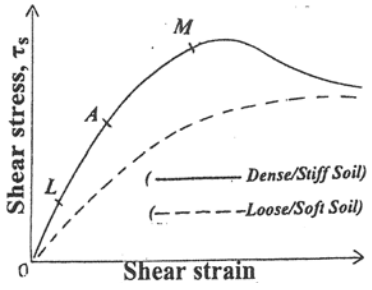

(b) Typical soil stress-strain curves

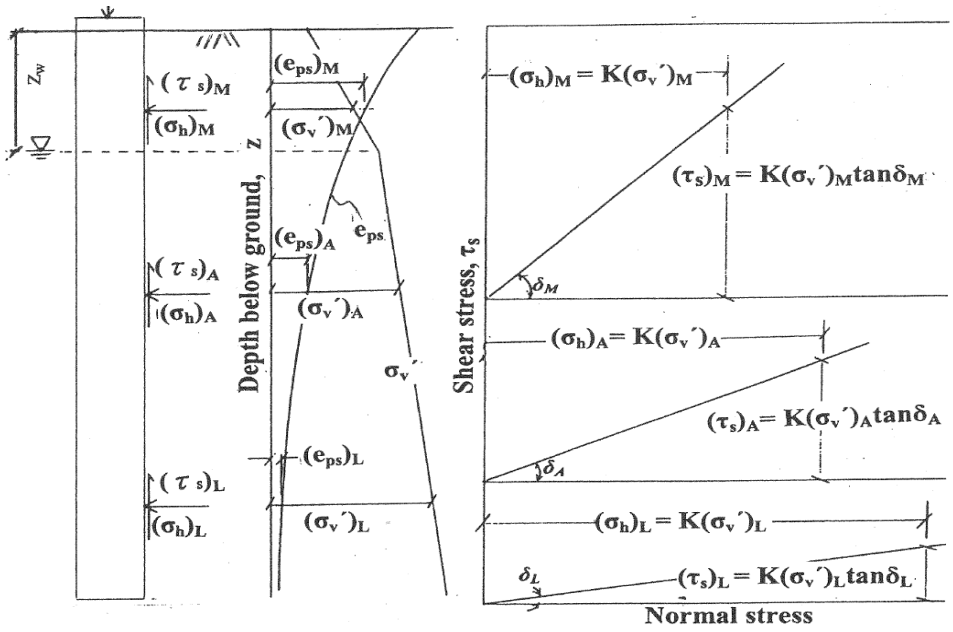

(c) Mobilization of friction vs shear displacement at pile/soil interface at various depths

(d) Variation of shear stress with normal stress at pile/soil interface at various depths

Figure 1: Basic stress and stress-strain relationship in soil and at pile/soil interface

2.2 Effect of horizontal earth pressure coefficient (K)

K depends pre-dominantly on construction method and is also the most variable when moving from one site to another with different pile construction methods (Kulhawy and Mayne 1990; Rollins *et al* 2005; Kulhawy and Chen 2007). This can easily change by several times to even more than 10 times. For a normally consolidated soil before pile construction, K can be considered to equal to K_o so that the following conventional equation $K_o = (1 - \sin\phi)$ can be assumed to be valid, where ϕ= effective internal soil friction angle. K_o can therefore vary from 0.577 to 0.357 for ϕ varying from a loose soil with a value of 25^o to a fairly dense soil with a value of 40^o. For an over-consolidated soil K_o can be in excess of 1.0. For a vertical pile embedded in soil, K will be lowest in the replacement piles and highest in displacement pile (O'Neill 2001). The lowest limit must be the installation of bored piles, with either bentonite slurry support or just no lateral support at all. Under such conditions, it is possible for K dropping to lower than K_a. On the other hand, for displacement piles, K will certainly be increased to larger than K_o, with the corresponding maximum K_p being the upper bound. As can be expected, K will increase with the increase in the amount of outward soil displacement during pile construction (Kan *et al* 2013).

2.3 Effect of effective vertical soil stress (σ_v')

In general at any depth below the groundwater table σ_v' is given by:

$$\sigma_v' = q + \gamma z_w + (\gamma - \gamma_w)(z - z_w) \quad (4a)$$

where q= surcharge at ground surface, γ= soil bulk density, γ_w= density of water, and z_w= depth of groundwater table.

For depth above ground water table,

$$\sigma_v' = q + \gamma z \quad (4b)$$

Eqts (4a) and (4b) indicate that: (1) the surcharge (q) is normally small, in the order of 5 to 10 kPa; (2) the soil bulk density (γ) does not vary too much in moving from site to site; (3) the density of water (γ_w) is a material constant; and (4) the only parameter that can vary more considerably from site to site is the depth of groundwater table (z_w). In the extreme case, z_w can be lowest along sloping ground with z_w being quite near to rock head. On the other hand, on reclaimed areas, z_w will be only a few metres below ground surface. These two extreme cases can be best illustrated in the following example, with length of pile equal to 30m, γ = 19 kN/m^3, z_w= 4 m in Site A and 30 m in Site B. Even in these extreme cases with z_w from 4 to 30m, σ_v' in Site A varies from 76 to 310 kPa whilst σ_v' in Site B only from 76 to 570 kPa.

2.4 Effect of friction angle (δ)

δ is a parameter that usually has not been properly defined or over-simplified in most design works. Very often, this is taken as friction angle at pile/soil interface or friction angle of soil immediately adjacent to pile/soil interface, whichever is smaller. Figure 1b shows a typical stress strain relationship for both a dense sand (or stiff clay) as well as for a loose sand (or soft clay) based on extensive actual test works (Taylor 1948; Terzaghi and Peck 1967). It shows that the frictional shear stress (τ_s) at the pile/soil interface is a function of the shear displacement (e_{ps}). In general τ_s will increase with the increase in e_{ps} (Figures 1c & 1d). However, this is not a linear increase as soil is not a linear elastic material (Frizzi and Meyer 2000; Misra and Chen 2004).

2.5 Summary

The above paragraphs discuss the individual effect of each of these three parameters. Nevertheless, what is more important is the combined effect in the form of $K\sigma_v' \tan\delta$ at various depths in a particular site. For a given site, K should remain more or less the same at various depths as there is normally no change in the construction method. σ_v' will increase with depth but the rate of increase will depend on the depth of the groundwater table. Nevertheless, the general trend is for $K\sigma_v'$ to increase with depth. Figure 1c shows that while $K\sigma_v'$ increases with depth, $\tan\delta$ decreases with the decrease in shearing displacement, which will in turn decrease with depth. Thus, the overall picture for the term $K\sigma_v' \tan\delta$ can be illustrated in a more quantitative manner in Figure 1d, with the plotting of the shearing stress (τ_s) versus normal stress ($K\sigma_v'$) carried out at the upper part, middle part and the bottom part as indicated in Figures 1c & d. There is a general trend of $K\sigma_v'$ being lowest and $\tan\delta$ highest at the upper part and this trend is reversed in moving to the bottom part. The resulting effect that the mobilized shear resistance decreases with depth can be observed in actual pile test results as indicated in Figure 3.

3 CURRENT METHODS OF DESIGNING FRICTION PILES AND THEIR LIMITATIONS

For some inexperienced designers, friction pile design in soil can be based simplest on Eq (3) with δ taken as soil friction angle determined from triaxial or shear box test and K equal to K_o. Alternatively, there is α(total stress) method for over-consolidated clay with $\tau_s = \alpha c_u$, where c_u= undrained cohesion (Tomlinson 1971). In Hong Kong, two other methods are commonly adopted, namely, β (effective stress) method and N-value method. β method is to evaluate at various depths the β value which is equal to $K\tan\delta$. There are again two approaches to evaluate this β value (Brown *et al* 2007). The first one is the depth-dependent β method by developing from field load tests its variation with depth. The second one is a more fundamental approach by evaluating in terms of K and δ. As for N-value method, this is just to correlate the SPT-N value directly to the shaft friction and is more commonly adopted in Hong Kong as the SPT-N values are readily available in nearly every project. However, though the SPT-N value is a measure of the shearing resistance available at various depths, this does not represent the shearing resistance that can be mobilized.

The above review of the fundamental theories governing the stress-strain relationship at the pile/soil interface at various depths shows that the soil friction in pile is controlled by the following three major factors: (1) pile construction method, (2) shear displacement along pile/soil interface at various depths, and (3) soil properties. As a result, there are two major short-comings of the above two methods. Firstly, as K can change very drastically with change in construction method, the variation of β with depth by most empirical equations cannot reflect this change. Neither can this be accounted for even if K is considered separately. Secondly, δ at various depths is not a constant even for the same type of soil because this depends on the

relative pile/soil displacement. This change in δ with depth can be in a way accounted for by the depth-dependent β method, but not by the N-value method as the SPT-N value will in general increase with increasing depth.

4 FIELD MEASUREMENTS

4.1 Instrumentation

In order to develop a simple and workable design equation for friction piles in soil especially including the effect of the pile construction method on the K value and the variation of tanδ with depth for each construction method, ArchSD has been carrying out loading tests on a number of meticulously instrumented friction piles (nominal diameter 300-600 mm or more) with different construction methods since the mid 1990s. Among these piles, at least four different construction methods have been adopted. The typical details of these piles are as summarised in Table 1, and the geology and soil strata of various sites (together with the SPT-N values versus depths) are summarised in Table 2.

Table 1: Typical details of instrumented friction piles studied by Arch SD

Site No.	Pile No	Site Location	Pile Type	Construction method	Nom D (mm)	L (m)	Max Load (kN)	Corr Sett (mm)	(2)E_{com} (MPa)	Strain Gauge	ζ (see Section 4)
1	1/1	Yuen	(1)CFA or	Boring with a		25	2922	6.28	27700	@3to	13.58
	1/2	Long	PIP	CFA to the		25	2922	6.50	27700	4m int.	13.58
			(Pakt-In-	required						from	
2	2/1	Tung	Place)	depth, and		38	5360	6.00	34750	2m	11.72
	2/2	Chung	piles	cement mortar		38	5540	4.78	34750	depth	11.72
				to be pumped							
3	3/1	Ma On		through the	610	45	4400	9.22	30050		9.70
	3/2	Shan		auger tip		45	4600	12.35	30050		9.70
		Area 90		under pressure							
				during lifting.							
4	4/1	Ma On				45	5400	10.13	31000		14.76
	4/2	Shan				45	5200	12.69	31000		14.76
		Area 100									
5	5/1	Kowloon	Bored	Barette type	2800	40	5430	9.35	27500	@2 to	2.52
		Bay	piles	pile supported	× 800					4m int.	
				by bentonite,						from	
6	6/1	Yeung		and RCD	1200	50	5400	21.90	27500	2m	1.89
		Long		method						depth	
				supported by							
				bentonite							
7	7/1	Mid-	Friction	Steel section		49	2600	7.43	50660	@5m	22.76
	7/2	Levels	minipiles	inserted into		49	2600	8.52	50660	int.	22.76
			with	pre-bored						from	
			shaft	hole; cement	305					1m	
			grouted	grout injected;						depth	
				tube-a-							
				manchette							
				post-grouting							

Notes : 1. Ordinary PIP piles with reinforcement cage of depth of 24m were used in Site No. 1, and PIP piles reinforced by a H-pile (305×305x149kg/m with length 24 to36m) were used for Site Nos. 2 to 4.
2. All friction minipiles were inserted with a built-up H-section in Site No. 7 for the whole length of pile.
3. E_{com} = elastic modulus of the combined section of sand/cement mortar (or concrete) and steel reinforcement/section.

Table 2: Geology and soil strata in each site studied

Site No.	Site Location	Geology	Soil strata	Average SPT-N value at depth (m)											Rock head level
				0 - 4	4 - 8	8 - 12	12 - 16	16 - 20	20 - 24	24 - 28	28 - 32	32 - 36	36 - 40	40 - 44	
1	Yuen Long	Marble area	Fill Alluvium Weathered soil	12	16	27	31	29	26	29	32	45	43	42	Sound rock at fairly great depth, normally over 50 – 60m to a max. over 100m
2	Tung Chung	Marble area	Fill Alluvium Weathered soil	19	17	21	38	40	29	30	29	34	36	40	
3	Ma On Shan Area 90	Marble area	Fill Marine deposit Alluvium Weathered soil	21	23	16	12	14	24	36	47	32	31	34	
4	Ma On Shan Area 100	Marble area	Fill Marine deposit Alluvium Weathered soil	13	10	17	16	12	25	34	43	41	39	42	
5	Kowloon Bay	Granitic area	Fill Marine deposit Alluvium Weathered soil	3	14	13	13	5	12	29	35	88	35	38	
6	Yeung Long	Volcanic area	Fill Alluvium Weathered soil	19	21	8	9	12	14	44	34	28	31	36	
7	Mid-Levels	Granitic area	Fill Alluvium Weathered soil	6	27	28	28	26	25	35	36	36	42	52	

For each of the two piles in Site Nos 1, 2, 3 and 4, strain gauges were installed along both sides of the web of the steel H-pile at about 3-4 m intervals. For Site Nos 5 & 6, strain gauges were installed on the reinforcement cage at about 2-4 m intervals (Wong 2003). The construction method in these two sites were quite similar as the end condition of the bored pile wall before concreting was the same, both being supported by bentonite slurry. For Site No 7, vibrating wire strain gauges were installed along the piles at 10 levels with two gauges at each level. The interval between each level was 5 m and started at 1 m depth (Kan *et al* 2013). In each fully instrumented pile, the axial force and deformation at various depths were measured at various load increments during loading tests, and these were then processed with SPT-N values measured before pile installation. With the axial pile force thus measured, the elastic pile shortening and hence the shear displacement at the pile/soil interface at each depth can be evaluated. The shearing resistance between successive depths can also be estimated from the corresponding difference in axial force. Accordingly, the shearing resistance/displacement relationship at various depths can be established.

4.2 Results

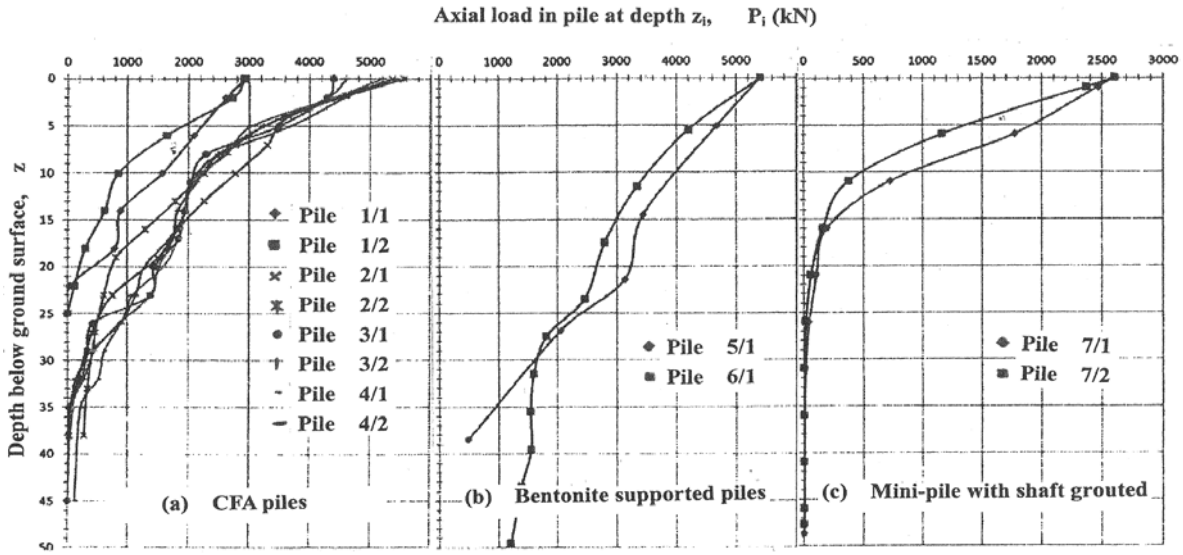

Figure 2: Axial load profile in piles with various construction methods

For each instrumented pile, the field test results comprise two major parts:

(1) settlement at pile top at various loading stages, which is basically the compliance test for a lot of piling works, and will yield the load-settlement curve for various loading stages; and
(2) readings of the strain gauges at each load stage of the pile load test as carried out in (1) above, which will yield the axial pile load at each instrumentation depth.

From the above results, the distribution of axial pile load at various depths is as shown in Figures 2a, b & c. Moreover, with a knowledge of the elastic modulus value of the pile materials, the corresponding shear displacement of the pile relative to the surrounding soil at this depth can also be deduced.

4.3 Analysis

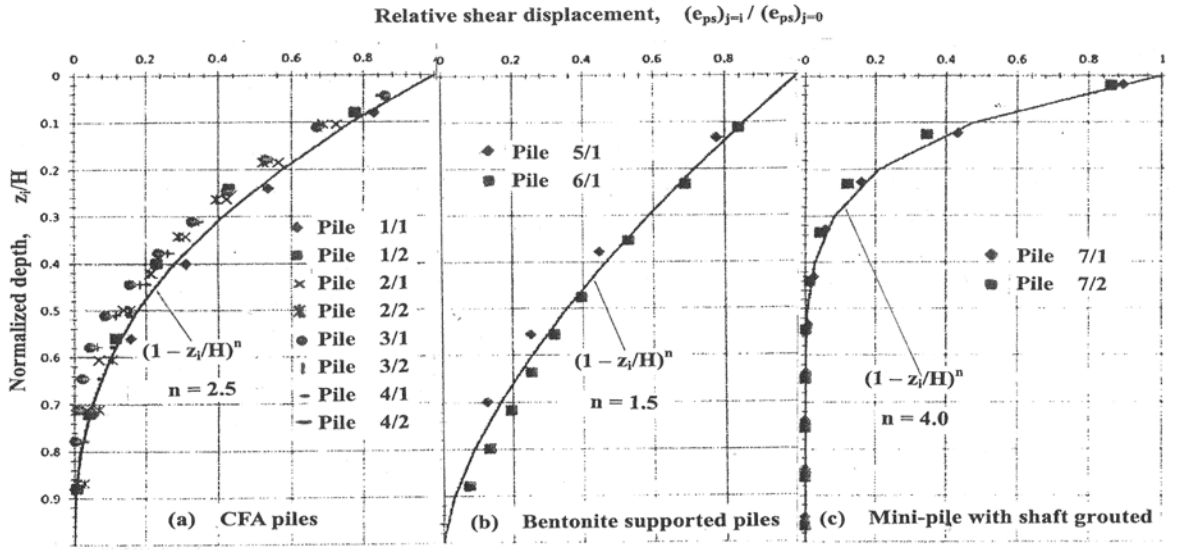

Figure 3: Normalized plot of relative shearing displacement for piles with various construction methods

Figures 3a, b & c are normalized plots with the ratio of the shearing displacement relative to the total at the pile top against z_i/H together with the trend lines. From Figures 2a, b & c and Figures 3a, b & c, the following can be observed:

(1) Both the shearing resistance and shearing displacement decrease with depth. This is in line with the fundamental soil mechanics theories as presented in Figure 1b that the lower the shearing displacement, the lower the shearing resistance.
(2) A very special feature of the normalized plot in Figures 3a, b, & c is that for piles constructed by the same method, all the plotted results will practically converge to the same curve. From these figures with $(e_{ps})_{j=i} = \sum_{j=\eta}^{i} \Delta(e_{ps})_j$, the following general equation appears to be valid:

$$(e_{ps})_{j=i} / (e_{ps})_{j=0} = (1 - z_i/H)^n \quad (5)$$

In the above equation, j is an integer varying from i to η, $z_\eta = H$, and n is a constant for a given method of pile construction. This means that $(e_{ps})_{j=i}$ is the total shear displacement between depth z_i and depth z_η. Accordingly, $(e_{ps})_{j=0}$ is the total shear displacement between depth z_0 and depth z_η (i.e. total shear displacement at pile top).
(3) For CFA piles in Figure 3a, n = 2.5,

$$\text{i.e. } (e_{ps})_{j=i} / (e_{ps})_{j=0} = (1 - z_i/H)^{2.5}. \quad (5a)$$

For bored piles supported by bentonite in Figure 3b, n=1.5,

$$\text{i.e. } (e_{ps})_{j=i} / (e_{ps})_{j=0} = (1 - z_i/H)^{1.5}. \quad (5b)$$

For mini-pile with shaft grouted in Figure 3c, n = 4,

$$\text{i.e. } (e_{ps})_{j=i} / (e_{ps})_{j=0} = (1 - z_i/H)^{4.0}. \quad (5c)$$

(4) In all cases, the decrease of $(e_{ps})_{j=i}/(e_{ps})_{j=0}$ with z_i/H is fairly rapid.

5 PROPOSED DESIGN METHOD

It has been well established that SPT-N value is a measure of the available shearing resistance in soil. Referring to basic soil stress-strain principles, this corresponds approximately to Point M of the stress-strain curve as in Figure 1b. However, in dealing with friction pile design in soil, the following have not been well established:

(1) the proportion of the shearing resistance that can be mobilized at various depths: Theses correspond to any points along the stress-strain curve OLAM in Figure 1b. From Eq (5), the following general equation appears to be valid for a pile at depth, z_i with total depth H:

$$(N_i)_{mobilized} = (N_i)_{measured} \times (e_{ps})_{j=i} / (e_{ps})_{j=0} \quad (6a)$$

where $(N_i)_{mobilized}$= proportion of shearing resistance that can be mobilized at depth z_i, and $(N_i)_{measured}$= SPT-N value measured at depth z_i.

Substituting Eq (5) into Eq (6a), the following equation can be obtained:

$$(N_i)_{moblized} = (N_i)_{measured} \times (1 - z_i/H)^n \quad (6b)$$

(2) the relationship between shearing strength and the $N_{mobilized}$ value: Denote this ratio by the parameter ζ.

With such results, for a pile with total depth of H having its SPT-N value measured at various depths z_i the maximum load P_{max} that can be developed will be given by the following equation:

$$P_{max} = \sum_{i=0}^{n} \zeta \times (N_{i+½})_{measured} \times (1 - z_{i+½}/H)^n \times (z_{i+1} - z_i)\pi D \quad (7)$$

6 CONCLUSIONS

With the N-value measured at various depths at or near the proposed pile location, the maximum pile capacity P_{max} can be estimated from Eq (7), provided that the two newly introduced parameters, namely n and ζ, are known. Both n and ζ have been found in this paper to be essentially the same for piles with the same construction method. To determine n, reference can be made to Figures 3a, b & c. The n value that will yield the best fitted curve $(1–z_i/H)^n$ to the test points is the required n. With n thus determined and the axial pile load at various depths measured, ζ can be evaluated from Eq (7). In case that no loading test results are available, ζ may be obtained from Table 1 for the corresponding construction methods. In either case in order to verify the design assumptions and parameters, loading test on a trial pile is recommended prior to the installation works. The purposes of the loading test on a trial pile are to establish and/or verify installation means and methods of construction, and to verify the design parameters and hence the load carrying capacity of the pile. One vital point is to note that the present proposed design method is based on the average SPT-N values of each site. It follows that its variation for site with particular soil type, stress history, pile size and pile construction method cannot be fully differentiated. More instrumented pile load tests are also recommended to be carried out with well defined drillhole with SPT-N values at the proposed pile location to verify the proposed design method.

ACKNOWLEDGEMENTS

The authors would like to record their thanks to the Director of Architectural Services, Hong Kong SAR Government for his kind permission in publishing this paper.

REFERENCES

Brown, D.A., Dapp, S.D., Thompson, W.R. and Lazarte, C.A. 2007. *Design and Construction of Continuous Flight Auger (CFA) Piles*. Federal Highway Administration, Washington DC.

Frizzi, R.P. and Meyer, M.E. 2000. Augercast Piles: South Florida Experience. In R.Y.S. Pak & J. Yamamura (ed), *Proceedings of Sessions of Geo-Denver 2000, 5-8 August 2000, Denver, Colorado*. American Society of Civil Engineers, Reston, VA, 382-96.

Kan, C.Y., Wong, C.T. and Leung, M.K. 2013. Relationship of friction and shear displacement along the depth of shaft-grouted mini-piles. *HKIE Transactions*, 20(4): 206-213.

Kulhawy, F.H. and Chen, J.R. 2007. Discussion of Drilled Shaft Side Friction in Gravelly Soils. *Journal of Geotechnical and Geoenvironmental Engineering*, 133(10): 1325-1328.

Kulhawy, F.H. and Mayne, P.W. 1990. *Manual on Estimating Soil Properties for Foundation Design*. Electric Power Research Institute, Palo Alto, CA.

Misra, A., Chen, C.H., Oberoi, R. and Kleiber, A. 2004. Simplified Analysis Method for Micropile Pullout Behaviour. *Journal of Geotechnical and Geoenvironmental Engineering*, 130(10): 1024-1033.

O'Neill, M.W. 2001. Side Resistance in Piles and Drilled Shafts. *Journal of Geotechnical and Geoenvironmental Engineering*, 127(1): 3–16.

Rollins, K.M., Clayton, R.J., Mikesell, R.C. and Blaise, B.C. 2005. Drilled Shaft Side Friction in Gravelly Soils. *Journal of Geotechnical and Geoenvironmental Engineering*, 131(8): 987–1003.

Taylor, D.W. 1948. *Fundamentals of Soil Mechanics*. John Wiley and Sons, New York.

Terzaghi, K. and Peck, R. B. 1967. *Soil Mechanics in Engineering Practice*, 2nd edition. John Wiley and Sons, New York.

Tomlinson, M.J. 1971. Some Effects of Pile Driving on Skin Friction. In *Proceedings of Conference on Behaviour of Piles*, 107–114.

Wong, H.Y. 2003. Design and construction of soil friction bored piles in Hong Kong, with particular reference to marble areas. *Presented at the Hong Kong Institution of Engineers Annual Seminar on Case Histories in Geotechnical Engineering in Hong Kong, 9 May 2003, Hong Kong.*

Geotechnical Design at Tseung Kwan O Reclamation Development

S.L. Chiu, Vic Pun & P.H. Lam
AECOM, Hong Kong

ABSTRACT

In recent years, Tseung Kwan O (TKO) reclamation area has been a hot spot for the blooming of building industry, particularly in land parcels nearby the Tseung Kwan O MTRC Station where a good number of private developers have bided lands for residential developments. At the time of this paper, the authors were handling over 10 different residential developments under various development stages from the site investigation planning stage to superstructure construction stage in the area. Due to the historical background of the reclamation area and other site specific constraints imposed by different existing infrastructures within TKO, the project developments faced complicated problems of soil-structure interactions that required design engineers to carry out sophisticated FEM analysis to deal with in the course of ELS and foundation designs.

The design parameters in particular the elastic modulus of soils and geological profile that were in need for the ELS and foundation designs had to be acquired through ground investigation (GI) at the very beginning of the projects. Some good quality data were obtained from the GI of the developments undertaken by the authors. This paper shares information about the geotechnical and geological aspects in this part of TKO area that has not been published before.

1 SITE DESCRIPTION AND CHARACTERISTICS

The Chief Executive presented his Policy Address 2013 casting the focus with a great concern on housing supply where a great demand of land supply is in desperate need for both short and long term solutions of housing problems.

The recent blooming of the building construction industry and the elite location of the Tseung Kwan O (TKO) reclamation area nearby the Tseung Kwan O MTRC Station attracted a number of private developers to acquire lands from the government. At one time, the authors were handling over 10 different residential developments under various construction stages from the site investigation planning stage to superstructure construction stage in the area at the end of year 2013. The rapid growth of building developments led to construction sites standing close to one another, resulting in construction activities that were influenced each other sometimes. Besides, the construction activities were required to be carried out in due care so that they would not affect the existing infrastructures and municipal utilities in the vicinity of the development sites. Therefore sophisticated FEM analyses were required to deal with the complicated designs of ELS and foundation as well as interfacing problems of the developments and the surroundings.

The authors were involved in several residential developments in this area. The locations of the sites are shown in Figure 1.

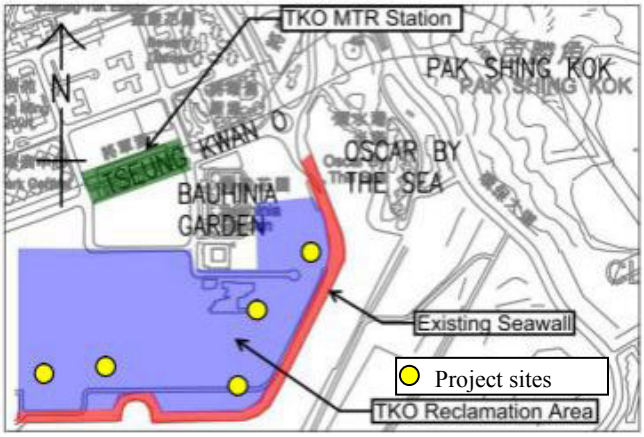

Figure 1: Site location plan

2 BACKGROUND INFORMATION AND DESK STUDY

2.1 Reclamation history

The sites where most of the development projects were carried out were situated in a piece of reclamation at Junk Bay. The reclamation and associated construction of the seawall as shown below in Figure 2 were carried out under two different contracts by the then Territory Development Department, namely Contract no. TK34/91 and TK36/93. During the construction of seawall, soft marine clay was dredged and underwater fill material type I was laid onto the alluvium layer to form the foundation for the seawall. The core of seawall was made of Grade 400 rock fill. The seawall surface was sloping 1:1.75 at the front face and inclined at a gradient of 1:1.5 at the back. The surface was protected with various sizes of rock armour. Geotextile was placed on the sloping back surface of the seawall with a layer of rockfill Grade 400 or Grade 200 on it. The geotextile was extended to the entire undredged seabed. As revealed from the drawings, general fill material was adopted as reclamation fill. The seawalls were completed in about 1997 and reclamation was completed in 1999.

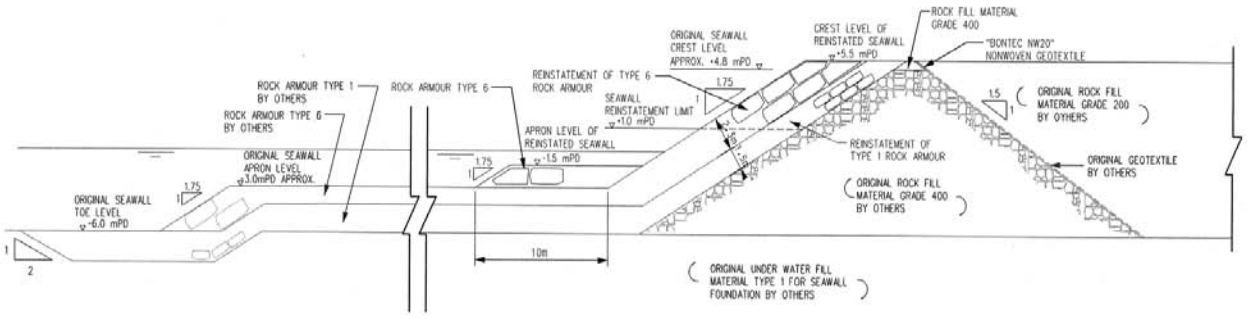

Figure 2: Typical Section of Seawall

2.2 Aerial photos interpretation (API)

The aerial photos showing the reclamation history is shown in Figure 3. From the aerial photos, the reclamation of this area was divided into two stages. The eastern portion of the seawall was constructed in 1995 and reclamation was completed in 1997, while the western portion of the seawall was completed in 1997 and reclamation was completed in 1999.

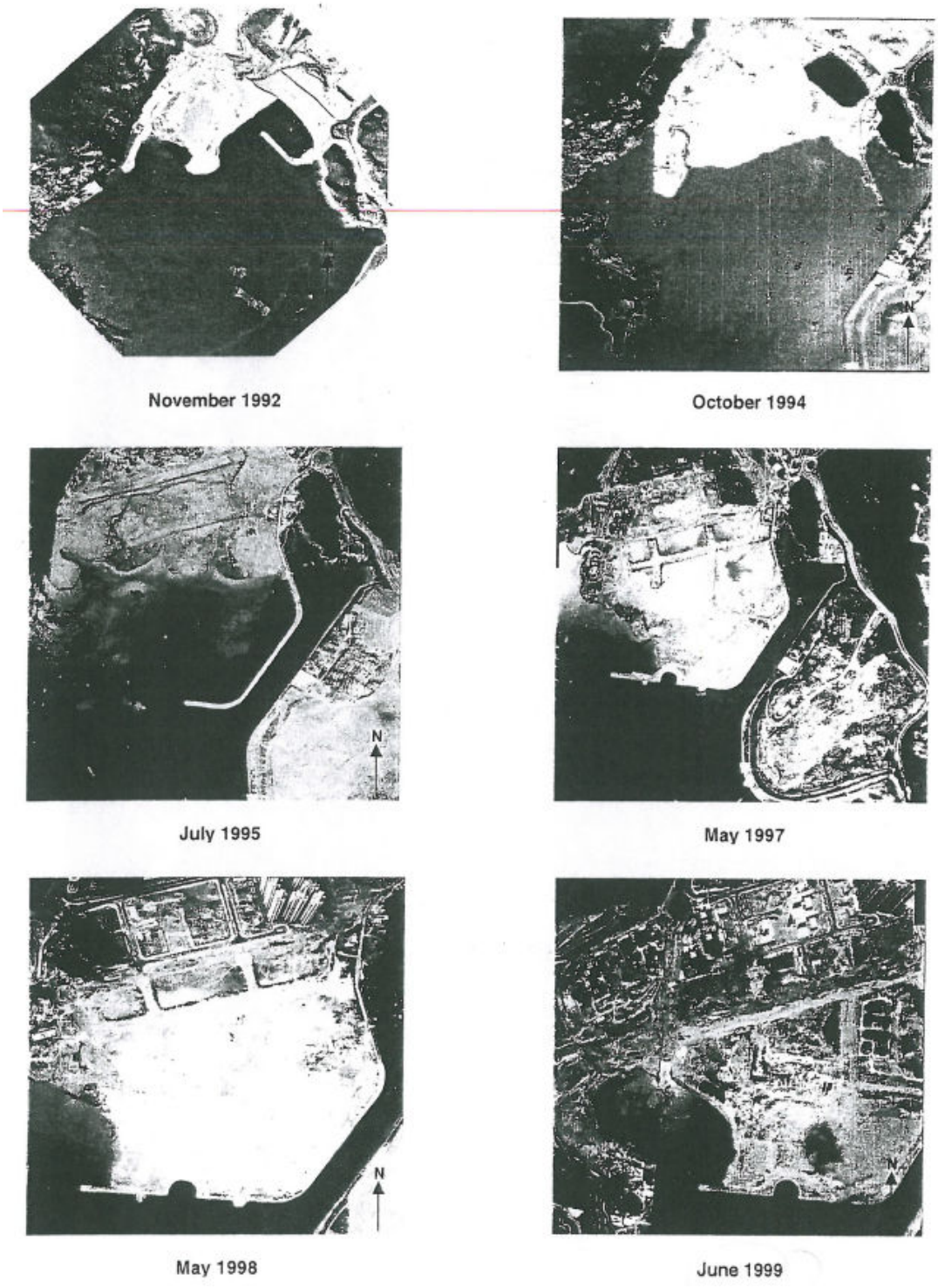

Figure 3: Aerial photos showing the reclamation history

3 SITE INVESTIGATION

According to the site investigation results, the general geology of the development sites in the reclamation area is fill layer that comprises cobbles and gravels on the top, overlying marine clay layer with occasional marine sand lenses, followed by sandwiched layers of alluvium clay and sand. Completely decomposed and highly decomposed tuff could be seen underlying the alluvial materials above bedrock which was encountered at various depths of 30m to over 60m below ground. A typical ground profile across the area is given in Figure 4.

Sand fill could be found adjacent to the existing seawall, extending deep down to depths of approximately 30m below existing ground where no marine deposits could be seen at boreholes in the vicinity of the seawall. Perhaps the marine deposits had been dredged and replaced by sand fill during the construction of the seawall.

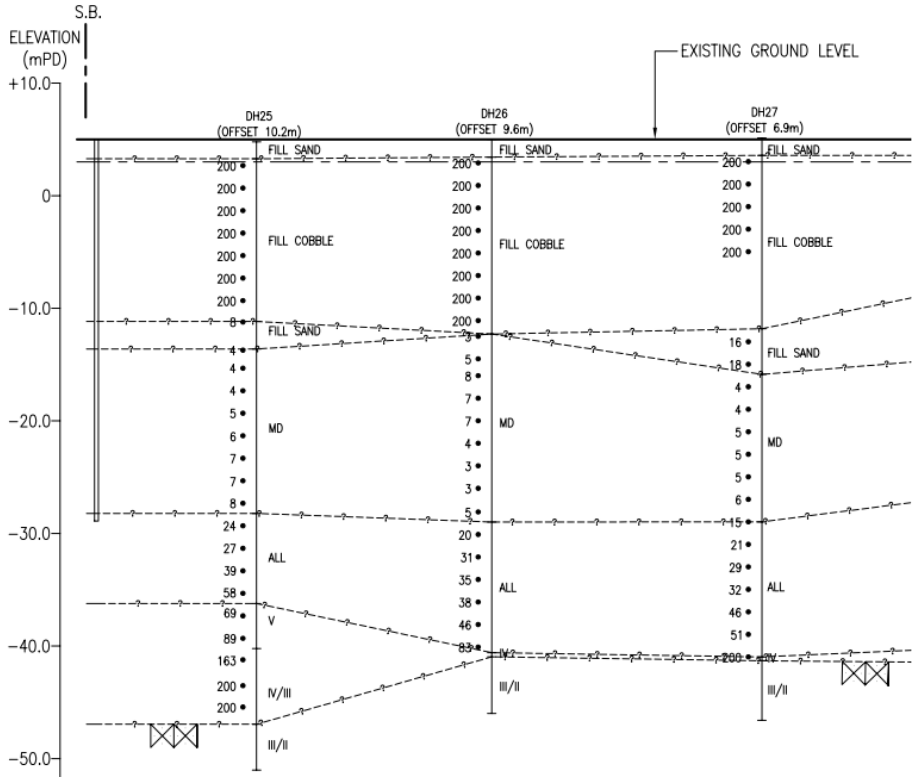

Fill (Cobble) - Loose to medium dense, brownish grey to dark grey, silty fine to coarse SAND and angular COBBLE & coarse gravel sized rock fragments
Fill (Sand) - Medium dense, gravelly silty fine to coarse SAND with shell fragments
Marine deposit - Soft to firm, grey to dark grey, silty CLAY with occasional shell fragments
Alluvium (Clay) - Soft to stiff, silty CLAY and loose to very dense, light grey to dark grey, clayey to coarse SAND with coarse gravel & cobble sized tuff fragments.
CDT - Extremely weak to moderately strong, completely to highly decomposed TUFF
MDT - Moderately strong to strong, moderately to slightly decomposed fine ash to coarse ash TUFF

Figure 4: Typical geological profile within the reclamation area

The field tests included standard penetration tests (SPT) to determine the SPT-N values, the pressuremeter tests for measurements of soil stiffness at various soil layers beneath the fill, plate load tests were conducted for the stiffness of the coarse grained fill where pressuremeter tests were in vain, field permeability tests and vane shear tests were also conducted in soft marine deposits and alluvial clays. The laboratory tests scheduled included unconsolidated undrained triaxial tests, single-stage and multi-stage consolidated undrained tests, oedometer tests, and particle size distribution tests, etc.

4 GEOTECHNICAL DESIGN ASPECTS

4.1 Selection of design parameters

The FILL layer at location near the existing seawall is about 30m in thickness with some local spots where thickness of fill was found extending to 60m in the TKO Reclamation Area. Most of the utilities are buried underground at various depths in the fill layer. The deformation of FILL due to excavation may lead to settlement problems with the utilities and roads within the area. FEM PLAXIS was used to assess the

excavation effects to the underground utilities as well as to the surroundings of the building sites. The input material parameters for each layer of material included basic soil properties and values of deformation modulus E, which in general practice in Hong Kong can be obtained by empirical correlation with SPT-N values or through in-situ field tests, such as pressuremeter test and plate load test. The advantages and limitations of the two ways namely correlation and in-situ tests for determination of the deformation modulus are given below in Table 1.

Table 1: Determination of elastic soil stiffness, E, by different methods

	Advantages	Limitations
SPT	Quick, cheap, easy to carried out	• For SPT in the cobbles, the N-values exceed 200 and E value is overestimated. • The countable SPT value in the FILL layer will normally the sand layer between cobbles; therefore, the N-value is not representing the entire FILL layer and the E value is underestimated.
Pressuremeter	Reliable E values base on the pressure and volume change	• The pressure bulb would be damaged in testing the angular cobbles, and thus, test results could not be obtained. • The pre-drilled hole may collapse in very loose sand material and test could not be carried out. • It is time consuming and costly because of difficult ground conditions against the penetration and testing with pressuremeter.
Plate Load Test	Reasonable E values	• The test can only be carried out on ground or in pit at shallow depth below ground above ground water. • Time Consuming (min. 3 days for carrying out 1 test) and costly. • The size of set up increases with increase in size of testing plate; in general, a 300mm plate is used which limits the depth of influence zone of the test.

For testing in both cohesive soil and cohesionless soil, and depending on the disturbance to the formation of test hole, pressuremeter test is considered adequate. Also, the following relationship between the SPT and Young's Modulus is suggested (GEO, 2006), where the stiffness of the soil related to uncorrected SPT-N value.

$$Ev' = 0.8N \text{ to } 1.2N \text{ (MPa)} \quad (1)$$

However, in the FILL layer, there were cobbles and sub-angular gravels that the pressure bulb might easily be damaged by the sub-angular gravels causing the pressuremeter test unsuccessful. Plate load tests were therefore employed to carry out at 1 m below the existing ground level. The results of the plate load tests gave values of E reasonably greater than the estimated values by correlation of N-value as shown above, the results were also reasonably consistent in comparison with that of SPT-correlated value for the fill layer of cobble and gravel. The E value (Bowles, 1997) from plate load tests are given below in Table 2.

Table 2: Plate load test results and the estimation of Young's Modulus (E) for Fill

	$k_s = q / \delta$		$E = k_s * B * (1-\mu^2)$		
Plate Load Test	k_{s1} (MPa)	k_{s2} (MPa)	E_1 (MPa)	E_2 (MPa)	E (avg)
TP1 (300kPa)	111	122	76	83	80
TP1 (1200kPa)	238	278	162	190	176
TP2 (300kPa)	75	86	51	59	55
TP2 (1200kPa)	97	94	66	64	65
TP3	34	35	23	24	24
TP4A (300kPa)	50	54	34	37	35
TP4A (1200kPa)	127	141	87	96	91

The shear strength parameters of soil were determined by the triaxial compression tests on undisturbed mazier samples collected at site specific ground investigation and by in-situ vane tests. However, given the nature of the FILL layer at top that comprised cobbles and gravels; therefore no undisturbed samples could be obtained from the FILL layer. As shown in Figure 5 below, the results from vane shear tests, the results from unconsolidated undrained tests, and the results from pressuremeter tests were used to estimate the undrained shear strengths, cu of different soils; and thus to determine the design parameters. For the pressuremeter test, the soil plasticity property enable the engineer to correlate the shear strength properties with the Young's Modulus (Bowles, 1997), where the Young's Modulus, as shown in Figure 6, can be correlated with the SPT-N value. (GEO, 2006)

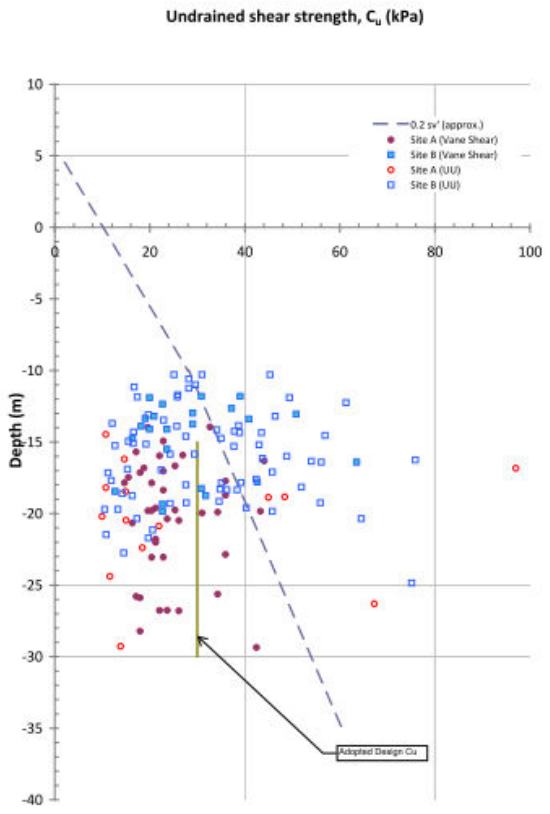

Figure 5: Estimation of undrained shear strength (C_u) for Marine Deposit Clay

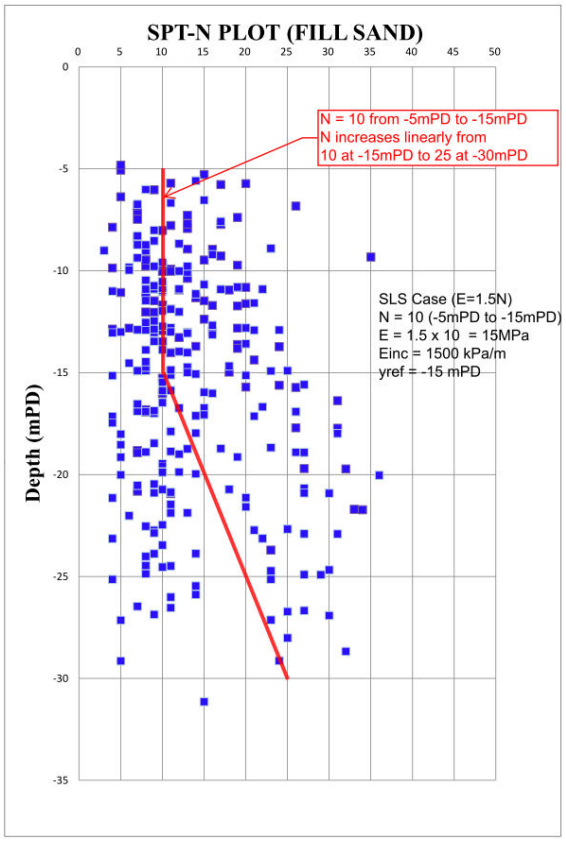

Figure 6: SPT-N values and estimated elastic modulus (E) for Fill

4.2 Drained or undrained analysis

Based on the site investigation results, there is generally a layer of alluvium CLAY between the Marine Deposit CLAY and alluvium SAND layers. Although majority of the alluvium underlying this area is described as silty CLAY or sandy CLAY in the borehole log, according to particle size distribution testing results, alluvium possessed SILT properties and is mainly described as sandy SILT/CLAY. Based on the field permeability tests carried out within various depth of alluvium, coefficient of permeability (k) of alluvium is in the order of 10-6m/s. On the other hand, field permeability tests revealed the permeability of marine deposit of this site is in the order of 10-7m/s. It becomes clear that the permeability of alluvium is in general one order higher than the marine deposit layer. In accordance with CIRIA C580, given the mass permeability is not low, drained conditions should be assumed in design. Therefore, in the subsequent design of ELS, the alluvium was considered as drained material. The results of permeability tests are given in Figure 7 for various soils of this area.

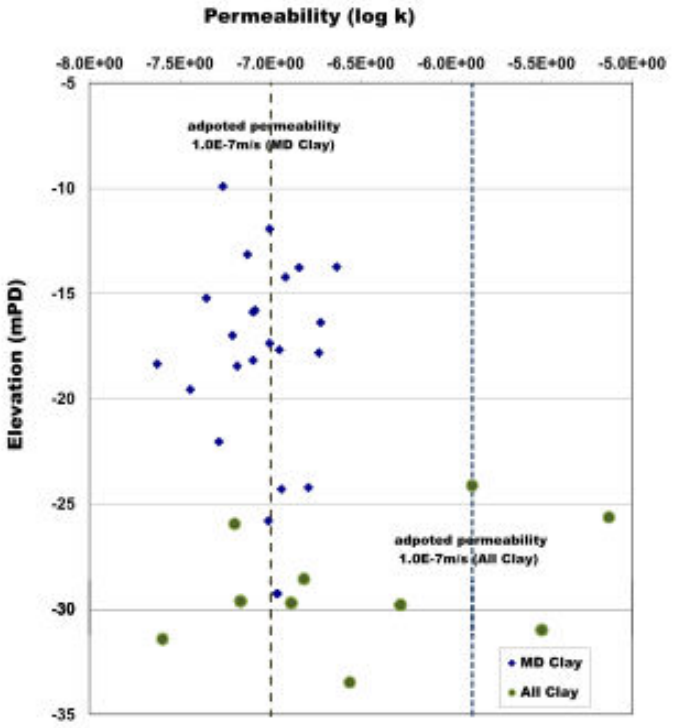

Figure 7: Summary of permeability test results

4.3 Design considerations of ELS works for neighbourhood development

As there were numbers of developments going on over the Tseung Kwan O Reclamation area at the time of this paper, it was observed that the construction activities at neighborhood sites would induce interfacing effect to the site at the common boundary. Of an ELS design, the effect of the site activities at the neighborhood lots should be taken into account for various scenarios in FEM analysis. For the concerned projects in TKO, PLAXIS model as shown in Figure 8 associated with the following scenarios were carried out:-

a) ELS works carried out simultaneously – The design parameters, ELS schemes, the construction sequences between both lots should be coordinated together. The effect of the proposed ELS works to each other should be considered in the ELS submission for both lots. Furthermore, sensitivity shall be carried out to consider the effect of the ELS works of the study lot when the construction works of adjacent lot is suspended at certain stage.

b) ELS works of the adjacent lots are completed – In this case, consider the effect of the ELS works to adjacent by setting the initial condition which bulk excavation of adjacent lot is completed and the struts are in function.
c) Superstructure works of adjacent lots are completed – The load transfer scheme of adjacent lot should be considered to check if there is wind load transfer to the proposed ELS works of the subject lot. The lateral load of the foundation systems within the studied area are usually resisted by the subgrade reaction of surrounding soil and the passive resistance of the basement structure. The effect of the lateral load on the proposed ELS works in the subject lot should be considered

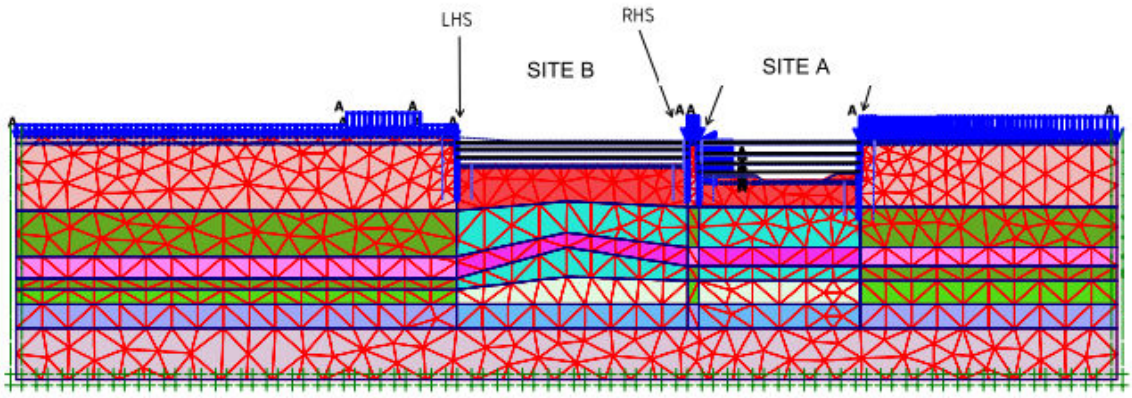

Figure 8: General case when considering interface

There were some other existing structures which might affect or be affected by the proposed ELS works in the concerned site area. Existing seawall, box culvert, newly constructed road and cycling track were situated near the development sites. The stability of these structures, which are founded on different foundations, shallow or deep, should be checked if they were affected by the proposed ELS works. There should be no excessive settlement which might affect the functionality of the structures.

4.4 Design consideration of foundation works

The reclamation of the area was completed in 1999, almost 17 years back from now that primary consolidation of the marine deposits underlying the FILL may have completed. The assessment of the effect of negative skin friction and the consolidation of marine deposits for the area revealed that consolidation of marine deposit could be considered completed if the thickness of clay layer was less than 6m;

Landfill time , t =	17	year
Coefficient of consolidation of MD (CLAY), $C_{v\ MD}$ =	1.1	m^2/year
Time factor, $T_{v\_MD} = C_v*t/d^2$ =	2.08	
For U > 0.6 $U = 1-\frac{8}{\pi^2}\exp(-\frac{\pi^2}{4}T_v)$ By this equation, U =	0.9952	

However, for some parts of the area where thick clay layers were encountered, consolidation of the marine deposits were still in process where the undrained strengths of the clay were low (for instance, ratio of Su/ v'< 0.2 as shown in Figure 5), negative skin friction effect to foundation could not be ignored in the foundation analysis and design.

Nevertheless, in most cases the development projects in the area would include deep basement structures where basement excavation would result in removal of most of the fill materials above the marine deposits which is a great relief of over-burden pressure on the marine deposits that could reverse the consolidation process. After evaluation of the degree of consolidation base on the laboratory test results, the remained

excess pore pressure can be estimated. Due to the course of the excavation works to certain depth, the stress change due to the removal of soil implies that there will not be any loading applied to the clay material and would not trigger the consolidation. Thus, NSF effect can be significantly eliminated in the design of pile foundation. However, the NSF effect to the foundations at the boundary should be handled with care as the unloading effect due to basement excavation was minimal at the boundary if not in vain at all. As a result, down-drag forces prevailing on the screen walls of the basement should be considered. To reduce the down-drag force, bitumen can be applied on the sheet pile wall before the construction of basement structure. In this connection, a friction angle of 5 degrees for the basement constructions had been adopted if a sandwiched bitumen layer of thickness of 10mm was provided.

The adopted foundation types in this area were bored piles, steel socketted H-piles, driven piles and driven piles to volcanic (TUFF) bedrock at various depths from about 40m to 60m in this area.

5 CONCLUSIONS

This paper presented the geotechnical parameters from site specific ground investigation works as well as design considerations associated with ELS and foundation works. The following concluding remarks are thus given:

a) Planning on site investigation, including field works schedule and laboratory testing is important to allow engineers to select proper soil parameters based on the results of site specific tests.
b) It is noted that the deformation modulus of FILL consisting of cobbles and sub-angular gravels could be obtained from in-situ plate load test.
c) Geotechnical design parameters were obtained from quality data of in-situ tests and laboratory tests of the site investigations carefully planned for the purposes of the developments.
d) In consideration of the interaction effects to a development site by other development works adjoining the sites, complicated scenarios of the interaction at different stages of the developments to one other were carefully assessed using FEM analysis.
e) Determination of representative geotechnical parameters was the key to the success of FEM analyses of the complicated design scenarios aforementioned.

REFERENCES

Bowles, J.E., 1997, *Foundation Analysis and Design (Fifth Edition*), McGraw-Hill International Editions. 316-317p

GCO (Geotechnical Control Office). 1990. *Review of Design Methods for Excavations. Geotechnical Control Office Publication No. 1/90*. Geotechnical Control Office, Hong Kong

CIRIA (Construction Industry Research and Information Association). C580. 2003. *Embedded Retaining Wall*

GEO (Geotechnical Engineering Office). 2006. *Foundation Design and Construction*, *GEO Publication No. 1/2006*. Geotechnical Engineering Office, Hong Kong

Foundation Design for the District Cooling System Building at Kai Tak

Leslie H. Swann & Irene Chung
Jacobs China Limited, Hong Kong

ABSTRACT

Jacobs China Limited (JCL) was appointed to carry out detailed design of the District Cooling System (Phase II Works) at Kai Tak Development. Foundation design at Southern DCS plant room and Seawater pump room was one of the challenges. As well as taking the load of the structure, the foundation had to be designed for the future development within the area. Given the very tight programme requiring the construction to be complete in a short period, a design that eliminated piling was sought. The base slab of the buildings was designed to be founded on lightly over consolidated Alluvial Clay and Sand. In order to achieve advantage in programme the principle of effective stress was used to eliminate all piling. An extended base slab was used to resist uplift forces. The site was pre-loaded by lowering the groundwater table before excavation in order to ensure that the settlement on reloading with the structure and future development was acceptable. As the load of the soil removed was similar to the total loading, the net increase in pressure at the soil supporting the raft footing was negligible.

1 INTRODUCTION

1.1 Project Background

The project to design, build, and operate a District Cooling System (DCS) (Phase II Works) at Kai Tak Development (KTD) is to provide an energy efficient cooling system to customers in line with the Hong Kong SAR Government's Policy to reduce carbon emissions.

The DCS (Phase II Works) consists of a seawater pump room with an associated intake, a southern DCS (SDCS) plant room with an associated outfall, a northern DCS plant room, and several sections of DCS chilled water pipelines and seawater pipelines under a design and build contract. Preliminary design of the whole system was required as part of the design. The construction of these remaining works will be carried out under other contracts while the operation of the whole DCS will fall under Phase II works until the end of the operation period.

1.2 Structural Form

Located at the disused runway of the former Kai Tak Airport, the southern DCS plant building is a reinforced concrete underground structure with a 2-storey basement measuring 130m by 32m approximately on plan. The adjacent integral seawater pump room building has a 2-storey basement measuring 100m by 36m approximately on plan. Raft foundation slab was extended with size as shown in Figure 1 below. The depth of the DCS building was 18.2 m below ground level and the depth of the seawater pump room was 14.1m below ground level. Initially, part of the seawater pump room was proposed as a single storey basement. However, to reduce the future net load as a consequence of a future development, it was agreed to increase the basement depth everywhere to a 2 storey basement.

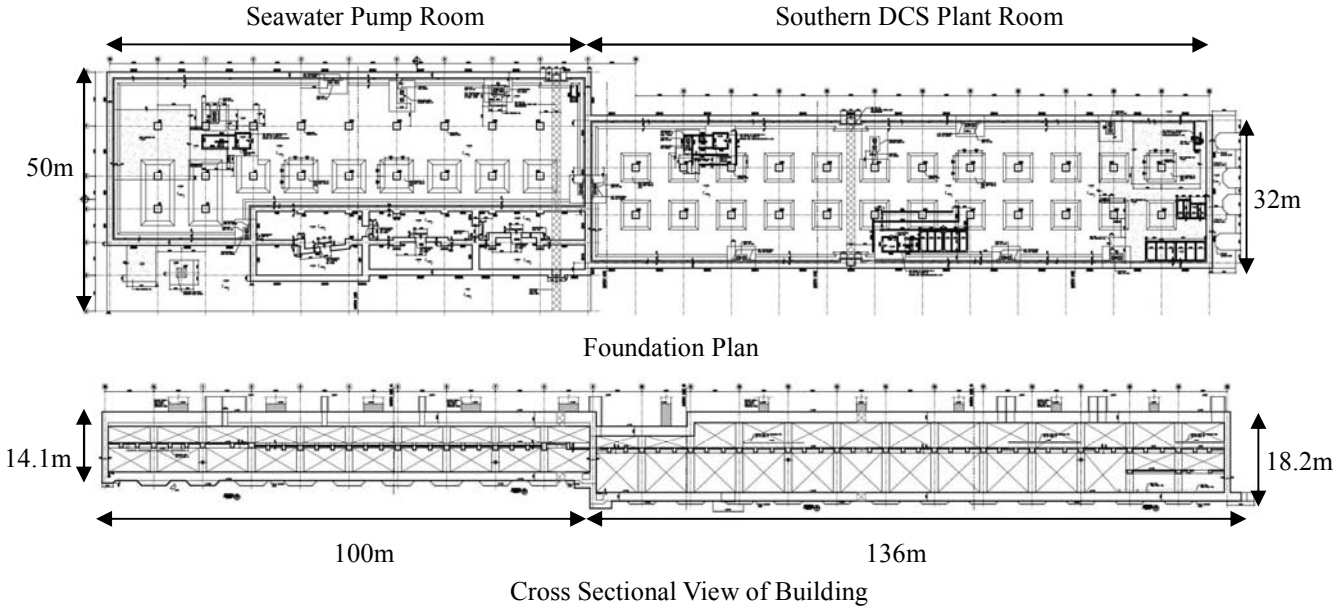

Figure 1: Foundation Plan and Cross Sectional View of Southern DCS Plant Room and Seawater Pump Room

2 DESCRIPTION OF GROUND CONDITIONS

2.1 Subsurface Profile and Design Ground Model

Based on published information, the geology of the site comprises a sequence of superficial soils including Alluvial and Marine Deposits, which overlaid completely decomposed granite (CDG) and medium grained granitic bedrock. It is understood that dredging was carried out during the previous development of the site to remove a majority of the Marine Clays and that only isolated pockets remained. Significant thickness of Reclamation Fill comprising a variety of soil and rock materials was anticipated across the site.

A project specific ground investigation at the Southern DCS area was undertaken in April 2011. It included twenty-five (25) boreholes drilled five metres into bedrock. SPT and permeability tests were undertaken on site and a series of laboratory tests were carried out to determine the geotechnical design parameters.

The results of ground investigation were generally consistent with the published geology, which revealed soil horizons that follow the sequence of Fill, Marine Deposits, Alluvial Deposits and CDG. Localised pockets of clay were encountered in the Marine and Alluvial Deposits. Within the Alluvial Deposits the clays were in lenses / layers generally less than 3m thick. Beneath the seawater pump house, the clay layers were up to 10m thick beneath parts of the foundation. However, all the deposits of the Marine Clay were above the base of the structure and hence were to be excavated. The Fill encountered comprises a highly variable layer of loose to medium dense Sand with some gravels.

A generalized ground model of the site used in design is presented in Figure 2 below.

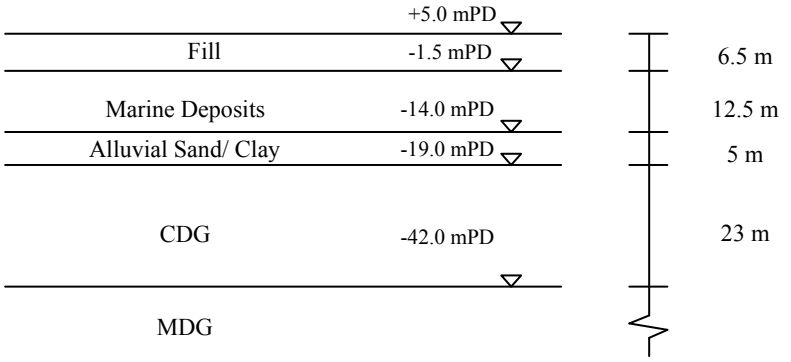

Figure 2: Design Ground Model

2.2 Design Groundwater Level

Groundwater level (GWL) at the site is subject to tidal influence due to the close proximity to the sea. A design GWL in the range between +1.0mPD and +4.0mPD was adopted taking into account monitoring during and subsequent to the ground investigation, and published tide levels at the Quarry Bay Tide Station. A mean GWL of +2.5mPD measured during the ground investigation was adopted for temporary works design.

2.3 Geotechnical Design Parameters

The geotechnical design parameters were selected based on typical published figures, in-situ and laboratory tests results. The existing fill and Marine Clay and sand were to be excavated and thus their compressibility properties were not significant with regard to the design.

The compressibility parameters (mv, Cc, Cr and Cv) were obtained from oedometer tests. Based on the Cc to Cr ratios, it was assumed that the settlement of the soil on reloading would be 10% of the settlement determined from the virgin compression curve. The design parameters are summarised in Table 1 below. The analyses concluded that the soil was over-consolidated with an average OCR of 1.15.

Table 1: Geotechnical Design Parameters

Soil Type	Mv (m2/MN)	Compression Index - Cc	Re-compression Index - Cr	Cc/Cr	Coefficient of Consolidation – Cv (m2/yr)
Alluvial Clay	0.09	0.15	0.02	9.2	5.52
Alluvial Sand	0.053	0.053	0.01	26.5	33.62
CDG	0.06	0.16	0.02	13.8	74.93

3 DESCRIPTION OF FOUNDATION CONCEPT

3.1 Foundation Design Approach

The total load of the SDCS building and the future development above is similar to the load of the soil removed. As a result the net load applied to the ground would be negligible. At tender stage, tension piles socketed into rock were designed to resist uplift on the base slab founded on consolidated Alluvial clay and sand. The final foundation design generally followed the same design approach, with the exception that it was agreed to extend the base slab to the south-east end of the SDCS building. The additional downward loading provided by the weight and soil friction of soil above the extended slab provided adequate resistance to the up-lift force and it was thus possible to eliminate the tension piles which gave programme advantages. However, time had to be allowed for preconsolidating the soil as described below.

A Factor of Safety of 1.1 against uplift was maintained in all temporary stages in accordance with the Code of Practice for Foundations. A Factor of Safety of 1.5 against uplift was designed at the final stage with the future development loading to comply with the project's Employer's Requirement.

3.2 Settlement Estimate and Control

The total foundation settlement is the sum of immediate settlement upon application of loading, and consolidation settlement of saturated clay soil due to dissipation of excess pore water pressure. The magnitudes of immediate and consolidation settlement are typically 30% and 70% of the total settlement respectively.

In order to limit the consolidation settlement of the SDCS building within acceptable limits, the design required the ground to be pre-consolidated by lowering the groundwater table from +2.5mPD to –17.85mPD before excavation commenced. As a result, the net increased effective stress at the soil supporting the raft footing would be negligible when the future development is constructed.

The change of effective stresses in the soil at the base of the structure at each stage of construction is indicated in Figure 3, based on the first six stages of construction:

Stage 0: Installation of sheet piles enclosing the temporary cofferdam prior to excavation;

Stage 1: Dewatering to -17.85 mPD i.e. 1 m below formation level of SDCS plant room;

Stage 2: Excavate to -16.85 mPD at SDCS plant room and -12.75 mPD at Seawater pump room;

Stage 3: Construction of building structure;

Stage 4: Stop pumping and allow groundwater recovers to original level;

Stage 5: Backfill 3m soil on top of roof slab of the building occupied by the Operator;

Stage 6: Construction of future development structure (Dead load only);

Stage 7: Operation of future development structure (Live load only, transient in nature) – not shown

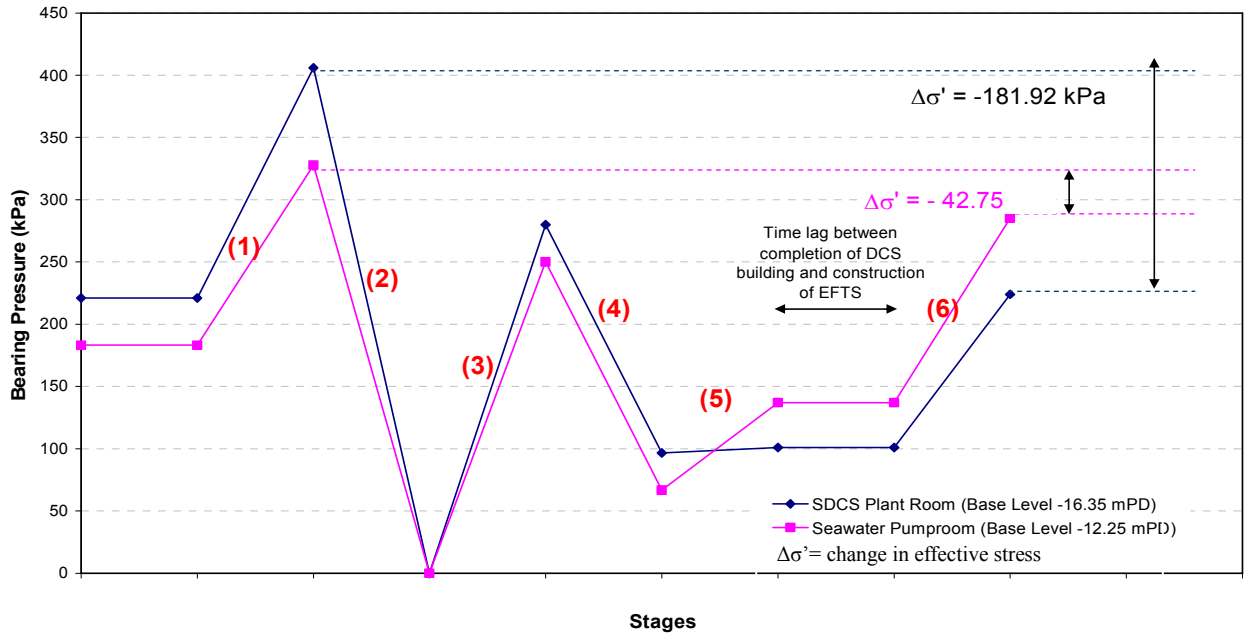

Figure 3: Load Path of Soil underneath the SDCS Building

The indicative soil stress- strain relationship relative to each stage of constructions is presented in Figure 4.

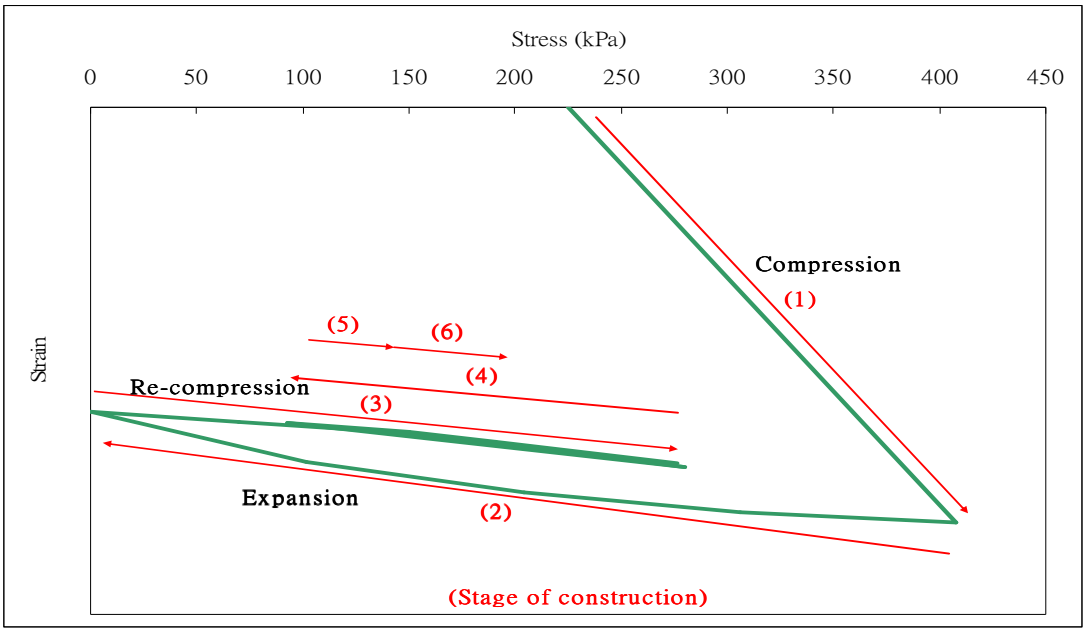

Figure 4: Stress-Strain Diagram for Soil below SDCS Building

Since the effective stress of soil at the base of the structure will always be less than the pre-consolidation pressure, settlement due to construction of the DCS structure and the future development will follow the re-compression curve (Stages 3 to 6).

The soil effective stress at each stage was estimated using the computer programme VDISP. The features of VDISP simulations include:

a) Each layer of soil is a semi-infinite, homogeneous, isotropic mass with a linear stress-strain relationship due to a point load on the surface. The stress distribution in the ground was determined by assuming a Boussinesq stress distribution.
b) Settlement is calculated using a profile of Young's modulus with depth. The modulus can be constant or vary linearly with depth for each soil layer.
c) Displacements and stresses can be calculated at several levels and at any location in plan. The location of the displacement/stress points is defined by means of displacement grids. These may be two-dimensional orthogonal grids, lines or points. The results from the grids can be displayed graphically as contours.
d) Loaded areas can be defined as rectangles or circles. Pressures are applied uniformly. Areas can be superimposed and placed at any level. All loads are completely flexible i.e. no allowance is made for stiffness of the structures.
e) The base of the model is defined by the specification of an equivalent rigid boundary.
f) The ground is modelled using a series of vertical soil profiles each consisting of a number of horizontal soil layers. The plan distribution of the soil profiles is specified in rectangular areas known as soil zones. These can be superimposed allowing the development of complicated ground models.

The rate of consolidation was estimated based on Terzaghi's theory of one-dimensional consolidation and the formula

$$Tv = \frac{Cv \cdot t}{d^2} \quad (1)$$

where Cv= Coefficient of Consolidation, t=time, *d = drainage path length [d = H for one-way drainage, d = H/2 for two-way drainage]*

At 90% degree of consolidation (U), Tv = 0.8 i.e. Cvt90/d2 = 0.80

The odeometer tests indicated average t90 = 0.48 min and 2.17 min for the CDG and Alluvial Sand samples respectively. Therefore, it was considered that settlement at CDG and sand layers would occur rapidly, almost immediately upon application of foundation loads.

Since the Alluvial Clays at the site were localised pockets within the sand layer, water could be drained from both the upper and lower boundaries. The drainage path of at the saturated clay was thus determined to be half of the thickness of the stratum.

Based on the average cv = 5.52 m2/year, using the average 3.5m thickness of Alluvial Clay, it was estimated that the time required for 90% degree of consolidation to occur would be 161 days, the time required for 50% degree of consolidation to occur is 41 days and the time required for 40% degree of consolidation to occur is 32 days.

Given the tight programme it was designed to hold the lowered groundwater level to –17.85 mPD for 30 days prior to excavations, in order to achieve 40% consolidation settlement of the localised clay pockets. In the pump room area there were zones where the clay thickness was found to be up to 10m thick. Sand drains to accelerate the consolidation were designed at the mid-north-western portion of the pump room area where localised thick Alluvial Clay pockets were found.

The foundation settlements calculated by VDISP, taking into consideration raft foundation rigidity (Tomlinson, 1975), were found to be within 25mm and differential settlement of the raft foundation was assessed to be within acceptable limits.

Results of VDISP analyses were validated by using the finite element software SAFE. The settlement contours from SAFE output is shown in Figure 5. It was predicted that the maximum settlement of 34mm will be present at the column along Grid B between grids 1A & 1for the future development structure. Apart from this local settlement, all the other areas of the raft foundation would have settlement below 25mm, which was consistent with the VDISP results.

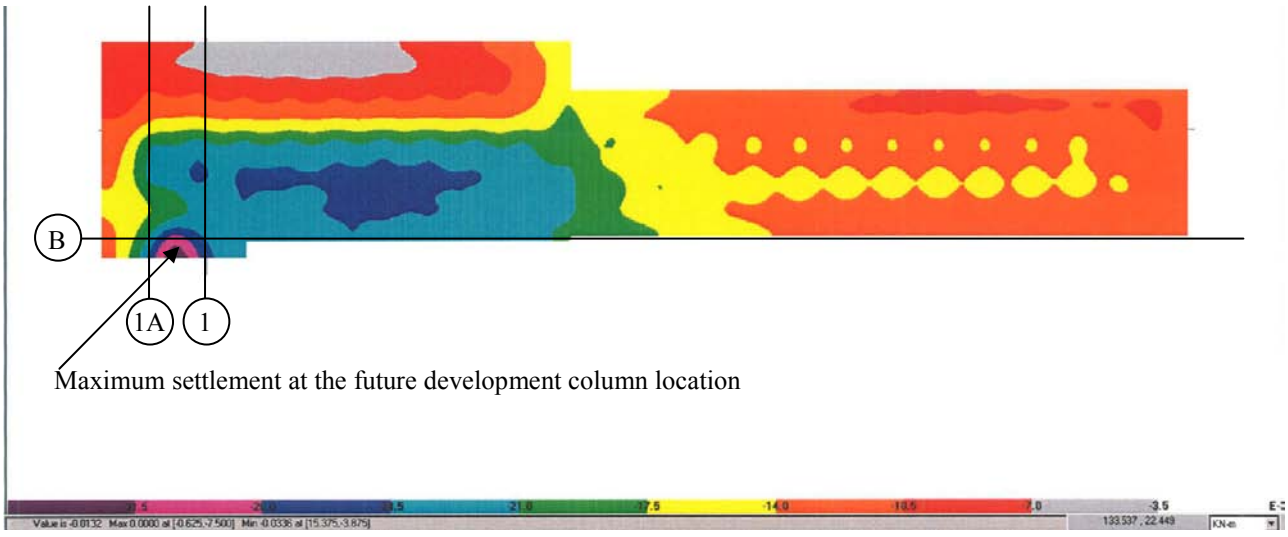

Figure 5: Settlement Contour of Raft Foundation

4 FOUNDATION CONSTRUCTION PERFORMANCE

Construction of foundation has been completed for more than a year and the superstructure was recently completed, with backfilling to ground level complete in March 2014. No significant settlement was reported during construction.

Dewatering at the Pumphouse and SDCS Plant Room continued with drawdown generally below the base of the foundation till backfilling was completed. No significant uplift was reported after the pumps were switched off and water levels allowed to recover.

5 CONCLUSIONS

An alternative foundation design has been undertaken at the Southern District Cooling Building for programme advantage. By using the principle of effective stress, and preloading by dewatering, long term settlement has been limited. Based on the available data the construction of the building has performed as anticipated.

ACKNOWLEDGEMENTS

The authors would like to thank EMSD and the Contractor for the project, Hong Kong District Cooling DHY Joint Venture, for giving permission to publish the paper.

REFERENCES

Tomlinson, M.J. 2001. *Foundation Design and Construction.* Pearson Education Limited.

Design and Analysis of a Piled-raft Foundation in Doha

L Tony Chen
Hyder Consulting Limited

ABSTRACT

Doha Tower is composed of 45 stories above the ground and a 4 level underground basement. The tower is cylindrical in shape, measuring approximately 45m in diameter and 231.5m in height above the ground. It is supported by a piled raft foundation system. This paper discusses the process and details of the piled raft design, focusing on ground investigation, selection of geotechnical design parameters, full scale pile load testing and 3D modeling of foundation – ground interaction. Numerical analyses have indicated that a longer pile tends to reduce pile settlement but the reduction rate decreases with increasing pile length, especially when it reaches about 20m. The full scale pile load testing has shown that the measured load - settlement response of a single pile is much stiffer than that assumed in the foundation design, indicating that the piled raft foundation system is adequately designed.

1 INTRODUCTION

Doha Tower is located in West Bay Doha. It comprises 45 stories above the ground and a 4 level underground basement. The tower is cylindrical in shape, measuring approximately 45m in diameter and 231.5m in height above the ground. The superstructure is primarily supported by 9 inclined perimeter columns and a core area, all in reinforced concrete. This was a design and build project. The construction commenced in 2005 and was completed in 2012.

In the reference design provided at the tender stage, the tower was indicated to be supported by large size barrette piles. However, a more cost effective foundation system comprising a piled raft was adopted in the final design as will be discussed in this paper. Piled raft foundations have been used to support tall buildings around the world and the topic has been widely discussed, see for example Poulos (2005).

This paper discusses the process and details of the piled raft design, focusing on ground investigation, selection of geotechnical design parameters, full scale pile load testing and 3D modeling of foundation – ground interaction.

2 GROUND CONDITIONS

Topographically the site is relatively flat. The Qatar Peninsula geologically represents a part of the Arabian Gulf Basin. This basin is mainly composed of extensive carbonate sediments with different ages overlying the basement rocks and may reach up to 10 km in thickness. The outcropping rocks in Qatar are mainly referred to as Quaternary and Tertiary Ages. The geology of the study area is mainly of the recent and Tertiary sediments Simsima Limestone and Rus Formation.

A ground investigation program was carried out at each of the concept design stage, detailed design stage and construction stage, comprising the following scope:

- Drilling 17 boreholes to depths ranging from 30 to 120m;
- Drilling 8 destructive boreholes to depths ranging from 25m to 40m;
- Carrying out various in-situ tests in selected cored and destructive boreholes, including 24 falling head permeability tests, 39 packer tests, 1 PS Suspension test and 198 pressuremeter tests;
- Carrying out various laboratory tests to determine the physical, mechanical and chemical properties of the ground materials.

The ground was found to generally consist of Hydraulic Fill, Marine Sand/Caprock, Simsima Limestone, Dukhan Alvelina, Midra Shale and Rus formation. Ground water levels were measured at depths ranging from 2.25m and 4m below the existing ground surface.

Due to the existence of the four basement levels, the top surface of the foundation was at -14.7m. The rock strata below this level are described briefly in Table 1.

Table 1: Descriptions of identified stratigraphical units

Rock strata	Thickness (m)	Description
Simsima limestone	6 to 9	fine to medium grained chalky crystalline/dolomitic limestone
Dukhann alveolina	0.5 to 1.5	white fossiliferous chalky limestone
Midra Shale	5.2	laminated shaley limestone or shale intercalated with thin bands of limestone or dolomitic limestone.
Fahahi valates	0.5-1.5	whitish, crystalline, compact fossiliferous limestone
Russ formation		chalky dolomitic limestone

Figure 1 shows the range of the measured unconfined compressive strength or UCS values, while Figure 2 shows the Young's modulus values obtained from both the Menard pressure-meter testing and PS Suspension testing.

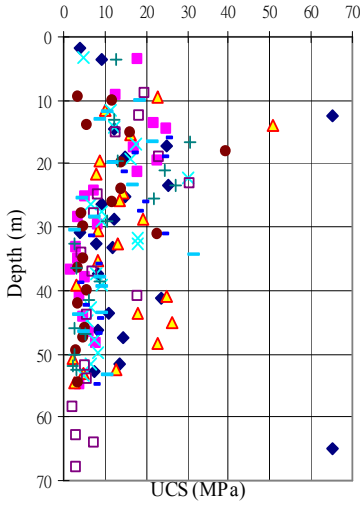

Figure 1: Measured UCS values

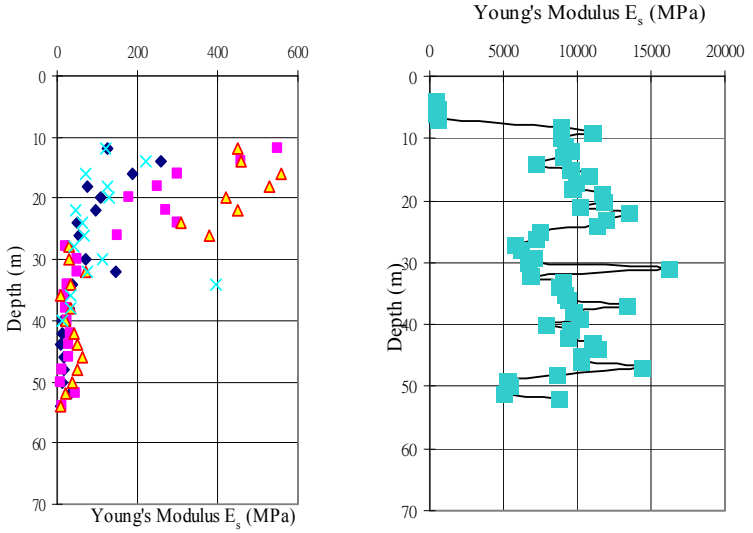

(a) Pressuremeter testing (b) PS Suspension testing

Figure 2: Measured Young's modulus values

3 ADOPTED GEOTECHNICAL MODEL AND DESIGN PARAMETERS

The adopted geotechnical model and design parameters for the five rock strata are presented in Table 2, involving the following assumptions:

- The allowable raft bearing capacity was conservatively taken as one tenth of UCS as recommended by Bowels (1996).
- The ultimate shaft friction of bored piles in the rock strata was estimated using the following equation as recommended by Horvath and Kenney (1979) (reported by Burland and Mitchell, 1989):

$$f_s = 0.25 (q_u)^{0.5} \quad (1)$$

where q_u is UCS in MPa.

- The ultimate end bearing capacity of bored piles was taken as one times the UCS as recommended by Bowels (1996).
- As for the Young's modulus values, it was noted that the results from the Menard testing and PS suspension testing differ significantly, with the latter being significantly larger than the former, mainly due to the strain level of the latter being much smaller than that of the former. Taking into account of the actual strain level of the ground and based on the author's experience, it was considered appropriate to adopt design Young's modulus based on the pressuremeter testing results factored up by about 10 times.
- The Poison's ratio was taken as 0.2 for all the rock strata.

Table 2: Adopted geotechnical model and design parameters

Rock type	Thickness (m)	Young's modulus E_s (MPa)	Allowable raft bearing capacity q_a (MPa)	Ultimate pile shaft friction f_s (MPa)	Ultimate pile end bearing capacity f_b (MPa)
Simsima limestone	7.5	1300	1.5	1.0	15
Dukhan alveolina limestone	1.0	500	-	0.7	7
Midra shale	4.0	500	-	0.7	7
Fahahil valates limestone	1.0	500	-	0.7	7
Russ formation (upper)	20	300	-	0.4	4
Russ formation (lower)	70	100	-	0.2	2

4 LOADINGS

The loadings used for foundation design were obtained from super-structure analyses. The key loadings are presented in Figure 3. The loadings were applied as concentrated loads at the individual column and wall locations on the raft. A number of ULS and SLS load combinations were considered in the design, however, only the Dead Load + Live Load – Water Pressure case will be discussed in this paper due to space limitations.

Table 3: Foundation loadings

Load source	Vertical N (MN)	Horizontal H_x (MN)	Horizontal H_y (MN)	Moment M_x (MNm)	Moment M_y (MNm)	Moment M_z (MNm)
Dead Load	-1004	0	0	0	0	0
Live Load	-200	0	0	0	0	0
Uplift water	256	0	0	0	0	0
Wind (x)	0	14	0	1714	0	-1
Wind (y)	0	0	14	0	2015	0
Seismic (x)	-115	23	24	8	9	0.3
Seismic (y)	-115	18	21	7	10	0.3
Seismic (z)	-100	13	14	5	6	0.2

5 FOUNDATION SYSTEM

In the reference design provided at the tender stage, the tower foundation consisted of 2.8 x 1.2m barrette piles arranged in several groups to support the perimeter columns and the central core area, with a minimum pile length of 24m. Loadings from the super structure were to be transmitted to the piles through a reinforced concrete cap of 1.8m thick above the piles and 0.5m thick between pile groups. In this design, all the foundation loads are to be taken up by the barrette piles only.

In view of the relatively high bearing capacity of the underlying rock layers, it was considered that a more cost effective and time saving option could be developed by adopting a piled raft foundation, whereby the loads are shared by both the raft and the piles while the settlement is reduced mainly by the piles.

Based on a series of numerical analyses (details to be discussed in the next section), the preliminary design adopted a piled raft system consisting of a 3m thick raft and a total of 113 bored piles, 1.2m in diameter, located under the perimeter columns and the central core area. All piles were 20 m long. Based on the adopted

geotechnical parameters shown in Table 2, the axial geotechnical capacity of each pile was estimated to be 11.3MN which was adopted as the design capacity. Figure 3 shows the adopted pile layout.

Compared with the reference design, the total concrete volume of the current design is about 33% less, resulting in cost savings.

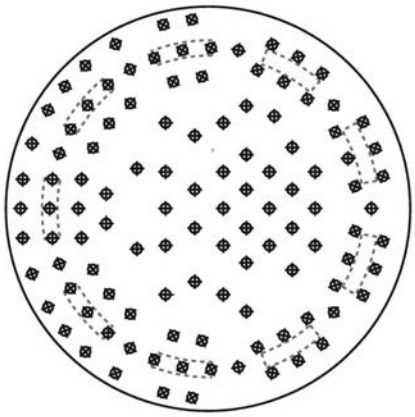

Figure 3: Adopted pile layout

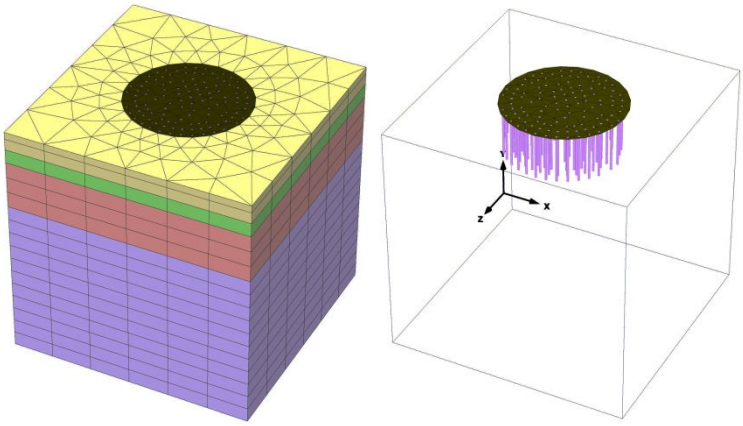

Figure 4: Adopted Plaxis model

6 ANALYSES

6.1 Analyses of single piles and piled raft

The piled raft design involved a series of single pile and pile group analyses. The analyses were initially carried out using the commercial computer program Ansys and later verified by the commercial computer program Plaxis 3D Foundation. The pile forces and settlements given by the two programs were found to be broadly similar. Due to space limitations, only Plaxis analysis will be discussed in the present paper.

Figure 4 shows the adopted Plaxis model. The rock was modeled as volume elements with Mohr-Coulomb model. The piles were modeled as beam elements connected directly to the surrounding 3D volume elements forming the rock, with limiting skin friction and end bearing capacity. The raft was modeled as plate elements with each loading point and pile point identified as nodes. The piles were connected to the raft by pile-head nodes.

Analyses of a single pile, 1.2m in diameter, were carried out to investigate the load – settlement behavior and the effect of pile length on settlement. Figure 5 shows the load – settlement response curve for a 20m long single pile subject to a load up to 2 times the pile working load of 11.3MN. As can be seen, the response is essentially elastic up to the working load level and thereafter becomes non-linear.

Figure 6 shows the computed pile head settlements for different pile lengths. As expected, a longer pile tends to reduce settlement but the reduction rate appears to diminish with increasing pile length, especially when the pile length reaches about 20m. Accordingly, a length of 20m was adopted for all piles. The corresponding pile head stiffness was estimated to be about 1,600 MN/m which would be used later to compare with that from full scale pile load testing for assessing the appropriateness of the adopted geotechnical design parameters.

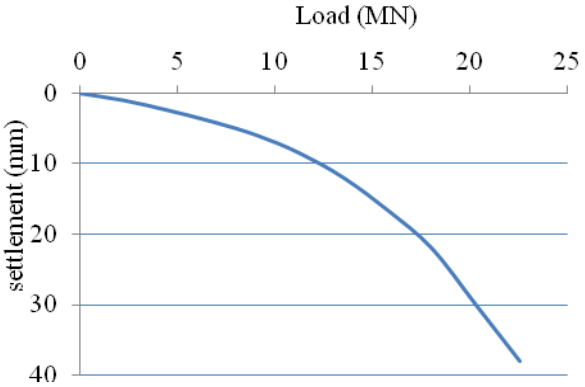

Figure 5: Predicted load – settlement response for a 20m long pile

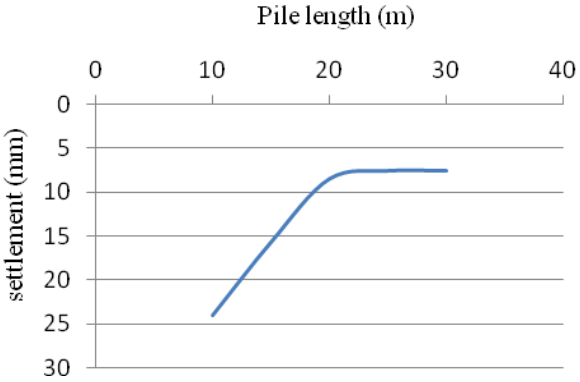

Figure 6: Pile length verses settlement

Piled raft analyses were then carried out to compute pile loads and settlements for different load combinations. The computed pile loads were all compressive with the maximum value being less than the adopted pile capacity of 11.3MN. The ground pressure underneath the raft was generally about 200kPa with localized areas reaching about 800kPa which was still less than its capacity. The load shared by the raft was about 30% of the total load.

The computed settlement contours corresponding to the load combination of Dead Load + Live Load – Water Pressure are presented in Figure 7. The maximum settlement, occurring at the raft centre, and the minimum, occurring at the raft edge, were about 72mm and 40mm, respectively. The resulting average angular rotation was thus about 1/780 which was within the normal limit for tall buildings and therefore acceptable.

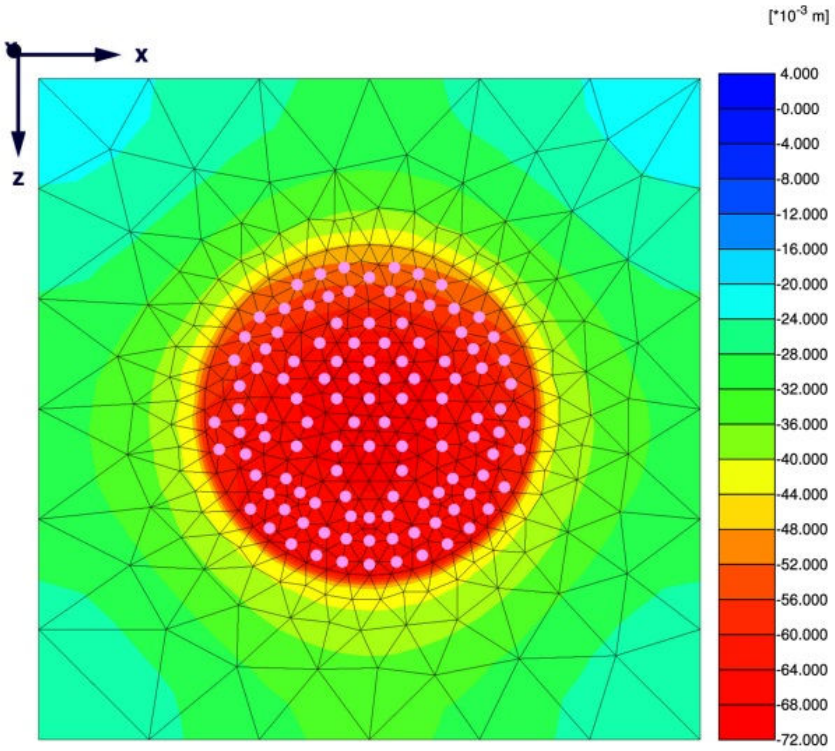

Figure 7: Computed settlement contours

6.2 Simple assessment of foundation stability

A simple assessment was also carried out to cross check the overall stability of the foundation system. In the assessment, the piled raft system was simplified as a foundation block with a depth of 2/3 of the pile + raft depth. The computed factors of safety against sliding and overturning were all well greater than 3.0, indicating that the foundation system was stable.

7 VERIFICATION BY PILE LOAD TESTING

7.1 Pile load testing

To verify the predicted pile capacity and hence the adopted piled raft design, preliminary pile load testing was carried out on two non-working piles, 1.2m in diameter and 20m deep below the ground surface, prior to construction of working piles. The test piles were loaded in three cycles, with each cycle being respectively up to 1, 1.5 and 2 times the adopted working load of 11.3MN.

As shown in Figure 8, the testing results indicated that the load-settlement response was essentially elastic up to a load level of approximately 19MN, approximately 1.7 times the adopted working load. For a load level up to 2 times the working load, the plastic or irrecoverable settlement was very small and less than 1mm. The computed pile head stiffness was approximately in the order of 6,000 MN/m which was much greater than that predicted by the Plaxis analysis, namely 1,600 MN/m as mentioned earlier.

As can be seen, the measured load – settlement response is broadly similar to that predicted by Plaxis analysis, albeit stiffer.

7.2 Design adjustment

The pile load testing results confirmed the adequacy of the piled raft design. Given that the measured pile response was much stiffer than that assumed in the design, it was considered reasonable to reduce the pile lengths and/or number of piles. However, due to reasons related to approval procedures, only the lengths of some piles subjected to relatively lighter loads were allowed to be reduced to 17m, justified by a re-analysis of the piled raft system using upward adjusted Young's modulus values of the rock strata.

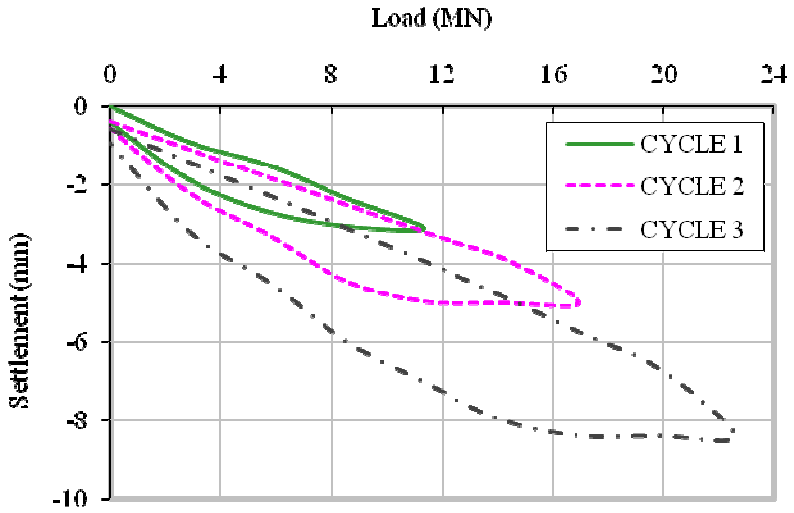

Figure 8: Load – settlement response measured from full scale pile load testing

8 CONCLUSIONS

This paper has discussed the process and details of design of a piled raft foundation system supporting a 45 story building, focusing on ground investigation, selection of geotechnical design parameters, pile load testing and 3D modeling of foundation – ground interaction. The following key conclusions may be drawn:

(a) The Young's modulus values of the rock strata derived from the pressuremeter tests appeared to be generally much smaller than the actual values, as demonstrated by the full scale pile load testing;
(b) Numerical analyses of single piles indicated that a longer pile tends to reduce pile settlement but the reduction rate decreases with increasing pile length, especially when it reaches about 20m;
(c) By allowing the raft to share foundation loads, a cost effective foundation design was achieved;
(d) The load - settlement response measured from the pile load tests appeared to be much stiffer than that assumed in the design as per Plaxis analysis, indicating that the piled raft design was adequate.

ACKNOWLEDGEMENTS

China State Construction Engineering Corporation is gratefully acknowledged for its assistance and support provided to the author while he was working on the project. The views expressed in this paper are those of the author only.

REFERENCES

Bowles, J.E. (1996). *Foundation Analysis and Design, 5th Edition*, The McGraw-Hill Companies, Inc., US

Burland, J. B., & Mitchell, J. M. (1989). Piling and Deep Foundations. *Proc. Int. Conf. on Piling and Deep Foundations, London, May 1989*.

Horvath, R. and Kenney, T.C. (1979). "Shaft resistance of rock-socketed drilled piers". *Presented at ASCE Annual Convention, Atlanta, GA*, preprint No. 3698.

Poulos, H.G. (2005). "Piled raft and compensated piled raft foundations for soft soil sites" *Geotechnical Spec Publications No 129*, ASCE, 214 - 234.

Padma Bridge, Bangladesh - Seismic Design Approach of the Pile Foundations

Suraj De Silva
SMEC Asia Limited, Hong Kong
Chao Li
Gammon Construction Limited, Hong Kong
Eric Yung, and Guoxiong Yu
AECOM Asia Co Ltd.

ABSTRACT

A Padma River is one of the largest rivers in the world. The river flow during the monsoon months is significant with flow rates reaching velocities in excess of 4.5 m/s. The high flow rates cause significant scour of the riverbed. Studies show that 100 year return period scour depth is 62 m. The width of the river in the dry season is about 6 kilometres. The site is seismically active. In order to establish the seismic design parameters of the site, a site specific seismic assessment was carried out in addition to extensive field and laboratory ground investigations. A detailed state-of-the-art ground investigation carried out comprised the recovery of very high quality undisturbed samples of sand using the GEL PUSH sampling technique and the self-boring in-situ friction tests (SBIFTs), cross-hole seismic shear wave and compression wave tomography, and other conventional tests. After establishing the static and dynamic design soil parameters, the ground response was determined using SHAKE, adopting five selected strong ground motions corresponding to a 475 year return period earthquake event. These ground response motions were then input into the MIDAS dynamic soil-structure interaction model incorporating the Penzien Method to design the piles and the superstructure, taking due note of the deep design scour depths. The analyses demonstrate that six 3 m diameter steel raking piles driven down to about 120 m are needed to support each bridge pier with the 150 m span truss girders placed on seismic isolation bearings.

1 INTRODUCTION

The Padma Multipurpose Bridge will be constructed a cross the 6 km wide Padma River at Mawa, about 50 km to the southwest of Dhaka, Bangladesh (see Figure 1 and 2). The project site is known to be challenging in three aspects – strong and deep riverbed scour, high site seismicity and extremely deep geology with bedrock encountered at a depth of approximately 12 km. One of the critical elements of the Padma Multi-purpose Bridge design was the design of the foundations. The foundation design was challenging, since the bridge is required to support large dead (150 m long steel truss, a bridge pier and a large pile cap) and live loads (live loads - the bridge is required to carry a freight train, gas mains, electricity cables, wind loads, ship impact loads and significant seismic loads), under significant river bed scour conditions. The scour depths corresponding to a 100 year return period has been estimated to be 50 m to 65 m across the river, thus resulting in free lengths of piles in the river of between 55 m to 65 m.

In order to support these foundation loads under these extreme environmental conditions during its design life, the bridge needs to be supported on large diameter steel tubular piles installed at a rake. The diameter of the piles required are 3 m installed at a rake of 1 horizontal to 6 vertical, driven into place. As the design scour is deep, the piles are also long, and estimated to be about 100 m to 120 m in length founded in dense to very dense sands.

This paper presents in brief the ground investigations that were carried out, the seismic design approach and parameters used, and brief pile design methodology. In the dynamic model the springs were connected through dashpots to masses that represent the free field; the technique being based on the modified Penzien

Method. The variations in the river bed with scour were hence represented by the depth of the springs, masses and dashpots along the piles. The design strong ground motions have then been imposed on the model at the stipulated depth to simulate the earthquake events for the dynamic analyses load cases. The design forces and stresses derived from the model have then been used in the structural design of the piles.

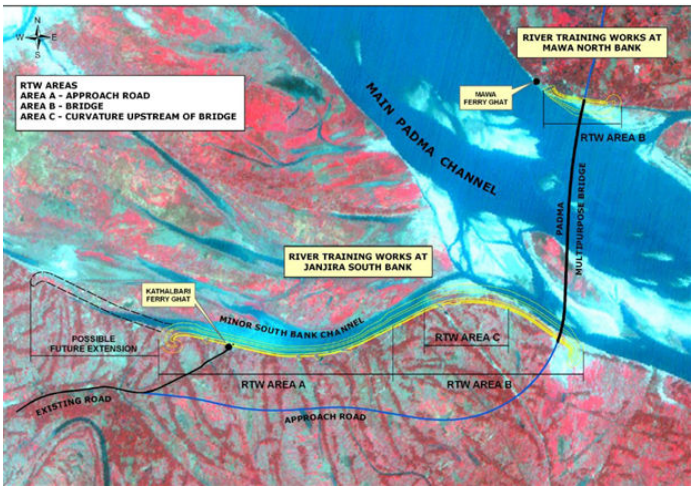

Figure 1: Padma River and Padma Bridge Location

Figure 2 : Computer Generated View of Proposed Bridge

2 SEISMIC HAZARD ANALYSIS

2.1 Site Seismicity

AECOM engaged the Bangladesh University of Engineering and Technology (BUET) to undertake a site specific seismic hazard assessment using the earthquake database available at the earthquake engineering department at the university. From this study the maximum PGAs derived using the Abrahamson & Silva attenuation relationship were recommended as the design PGA values at an depth (at an elevation of -120 m PWD considered to be stiff ground or the "pseudo bedrock") in the Padma Bridge design. These recommended values are presented in Table 1.

Table 1: Seismic design parameters

Return Period (Years)	Recommended Horizontal PGA in cm/s^2 (Abraham and Silva 2008) at -120 mPWD	Recommended Horizontal PGA in terms of " g " at -120 mPWD	Recommended Horizontal PGA in terms of " g " at riverbed/ground level
2	4	0.004	0.008
10	11	0.011	0.022
50	32	0.032	0.064
100	51	0.051	0.102
200	80	0.080	0.160
475	141	0.141	0.282
1000	230	0.230	0.460

2.2 Ground Motions

The ground motions adopted design contains both those from the seismic hazard analysis and strong ground motions from Japanese design codes and are shown in Figure 3.

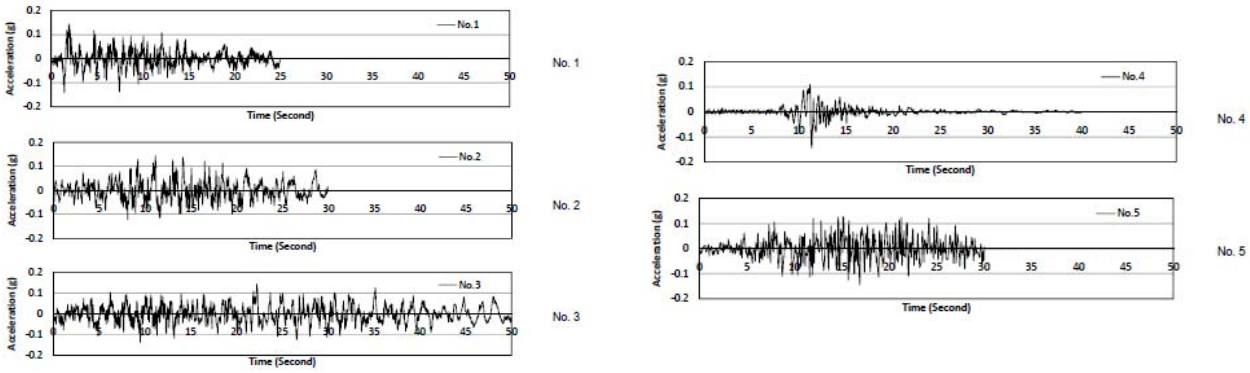

Figure 3: Input Ground Motion Adopted at - 120 mPWD for Ground Response Analysis

3 GROUND INVESTIGATION

The site investigation for this project was in two phases. Phase 1 comprised 5 marine boreholes to 120 m depth with Standard Penetration Test (SPT). The information was used in scheme design of the foundations and then to determine the scope of the Phase 2 ground investigation program, which comprised 19 additional boreholes down to 130 m depth, 6 boreholes down to 85 to 90 m depth, and 6 cross-hole geophysics boreholes down to 150 to 160 m depth, and Piezocone penetration tests down to about 60 m depth. In the 19 boreholes down to 130m depth, SPTs, conventional sampling and Flat Plate Dilatometer Tests were carried out. For the 6 boreholes down to 90 m, state-of-the art GEL PUSH sampling and Self Boring Internal Friction Tests (SBIFTs) were carried out along with SPTs. Cross-hole geophysical surveys were carried out down to 160 m depth to determine the shear and compression wave velocities and hence the dynamic soil parameters such as the initial/maximum shear moduli, G_0, of the soil strata. The high quality undisturbed GEL PUSH samples recovered were sent to Japan for laboratory testing. In addition to the conventional tests such as particle size distribution tests, specific gravity, mica content tests, consolidated undrained triaxial compression and extension tests, K_0 -consolidated undrained triaxial tests. Cyclic Triaxial Tests were used for the determination of soil dynamic curves including shear modulus degradation curves and damping ratio curves for various soil layers. Bender Element Tests were also carried out to obtain the initial/maximum shear moduli, G_0, of the soil strata.

4 GEOLOGICAL PROFILE

From the Phase 1 and 2 Ground investigation program, the geological profile of the site was established (Figure 4). The design parameters of major soil units are shown in Table 2. The location of the bridge alignment lies on the Padma River in Bangladesh between Mawa and Janjira. Geological sections across the river have been developed (Figure 3) to present the ground conditions. The soil within the main bridge area is predominantly micaceous sand with an average mica content of about 8 to 10% interspersed with occasional thin layers of clay/silt. The ground condition shows a layer of clay and silt is present at the banks with Unit 2 (less than 20% fine materials) extending down to depth of 120 to 130 m, below which a stiff to hard mottled clay layer was encountered. Very dense sand was once again encountered below the stiff to hard clay layer. Approximate 20 m thick layer of very dense sand with some gravel (Unit 3 soil with less than 20% fine materials with some gravel) stratum is identified from generally -60 m PWD to -90 m PWD. In general, SPT-N values increases with depth due to increase compaction. Loose fine-grained sand and silty sand was encountered down to a depth of about 10 m to 15 m. The stratigraphy of sub-units change with depth but the south bank generally shows lower SPT-N values than the north bank at the same depth, down to about 20 m. More fine materials are evident on the Mawa side. Section above indicates up to 15 m thickness of superficial strata Unit 1a present on the north bank (Mawa) of the River. The definition of the Geological Units is shown in Table 2.

Table 2: Definition of Geological Units and Some Basic Soil Parameters

Soil Unit	Soil Type Description	SPT N-Value Range	Bulk Unit Weight kN/m^3	Friction Angle, φ' Degrees
Unit 1a	Clay	0 < N ≤10	16	-
Unit 1b		10 < N≤17	17	-
Unit 2a & b	Micaceous Sand	0 < N ≤10	17.5	25
Unit 2c		10 < N≤17	17.5	25
Unit 2d		17 < N ≤ 32	19	28
Unit 2e		32 < N ≤ 50	19	30
Unit 2f		N>50	19.5	32
Unit 3e	Micaceous Gravelly Sand	32 < N ≤ 50	19	30
Unit 3f		N>50	19.5	32

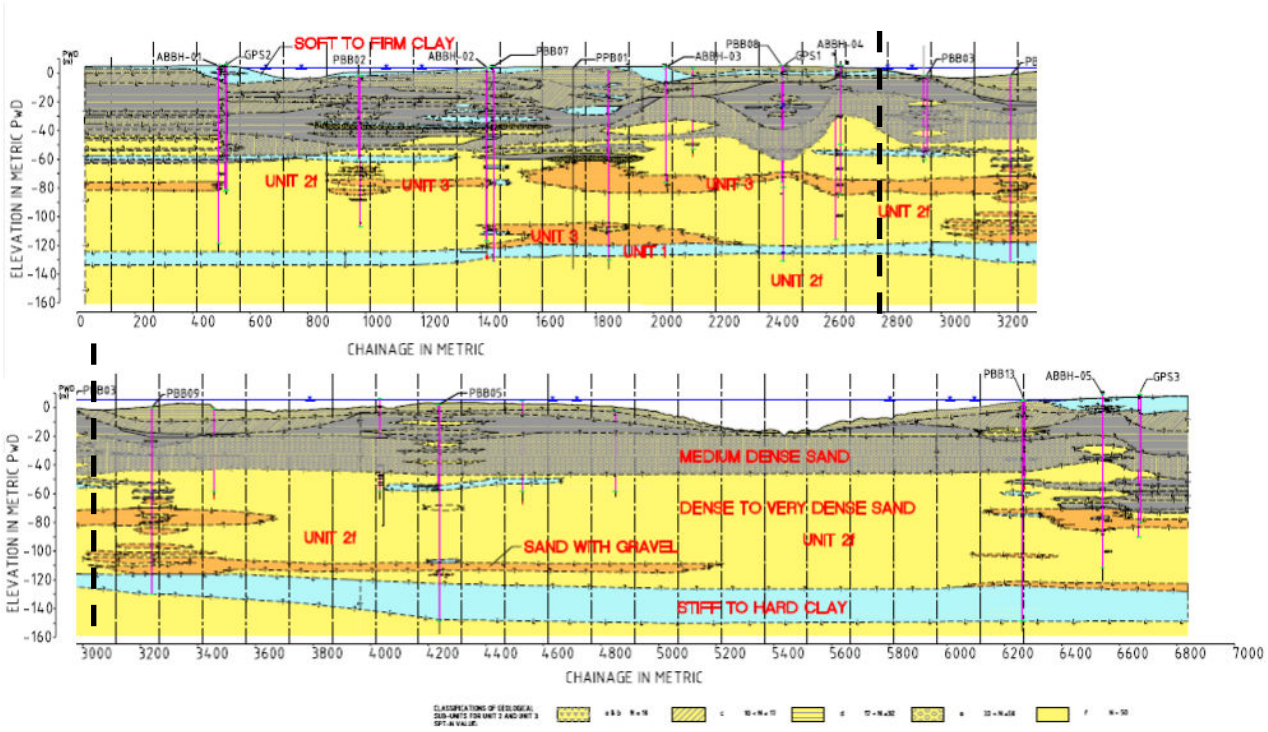

Figure 4: Geological Profile along Bridge Alignment

5 DYNAMIC SOIL PARAMETERS

5.1 Initial/Maximum Shear Modulus, G_o or G_{max}

In this project, various techniques were used to determine initial/maximum shear modulus. These techniques included both in-situ and laboratory methods. The in-situ methods can be further divided into methods through empirical correlations, and direct measurement from geophysical techniques. Empirical correlations between SPT and CPT tests and shear wave velocity were developed by researchers through historical data. In-situ direct measurement of shear wave velocity usually takes the form of geophysical methods, including the cross-hole and/or down-hole method and the spectral analysis of surface waves (SASW) method. For this project, SPT Tests and Cross-hole Geophysics Surveys were carried out as in-situ tests. Laboratory methods used for this project included Bender Element Tests and Cyclic Triaxial Tests. The results from all types of

tests quite consistently showed a trend of increasing initial/maximum shear modulus with depth. The initial/maximum shear moduli at shallow depth (0 m to 20 m) range from 50 MPa to 150 MPa, and at depths of 100 m to 120 m, the initial/maximum shear moduli increased to 300 MPa to 700 MPa. The G_0 obtained from different tests are plotted together in Figure 5. As shown in the Figure, the profile is divided into three depth ranges, i.e., 0 ~ 75 m, 75 ~ 100 m and 100 ~ 160 m. For depth range 0 ~ 75 m, data from cyclic triaxial tests, bender element tests and cross-hole geophysical survey are available. Due to the fact that cross-hole tests provide most data, results from cross-hole tests are considered as one data set, while results from Bender Element Tests and dynamic triaxial tests are grouped together to form another data set. In Figure 5, the green line is the trend line for cross-hole tests and the pink line is for data from Bender Element tests and cyclic triaxial Tests. An approximate average line (red line) between the two trend lines was recommended to be the design G_0 profile for the Padma Bridge Project for the depth range 0 ~ 75 m. For the depth range of 75 ~ 100 m, the trend line from cross-hole tests is a good fit to the data points from other two tests as well, and is thus used as the recommended design G_0 profile. For depth range of 100 ~ 160 m, the G_0 is taken as a constant. The shear modulus, G, and hence the degradation of the ratio, G/G_0 and the damping ratio with increasing shear strain obtained from cyclic triaxial compression tests are shown in Figure 6 and 7.

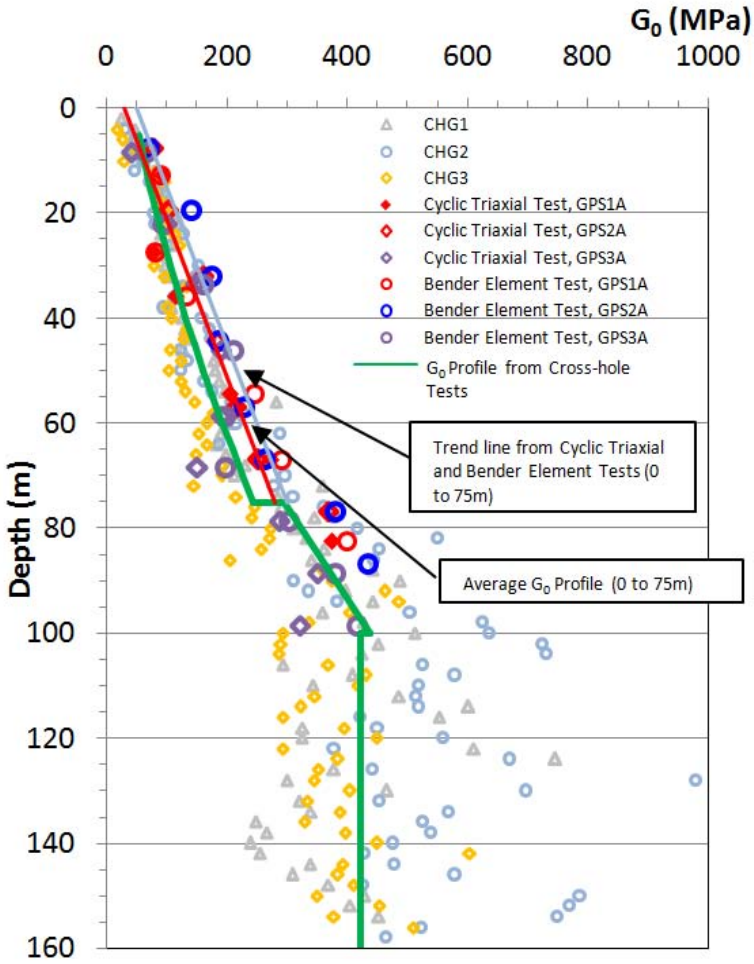

Figure 5: Initial Shear Moduli versus Depth Profile Obtained from Various Tests and Measurements

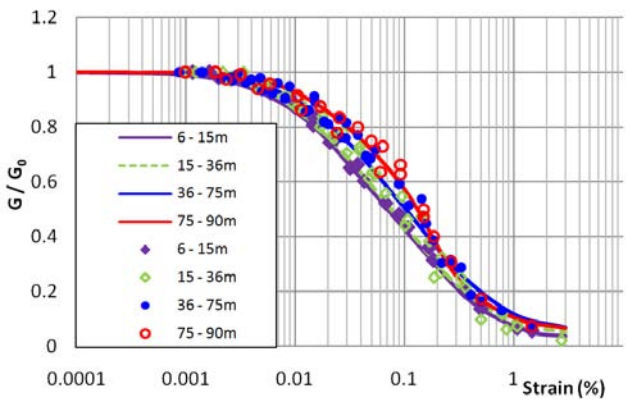

Figure 6: Degradation of Shear Modulus with Shear Strain Plots from Various Tests and Techniques

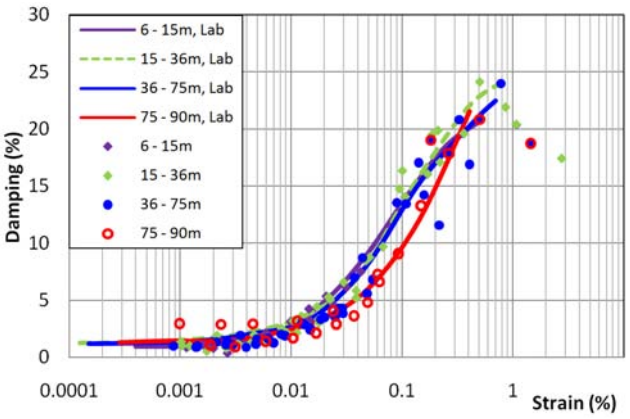

Figure 7: Variations of Damping Ratio with Shear Strain from Cyclic Triaxial Compression Tests

6 GROUND RESPONSE ANALYSIS WITH SHAKE

For five different input ground motions, specified at elevation of -120 mPWD, ground response analyses with SHAKE were performed to generate dynamic response of the free-field. In this process, the converged dynamic properties of soils are also generated. The dynamic soil parameters obtained from the ground investigation, the initial shear moduli G0 and the variation of G/G0 and damping ratios at different shear strains were used as input parameters when carrying out SHAKE analyses. Upon convergence of the SHAKE analyses, these converged dynamic soil properties together with the input motions described above were then used as input parameters in the MIDAS model developed incorporating the modified Penzien Method.

7 DESIGN OF PILES

7.1 Seismic Design

The approach to pile design in this assignment can be summarised as follows: (1) a six span (6 × 150 m = 900 m long) structural module was developed using the structural analyses program MIDAS. The various load cases were imposed on this model, including the dynamic load cases (ship impact and seismic) to determine the loadings on the pile caps; (2) another structural model using MIDAS was developed for a single pier with the soil/structure interaction modelled as springs and dashpots following the Penzien Method; (3) the forces and bending moments obtained from the 900 m long structural model is then imposed on the single pier structural model and the strong ground motions are imposed at the base of the spring-dashpot column at – 120 m PWD to simulate strong ground motions. The results from these seismic load case analyses and the other load cases are compared to generate force and bending moment envelopes for the piles, which was then used for the structural design of the piles; (4) PIGLET models were also developed to better model the static soil-structure interactions. The forces and the moments obtained from the 900 m long structural module was then imposed on the PIGLET model to obtain the settlement and lateral deflection of the pile group at the individual pier locations, and to obtain the loads and bending moments of the individual piles. These were compared with those from the structural model and larger values were used in the geotechnical design of the piles. The following factors of safety were adopted for the various load cases when determining the geotechnical capacity of the piles.

Table 3: Geotechnical Factors of Safety used for Various Load Cases when Designing Piles

Load Case	Load case	FOS on Skin Friction in Compression	FOS on Skin Friction in Tension	FOS on End Bearing
1	SW + SDL + LL	1.5	3	3
2	SW + SDL + Ship Impact	1.25	2.5	2.4
3	SW + SDL + LL + W	1.25	2.5	2.4
4	SW + SDL + LL + Ship Impact + 10 yr Scour	1.25	2.5	2.25
5	SW + SDL + 1/3 HA (1 lane) + RL + 100 yr Earthquake + 100 yr Scour	1.25	2.5	2.4
6	SW + SDL + 1/3 HA (1 lane) + RL + 475 yr Earthquake+ 100 yr Scour	1.1	2.2	1.1
7	SW + SDL+ Check Flood Scour (500 yr scour) down to -70 m PWD	1.25	2.5	2.4

Note: SW – Self Weight; SDL – Superimposed Dead Load; LL – Live Load; W – Wind Load: HA – Highway Loading: RL – Railway Loading

7.2 Geotechnical Pile Design

The forces obtained for the various load cases have also been imposed on a foundation model developed using the soil structure interaction program, PIGLET, to determine the overall group behaviour of the piles, the settlement of the pile cap, the individual pile settlements, lateral deflections and the bending moments. The axial forces on the piles determined from PIGLET were then used to carry out the geotechnical design of the piles and to determine the pile length based on the required geotechnical capacity of the piles.

Table 4: Summary of the Geotechnical Pile Design

	Near Banks - 6 Piles with seismic Isolation	**Mid River - 6 Piles with Seismic Isolation**	**Transition Piers at Banks (3m vertical bored piles without seismic Isolation)**
Type of Piles	Steel Raking	Steel Raking	Vertical Concrete
No. of Piles	6	6	12
Diameter (m)	3	3	3
100-year Scour Level (mPWD)	-62	-62	No scour
Pile Founding Level (mPWD)	-114	-98	-80
Critical Axial Load (MN)	87.6	84.5	81.0

7.3 Brief Description of Structural Design Approach of the Piles

A 3-dimensional, non-linear time history dynamic analysis has been performed for the structural design of the foundations to determine the impact of seismic ground motions on the piles and the structure. For the plan alignment of the main bridge, the subtended angle is less than 18 degree (the radius is 3000 m and one module of the Main Bridge is 900 m), the whole bridge may be modelled as a straight line in plan. The seismic analyses have considered soil structure interaction using an appropriate range of soil parameters reflecting the actual site conditions. Since there is no active fault within 5 km from the construction site, and as the bending moments in the piers due to permanent loads are small, the vertical component of seismic action was not considered (see BS EN 1998-2, 4.1.7). In the nonlinear dynamic analysis, the bending moment and curvature relationship can be used to describe the nonlinear behaviour of the plastic hinge. Each pier (column) shall have a minimum lateral flexural capacity (based on expected material properties) to resist a lateral force of 0.1× Pdl , where Pdl is the tributary dead load applied at the center of gravity of the superstructure. For large amplitude deformations P-δ effects have been considered. Plastic hinges were detailed in accordance with AASHTO LRFD Clauses 5.10.11.4 and 5.10.12.

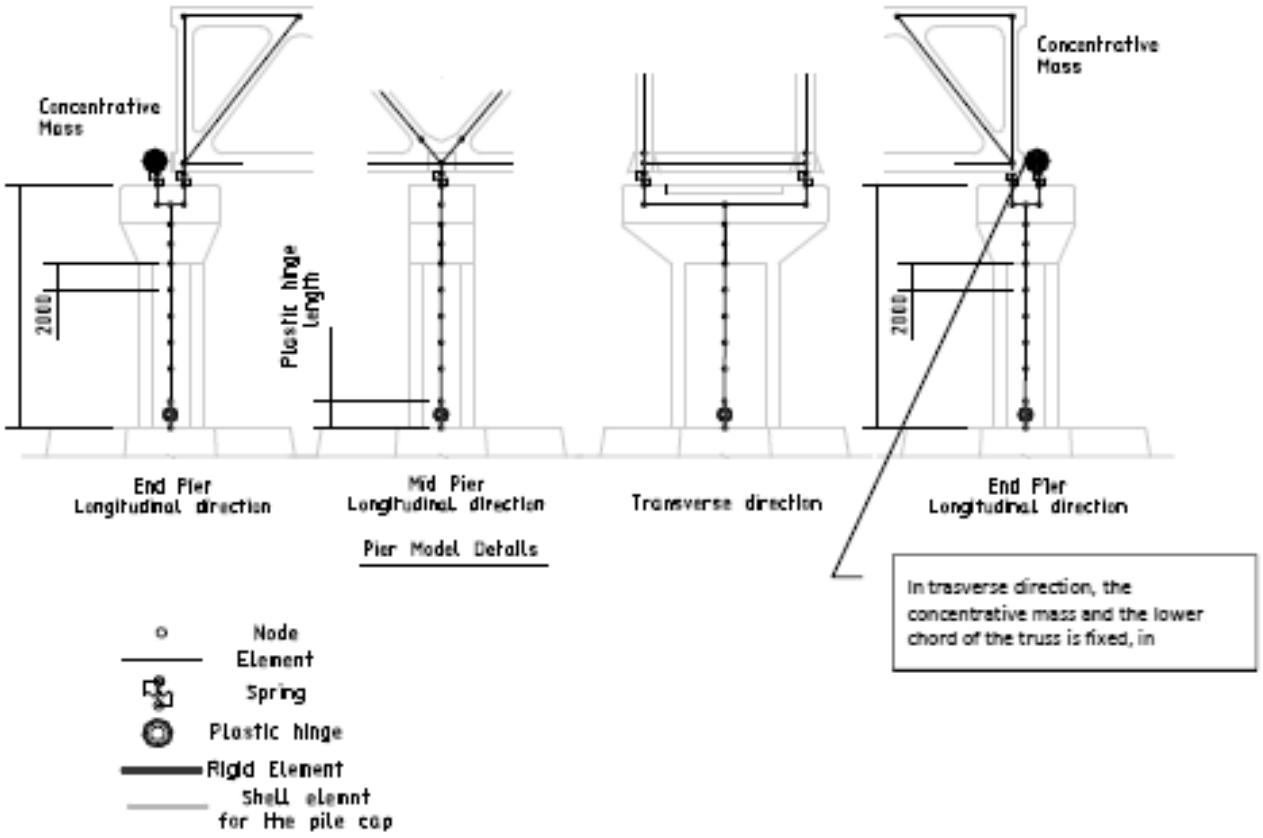

Figure 8: Pier Structural Modelling Details

This main bridge behaves in a complicated manner due to its height (120 m) and the large mass of the superstructure, the pile cap and the piles. A three dimensional non-linear time history dynamic analysis, using a modified Penzien model (see Figure 8), has been adopted for carrying out the detailed design. This model is divided into two parts, the structure and the free-field soil. The interactions between the structure and the free field are simulated by lateral springs attached to masses. Related to the free-field part, in order to determine the equivalent mobilised shear moduli, G, and effective damping ratio, D, at each layer of soil, free-field analyses of the soil columns was carried out beforehand using the program SHAKE to determine the ground response. Subsequently, 3-dimensional dynamic analyses were carried out using the equivalent shear moduli and effective damping ratios obtained from the SHAKE analyses as input data into the 3D structural model. The schematics of the structural MIDAS models are shown in Figures 8, 9, 10 and 11.

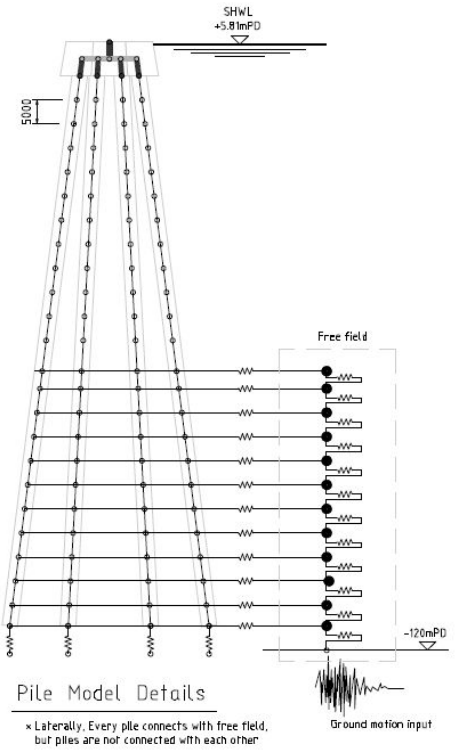

Figure 9: MIDAS Structural Model of a Single Pier Adopting the Penzien Method

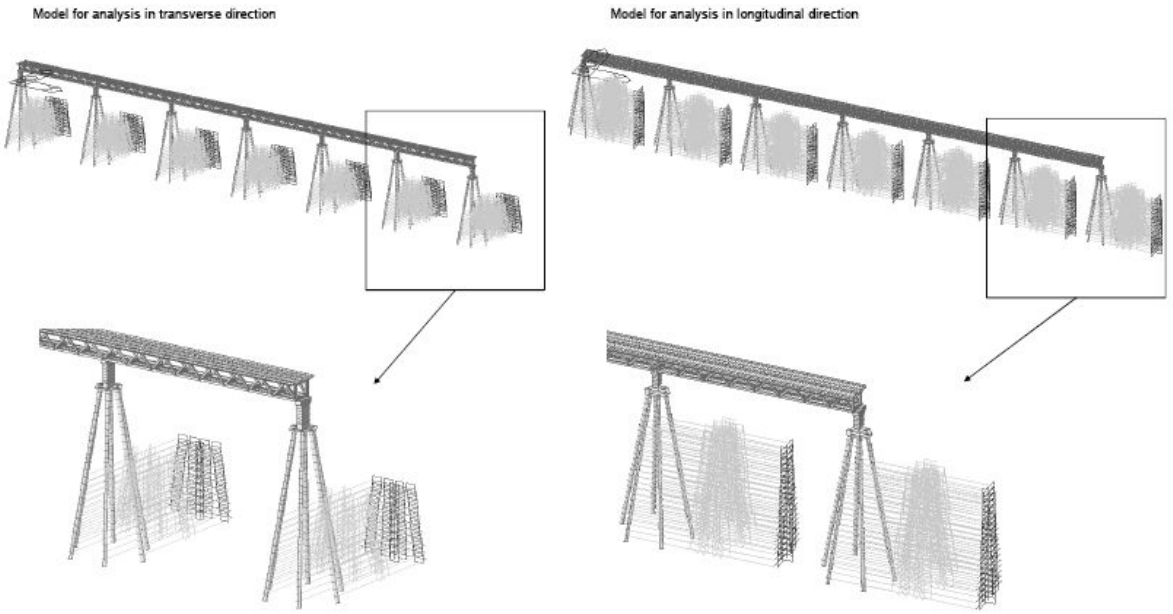

Figure 10: Global Modelling of the Piers including the Deck Structure in a 3D Structural Penzien Model

In the dynamic model the springs were connected through dashpots to masses that represent the free field; the technique is based on the modified Penzien Method. The variations in the river bed with scour were hence represented by the depth of the springs, masses and dashpots along the piles. The design strong ground motions have then been imposed on the model at the stipulated depth to simulate the earthquake events for the dynamic analyses load cases.

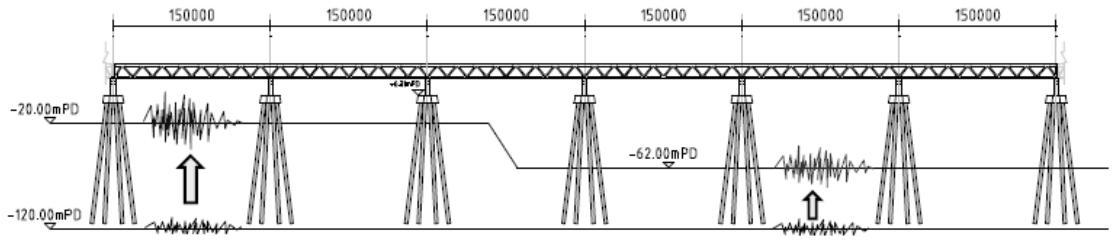

Figure 11: Application of Seismic Motions to Global Model

The design forces and stresses derived from the model have then been used in the structural design of the piles. Each of the cases represents a different combination of scour for an individual bridge module. Through this exercise, bending moments were examined along the pile to make sure conformance and economic design. It was observed that for piers with deep scour, large bending moments extend a long way down the pile, making it impossible to reduce the structural steel thickness of pipe piles with depth.

8 PILE DESIGN

For the main bridge piled foundations of the piers located in the river a symmetrically installed 6 pile arrangement has been adopted. A plan and a sectional view of the piles are shown in Figure 12. The piles are 3 m diameter, in-filled steel tubular piles (formed from steel plates of 60 mm thickness) installed in a 1H:6V rake. The pile cap is a hexagonal shaped 7 m thick reinforced concrete cap encasing all the pile heads and supporting the bridge piers. The founding elevations of the piles are at -120 m PWD Elevation – the piles are 130 m long embedded in very dense sands and gravels. The API guidelines and design approach was used when designing the driven steel piles.

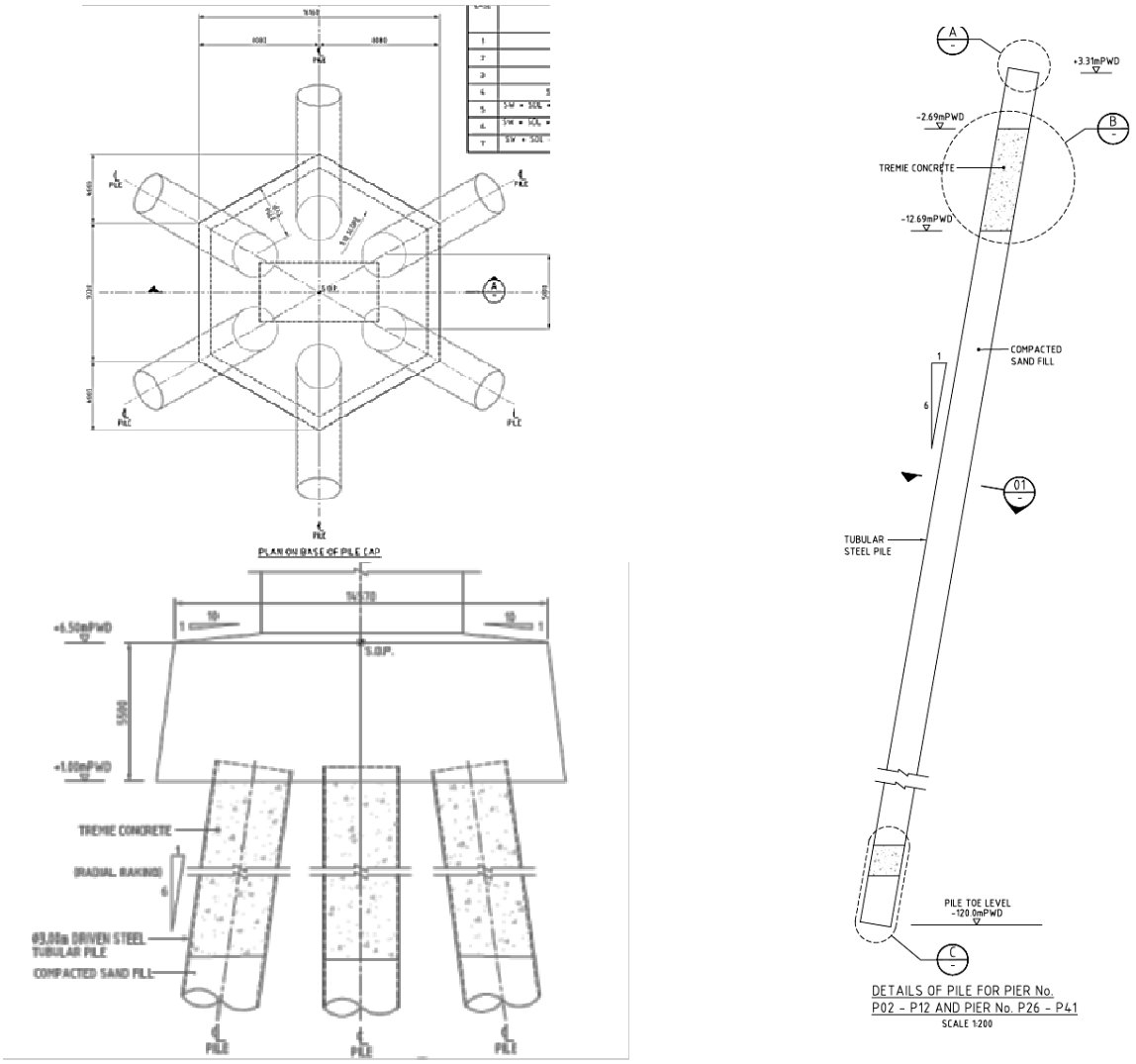

Figure 12: Main Bridge Pier Raking Steel Tubular Pile Foundation Arrangement

9 CONCLUSIONS

The difficult ground conditions and severe environmental conditions have made the foundation design for the Padma Multipurpose Bridge one of the most challenging aspects of the whole bridge design. Deep scour combined with earthquake loading required piles to be designed for large lateral loads with the piles unsupported for a length of 65 m. In developing suitable foundation design solutions, a comprehensive risk based basis of design, and a state-of-the-art structural model incorporating the modified Penzien Method in the dynamic MIDAS model where the results of SHAKE analyses were used as inputs were developed. Sophisticated insitu and laboratory tests were carried out to depths of 160 m to establish the dynamic design soil parameters that were then used in the modelling and analyses to provide the bridge with a robust foundation system that should require minimal maintenance.

REFERENCES

Sham, S.H.R. & Tapley, M.J. 2010. The design of Padma Multipurpose Bridge – challenges and solutions in design of the river spans. *Proc. IABSE-JSCE Conference, Dhaka, 10-12 August 2010*

De Silva, S., Wightman, N.R. & Kamruzzaman, Md. 2010. Geotechnical ground investigation for Padma Main Bridge. *Proc. IABSE – JSCE Conference, Dhaka, 10-12 August 2010*

Tianjin 117 Mega Tower Deep Foundation

G.X.W. Ge, F.H.Y. Chu, W.W.B. Wei & S.Y. Gao
Ove Arup and Partners Hong Kong Limited

ABSTRACT

The Tianjin 117 Mega Tower consists of a 597m tall 117-storey tower with a 4-level basement accounting for a total excavation depth of over 26m. The soft ground characteristics of the site pushed foundation construction to its extremes in terms of bearing capacity, constructability and settlement control. 1m diameter bored pile of 95.5m effective length (120m construction length from ground level) with shaft and toe grouting was originally proposed. The long length is partly due to the need for shear transfer along the pile shaft as well as settlement control requirements. Before having the long slender bored pile option, comprehensive option study had been conducted including steel pipe pile and barrette. Fully instrumented trial pile tests were conducted to verify both the pile capacity and the constructability of the proposed bored pile option using C50 tremie high strength concrete with a construction length of 120m/100m from ground level, which were tested to 42MN with double-sleeves at the equivalent basement depth for eliminating friction. After careful considerations of the geotechnical conditions and local experiences, a shortened version of piles with about 76m effective length was selected at the detailed design stage. This paper briefly introduces the foundation option study and trial piling process of Tianjin 117 Mega Tower, as well as the key design aspects of the foundation system.

1 INTRODUCTION

Tianjin City is fast emerging as one of the economic hubs in North China and is closely integrated with capital Beijing. Numerous large-scale developments and super high-rise buildings are being constructed. The Tianjin 117 Mega Tower is located in the Comprehensive Auxiliary Zone of Tianjin Software and Service Outsourcing Base, which is located to the west of the Tianjin City in the Xiqing District (Figure 1).

The total site area for the development is over 100,000m2, comprising a skyscraper, commercial buildings, a convention centre, luxurious shopping areas, luxury residences, service apartments and a polo sports club (Plate 1). The Tianjin 117 Mega Tower is the major element of the Client's Phase I development, which involves the construction of a 597m tall 117-storey tower with a 4-level basement accounting for a total excavation depth of over 26m. The gross floor area of the tower is about 370,000m2, with a footprint of 65m×65m at ground level, gradually reduced to 45m×45m at the roof level. When completed, this building will become the tallest building in North China. The tower will be used mainly as Grade A offices with the top 20 levels as 6-star hotel rooms. Entertainment facilities, restaurants and an observation deck will also be located at the top of the tower, featuring a diamond-shaped glazed top where guests can enjoy an eye-catching and spectacular view from the highest level of the city (Plate 2, Copyright© by P & T Group).

.

2 SITE CONDITIONS

2.1 Stratigraphy

Site investigation (SI) for the tower area was carried out in August 2008. 24 boreholes were located within the tower foundation footprint with drillhole depth varying from 140m to 196.4m. The scope of the site investigation included boreholes, SPT, wave velocity measurements, CPT, pressuremeter and lab tests, etc..

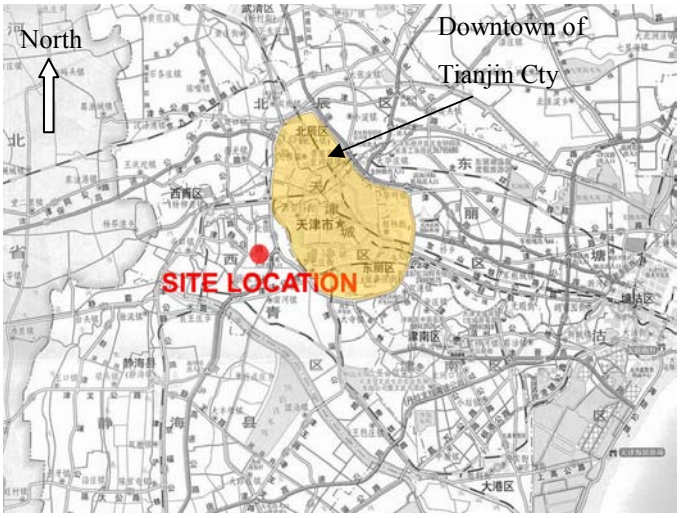

Figure 1: Site location (not to scale)

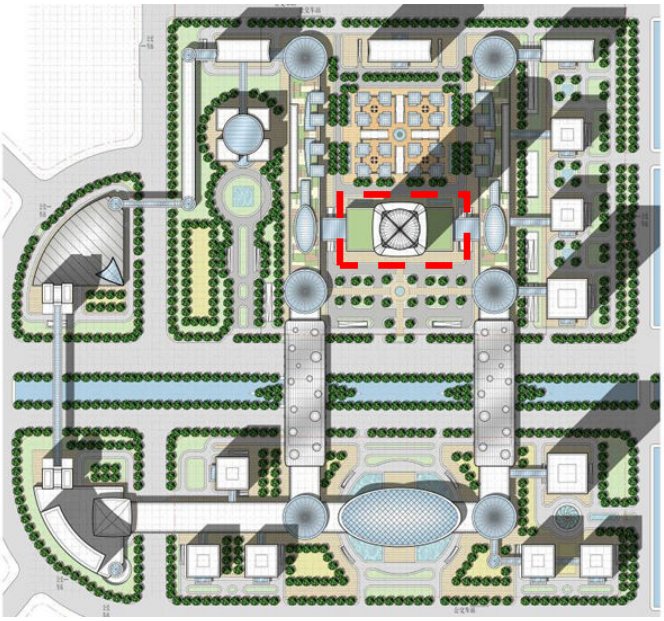

Plate 1: Master layout plan

Plate 2: Perspective of the tower

The topography of the site is generally gentle and flat, with a few gullies and a fishpond, which had been backfilled with construction wastes. The average ground level is +2.52m (Dagu Datum). The relative datum adopted was taken at +3.45m Dagu Datum. The ground is mainly composed of fill, Silt, silty Sand, silty Clay and Clay interbeddings.

The strength and deformation parameters were assessed by refereeing to the in-situ test results, stress level and lab-tests. Figure 2 gives an illustration of the SPT profile along depth. The silty Sand layer at around 100m or 120m in depth was considered to be a good founding layer for deep foundation.

2.2 Hydrogeology

Due to the presence of interbeddings of Silt, Sand and Clay layers, there are a number of aquifers underneath the site. It was observed that there were one phreatic aquifer and four confined aquifers within 100m in depth. The hydrostatic water level of the phreatic aquifer was at 2.1m~2.7m in depth during site investigation period, whilst that of the first confined aquifer was at 2.1m~2.9m in depth. All the phreatic and confined aquifers were found to be highly affected by adjacent excavation and dewatering works.

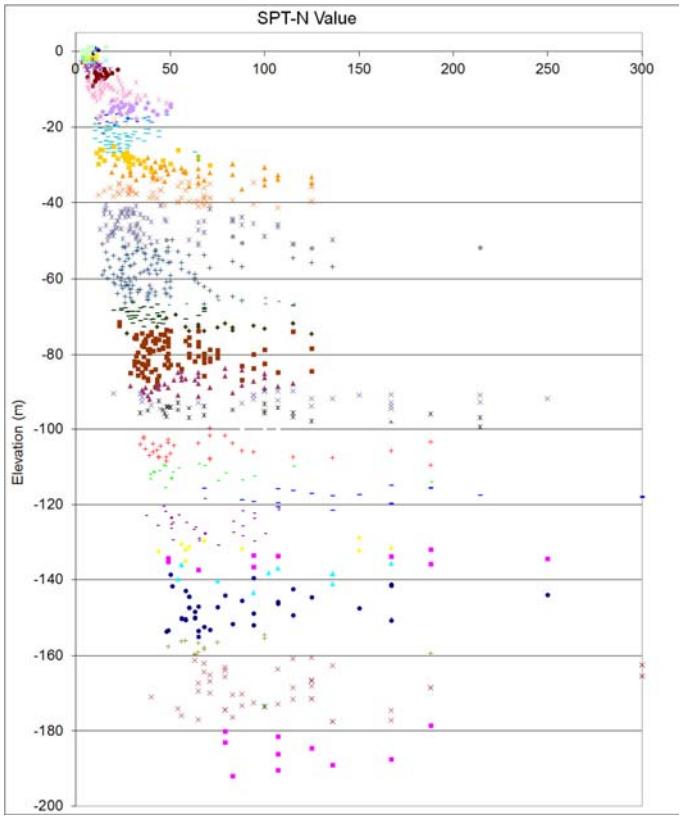

Figure 2: Profile of SPT-N value

2.3 Seismic effect

According to the Chinese National Standard "Code for seismic design of buildings" (GB50011-2010), the seismic precautionary intensity of the site is VII, the design basic acceleration of ground motion is 0.15g under the first design earthquake group, and the site is classified as Construction Site Category III.

Based on the site investigation, within the top 20m of the ground, there existed Silt layer 2-2, Silt layer 3-2, silty Sand layer 3-3 and Silt layer 4. In accordance with the National Standard GB50011-2010, standard penetration test results had been used to justify the liquefaction potential of the ground, and it was found that when the seismic intensity achieves VII with the highest groundwater level close to the ground surface, the site is assessed to be non-liquefiable.

3 FOUNDATION OPTION STUDY

Three options were proposed at the inception of the project – driven steel pipe pile, barrette and bored pile.

Steel pipe piles were used in two of the three mega towers in Shanghai, while for the third one under construction, Shanghai Centre, bored piles were adopted. Barrettes, which are commonly used for high-rise buildings in Hong Kong, are rarely used in Mainland China.

Comprehensive comparisons had been conducted at the schematic design stage (Table 1), and further discussions with local authorities were also made. It was concluded that the foundation scheme would adopt the use of bored piles, primarily due to: (1) cost considerations; (2) for barrette option, lack of competent contractors and construction expertise and no past experience locally.

4 TRIAL PILES

Based on the site investigation results, the characteristic value of single pile capacity of 76m and 95.5m pile (effective length) is in the order of 10.5MN and 14MN, respectively. It was decided to carry out trial piles before the design to verify the pile capacity and to identify appropriate construction parameters. Two

Table 1: Foundation option study

Issue	Bored Pile	Driven Steel Pipe Pile	Barrette
Construction Method	Commonly used	There were case histories with comparable height	Seldom used, may have difficulties finding competent contractors
Settlement (from past experiences)	Usually within predictable range	Often greater than predictions	No actual data
Approval	More straight forward	Straight forward	Envisaged difficulties due to lack of past experience and competent contractors
Construction from Ground Level	Yes	Yes	Yes
Impact on Adjacent Constructed Piles	Less effect	Without additional relieving works, may create additional lateral pressures on adjacent piles	Less effect
Material	High strength concrete maybe used, but little precedence	Available	High strength concrete maybe used, but little precedence
Cost	X	2.3X	1.3X
Overall	Recommended	Not recommended	Not recommended

packages with total 8 tests were carried out at Pile No. 3, 6, 9, 12 and S1, S2, S3, S4. C50 tremie concrete was used for concreting. Double-sleeves were used to minimize the frictional effects to sections of the trial piles from ground level to the design cut-off level of the corresponding working piles. Shaft grouting and toe grouting were adopted for Pile No. 3, 6, 9, 12, S1, S2, whilst only toe grouting was adopted for S3 and S4. Double cycle loading was carried out for Pile No. 6 and S1~S4. Typical pile load versus settlement curves are shown in Figure 3.

All trial piles were tested to 42MN without failure except S4 (Table 2, Table 3). The test results were carefully assessed and it was determined to use 76m effective length bored pile with a characteristic value of single pile capacity of 16.5MN in the design considering various construction factors.

Table 2: Trial pile test (Package 1)

Pile No.	Dimension	Construction length （m）	Effective length（m）	Final test load（MN）	Vertical disp.（mm）	Ultimate capacity（MN）
3	Φ1.00 × 120m	120.57	95.50	42	55.72	≥42
6	Φ1.00 × 120m	120.51	95.50	42	58.92	≥42
9	Φ1.00 × 100m	100.84	76.00	42	50.54	≥42
12	Φ1.00 × 100m	101.13	76.00	42	52.25	≥42

Table 3: Trial pile test (Package 2)

Pile No.	Dimension	Construction length （m）	Effective length（m）	Final test load（MN）	Vertical disp.（mm）	Ultimate capacity（MN）
S1	Φ 1.00 × 100m	98.49	76.00	42	47.62	≥42
S2	Φ 1.00 × 100m	98.40	76.00	42	52.54	≥42
S3	Φ 1.00 × 100m	98.33	76.00	42	56.96	≥42
S4	Φ 1.00 × 100m	98.27	76.00	42	93.54	37.5

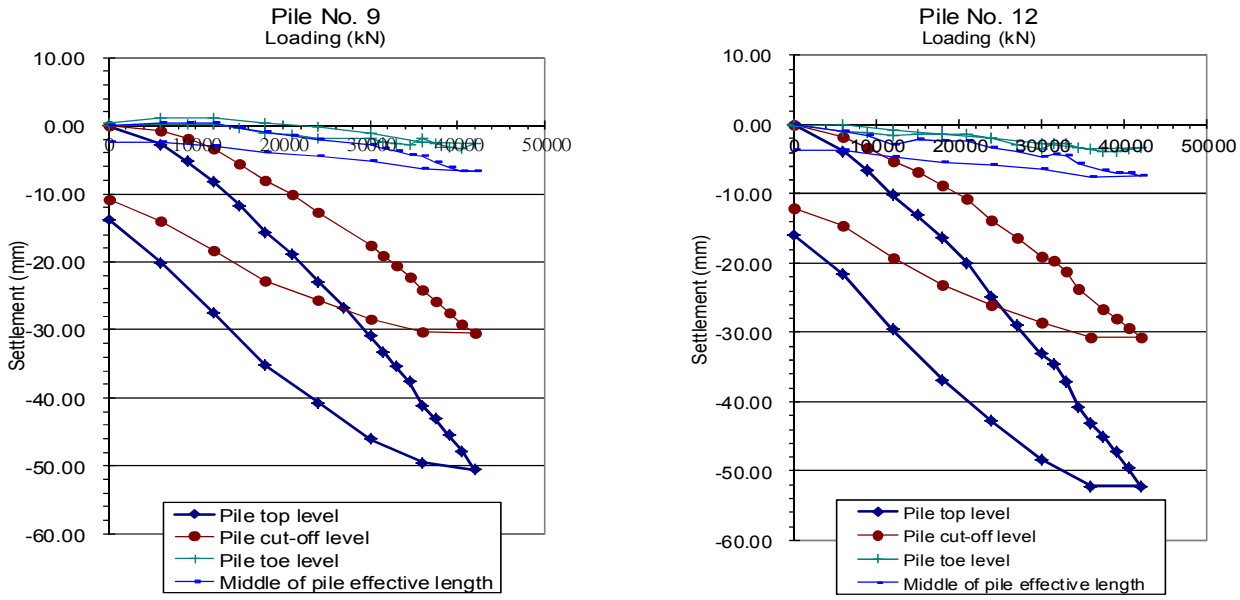

Figure 3: Load versus settlement curves of Pile No. 9 and Pile No. 12

5 PILE DESIGN

5.1 Structural system and loading schedule

The superstructure is composed of mega-brace tube and mega-frame as the perimeter structure plus the central core. Pile cap dimension was designed as 86m×86m×6.5m. Gravity loading information is listed at Table 4.

Table 4: Gravity loading schedule

Item	ETABS Results
DL(MN)	7,547
LL(MN)	1,392

Various nominal loading combinations of serviceability limit states were checked against pile geotechnical capacity, whilst different fundamental load combinations of ultimate limit states were checked against pile structural strength.

5.2 Settlement analysis and structure-pile-soil interaction analysis

In order to obtain more realistic input parameters for foundation settlement assessment, back analysis was conducted by simulating trial pile results with an axisymmetrical model using finite difference program FLAC-2D Version 6.0 software. The modulus of compressibility Es (Young's Modulus under K0 condition) values recommended by the SI contractor (SI contractor's recommendation is compulsory in Mainland China) were taken from the oedometer test results in accordance with in-situ stress level. These recommended Es values were nearly the same if correlating the in-situ SPT-N value by Es = 1×'N' = 'N' MPa. When the input Es value (an averaged value) in the numerical model is about 5 times of the recommended value from the SI report through sensitive analyses (concrete's elastic modulus is based on testing data and is in the order of 34.5GPa), the pile settlement curve is close to the corresponding trial pile result (Figure 4). Small strain Ed was also calculated from wave velocity test results, i.e., dynamic elastic modulus derived from the shear and compression wave velocity, vs and vp, and soil densities. The calculated Ed value is about 10 times of the Es value from oedometer tests. It is well known that soil stiffness decreases with the increase of strain. Soil stain of pile foundation is thought to be between small dynamic strain and large consolidation strain, which gives confidence to adopt the aforementioned calibrated Es values in analyzing structure-pile-soil interaction of pile group. In terms of pile group effect, for thick interbedding subsoil, if pile centre to centre (c/c) spacing ≥ 3D (D is pile diameter), the Chinese Industrial Standard "Technical Code for Building Pile Foundation" (JGJ94-2008) suggests to ignore such effect based on past experiences.

In order to study the rebound and recompression and settlement behavior of the pile group during pit excavation and basement and superstructure construction, a simplified axisymetrical model using FLAC-2D 6.0 was adopted. The 86m×86m square shape raft was simplified to a circular shape with the same planar area (See Figure 5); The pile group was simulated by 18 rows of solid elements (See Figure 6); Interface elements were adopted between the pile elements and the corresponding soil elements; Bulk modulus and shear modulus using the calibrated Es values for different soils (no other more reliable elasto-plastic soil parameters were available at that moment) and other soil physical parameters were adopted in the analysis. Following steps were simulated: (1) In-situ equilibrium state; (2) Pile and diaphragm wall installations; (3) Dewatering; (4) Pit excavation; (5) Basement and superstructure construction and groundwater resuming.

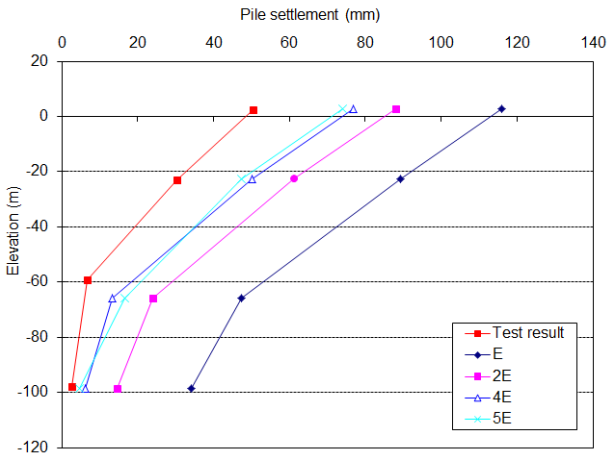

Figure 4: Sensitive analysis with single pile settlement

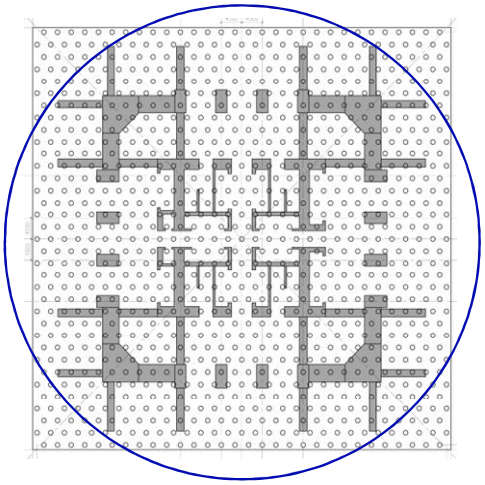

Figure 5: Equivalence of the raft from square to circular shape

In addition, a settlement calculation software VDisp and a structural finite element software SAFE were adopted to achieve a convergence of the iteration process of raft-pile-soil interaction. In this approach, a more elaborated 3D structural model using SAFE software was set up, in which the stiffness of superstructure, basement and pile cap was simulated, to check the reaction force and settlement of each pile. Detailed results of the two approaches as mentioned above are not shown here due to page limit.

The total settlement of the pile group is composed of pile group consolidation settlement, rebound and recompression of the excavation pit and elastic shortening of the pile shaft. Quasi-permanent load combinations of serviceability limit states were used to calculate the pile group settlement. On top of the finite differences and finite elements method as mentioned above, an equivalent pier layerwise summation method as specified in the Chinese Standard JGJ94-2008 was also used to check the settlements at centre point and corner point of pile cap, followed by a settlement contour analysis using VDisp. The approach at JGJ94-2008 adopts various coefficients to account for the effects of the shape, dimension and stiffness of pile cap, number of piles, pile dimension and spacing, post-grouting and etc., which are based on past experiences.

It was envisaged that about 35% of the total settlement would have been completed during building construction. The residual settlement was estimated as shown in Table 5.

Table 5: Residual settlement after building construction

Consolidation settlement (mm)	Rebound and recompression (mm)	Pile shaft elastic shortening (mm)	Residual settlement (mm)
112	58	0	170

5.3 Foundation scheme

Based on pile option study, trial piling results, envisaged loading schedule and distribution, pile reaction and settlement analysis results, the final pile foundation scheme is to have 941 nos. bored piles using C50 tremie concrete (Figure 7), 76m effective length, 3m c/c, and the rebar ratio of majority of the piles is less than 3%.

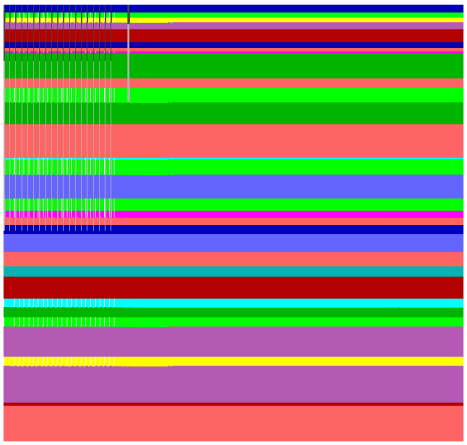

Figure 6: Axisymetrical FLAC-2D model (200m wide, 196m deep)

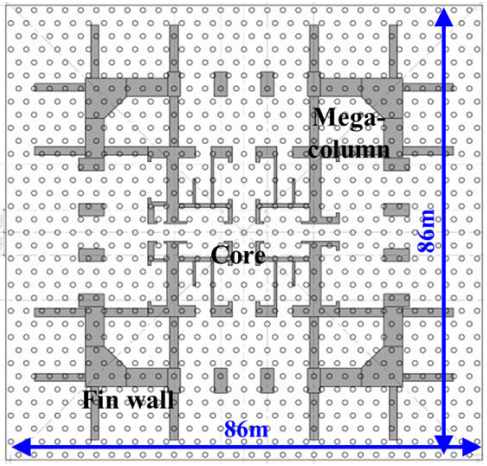

Figure 7: Plan layout of working piles

6 CONCLUSIONS

Upon careful foundation option study, large-scale trial piling, as well as comprehensive calculations and analyses, the 76m effective length slender bored pile scheme for Tianjin 117 Mega Tower had been verified and was put forward for construction. All piling works had been successfully completed by 2010 with all the necessary post-construction pile loading tests, coring, and pile integrity tests completed. Whilst the super-structure construction is underway, field instrumentation is still ongoing. The pile group behavior will be further reviewed once the field instrumentation data are available.

ACKNOWLEDGEMENTS

The authors would like to express their gratitude to the Technical Sub-committee of HKIE Geotechnical Division for their constructive advices to this paper. Comments from Ir. James W. C. Sze are also highly appreciated.

3D Finite Element Analysis for Deep Foundation Case Histories

F. Tschuchnigg & H.F. Schweiger
Graz University of Technology, Graz

ABSTRACT

In this paper results from numerical analyses of two deep foundation projects are presented. The first project concerns the deep foundation for the Donau City Towers in Vienna. Due to the fact that the towers are located very close to each other interaction between the two towers has to be taken into account by means of three-dimensional numerical modelling. In the second part of the paper the foundation of a tower which is part of a shopping mall in Bucharest is considered. Again, due to the geometric layout 2D analyses proved to be too conservative and therefore a number of 3D analyses have been performed. Different arrangements of diaphragm wall panels have been investigated to find an economical and technical feasible solution for the layout of the foundation elements. It could be shown for both projects that the chosen foundation concept leads to acceptable settlement behaviour.

1 INTRODUCTION

Deep foundations such as pile foundations require in general three-dimensional numerical analyses because in general the geometry and the layout of the foundation elements do not allow a plane strain representation. One of the key aspects in numerical modelling of this type of problems is an appropriate model to take into account the interaction between piles or diaphragm wall barrettes and surrounding soil. This interaction behaviour is different depending on the type of foundation, e.g. piled raft foundations as compared to a standard pile foundation, and strictly speaking also depends on pile type and the construction method. When foundation elements are modelled with volume elements so-called interface elements with specified (frictional) properties are usually employed to model the interaction between pile and surrounding soil. The disadvantage of modelling individual piles with volume elements is the large number of elements required leading to very demanding numerical models. Another option for modelling piles is the concept of a so-called embedded pile element. This special element consists of a beam element which can be placed in arbitrary direction in the subsoil, embedded interface elements to model the interaction of the structure and the surrounding soil and embedded non-linear spring elements at the pile tip to account for base resistance.

2 EMBEDDED PILE CONCEPT

The advantage of this concept is that different pile lengths, spacing and orientations can be studied without regenerating the entire finite element mesh. If a large number of piles have to be considered the number of elements in the system is significantly reduced as compared to finite element models with volume piles. Although the diameter d is assigned to the embedded beam element, it remains a line element in the finite element model. When modelling an embedded pile additional nodes are automatically generated inside the existing finite elements and the pile-soil interaction behaviour is linked to the relative displacements between the pile nodes (u_p), the virtual soil nodes (u_s) and the embedded interface stiffnesses K (Sadek and Shahrour, 2004). Additional to the diameter d which determines an elastic zone in the soil around the beam in order to avoid failure in a soil element (Engin, 2006), the unit weight γ, the stiffness E and the maximum skin and base resistance has to be assigned to an embedded pile. It is important to notice that this definition implies that the bearing capacity of the pile is an input and not a result of the analysis. Figure 1 illustrates the embedded pile concept. In order to assess the applicability of the embedded pile approach for practical problems various examples from the literature have been recalculated employing the embedded pile concept. Details of this comprehensive study can be found in Tschuchnigg (2013).

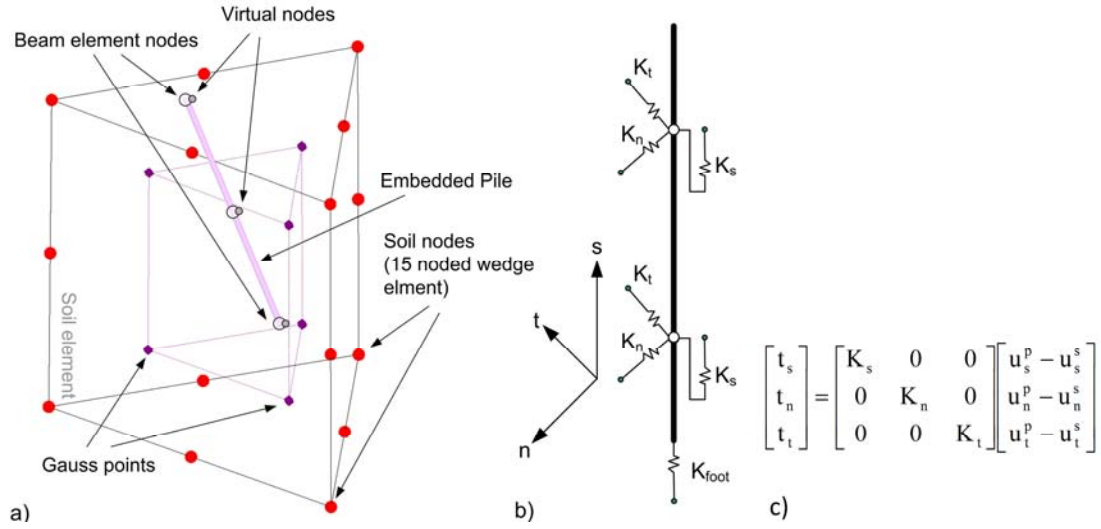

Figure 1: Embedded Pile concept: (a) Schematic overview, (b) Embedded interface stiffnesses, (c) Constitutive equation

3 CASE HISTORY I – DONAU CITY TOWERS VIENNA

3.1 Project overview

The projects discussed are two very high and slender towers. In this particular case the deep foundation elements have the form of diaphragm wall barrettes with a unit length of 3.6 m and a unit width of 0.6 m. Tower I has a total height of about 220 m and tower II of 165 m. It is planned to build the foundations for both towers at the same time but to construct the superstructure of tower I first. Due to the fact that the distance between the two towers is only 24 m it is necessary to take the loads from the later built tower II into account for the design of the foundation system of tower I. The excavation depth for constructing the base slabs of both towers is about 8.5 m.

3.2 Soil conditions and numerical modelling

The soil profile as defined in the finite element calculations is based on core drillings with depths down to 70.0 m. The first 4 to 5 m consist of deposits, followed by a 6.5 m thick layer of gravel and then alternate layers of either sands or sandy silts are present (Martak *et al*. 2008). The Hardening Soil Small model (HSS), as implemented in the finite element code Plaxis 3DF (Brinkgreve and Swolfs, 2007), is used to model the soil behaviour (Benz, 2007). The HSS model needs, compared to the Hardening Soil Model (for details see Schanz et al. 1999), two additional parameters to describe the stiffness behaviour at small strains. These are the initial shear modulus G_0 and the shear strain level $\gamma_{0.7}$, which represents the shear strain where the secant shear modulus is reduced to 70% of its initial value. Detailed information about the geological conditions and the soil properties are given in Tschuchnigg & Schweiger (2010). All slabs behave linear elastic and the diaphragm wall elements are modelled with the Mohr-Coulomb model (linear elastic - ideal plastic model). In addition the tensile strength of the barrettes is limited to a value of 3000 kPa.

3.3 Results

All calculations are carried out as a drained analysis, thus final settlements are presented. To obtain realistic final deformations a reliable stress distribution in the soil after the excavation is required, consequently it is necessary to model the construction process. In total 10 calculation phases were modelled in all FEA. For the generation of the initial stress state it is important to take the overconsolidation of the soil into account. This is done with the so called pre-overburden-pressure (POP). For all soil layers a POP value of 600 kPa is defined and the earth pressure coefficient K_0 is increased from K_0^{nc} to a value of 0.7. As a consequence the volumetric

and deviatoric yield functions are shifted and the elastic region of the Hardening Soil Small model is increased. Figure 2a shows a top view of the finite element model used and additionally some geometrical information of the project. This model consists of around 137 000 15-noded wedge elements and the 317 diaphragm wall barrettes are modelled as volume elements. In order to obtain a reasonable symmetric settlement trough despite a highly non-symmetric load distribution with respect to the centre of the foundation slab the length of the barrettes varies across the foundation slab. Several calculations have been performed to optimize this layout. Figure 2b illustrates the final layout of the deep foundation elements and the contours of calculated vertical displacements. Results of this model will not be discussed in detail here (see Tschuchnigg and Schweiger 2010). But a numerical study was performed to investigate whether a piled raft foundation with a smaller number of piles would have been feasible from a theoretical point of view, not considering other issues (contractual or conceptual) which may have prevented such a solution for this particular project. In the following different piled raft geometries are presented and emphasis is put on the different modelling strategies of piled raft foundations. The first layout considered consists of 75 piles (referred to as layout 1 in the following). The piles are modelled by means of volume piles (VP) and alternatively by embedded piles (EP). The models consist of approximately 240 000 elements and the pile length varies between 20 - 30 m, similar to the final concept with diaphragm wall panels. The aim of these analyses is mainly a comparison of the two modelling approaches. In this calculation the pile-soil interaction, when using volume elements for the piles, is taken into account by means of interface elements with a strength reduction factor R_{inter} of 0.8. When using the embedded pile approch the shaft and base resistance of the pile is an input and not a result of the analysis. The influence of ultimate embedded pile capacity on the embedded pile behaviour is investigated in Tschuchnigg & Schweiger (2009). And the effect of different definitions of the pile-soil interaction on the settlement behaviour of the Donau City Towers is studied in Tschuchnigg & Schweiger (2010). Figure 3a shows that the maximum vertical displacements obtained from both models are almost identical. However, both the maximum vertical displacements and the differential settlements are not acceptable from a practical point and as a consequence the layout is modified in a way that the spacing of the piles is decreased in the high loaded regions (layout 2). In this model the number of piles is 113 for tower 1 and 128 for tower 2 respectively. The length of the piles is again similar to the barrette foundation.

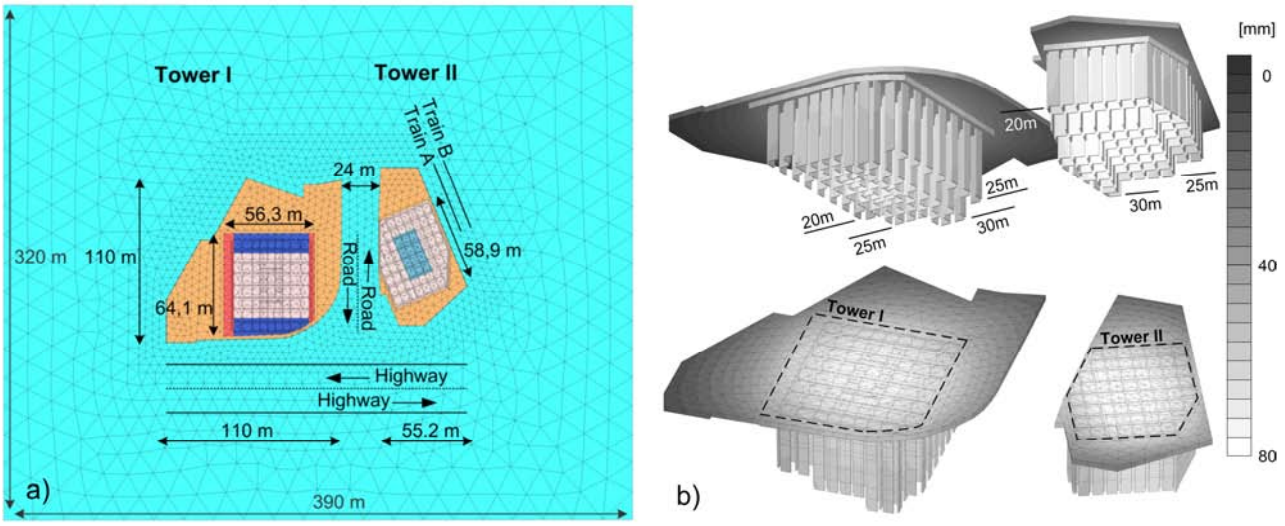

Figure 2: (a) Top view of 3D FE model, (b) Optimised barrette layout for tower I and tower II

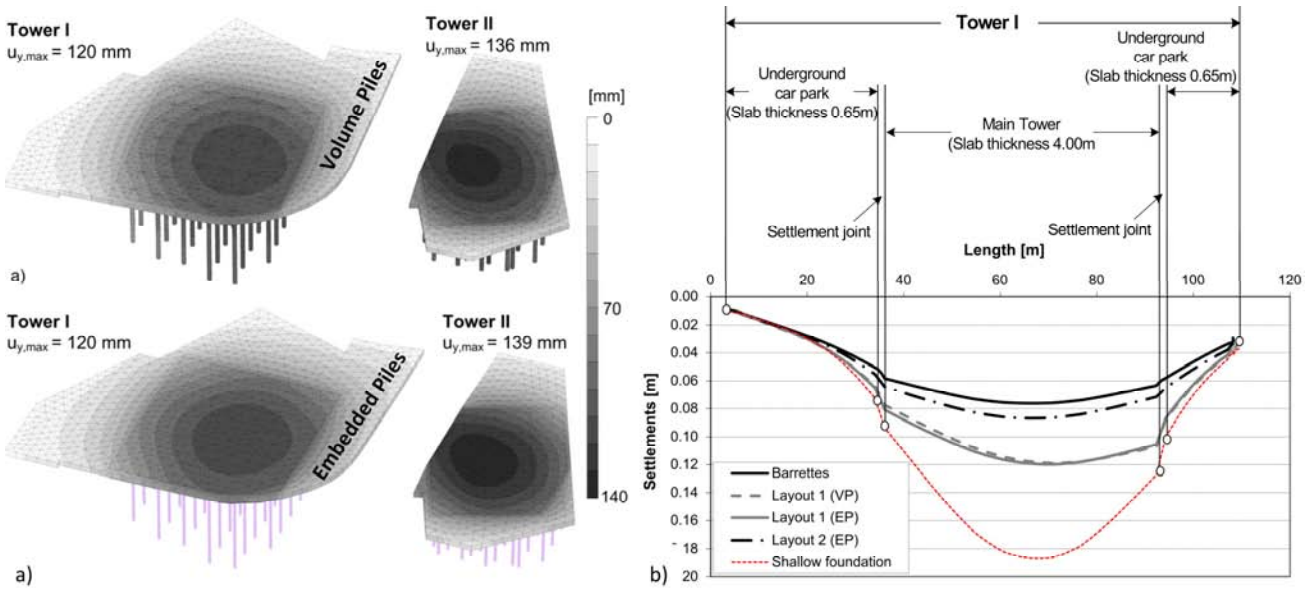

Figure 3: (a) Contours of vertical displacements for layout 1, (b) Comparison of settlement troughs

This piled raft foundation reduces maximum vertical displacements of tower I from 120 mm to 87 mm and settlements of tower II from 139 mm to 88 mm. Also the differential settlements are significantly reduced. Figure 3b shows the calculated settlement troughs of tower I (cross section through the centre of the raft) for the different models. The barrette foundation concept is compared with piled raft foundation layout 1, layout 2 and a shallow foundation, which is added here purely for the comparison because this option is of no practical relevance as it yields, as to be expected, too large vertical and differential settlements. At the time of this writing the tower I is still under construction having reached its final height, but is not yet completely finished. Measured settlements so far amount to approximately 40 mm. Considering that some changes have been introduced as compared to the assumptions made in the analysis and taking into account that variable loads and long term effects are not included in this figure it can be concluded that the calculated settlements provided a reasonable but somewhat conservative estimation of the actual settlement behaviour.

4 CASE HISTORY II – SKY TOWER

4.1 Project description

The Sky Tower is part of the so called Floreasca City Center in the north-eastern part of Bucharest. The site consists of the Promenada mall which is the shopping and entertainment centre and two office buildings, namely the Office Wing and the Sky Tower. With a total height of more than 130 m the latter will be the highest building in Bucharest. The deep foundation concept is similar as for the previous example and consists of diaphragm wall panels. The top view of the project layout is shown in Figure 4a. The excavation has a maximum length of 93.4 m and a maximum width of 61.7 m. The bottom of the foundation slab is 20.4 m below the ground surface. The two egg-shaped areas represent the regions where high point loads, up to 14 900 kN are acting. The thickness of the foundation slab is 2.5 m in the inner region of the excavation pit and 1.6 m in the outer areas. The diaphragm wall panels have a thickness of 0.8 m beneath the high loaded areas and the sensitive zones and 0.6 m in the other regions respectively. The diaphragm wall which acts as a retaining wall for the excavation and as a foundation element has a thickness of 1.0 m. It is planned to install the deep foundation elements from the ground surface and to realise the excavation afterwards with the top-down method. As a consequence the panels are acting as tension elements (against uplift) and minimise the heave during excavation. Due to the high loads in the core of the construction large differential settlements of the foundation slab are expected. The aim of the 3D finite element analysis is to find an optimum layout for the deep foundation elements in order to minimise both the total deformations and, even more important, the differential displacements of the slab. Therefore different arrangements of diaphragm wall panels have been

investigated to find an economical and technical feasible solution for the layout of the foundation elements (see Tschuchnigg and Schweiger 2010), but only the final foundation arrangement will be presented here.

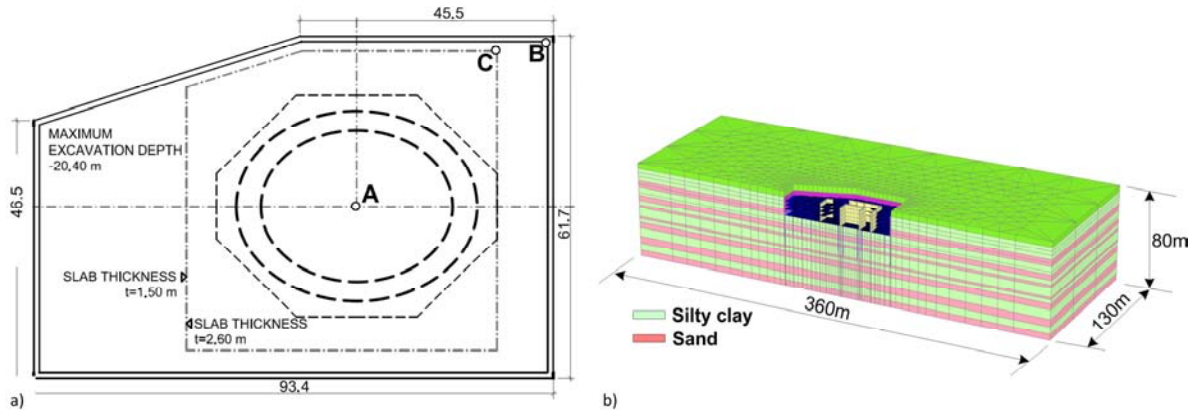

Figure 4: (a) Top view of construction layout, (b) FE model with illustration of ground profile

The soil profile for the finite element simulation is based on core drillings with depths down to 60.0 m from the surface. All borehole logs show alternate layers of either sands or silty clays (Figure 4b) with layer thicknesses between 1 to 8 m. All walls and floors in the FE model behave as linear elastic material with a Young's modulus of 3E7 kN/m^2 and a Poisson's ratio of 0.2. The diaphragm wall elements are modelled with volume elements and described with the Mohr-Coulomb model. The tensile strength of the barrettes is limited to a value of 3 000 kPa.

4.2 Results

All calculations in this paper are drained analysis, which means final settlements are presented. This seems to be justified because of the alternate layers of sands and silty clays, which speeds up the consolidation procedure. The real building process was modelled with 15 calculation phases. To include the high stiffness of the superstructure, which influences both the stress distribution in the foundation slab and the calculated settlements, the core walls of the basement floors are also modelled. The displacements presented and discussed in the following are obtained after the final calculation phase. The final layout of barrettes consists of two discontinuous circles of panels which are arranged in the area of concentrated loads (Figures 5). Only a quarter of the structure was modelled, which allows for a finer discretization at the same time keeping the model size within acceptable limits. The vertical settlements calculated are about 105 mm. Figure 6a shows the contour lines of vertical displacements of the entire 3D model. The differential settlements of the foundation slab are presented in Figure 6b. Between point A and B about 65 mm of differential settlements are expected and approximately 47 mm within the 2.6 m thick slab (point A to point C). A further variation involves the replacement of a sand layer by a silty clay layer below -60 m in order to take the uncertainty with respect to ground conditions at deeper layers into account. It follows from this calculation that settlements increase by 10 mm to approximately 115 mm.

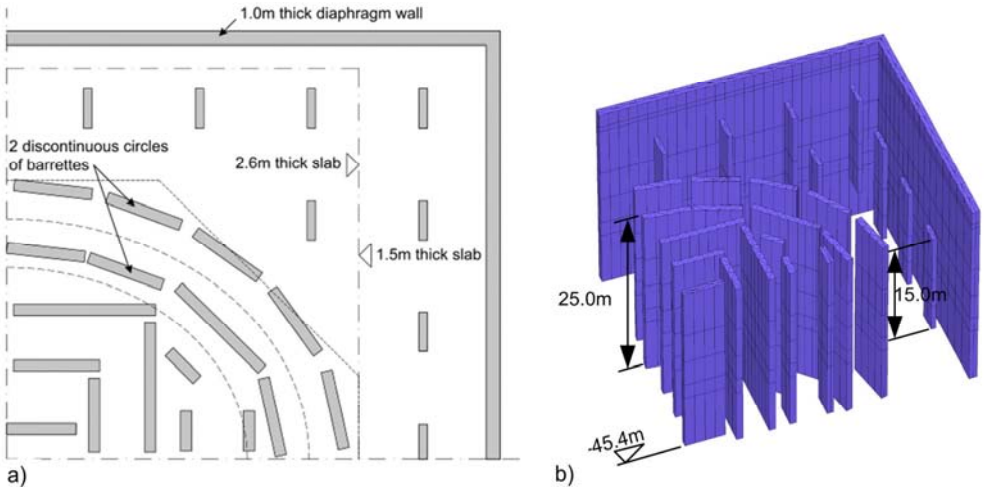

Figure 5: (a) Top view of final foundation concept, (b) 3D view of arrangement of barrettes

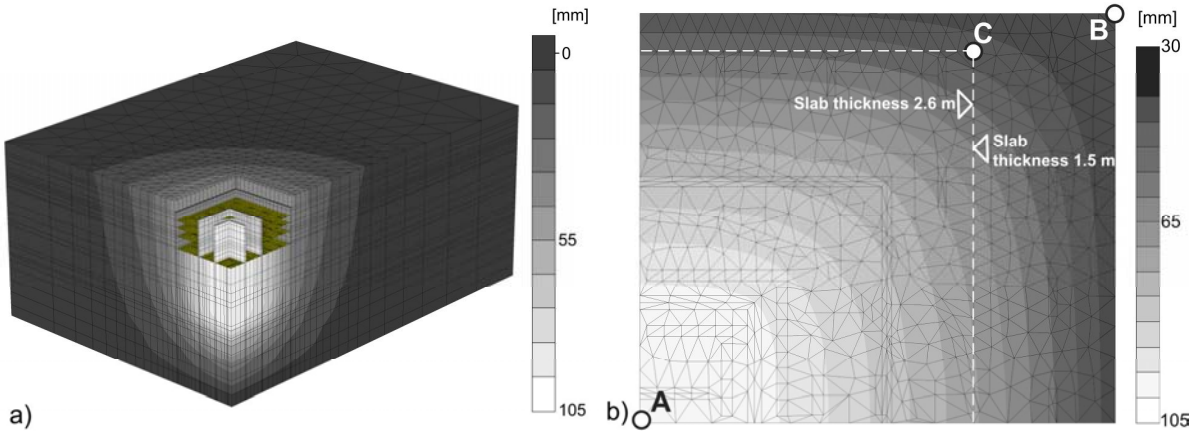

Figure 6: (a) Contours of vertical displacements, (b) Contours of vertical displacements of the foundation slab

5 CONCLUSIONS

3D finite element analyses for two case histories involving deep foundations have been presented. In the first example the settlement behaviour of two adjacent towers (DC-Towers Vienna) has been assessed. As a consequence of eccentric loading conditions and the small distance between the two towers the deep foundation elements have different lengths at different positions. The designed foundation system consists of diaphragm wall panels with lengths between 20 to 30 m. The expected settlement of both towers is less than 80 mm. Emphasis has been put on modelling aspects, namely employing a standard technique where the foundation elements are modelled by means of volume elements and a computationally more economic technique employing a so-called embedded pile formulation. It could be shown that both modelling techniques yield very similar results. Thus it can be concluded that the embedded pile concept is a very attractive technique of modelling large pile groups in numerical analyses. The second example concerns the settlement behaviour of the Sky Tower, Floreasca City Center in Bucharest. Due to the geometric layout 2D analyses proved to be too conservative and therefore a number of 3D analyses have been performed investigating different arrangements of diaphragm wall panels. The final concept of the deep foundation consists of two discontinuous circles of diaphragm wall panels beneath the high loaded areas. Expected maximum settlements are in the range of 105 mm and differential settlements in the foundation slab around 65 mm.

REFERENCES

Benz, T. 2007. Small-strain stiffness of soils and its numerical consequences. *Ph.D. Thesis, Mitteilungsheft Nr. 55, Institute for Geotechnical Engineering*, University of Stuttgart.

Brinkgreve, R.B.J. and Swolfs, W.M. 2007. *PLAXIS 3D Foundation, Finite element code for soil and rock analyses, Users Manual*, Plaxis bv, Delft, The Netherlands.

Engin, H.K. 2006. *A report on embedded piles*, Plaxis internal report.

Martak, L., Mayerhofer, A.F., Tschuchnigg, F. and Vorwagner, A. 2008. Bahnhof Wien Mitte – Ein zentrales Infrastrukturprojekt im Herzen Wiens, *Proc. 23th Christian Veder Kolloquium*, M. Dietzel et al. (eds.), Graz, pp 79-96.

Sadek, M. and Shahrour, I. 2004. A three dimensional embedded beam element for reinforced geomaterials, *Int. J. f. Numerical and Analytical Methods in Geomechanics* 28(9), pp 931-946.

Schanz, T., Vermeer, P.A. and Bonnier, P.G. 1999. The Hardening-Soil Model: Formulation and Verification. *Beyond 2000 in Computational Geotechnics, Brinkgreve* (ed.), Rotterdam, Balkema, pp 281-290.

Tschuchnigg, F. & Schweiger, H.F. 2009. Numerical study of simplified piled raft foundations employing an embedded pile formulation. *Proc. intern. Conf Conference of Computational Geomechanics*; S.Pietruszczak et al. (eds.), Juan-les-Pins, 2009, pp. 743-752.

Tschuchnigg, F. and Schweiger, H.F. 2010. Study of a complex deep foundation system using 3D finite element analysis, *Proc. European Conference of Numerical Methods in Geotechnical Engineering*, Benz & Nordal (eds.), Trondheim, 2-4 June 2010, pp 679-684.

Tschuchnigg, F. and Schweiger, H.F. 2011. Comparison of deep foundation systems using 3D Finite Element analysis, *Proc. 13th Intern. Conf. Computer Methods and Advances in Geomechanics,* Khalili & Oeser (eds.), Melbourne, 2011, pp 970-975.

Tschuchnigg, F.; Schweiger, H. F; Fröhlich, K. 2010. 3D Finite Element analysis of a deep foundation with diaphragm wall panels. *Proc. Int. Geot. Conf., Geotechnical Challenges in Megacities*, Moscow, GRF, St. Petersburg, Vol.2, 471-478.

Tschuchnigg, F. 2013. 3D Finite Element Modelling of Deep Foundations Employing an Embedded Pile Formulation. *Ph.D. thesis, Mitteilungsheft Nr. 50*, Graz University of Technology.

A Case Study of Marine Structures Foundation Design

Henry Wang, Herman Wong & Eddie Wong
AECOM Asia Company Limited

ABSTRACT

This paper presents a case study of foundation design of marine quay structures as an extension to an existing container terminal. The project site is located at Port Said East of Egypt at the northern end of Suez Canal in Egypt and lies within seismic zone 3 as defined in the relevant Egyptian Code.

The soil stratification at the site comprised of a number of interbedded layered cohesive and cohessionless soils extending to a considerable depth of approximately 60m. Conventional rectangular and T-shape barrettes were used as foundation of the quay structures. Transverse and capping beams are constructed to connect the barrettes together to form a quay deck. A curtain wall in form of diaphragm wall was placed between the front row barrettes to maintain the required dredged level in front of the quay deck. Sophisticated numerical 3-dimensional static and 2-dimensional dynamic analyses were carried out for foundation design to demonstrate on compliance on deformation limits in all the construction, operation and earthquake conditions.

Complexity of ground conditions gave a major challenge in this project. The base layer of soft clay turn out to be under-consolidated and to be thicker than the originally assumed as uncovered in the additional ground investigation carried out after the contract award.

1 INTRODUCTION

1.1 Project Descriptions

The Port Said Container Terminal, Phase 2 project (Project) is situated in Port Said, Egypt at the mouth of the Suez Canal on the Mediterranean Sea. It is a major transshipment hub for the Eastern Mediterranean region. Figure 1 presents the Site Vicinity Map. The project involves the construction of the port facilities incorporating all marine and port related infrastructures as the extension to the existing container terminal Phase 1. The site layout is presented in Figure 2. The proposed quay structure is 1200m long in the structural form of reinforced concrete barrettes with curtain (diaphragm) walls at waterside and landside. In addition, internal barrettes are constructed between curtain walls. Transverse beams and capping beams are connecting between barrettes. Suspended slabs are spanning one-way over transverse beams. The major scopes of design works include design of quay structures foundation, as well as dredging, reclamation and ground improvement works. The quay structure and associated fittings are mainly designed in order to:-

- Provide 1200m of operational continuous quay for berthing and mooring of container vessels and feeder vessels in the range 212 TEU to 14,500 TEU;
- Support high-capacity rail-mounted electrically operated ship-to-shore gantry cranes and container handling equipment;
- Provide access for delivery, erection, commissioning, operation and maintenance of quay-side gantry cranes, vessel berthing and mooring operations, victualling, bunkering and stores to vessels for emergency vehicles and emergency escape routes;
- Provide stowage pin and anchorage points slots for securing the quay-side gantry cranes against movement parallel to the quay and overturning; and
- Provide for handling and storage of containers and vessel hatch covers under the crane or the backreach, and for tractor-trailer operations.

Figure 1: Site Vicinity Map

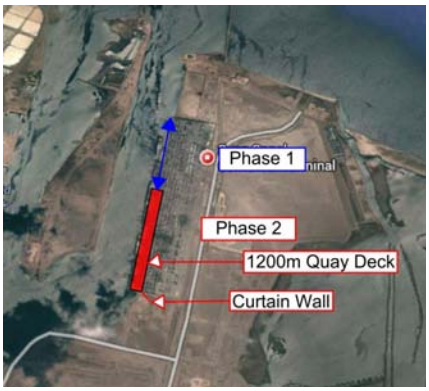

Figure 2: Site Location Plan

1.2 Foundations Descriptions

The quay structure is about 1200m long and 35m wide approximately. Deck level is generally about +2.5mCD. Berth pocket in front of quay structure was dredged down to -17.5mCD but it was designed to allow for future deepening to -18.5mCD. Dredging limit is also the site boundary which is 135m approximately seaward of the 1200m long copeline. Existing ground at landward of 45m approximately behind the landside edge of quay structure was treated to mitigate the risk of liquefaction under the designed earthquake events. The general port layout is shown in Figure 3.

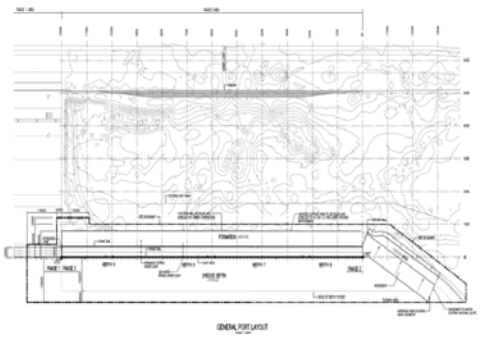

Figure 3: General Port Layout

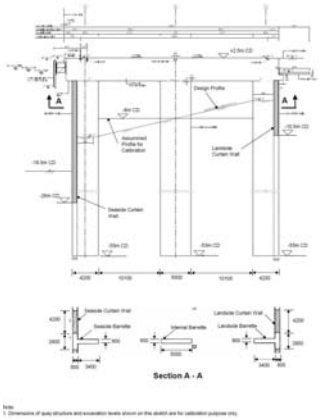

Figure 4: Typical Section of Quay Structure

Figure 5: Barrette Construction

Three rows of cast-in-situ reinforced concrete T-shape barrette / diaphragm wall with tie-beams was proposed after various options of quay structures had been considered. The performance and form of the proposed structure are similar to the foundation option (four rows of diaphragm wall per grid) of existing Phase 1 but the construction time would be shorter and early completion of the quay could be achieved. The proposed option would also cause less disruption to the existing terminal and canal operations. A reinforced concrete tie beam is connected between the front wall panel and the rear anchor wall panel. The seaside crane beam is supported on the front T-shape barrette and the landside crane beam is supported on the rear T-shape barrette. There is a middle diaphragm wall between the seaside and landside diaphragm walls i.e. three rows of diaphragm wall per grid. Curtain walls are as lagging for the T-shape barrettes. The typical section of the

quay structure is shown on Figure 4.

1.3 Design Considerations

The design life of the quay structure is 50 years. The quay structure is designed for berthing and mooring of container vessels and feeder vessels in the range 212 TEU to 14,500 TEU and supporting high-capacity rail-mounted electrically operated ship-to-shore gantry cranes and container handling equipment. Stringent settlement limitation is imposed to ensure safe operation of gantry cranes and container handling equipment on quay-side gantry crane tracks. It limits net vertical rail displacement produced under working loads to a maximum of 15mm with the design life of the crane rails.

The project site lies within Zone 3, which corresponds to earthquake intensity level VIII, as defined in the "Regulations for Earthquake-Resistant Design of Buildings in Egypt, 1998". The quay structure has to be designed to satisfy the performance requirements under the design earthquake. For seismic design, the performance-based design method as described in the "Seismic Design Guidelines for Port Structures", PIANC Working Group 34, 2001 (WG34) is adopted as the main guidance document. Two earthquake event levels (Level 1 & Level 2) were considered with different acceptable degree of impacts to the quay structure. Level 1 earthquake event (L1) and Level 2 earthquake event (L2) are motions with probability of exceedance of 50% and 10% during the lifespan of a structure respectively. The earthquake events L1 and L2 correspond to the design earthquake events with return periods of 72 years and 475 years.

2 SITE GEOLOGY AND CONIDTIONS

The soil stratification at the site comprises a number of inter-bedded layers of cohesionless and cohesive materials extending to considerable depth below current ground level. The descriptions of the stratigraphies and properties of soils are outlined as below. A typical geological profile is shown in Figure 6.

Soil Unit 1: Surcharge material placed on the Phase 2 site prior to the commencement of the Contract. The Unit generally comprises silty sands with shell fragments but may also contain layers of silt and clay. This Unit has been overlain in parts by sands, silts and clays removed from the area of the Phase 1 works during construction.
Soil Unit 2: Hydraulically placed material derived from excavations for the nearby Suez Canal by-pass channels. The Unit variously comprises layers of very soft to soft clay, highly dilatants sandy silt and dilatants silty sand, sometimes with shell bands.
Soil Unit 3: Generally a medium dense to dense, becoming very dense, fine to medium naturally occurring sand with many sand-sized shell fragments. The top level of this Unit tends to deepen and the stratum to thin towards the south of the Site. The stratum becomes inter-layered with clay in the south.
Soil Unit 4: An inter-layered deposit of very soft to firm clay, clay/silt and clayey silty fine sand. The Unit is predominantly cohesive.
Soil Unit 5: Consists of a considerable thickness of soft clay which becomes soft to firm and more plastic with depth. This about 30m – 40m thick layer of soft clay imposed the major challenge in this project. It was found under-consolidated with low undrained shear strength of 20kPa - 70kPa. The additional ground investigation after contract award indicated it is thicker than the originally expectation. This layer contributed the major movement of the quay structure under both construction and operation stages.
Soil Unit 6: Consists of generally dense to very dense, slightly silty to silty, slightly gravelly, fine to medium sand.
Soil Unit 7: Generally found as inter-bedded layers within Soil Unit 6 and comprises stiff to very stiff, highly plastic clay.

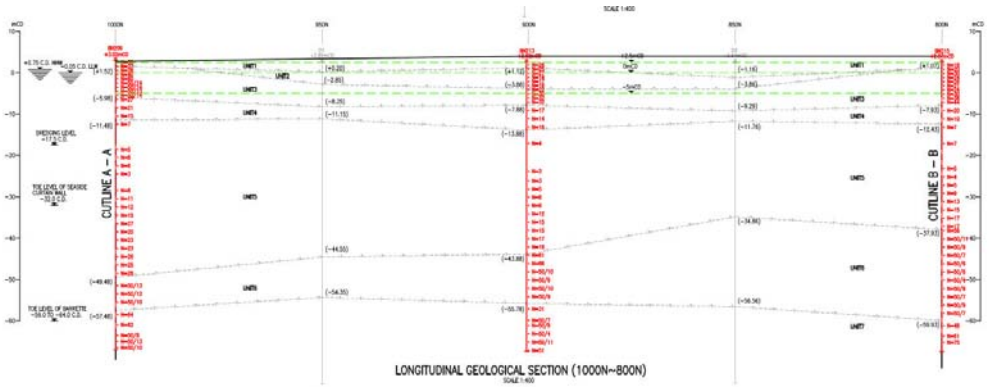

Figure 6: Typical Geological Profile along Quay Structure

3 DESIGN METHODOLOGY AND ANALYSIS APPROACH

3.1 Analysis Approach

From the site specific ground investigation record, the base layer of soft clay turned out to be under-consolidated and to be much thicker than the expectation. This soft layer contributed the major movement of the proposed quay structure. To take into account this non-typical soil-structure interaction in structural analyses, a calibration exercise was carried out to verify the validity of the soil spring and earth pressure used for structural analysis. In addition, sophisticated numerical 3-dimensional static and 2-dimensional dynamic analyses were carried out for foundation design to demonstrate on compliance on deformation limits in all the construction, operation and earthquake conditions as mentioned in Section 1.3.

3.2 Calibration of Soil Springs for Structural Analysis

The structural analysis of proposed quay structure was carried out by using 3-D structural analysis program, namely Microstran V7, which cannot take account of soil-structure interaction. In order to verify the validity of the soil spring and earth pressure used for structural analysis, a calibration exercise had been carried out by comparing the structural analysis results of a 7m pile bent, with that from 3-dimensional soil-structure interaction analysis by using PLAXIS 3D. The typical section of the quay structure as shown in Figure 4 was used in calibration exercise for comparison purpose.

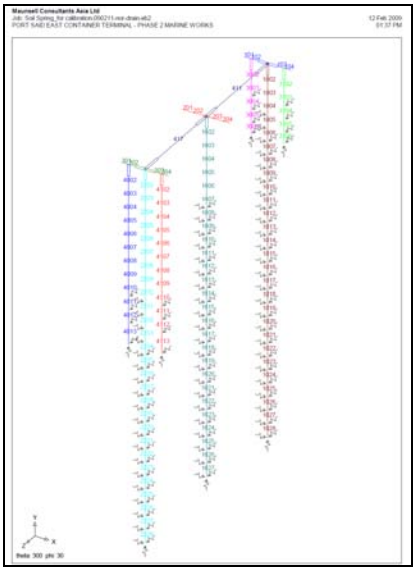

Figure 7: Microstran Model for Calibration

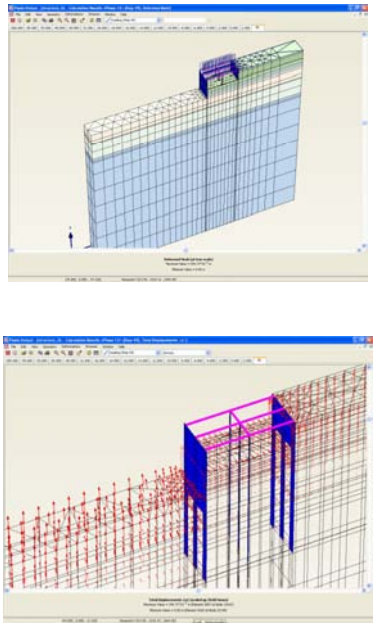

Figure 8: PLAXIS Model for Calibration

The soil strata as shown in Table 3.1 were adopted for the calibration models. The adopted geological profile is a typical profile of the site.

Table 3.1 – Soil Strata for Modeling

Soil Unit	Top Level of Soil Unit
Unit 2	+2.5m CD
Unit 4	-12m CD
Unit 5	-16m CD
Unit 6	-50m CD

In the structural model, lateral resistance of soil to embedded structural element was simulated by provision of soil springs determined from soil modulus. The coefficient of subgrade reaction would be corrected with a reduction factor for the effect of pile group subject to lateral load. The pile reduction factor for coefficient of sub-grade reaction for a lateral loaded pile group was made reference to Canadian Foundation Engineering Manual. The vertical spring stiffness was derived based on settlement calculation.

At-rest hydrostatic earth pressure was adopted for structural analysis. The initial stress in the model is generated using Ko procedure by PLAXIS. The initial pressure diagram generated was provided below. The pressure distribution generated using PLAXIS and the at-rest hydrostatic earth pressure for the structural model are found compatible. Passive Soil Resistance in the structural model was modeled as the maximum allowable reaction force at individual soil spring of the structural model which was considered equivalent to the passive soil pressure provided by the equivalent area covered by the spring.

For structural analysis, soil spring for long term condition (i.e. drained condition) was adopted. The reaction at individual spring would be checked. In case the reaction force exceeded the passive earth pressure, the spring would be removed and replaced with the allowable passive resisting force. For deformation assessment, PLAXIS 3D Analysis was adopted to simulate the staged excavation and evaluate the ground movement and soil-structure interaction throughout the excavation and application of operation loads. The barrette and curtain wall elements used in PLAXIS model were analyzed as elastic elements. In order to make direct comparison, only two relative simply load cases were carried out for this calibration assessment as below.

Table 3.2 – Loading Cases for Calibration Exercise

Loading	Case 1	Case 2
Self weight	yes	Yes
Surcharge on road (20kPa)	No	Yes
Surcharge on top of quay (60kPa)	No	yes

Three aspects were assessed in this calibration assessment, including lateral earth pressure, displacement and incremental bending moment.

a) Lateral earth pressure

For structural analysis of long-term condition, at-rest earth pressures were assumed at both sides of the barrettes/curtain walls. To verify this assumption, the at-rest earth pressure used in structural analysis is compared with the lateral earth pressure calculated by PLAXIS 3D and the results are shown below. As shown in the plots for comparison of net earth pressure, the net earth pressure applied at the barrettes and curtain wall for structural analysis were generally more conservative than that evaluated with PLAXIS 3D model.

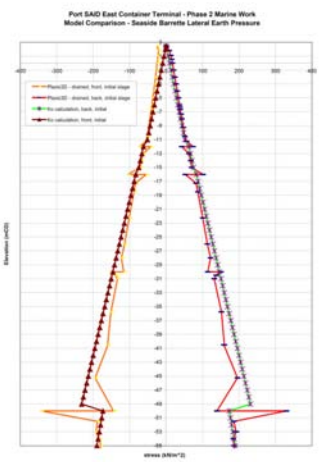

Figure 9: Initial Stress Comparison

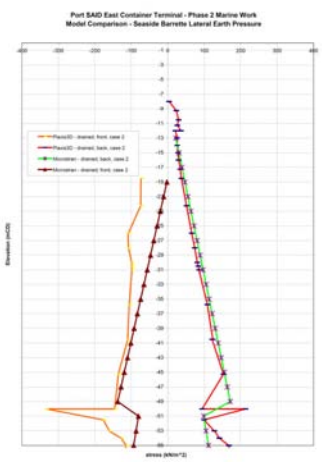

Figure 10: Lateral Pressure Comparison

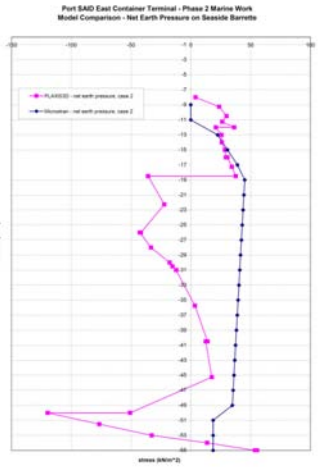

Figure 11: Net Earth Pressure Comparison

b) Displacement

The maximum horizontal displacement of the quay under load case 1 calculated by PLAXIS3D was 52.5mm and was consistent with the observed horizontal movement of the Phase 1 quay after completion of the excavation work which ranged from about 50mm to 70mm. As the soil modulus used in the PLAXIS 3D model is based on site-specific ground investigation results and the calculated movement is consistent with the movement observed during construction of similar quay structure in Phase 1, it is considered that the PLAXIS 3D model developed for this study is reliable.

To compare the deformed shape of seaside barrette in Microstran and PLAXIS 3D model, the relative horizontal displacement from the toe were plotted as below. Both the Microstran and PLAXIS 3D model gave similar mode of deflection of the quay structure. The estimated deflection of the quay calculated in Microstran was smaller than that estimated by PLAXIS 3D, which difference may be because of that PLAXIS 3D model taking into account the soil-structure interaction behaviour and the ground heaving induced by excavation sequence.

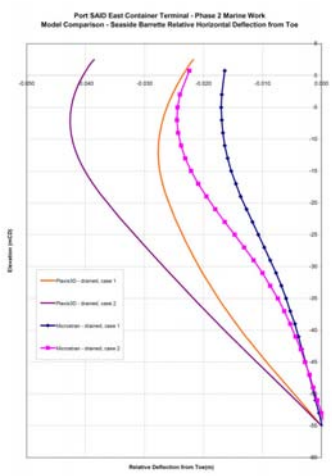

Figure 12: Horizontal Deflection Comparison

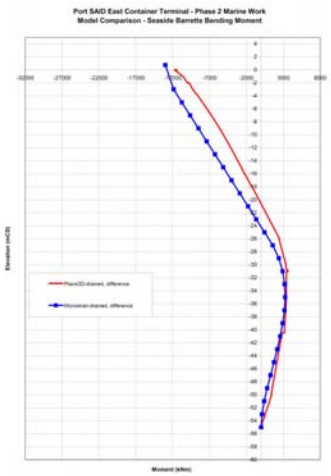

Figure 13: Bending Moment Comparison

c) Incremental bending moment

The calculated incremental maximum bending due to surcharge (i.e. difference between Case 2 and Case 1) was monitored at the top of seaside barrette in both models and the results are summarized in table below. From the above graphical plot of incremental bending moment comparison, they were found compatible to each other and the values from the two models were generally of the same order with about 10% difference in magnitude.

Table 3.3 – Calculated Maximum Incremental Bending Moment of Seaside Barrette

Load Case	Microstran	PLAXIS 3D
Case 2 – Case 1 (drained) (above -24mCD)	12997 kNm	11700 kNm
Case 2 – Case 1 (drained) (below -24mCD)	3250 kNm	3390 kNm

Hence, the proposed soil springs and earth pressure derived for structural analysis were found valid based on soil-structure interaction analysis set up with PLAXIS 3D program to evaluate the structural behaviour.

3.3 Three Dimensional Static Deformation Assessment

The quay structure is designed for berthing and mooring of container vessels and feeder vessels and supporting high-capacity rail-mounted electrically operated ship-to-shore gantry cranes and container handling equipment. Stringent movement limitation is imposed to ensure safe operation of gantry cranes and container handling equipment on quay-side gantry crane tracks. It limited net vertical rail displacement produced under working loads to a maximum of 15mm with the design life of the crane rails.

Eight 3 dimensional models were set up using PLAXIS 3D Foundation to assess the deformation along the quay structure with consideration of the variation in geological conditions as well as loading patterns. The quay structure is composed of 29 bays frame structure, except the two end bays, each bay is 42 m long. The models were developed to represent different geological or structural conditions.

The modeling sequence had fully taken into account the proposed excavation sequence. The excavation under the quay deck would be carried out before dredging in front of the seaside barrette. The stress release due to dredging in front of seaside barrette was considered and the unloading soil stiffness was assumed to be three times of the virgin soil modulus of clayey layer. Since no movement would be expected to occur at

existing Phase 1 Quay Structure, a very stiff existing structure was therefore introduced at the end of the model with a relative low stiffness (0.0001 time) interface connection to the proposed Phase 2 structure. The stiffness of sandy soils was assumed based on empirical formula of E=1N60 (MPa) and Mohr-Coulomb soil model was adopted in modelling. As Mohr-Coulomb soil model has its limitations on modelling of soft soil with respects to unloading-reloading behaviour, an advance soil model – Soft Soil Model, was adopted to model the clayey layers (i.e. units 4, 5 & 7). Benefits of using Soft Soil Models include:

- Stress dependent stiffness (logarithmic compression behaviour)
- Distinction between primary loading and unloading-reloading
- Memory of pre-consolidation stress
- Failure behaviour according to the Mohr-Coulomb criterion

The quay structure was analyzed in three dimensions by using PLAXIS 3D Foundation. PLAXIS 3D Foundation is finite element software for three-dimensional deformation analysis of soil-structure interaction. The typical model is presented in Figures 14. The whole construction sequence had been taken into account in the modeling, including initial stress at reclamation, construction of quay structures, staged excavation under the quay deck, staged dredging in front of the quay structures, and application of external loading of crane load, mooring, berthing, etc. Additional models with drained condition were also carried out to assess the long-term deformation of the proposed quay structures.

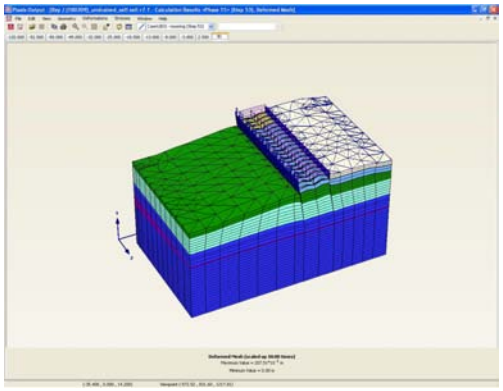

Figure 14: Isotropic View of Model

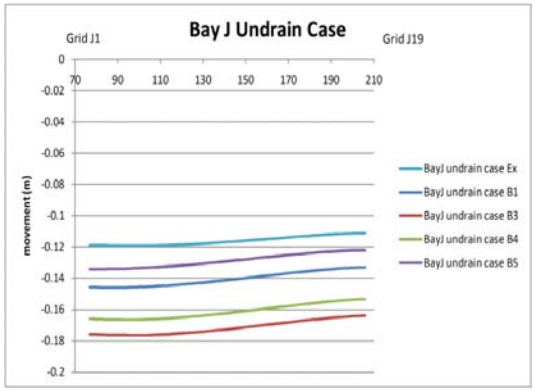

Figure 15: Differential Settlement of Typical Bay

The estimated differential settlement of a typical bay under different loading cases is shown in Figure 15. The maximum differential settlement was expected to occur at the most critical load case B3 (i.e. mooring case). The estimated value was within 20mm and this order could fulfill the rail maintenance criteria of 1 in 1000. The assessment was also checked against with the wall movement data of the Phase 1 prepared by Hamza Associates (Phase 1 designer). Four barrettes (in a bent) are adopted for the Phase 1 but with low stiffness individually in comparison with the Phase 2 scheme. The field measurement of the wall deflection after dredging ranged from 50mm to 70mm. In comparison with the numerical analysis results, the estimated wall deflection was about 70mm to 100mm and this indicated the modeling was compatible and on the conservative side.

3.4 Dynamic Deformation Analyses

Two earthquake design events were considered. Under the L1 events, container handling operations is required to be able to recommence immediately after the seismic event while minor repairs are carried out (Degree I Damage). Under the L2 event, the structure can be reasonably repaired and restored to operation in a reasonable period of time, not exceeding 3 months (Degree II Damage). The peak horizontal ground

acceleration at rock head level were taken as 0.08g and 0.12g for L1 and L2, respectively.

Due to the lack of characteristic earthquake time-histories form the site, the scaled physical earthquake recordings were used as input motions. Three earthquake events were considered, including Loma Prieta earthquake (1989), Aqaba earthquake (1995) and Alaska earthquake (2002). The earthquake motions are shown in Figure 16. These time histories were selected because they are consistent with the overall characteristics of earthquakes dominating the hazard at the site, including magnitude, recording distance, and faulting mechanism. When dealing with soil parameters in dynamic analysis, an important factor is the shear strain level under the design earthquake shaking. Depending on the strain level, the dynamic properties (or stiffness properties under dynamic loadings) of soils can be significantly different from those used in static analysis. Description of the dynamic soil parameters usually takes the form of a set of curves which show the shear modulus degradation and increase in damping ratio with the built-up of shear strain level, based on the underlying assumption of horizontal soil layers and uniform strain within each soil layers. Due to the lack of detailed information about the dynamic soil properties for this project, a sensitivity study was carried out in which three sets of shear moduli are used as input and the resultant displacements are compared. Through a sensitivity study, from the point of view of engineering conservatism the following parameters are chosen for dynamic analysis in estimating the permanent and residual displacements of the quay structure:

- Damping Ratio: 5% damping is selected
- Material Constitutive Model: Mohr-Coulomb material model with undrained type applied to clayey soils in the design cases
- Soil parameters: static soil parameters are chosen to provide a conservative estimation of dynamic displacements

The seismic analyses were carried out by PLAXIS Dynamics Version 8, the output information takes the form of time history of displacements at the pre-defined monitoring points to estimate the maximum and residual differential horizontal movement (between Point A and Point D) of the quay structure. The pre-defined monitoring points are shown in Figure 17.

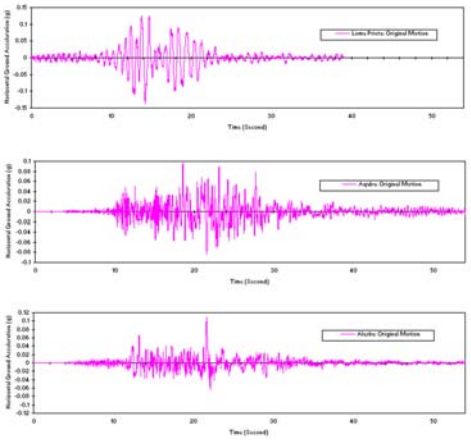

Figure 16 : Earthquake Motions of Loma Prieta (1989); Aqaba (1995); Alaska (2002)

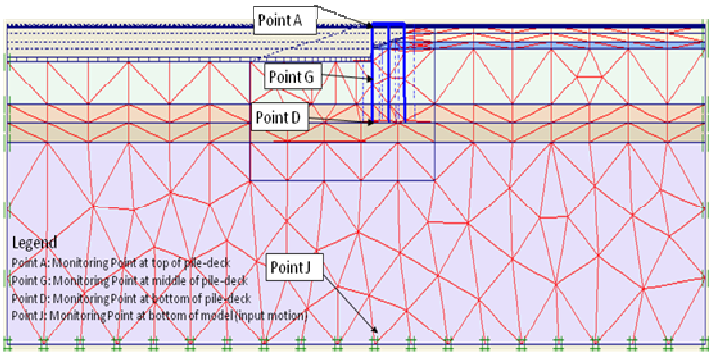

Figure 17 : Monitoring Points in Dynamic Model

The maximum differential movement was occurred under the earthquake motion of Loma Prieta. Under the L1 event, the maximum differential movement and residual differential movement estimated are 145mm and 77mm respectively (see Figure 18). The quay structure is about 20m above the mud line and the residual horizontal displacement is well within the Degree I damage criteria of 1.5% (i.e. 300mm) as classified in Table 4.2 in Chapter 4 Damage Criteria, 'Seismic design guideline for port structures', PIANC working group 34.

Under the L2 event, the maximum differential movement and residual differential movement estimated are 262mm and 179mm respectively (see Figure 19). The estimated value is also within the differential movement of 1.5% although the seismic design under the L2 event is structural control instead of displacement control in accordance with Table 4.2 in Chapter 4 Damage Criteria, 'Seismic design guideline for port structures', PIANC working group 34. The dynamic analyses under both the Level 1 and Level 2 earthquake events indicated only a slight tilting of the barrettes caused and hence found to be acceptable.

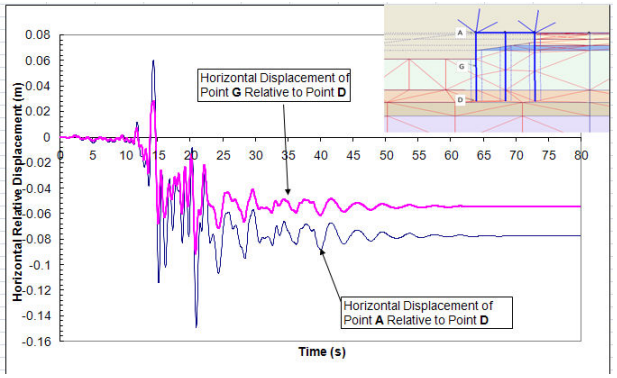

Figure 18: Level 1 – Deformation of Quay-Deck System, Loma Prieta

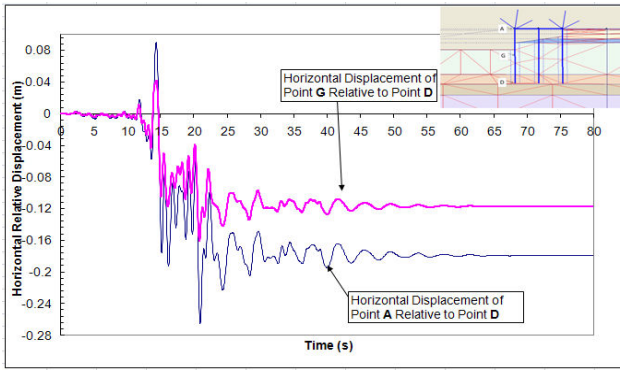

Figure 19: Level 2 – Relative Displacements of Quay-Deck System, Loma Prieta

9 CONCLUSIONS

This paper presents a case study of foundation design of marine quay structures in complex ground conditions which gave a major challenge in this project. The base layer of soft clay turn out to be under-consolidated and to be much thicker than the expectation Structural analyses taken into account the soil-structural interaction and deformation of the proposed quay structures under both operation condition and earthquake condition are the key criteria to demonstrate the design satisfying the project requirements. Sophisticated numerical 3-dimensional static and 2-dimensional dynamic analyses were carried out for foundation design to demonstrate on compliance on deformation limits in all the construction, operation and earthquake conditions.

REFERENCES

Canadian Geotechnical Society, 1992, *"Canadian Foundation Engineering Manual (3rd edition)"*. Canadian Geotechnical Society, Ottawa.

Hamza, M. Hamed, H., 2002, "Port Said East – Quay Wall Behaviour during Dredging"*, Marinetime Engineering and Ports II*.

Hamza, M. Hamed, H., 2002, "Three Dimensional Soil-Structure Analysis of Port-Said East Quay Wall", *Marinetime Engineering and Ports II*.

PIANC Working Group 34, 2001, "Seismic Design Guidelines for Port Structures", *International Navigation Association*.

Seismic Geotechnical Design of T-Shape Barrette Piles

Herman Wong, Henry Wang & Eddie Wong
AECOM Asia Company Limited

ABSTRACT

This paper presents a case study of geotechnical design of barrette pile to support a wing wall under earthquake excitation. The project site is located at Port Said East of Egypt at Suez Canal and lies within seismic zone 3 as defined in the relevant Egyptian Code. The proposed wing wall has to be designed to satisfy the performance requirements under the design earthquake.

While the retaining soils behind the wing wall is to be improved to prevent liquefaction hazard, significant strength loss and deformation are anticipated for the soils in front of the wall where ground improvement works in marine environment was found to be difficult. In order to maintain stability and minimize ground settlement behind the wing wall, a series of T-shape barrette pile is proposed to enhance the lateral load resistance of the wing wall system.

Due consideration is given to the seismic behavior of the site soils in front of the wall during and after the design seismic event. Deformation of the T-shape barrette pile is determined based on anticipated soil behavior. Mitigation measures have been proposed for based on the performance requirement set forth in the technical specification of the project.

1 INTRODUCTION

1.1 Project Descriptions

The Port Said Container Terminal, Phase 2 project (Project) is situated in Port Said, Egypt at the mouth of the Suez Canal on the Mediterranean Sea. It is a major transshipment hub for the Eastern Mediterranean region. Figure 1 presents the Site Vicinity Map. The Project involves the construction of the port facilities incorporating all marine and port related infrastructures as the extension to the south of the existing container terminal Phase 1. The Site Location Plan is presented in Figure 2. The major scope of design works include site preparation works, construction of 1200m long retaining quay structure and a 60m long wing wall structure, as well as dredging, reclamation and ground improvement works.

Figure 1: Site Vicinity Map

Figure 2: Site Location Plan

At the southern end of the quay deck structure, a wing wall with about 60m in length and a slope revetment in front of the wall are provided to enable the full dredged depth to be extended into the turning area. Figure 3 present the Wing Wall and Revetment Layout Plan.

The wing wall structure consists of T-shape barrette as well as curtain walls between the barrettes. The spacing of barrettes is 9m c/c. The T-shape barrette has dimension of 2.8m x 2.8m flange and 0.8m x 4.2m web while the curtain wall is 6.2m x 0.8m in size. The proposed revetment in front of the wing wall is in 1:4 gradient with the berm of 30m wide which geometry is similar to the existing northern revetment slope and match the turning area.

The top and the bottom levels of the T-shape barrette is at +2.5mCD and -52.5mCD. For the curtain wall in between, the top and bottom levels are at +2.5mCD and -22.5mCD)

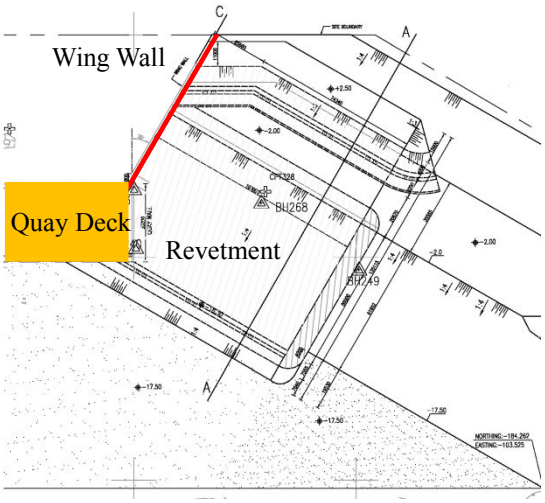

Figure 3: Wing Wall and Revetment Layout Plan

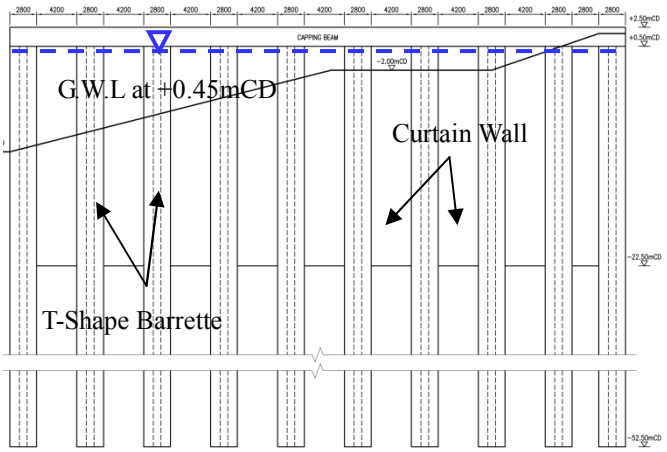

Figure 4: Wing Wall Elevated Section

1.3 Seismic Requirements

The project site lies within Zone 3, which corresponds to earthquake intensity level VIII, as defined in the

"Regulations for Earthquake-Resistant Design of Buildings in Egypt, 1998". The wing wall structure has to be designed to satisfy the performance requirements under the design earthquake. For seismic design, the performance-based design method as described in the "Seismic Design Guidelines for Port Structures", PIANC Working Group 34, 2001 (WG34) is adopted as the main guidance document.

Based on WG34, two earthquake event levels (Level 1 & Level 2) should be considered with different acceptable degree of impacts to the proposed wing wall structure. Level 1 earthquake event (L1) and Level 2 earhtquake event (L2) are motions with probability of exceedance of 50% and 10% during the lifespan of a structure respectively. For a design lifespan of 50 years for the wing wall structure, the L1 and L2 correspond to the design earthquake events with return periods of 72 years and 475 years.

Under the L1 events, container handling operations is required to be able to recommence immediately after the seismic event while minor repairs are carried out (Degree I Damage). Under the L2 event, the structure can be reasonably repaired and restored to operation in a reasonable period of time, not exceeding 3 months (Degree II Damage).

In this Project, the peak horizontal ground acceleration at rock head level is taken as 0.08g for L1 event. For the L2 event, the peak horizontal ground acceleration at rock head level is taken as 0.12g.

2 SITE GEOLOGY AND CONDITIONS

Based on the available ground investigation information, groundwater table was detected at about 3m below existing ground level of about +2.5mCD. Besides, the site soils could be differentiated into 7 soil units down to large depth of more than 70m below the existing ground and are briefly described as follows:

Soil unit 1- Surcharge material placed on the Phase 2 site prior to the commencement of the previous work. The Unit generally comprises of silty sands with shell fragments but may also contain layers of silt and clay. This Unit has been overlain in parts by sands, silts and clays removed from the area of the Phase 1 works during construction over few years back. Thickness varies but generally over 2m.

Soil unit 2 - Hydraulically placed material derived from excavations for the nearby Suez Canal by-pass channels. The Unit variously comprises layers of very soft to soft clay, highly dilatant sandy silt and dilatant silty sand, sometimes with shell bands. Average thickness varies from 5 to 6m.

Soil unit 3 - Generally a medium dense to dense, fine to medium naturally occurring sand with many sand-sized shell fragments with SPT N-value between 19 to 26. The top level of this Unit tends to be deeper and the stratum tends to be thinner towards the south of the Site. The stratum becomes inter-layered with clay in the south. Average thickness varies from 5 to 6m.

Soil unit 4 - An inter-layered deposit of very soft to firm clay, clay/silt and clayey silty fine sand. The Unit is predominantly cohesive. Thickness varies from 3 to 5m.

Soil unit 5 - Consists of a considerable thickness of soft clay which becomes soft to firm and more plastic with depth. Thickness varies from 25 to 40m.

Soil unit 6 - Consists of generally dense to very dense, slightly silty to silty, slightly gravelly, fine to medium sand. Thickness varies and was about 9m. This layer is considered at the founding material for the T-shape barrettes.

Soil unit 7- Generally found as inter-bedded layers within Soil Unit 6 and comprises stiff to very stiff, highly plastic clay. Thickness detected over 20m.

3 SEISMIC ASSESSMENT

3.1 Liquefaction Susceptibility

Soil liquefaction is one of the major seismic hazards in seismic region which causes ground failures, building damages or instability of earth structures. Therefore, evaluation of soil liquefaction potential is an important aspect of geotechnical engineering practice. Quantitative evaluation for liquefaction hazard using "simplified procedure" in accordance with Youd et al (2001) which based on cone penetration test (CPT) results has been adopted. The analysis has taken factor of safety (FOS) of 1.25 in accordance with the requirement specified in Section 4.1.4 of Eurocode 8: Design of Structures for Earthquake Resistance – Part 5: Foundations, Retaining Structures and Geotechnical Aspects

Based on the liquefaction analysis, soil units 1 and 3 behind the wing wall are considered liquefiable

during the design earthquake. Such soils can be removed and replaced with compactable material followed by vibro-compaction ground improvement method being implemented from about -8.5mCD to the ground level to eliminate the liquefaction risk. However, such ground treatment method is found to be difficult for the soils in front of the wing wall due to site constraints in marine environment.

Since the soil units 1 and 3 in front of the wing wall is identified to be liquefiable at the free-field revetment slope, the liquefaction would cause lateral spreading. However, the amount of lateral spreading is difficult to be evaluated due to the lack of site specific seismicity information. Therefore, it is conservatively adopted that the lateral spreading will cause half of the liquefiable mass to flow away and hence, the overburden surcharge contributed by the liquefiable soil in front of the wing wall is reduced by a half and residual undrained shear strength of the remained liquefied soil is adopted as 15kPa. The residual undrained shearing strength is based on the sleeve friction (fs) measured from CPTs in the vicinity of the wing wall area. The liquefiable soil effect is considered in both seismic and post earthquake conditions.

3.2 Cyclic Softening Assessment

The clayey soil (soil units 4 & 5) at levels of about -10mCD to -35mCD are subject to cyclic softening, the cyclic softening assessment has been carried out in accordance with Lunne et al (1997) using the CPTs results in the vicinity of the wing wall.

The use of remould shear strength after softening is based on remould strength measurement obtained by vane shear test on the clayey soil units 4 & 5. Taking into consideration also of sleeve friction CPTs data, the remould shear strength to be adopted for both seismic and post earthquake conditions are as follows:

Table 1: Proposed Remoulded Undrained Shear Strength

Soil Unit	Remoulded Undrained Shear Strength (kPa)
4	23
5 (-25mCD or above)	15
5 (-25mCD or below)	15+d*

*d=depth below -25mCD in meter

3.3 Earthquake Data for Seismic Assessment

Due to the lack of characteristic earthquake time-histories at the site, the scaled physical earthquake recordings are used as input motions. Three earthquake events are considered are Loma Prieta earthquake (1989), Aqaba earthquake (1995) and Alaska earthquake (2002). These time histories were selected because they are consistent with the overall characteristics of earthquakes dominating the hazard at the site. Characteristics considered included magnitude, recording distance, and faulting mechanism.

Each earthquake accelerogram is linearly scaled to the PHGA (Peak Horizontal Ground Acceleration) of the design earthquakes, i.e., 0.12g for Level 2 and 0.08g for Level 1 earthquake events respectively.

3.4 Numerical Analysis for Seismic Condition

The seismic analysis is carried out by PLAXIS Dynamics, the output information takes the form of time history of displacements at the pre-defined monitoring points to estimate the differential horizontal movement during and after the design earthquake. The monitoring points as shown in Figure 5 are set up to output the displacement, velocity and acceleration time histories.

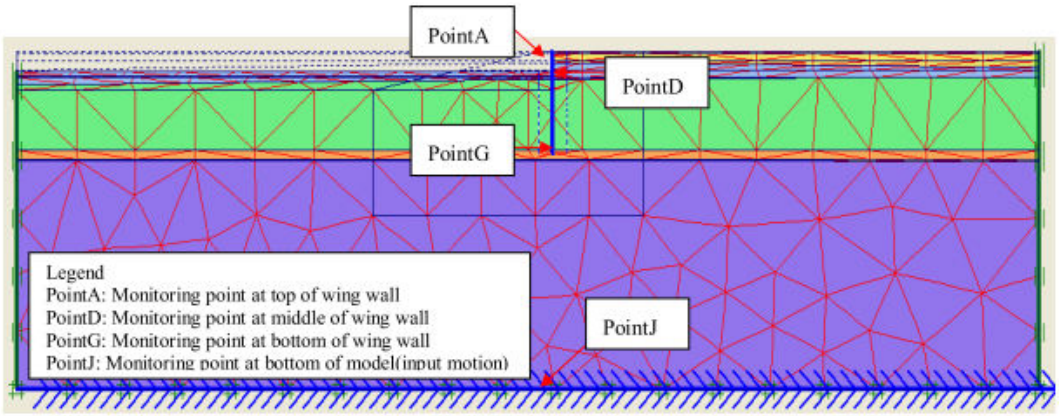

Figure 5: Geological Profile and Boundary Condition

For discussion, the L1 and L2 displacement time histories using Aqaba earthquake (1995) input is presented in Figure 6 and Figure 7.

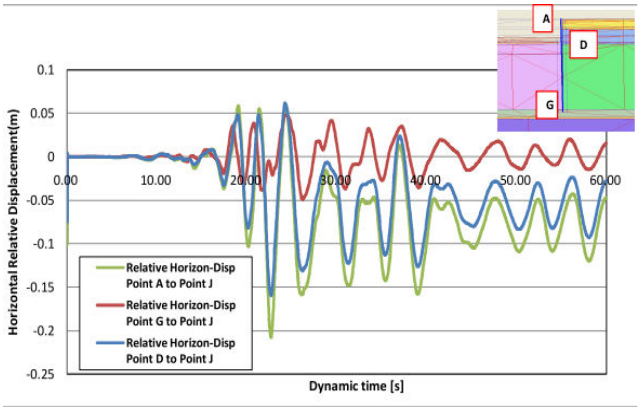

Figure 6: Level 1 – Displacements Due to Earthquake Motion, Aqaba

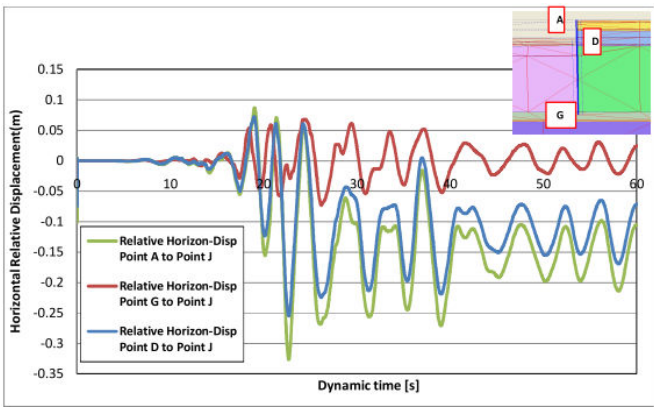

Figure 7: Level 2 – Displacements Due to Earthquake Motion, Aqaba

The maximum displacement relative to ground motion is approximately 207mm at point *A* (wall top, ground surface) for L1 earthquake events with a horizontal residual displacement of 80mm. As the maximum possible residual horizontal displacement is below this limit (300mm) classified as *Degree I Damage* in accordance WG34, it is expected the quay structure to be serviceable after a level 1 earthquake

The maximum displacement relative to ground motion is approximately 324mm at point *A* (wall top, ground surface) for L2 earthquake events with a horizontal residual displacement of 155mm. According to WG34, *Degree II Damage*, displacement conditions do not control for L2 earthquake event. In stead, peak response in stresses is the controlling factor and would be satisfied with appropriate structural design.

3.5 Numerical Analysis for Post-Seismic Condition

PLAXIS 3D Foundation is finite element software for three-dimensional deformation analysis of soil-structure interaction. Prime objective of the PLAXIS 3D models is to evaluate the deformation of the wing after design earthquake (post-earthquake condition). Figure 8 is the isometric view of the typical model.

Under the post-seismic condition, the operation behind the wing wall is assumed to be suspended and the surcharge behind the wall is reduced. In addition, collapse of the revetment in front of the wall is simulated.

The slope collapse begins the progression towards the post-earthquake condition. Subsequently, continuous static analyses are performed with cyclic softened and liquefied soil strength parameters to represent post-earthquake condition.

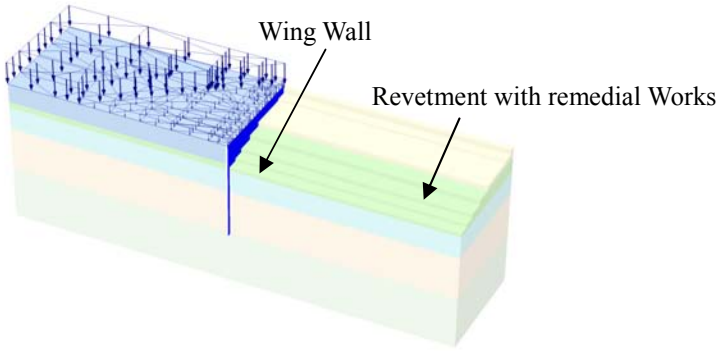

Figure 8: Isometric View of PLAXIS Model for Post Seismic Analysis

Based on the result of analysis, it is difficult to maintain sufficient stability under post-seismic condition considering the collapsed revetment as well as soil strength reduction due to both liquefaction and cyclic softening of revetment soil. Therefore, remedial works of the revetment is proposed to be implemented immediately after an earthquake. The components of the revetment remedial work include construction of rock fill berm at the toe of revetment, excavation of revetment crest soil to a minimal level and restriction of operation activity immediately after an earthquake.

Since remedial work is assumed, the northwestern end of the wing wall, where maximum dredging is carried out, will be remediated with additional rock fill berm to provide restraint at the northwestern section of wing wall. Therefore, the maximum deformation is reduced with horizontal wall deflection of 519mm. That would produce the wing wall inclination of 1.06%. Since there is no requirement on the post-seismic case specified in the Employer's Requirement, the Degree I Damage criteria of 1.5% inclination is considered to be serviceable. Hence, the wall inclination in post-earthquake case is also acceptable.

4 CONCLUSIONS

The paper presents the general approach for seismic and post-seismic analysis of the wing wall structure supported by the T-shape barrettes. With considerations of soil properties during and after the design earthquake events, PLAXIS analyses are adopted to estimate the wall deflection. The calculated deflections are check against the requirements as set forth in "Seismic Design Guidelines for Port Structures", PIANC Working Group 34, 2001 to ensure the wing wall deflections are acceptable.

In post-seismic condition, it is required that the terminal should be back to operation within 3 months after a Level 2 earthquake. Urgent remedial work will be carried out before the terminal is brought back to operation in order to maintain adequate stability. After the earthquake, the operation loads behind the wing wall should be removed to prevent further deformation due to soil softening, only construction load is allowed entering this area until the urgent remedial is completed.

REFERENCES

Egyptian Society for Earthquake Engineering, 1998, "*Regulations for Earthquake-Resistant Design of Buildings in Egypt*".

Lunne, T., Robertson, P.K., and Powell, J.J. M, 1997, *"Cone Penetration Testing in Geotechnical Pratice"*, Blackie-Academic Publishing /London.

PIANC Working Group 34, 2001, "*Seismic Design Guidelines for Port Structures*", International Navigation Association.

R.W. Boulanger & I.M. Idriss, 2004, *"Evaluating for Liquefaction or Cyclic Failure for Silts and Clays", Report No. UCD/CGM-04/01, Center for Geotechnical Modeling*, Department of Civil and Environmental Engineering, University of California at Davis.

The European Standard EN1998-5:2004, *"Eurocode 8: Design of Structures for Earthquake Resistance – Part 5: Foundations, Retaining Structures and Geotechnical Aspects"*.

Youd, T.L. et al. 2001, Liquefaction Resistance of Soils: Summary Report from the 1996 NCEER and 1998 NCEER/NSF Workshops on Evaluation of Liquefaction Resistance of Soils. *Journal of Geotechnical and Geoenviromental Engineering,* 127(4): 297-313.

WHEN **EXPERIENCE** COUNTS...





... COUNT ON **FUGRO**

Fugro provides a comprehensive range of foundation testing services for both land and marine projects in the Asia Pacific region.

We have been helping our clients deliver their success stories since the early 1970s and with offices located throughout China, South East Asia and Australia, we can truly provide local support with a global reach.

For further information:
onge-apac@fugro.com
www.fugro.com

Kai Tak Cruise Terminal Building, Hong Kong

ON SOLID GROUND

AECOM is a leading global provider of design and engineering professional services for both public and private clients. Our geotechnical consulting practice is one of the largest in Asia Pacific, supported by over 500 professionals and technical staff across the region. Leveraging a global force of 45,000 professionals, AECOM provides full range of geotechnical services and is dedicated to creating innovative and cost-effective solutions to tackle complex challenges.

Contact us: askgeotechnical@aecom.com | www.aecom.com

AECOM